The Activity and Dynamics of Enzymes

A thesis
submitted in partial fulfilment
of the requirements for the Degree of
Doctor of Philosophy in Biological Science at the
University of Waikato by

Rachel Dunn

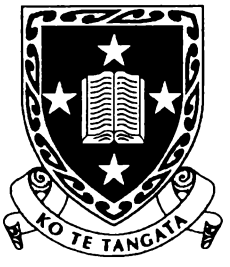

The
University
of Waikato
Te Whare Wānanga
o Waikato

2002

Abstract

It is generally accepted that enzymes require internal flexibility, or the activation of anharmonic motions, for catalytic activity. However, in general, the timescales and forms of the functionally important motions coupled to progress along the reaction pathway remain poorly understood. A number of biophysical studies have shown that protein dynamics undergo a temperature-dependent transition from harmonic to anharmonic motion. The purpose of this study was to further investigate the relationship between protein dynamics and catalytic activity, and also to investigate the nature of the observed dynamic transition.

The activity and dynamics of the single subunit enzyme xylanase, were measured under similar conditions, from –70 to +10°C. The activation of anharmonic picosecond-timescale motions is seen above –50°C, whereas the activity was seen to follow Arrhenius behaviour over the entire temperature range investigated. This result suggests that the enzyme rate-limiting step is independent of fast anharmonic motions below –50°C. Cryoenzymology studies of the temperature dependence of catalase and alkaline phosphatase activity showed no deviations from Arrhenius behaviour down to temperatures near –100°C. These results, as well as earlier studies on glutamate dehydrogenase, indicate that the observed independence of low temperature activity on global anharmonic picosecond-timescale motion may be a general property of both single- and multi-subunit enzymes.

Characterisation of cryosolvent properties, such as viscosity and phase changes, by DSC, DMTA, and X-ray scattering techniques, was used to select cryosolvents suitable for low temperature dynamic and activity measurements. A cryosolvent consisting of 70%methanol/10% ethylene glycol/20% water was particularly ideal, as it was the least viscous and free of phase-changes down to at least -160°C.

The effect of cryosolvents on enzyme properties was investigated, to enable the effect of solvent and temperature on the enzyme to be distinguished. The effect of varying solution composition on the picosecond timescale dynamics of xylanase was investigated by dynamic neutron scattering. The results indicate a significant

effect of the solvent, as the picosecond fluctuations of the protein solution largely follow that of the corresponding pure solvent. The results also indicate that the picosecond-timescale atomic motions respond strongly to melting of pure water, but are relatively invariant in cryosolvents of differing compositions and melting points.

The temperature dependence of the dynamic transition observed for glutamate dehydrogenase-cryosolvent solutions was also determined. Dynamic neutron scattering experiments were performed with two instruments of different energy resolutions, allowing the separate determination of the average dynamical mean-square displacements on timescales of up to approximately 100 ps and 5 ns. The results showed a significant dependence on the timescale of the temperature profile of the mean-square displacement. The lowest temperature at which anharmonic motion is observed is dependent on the time window of the instrument used to observe the dynamics. These results suggest that the temperature dependence of the dynamic transition in average protein motions is timescale dependent. A possible explanation is that motions over a given timescale are progressively replaced by slower motions, as the temperature is reduced.

Preface

The research for this thesis was conducted as part of an international collaboration to study the relationship between protein dynamics and enzyme activity. The group leaders are Prof. Roy Daniel, Prof. John Finney and Dr. Jeremy Smith, who provide expertise on enzyme catalysis, protein-solvent interactions, and molecular dynamics simulations, respectively. Due to the collaboration between groups, the research is obviously divided, with each group primarily contributing to their area of expertise. My role in the collaboration was primarily related to the cryoenzymology studies of several enzymes, to enable comparison with the dynamic data. I was also involved in the optimisation of enzyme assay procedures, and the further selection and characterisation of cryosolvents.

In many parts of this thesis, my own work has been placed in the context of the overall research effort. Where this has occurred, a clear distinction is made as to who conducted each part of research. It is felt that the presentation of the work in this context is necessary to enable the rationale for the conclusions to be evident. In Chapter Two the later DSC characterisation of cryosolvents was primarily my work, while the X-ray scattering and early DSC data, published in the paper included in Appendix A, were conducted by other members of the research group. In Chapter Three my work included the DSC characterisation of protein-cryosolvent solutions, and the determination of xylanase stability and activity. However, the neutron scattering data of protein-cryosolvent solutions was analysed by other members of the research group, although I was present to assist in sample preparation and loading. The cryoenzymology trials of Chapter Four were all my own work. It should be noted that the Rt8B.4 xylanase discussed in this chapter is different to the Thermotoga xylanase that was used in all other work mentioned throughout the thesis. Chapter Five contains the published paper on the temperature dependence of enzyme reactions (Bragger et al., 2000). I performed the cryoenzymology work with alkaline phosphatase, while another member of the research performed the cryoenzymology work with catalase. I was not directly involved in the dynamic neutron scattering experiments detailed in Chapter Six.

The published papers from this work are attached in the Appendices to enable easy access to the results of the research group as a whole. A statement concerning my contribution is given at the beginning of each of these papers. The majority of the xylanase cryoenzymology data and all of the glutamate dehydrogenase cryoenzymology data presented in Appendices D and C, respectively, were obtained as part of my Masters research.

Acknowledgements

I would first like to thank my supervisor, Roy Daniel, for the continual guidance, encouragement and patience he has shown throughout this study. I would like to thank Dion, Penny, and Warren, for making the laboratory an entertaining and encouraging environment. I would also like to thank Colin Monk for technical assistance, from heat shrink tubing to stubborn computers. To everyone else in the Thermophile Research Unit, I extend many thanks for making it a friendly and helpful environment. I am also grateful to the many people in the Chemistry Department who were always willing to help, and who let me borrow their equipment. In particular, I would like to thank Merilyn Manley-Harris, Wendy and Pat, who assisted with my electrospray experiments. I would also like to thank Cameron for being the willing provider of chemistry "know-how", which included drying solvents to finding stoppers.

I would also like to thank the NZFUW for the Merit Study Award, and to the NZVCC for the grant of a Claude McCarthy Fellowship, which made my visit to Don Cowan's laboratory at UCL, London, possible. Also to be thanked are Don Cowan for allowing me to visit his laboratory, and to Rory, Steve and Inma' who made my stay there enjoyable. I thank John Finney for helpful discussions while I was at UCL. A special thank you goes to Marianne Odlyha who assisted me greatly in the DSC and DMTA experiments.

The ability of Marcel to fix annoying computer problems, and the support and patience shown by my friends and family are also greatly appreciated.

Table of Contents

List of Tables

List of Figures

List of Abbreviations

κ	measure of the orientation of the electronic transition moments of the emitting and absorbing species (fluorescence)
τ	correlation time (NMR)
f	Lamb-Mössbauer factor
η	viscosity of a solution
ν_c	peak of fluorescent spectrum
τ_f	lifetime of excited chromophore (fluorescence)
τ_N	lifetime of Mössbauer nucleus
τ_p	period of dipole relaxation
$\langle u \rangle^2$	average dynamical mean-square displacement
$\langle x^2 \rangle$	mean-square displacement
A(t)	anisotropy at time t after excitation
$\bar{b}$	average scattering length
b	scattering length
B_j	temperature factor for atom j
c	speed of light
CD_3OD	perdeuterated methanol
cP	centipoise, unit of viscosity
C_P	heat capacity at constant pressure
D	diffusion coefficient
D_2O	deuterium oxide
DMF	dimethyl formamide
DMSO	dimethyl sulfoxide
DMTA	dynamic mechanical thermal analysis
DSC	differential scanning calorimetry
E*	complex tensile modulus
E'	storage modulus
E''	loss modulus
E_A	energy of activation
E_o	neutron energy
E_o	nuclear transition energy
ES-MS	electrospray mass spectrometry
ESR	electron spin resonance
F	electrostatic force between two charged species
F(Q)	structure factor (X-ray)
$G_s(r,t)$	self pair correlation function
h	Planck's constant
H	enthalpy
$\hbar$	$h/2\pi$
HPAE-PAD	high-performance anion-exchange chromatography with pulsed amperometric detection
$\hbar q$	neutron momentum change
$\hbar\omega$	neutron energy change
J	spectral-overlap integral (fluorescence)
k	incident wave vector

k	rate constant
k'	scattered wave vector
k_B	Boltzmann constant (gas constant per molecule, R/N)
K_M	Michaelis constant
m	rest mass
MeOH	methanol
Me-Xyl	methyl-β-D-xylopyranoside
Me-Xyl_2	methyl-β-D-xylobioside
MQ	milli Q water
n	refractive index of medium
N_A	Avagadro's number
NMR	nuclear magnetic resonance
NPh	*o*-nitrophenol
ONP-Xyl_2	*o*-nitrophenyl-β-D-xylobioside
ONP-Xyl_3	*o*-nitrophenyl-β-D-xylotrioside
ONP-xylose	*o*-nitrophenyl-β-D-xylopyranoside
pa_H	apparent pH
q	scattering wave vector
R	gas constant
r	hydrodynamic radius of diffusing species
$S(q,\omega)$	dynamic structure factor
$S_{INT}(T)$	integrated elastic intensity
T	temperature
T	temperature in Kelvin
T_1	spin-lattice relaxation
T_2	spin-spin relaxation
tan δ	loss tangent
T_g	glass transition temperature
v_o	neutron velocity
$W(Q)$	Debye-Waller factor
Xyl_2	xylobiose
Xyl_3	xylotriose
δ	phase angle
ΔG^*	free energy of activation
ΔH^*	enthalpy of activation
ΔS^*	entropy of activation
ε	tensile strain
ε_o	permittivity of a vacuum
ε_r	dielectric constant of the medium
θ	scattering angle
λ_o	de Broglie wavelength
σ	tensile stress
σ	total scattering cross section

Chapter One

Introduction

1.1 Introduction

It is widely accepted that enzymes require internal flexibility for catalytic activity (e.g., Frauenfelder et al., 1979; Artymiuk et al., 1979; Karplus and Petsko, 1990; Gerstein et al., 1994; Brooks et al., 1988; Huber and Bennett, 1983). It is implicit in the concept of the induced fit (Koshland, 1958; Yankeelov and Koshland, 1965) that an enzyme must flex over a timescale in keeping with its catalytic-centre activity.

A number of biophysical studies have shown that a transition in the equilibrium fluctuation of several proteins occurs at approximately 200 to 220 K (refer to references below). Below the transition temperature, the overall motion of groups of atoms ceases, and all that remains are the harmonic vibrations of the individual atoms. Above the transition temperature, the anharmonic dynamics may involve continuous and/or jump diffusion between potential energy wells associated with 'conformational substates' of slightly different structure in which the proteins are trapped below the transition temperature (Elber and Karplus, 1987; Kneller and Smith, 1994; Frauenfelder et al., 1979). Correlations have been found between protein function, such as ligand binding or proton pumping, and the presence of anharmonic motion (Ferrand et al., 1993; Rasmussen et al., 1992). These results suggest that protein function will also cease at the dynamic transition temperature, due to the observed dependence of activity upon flexibility.

The increased flexibility of proteins above the transition temperature may indeed be necessary for some proteins to rearrange their structures to achieve functional conformations. However, the timescales and forms of the functionally important motions remain poorly understood. Recent studies on mesophilic and thermophilic enzymes have demonstrated activity at temperatures below the dynamic transition temperature (More et al., 1995; Daniel et al., 1998). This indicates that the rate-limiting step is independent of the transition observed in the

picosecond timescale dynamics. The direct comparison of activity with dynamic measurements was made with the large, multi-subunit enzyme glutamate dehydrogenase. However, it is not clear whether the observed dependence of activity on picosecond dynamics can be applied to all enzymes. Both the enzyme assays and dynamic measurements were made on cryosolvent solutions containing the enzyme. This enabled the subzero determination of enzyme activity, and ensured that the activity and dynamic data were comparable.

The current research focused on several areas of further exploration, from the preliminary work mentioned above.

Initially, the applicability of the observed independence of the rate-limiting step on picosecond dynamics was determined by conducting similar experiments on the small, single subunit enzyme, xylanase.

Another goal of this work was to try and attempt activity measurements at significantly lower temperatures than previously determined. There were also indications that dynamic transitions were present at temperatures lower than that previously detected. Therefore, to enable correlations between activity and lower temperature dynamic transitions, it was important to measure activity to as low a temperature as possible.

To further understand the nature of dynamic transitions in proteins, it is also important to characterise solvent effects. Solvent can in principle affect protein dynamics by modifying the effective potential surface of the protein and/or by frictional damping (Brooks and Karplus, 1989; Smith et al., 1990). To enable the dependence of dynamics on the solvent environment to be determined, measurements of protein dynamics were conducted on enzyme samples dissolved in a range of cryosolvents.

The timescale dependence of the dynamic transition observed for proteins was also determined. This was accomplished by conducting parallel dynamic measurements on different timescales.

In conjunction with the above experiment, investigations to find and characterise an ideal low temperature cryosolvent were conducted.

1.2 Protein Dynamics

1.2.1 Structure of Proteins

A discussion of the primary protein structure shall initially be covered as it is useful in demonstrating the origin of the inherent flexibility of proteins. Each protein consists of a polypeptide chain formed from amino acids linked together by peptide bonds. The polypeptide chain is composed of repeating units that differ in their substituent groups, or side chains. The sequence of amino acids is referred to as the primary structure. The structure of a short section of polypeptide chain is shown in Figure 1.1.

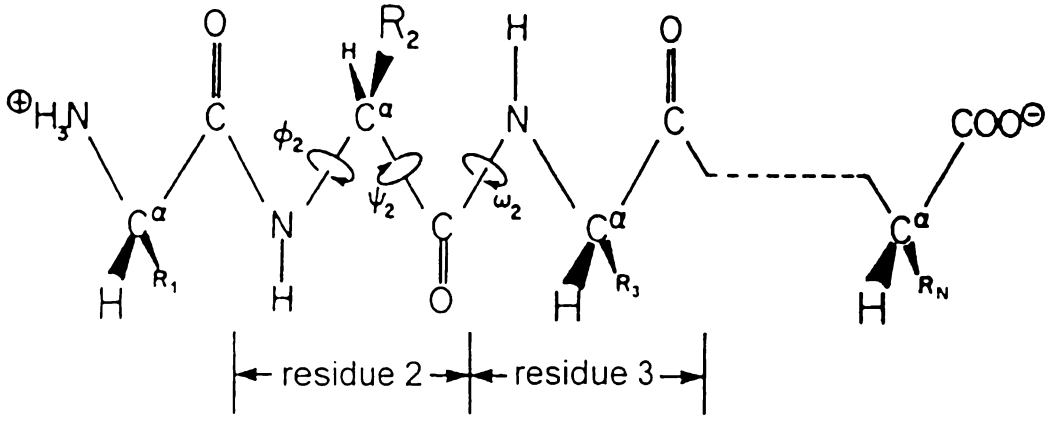

Figure 1.1. Structure of a polypeptide chain. The covalent bonds and bond angles are rather rigid, but sizable rotations can occur around certain bonds. The dihedral angles $\emptyset_i$, Ψ_i and ω_i, measure the torsion around the bonds in the backbone of residue i. The labels R_i represent the side chains. Reproduced from McCammon and Harvey, 1987.

The polypeptide chain is intrinsically flexible as many of the covalent bonds that occur in its backbone and side chain are rotationally permissive (McCammon and Harvey, 1987). Rotation around the dihedral angles, Ø and Ψ, of the main chain is permitted. The dihedral angle, ω, is relatively rigid with respect to twisting due to the partial double bond character of the C-N bond. Also, all of the side chains, except glycine, have one or more single bonds about which internal rotation can occur. The main limitation to rotation for the backbone dihedral angles, Ø and Ψ, arises from non-bonded interactions. The steric repulsion caused by the overlap of atoms, make certain values for Ø and Ψ energetically unfavourable.

1.2.2 Diversity of Protein Dynamics

This section will be a brief overview of the dynamical motions found in proteins. For a comprehensive coverage of protein dynamics refer to McCammon and Harvey (1987) and Brooks et al. (1988).

Due to the intrinsic flexibility of the primary structure of proteins, proteins have a wide variety of internal motions. The groups linked by the rotationally permissive covalent bonds are themselves comparatively rigid, for example the CONH peptide group and the ring in the tyrosine side chain, and constitute the fundamental dynamical elements in a protein molecule (McCammon and Harvey, 1987). Within these groups, only small atomic displacements occur due to the cost of deforming bond lengths, bond angles, and dihedral angles about multiple bonds. The important motions in proteins involve the relative displacement of such groups. This yields a vast dynamical spectrum that ranges from the rapid local motions of the individual groups to slow collective distortions of large regions within the molecule. High frequency vibrations of the atoms occur within the groups, but do not affect the relative displacements. The motions cover a wide range of amplitudes (0.01 to 100 Å) and timescales (10^{-15} to > 1 s). The types of internal motions have been summarized in Table 1.1.

Because of the high packing density in protein molecules, their atomic motion displays similarities to that seen in other dense materials. Over short periods of time ($\leq 10^{-12}$ s), the small amplitude motions (≤ 0.2 Å) show similarities to the motions of a molecule in a liquid. The groups display rattling motions in a cage consisting of the neighbouring atoms, or surrounding solvent if the group is at the protein surface. For many processes with longer characteristic times, the types of motions that develop are typical of solid materials. This is expected as the atoms in a protein have definite average positions corresponding to the native molecular structure (McCammon and Harvey, 1987). More substantial displacements of groups of atoms occur over longer time intervals, and involve concomitant displacements of the cage atoms (Brooks et al., 1988). These collective motions may have either a local or rigid-body character. Local motions involve changes in the cage structure and the relative displacement of the neighbouring groups. Such motions are subject to large restoring forces associated with the distortion of the

cage surrounding the group. An example of such a motion is the rotational isomerisation of the tyrosine rings, corresponding to an 180° change in the dihedral angle. Rigid-body motions involve the relative displacement of different regions of the protein, but only small changes on a local scale. The distortion is therefore distributed over many residues in the molecule, and the protein can be thought of as behaving like a continuous elastic material (McCammon and Harvey, 1987). The hinge bending motion that occurs in proteins with two globular domains is a good example of a rigid-body motion. A useful collection of known examples of domain movements in proteins is given by Gerstein et al. (1994).

In addition to the local structural transitions and global elastic motions, proteins undergo more complicated dynamics on long timescales. The native conformation of a protein comprises a large number of slightly different structures that correspond to local minima in the potential energy surface of the system. The interconversion between some of these substates may occur on a comparatively long timescale. Transitions among some of these substates are of biological importance, for example, binding of an appropriate regulatory ligand may increase the population of substates with greater activity. The global character of some transitions is due to the dense packing of the proteins, as movement in one region will depend on the small rearrangements of surrounding regions.

The relationship between the various fluctuations occurring in proteins has been discussed by a number of authors. Brooks et al. (1988) suggested that the small-amplitude fluctuations are essential to all other motions in proteins, and "serve as the "lubricant" that makes possible larger-scale displacements, such as domain motions, on a physiological time scale. A similar statement was given by McCammon and Harvey (1987), who proposed that the "fast motions represent a kind of dynamic background that partly determines the nature of all slower motions". Similar conclusions have been made from dynamic studies on, for example, myoglobin (Doster et al., 1989) and bacteriorhodopsin (Lehnert et al., 1998).

Table 1.1. Internal motions of proteins. Adapted from Brooks et al. (1988).

I. *Local motions* (0.01 to 5 Å, 10^{-15} to 10^{-1} s)

- a) Atomic fluctuations
  1. Small displacements required for substrate binding
  2. Flexibility required for 'rigid-body' motion
  3. Energy 'source' for barrier crossing and other activated processes
- b) Side chain motions
  1. Opening pathway for ligand to enter and exit
  2. Closing active site
- c) Loop motions
  1. Disorder-to-order transition
  2. Rearrangement as part of rigid-body motion
- d) Terminal arm motions
  1. Specificity of binding

II. *Rigid-body motions* (1 to 10 Å, 10^{-9} to 1 s)

- a) Helix motions
  1. Induction of large-scale structural change
  2. Transitions between substates
- b) Domain (hinge-bending) motions
  1. Opening and closing of active-site region
  2. Increasing binding range of antigens (antibodies)
- c) Subunit motions
  1. Allosteric transitions (hemoglobin)

III. *Large-scale motions* (>5 Å, 10^{-7} to 10^{4} s)

- a) Helix-coil transition
  1. Activation of hormones (glucagons)
  2. Protein folding transition
- b) Dissociation/association and coupled structural changes
  1. Formation of viruses
  2. Activation of all fusion proteins
- c) Opening and distortional fluctuations
  1. Binding and activity (calcium-binding proteins)
- d) Folding and unfolding transition
  1. Synthesis and degradation of proteins

1.2.3 Effect of Temperature on Protein Dynamics

A number of studies have investigated the effect of temperature on protein structure and dynamics. Frauenfelder et al. (1987) studied the thermal expansion of metmyoglobin crystals, by analysis of the refined crystal structures at 80 K and 255 to 300 K. The internal volume occupied by myoglobin increased by approximately 3% on heating from 80 K to 300 K. The internal volume change was attributed to an increase in the small, subatomic free volumes between the atoms. Expansion of the protein is non-uniform, with particular regions of the protein showing greater changes between the low temperature and room temperature structures. Thermal expansion occurred mainly in the protruding loops, implying a lower thermal sensitivity for the tightly packed protein core. The anisotropy of the thermal expansion reflects the distribution of interactions that stabilise the average structure and govern the fluctuations.

Protein dynamics has also been shown to be affected by temperature. The most interesting phenomenon is a 'sharp' transition observed in protein dynamics at approximately 180 K to 220 K. A variety of enzymes have been studied by different techniques, and have all shown a similar transition temperature in the observed dynamics. The timescales of the motions detected by each technique vary from approximately 10^{-7} s, for Mössbauer spectroscopy, to approximately 10^{-12} to 10^{-13} s, for neutron scattering. X-ray diffraction studies of metmyoglobin (Hartmann et al., 1982) and ribonuclease-A (Tilton et al., 1992) show transitions in the mean-square displacement of particular atoms at approximately 200 K. Mössbauer spectroscopy on deoxymyoglobin crystals (Parak et al., 1982; Bauminger et al., 1983) and metmyoglobin crystals (Bauminger et al., 1983), showed a transition in the dynamics at approximately 200 to 220 K. A number of proteins have been studied by neutron scattering, including hydrated powders of superoxide dismutase (Filabozzi et al., 1996) and myoglobin (Doster et al., 1989; Cusack and Doster, 1990), and bacteriorhodopsin in hydrated purple membranes (Ferrand et al., 1993; Fitter et al., 1997), and have also shown low temperature transitions in the dynamics of these proteins. The transition occurred at approximately 180 to 220 K for myoglobin and superoxide dismutase, and at approximately 220 to 230 K for bacteriorhodopsin. Conformational dynamics

within the complex between Zn-substituted cytochrome *c* peroxidase and cytochrome *c*, was studied by examining the fluorescence quenching of the triplet state of the zinc in the cytochrome *c* peroxidase by the ferriheme of cytochrome *c*. A transition region was seen in the decay traces of the complex from 220 to 250 K (Nocek et al., 1991).

Some refer to the observed transition in protein dynamics workers as the 'glass transition', due to certain characteristic features that are also found in the dynamics of dense glass-forming systems (Iben et al., 1989; Angell, 1995). Below the glass transition, the protein motions are purely harmonic vibrations of the atoms. In the inelastic neutron scattering studies on myoglobin by Doster et al. (1989), the elastic intensity at temperatures between 4 and 180 K had the Gaussian form expected for a harmonic solid. The vibrational motion can be described by a Debye-Waller factor, where the mean-square displacement, $\langle \Delta x^2 \rangle$, increases linearly with temperature.

Above the glass transition temperature, anharmonic motions become apparent, in addition to the harmonic vibrations of the atoms. In the neutron scattering experiments by Doster et al., (1989), an extra decrease in the elastic intensity at low q (where q is the scattering wave factor) is observed above the glass transition temperature near 200 K. This is proposed to indicate the excitation of new degrees of freedom. In the studies by Filabozzi et al. (1996), a marked decrease in the elastic intensity above the transition temperature was also seen. The anharmonic contribution is attributed to the onset of torsional jumps of protons among distinct sites with slightly different energy, i.e. conformational substates.

The decrease in elastic intensity is compensated for by an increase in the quasielastic scattering, which is seen as a broad continuous region centered about the elastic peak. Quasielastic scattering is due to stochastic processes that occur over long timescales, for example, rotational or diffusive motions that involve the crossing of energy barriers (Loncharich and Brooks, 1990).

From an analysis of the quasielastic spectra, obtained by subtraction of the vibrational background, two spectral components with different shape and temperature dependency were recognised (Doster et al., 1989). The first was a fast β-process, with a broad line that increased in intensity with increasing

temperature, consistent with local jumps between different energy states. A slower α-process was also identified, where the linewidth broadened with increasing temperature. These processes were compared to the results derived from a mode coupling theory of the liquid glass transition in a hard-core liquid. A detailed discussion of mode coupling theory and its relationship to protein dynamics is given by Doster et al. (1990). The α-process reflects a collective effect, its shape arising as a result of non-linear coupling between density fluctuations. The β-process corresponds to local motions of the atoms in the cage formed by their neighbours. It is suggested that the diffusive motions in proteins resemble those in other close-packed systems dominated by hard-core interactions. Therefore, Doster et al. (1989) proposed that the dynamical features of myoglobin suggest a coupling of fast local motions to slower collective motions.

A later analysis of the neutron scattering data from myoglobin was conducted by Kneller and Smith (1994), and leads to an alternative explanation for the non-vibrational component of the dynamics. When the dihedral angles were constrained in a molecular dynamics simulation, the resulting rigid side chain motions were found to account for the full dynamics. The non-vibrational contribution to the mean-square displacements was therefore attributed to the liquid-like diffusive motions of the side chains, rather than conformational transitions in the side chains themselves.

As mentioned already, the transition in protein dynamics has also been observed in X-ray diffraction studies of crystals, and is manifested as a transition in the mean-square displacement. The effect of temperature on the crystal structure of ribonuclease-A was studied by Tilton et al. (1992). The average mean-square displacement showed a biphasic behaviour, with the transition occurring at approximately 200 K. Histograms of the individual Debye-Waller factors indicated that, as well as an increase in the overall Debye-Waller factor with temperature, a broadening of the distribution occurred. The more complicated distributions at the higher temperatures were suggested to reflect increasing anharmonicity in the atomic motions. A strong anisotropy in the temperature

dependence of the Debye-Waller factor was observed, and implies that the forces stabilising the protein structure are not uniform throughout the protein.

The temperature dependence of the dynamics of metmyoglobin crystals was also investigated by X-ray diffraction (Hartmann et al., 1982). A transition in the mean-square displacement of the iron atom, and the atoms in the heme plane, was observed around 200 K. The X-ray data was compared to that obtained from Mössbauer experiments, which was found to exhibit a dynamical transition at a similar temperature. When the overall mean-square displacement was extrapolated to 0 K, non-zero values were obtained, suggesting conformational substates of the metmyoglobin molecule. In addition, even at 80 K, some of the atoms of myoglobin were found to have mean-square displacements greater than 0.1 $Å^2$, also providing evidence for conformational substates. The presence of substates in myoglobin was first suggested by the temperature dependence of ligand binding (Austin et al., 1975). In the study by Frauenfelder et al. (1979), the presence of conformational substates was also demonstrated. Detailed discussions of protein conformational substates, with particular reference to myoglobin, have been given by Frauenfelder et al. (1991), Ansari et al. (1985), and Elber and Karplus (1987).

A number of studies have also shown that the solvent environment of a protein influences its dynamics. This aspect of protein dynamics is discussed in Section 3.2.2.

1.2.4 Mobility and Catalytic Activity

The fact that proteins are dynamic entities is well known, as demonstrated in the previous section. The importance of the dynamic flexibility of proteins with respect to their biological functioning is well established (McCammon and Harvey, 1987; Brooks et al., 1988). However, the direct relationship between enzyme flexibility and activity is not as well characterised as the motions themselves, and is an intense area of research.

Enzymes are the catalysts of biological systems; the characteristics of enzymes are their specificity and catalytic power. A significant proportion of the catalytic power of enzymes comes from their bringing of substrates together in favourable

orientations in enzyme-substrate complexes. The specificity of substrate binding depends on the precisely defined arrangement of atoms in the active site. To fit into the active site a substrate must have a matching shape. Fischer first proposed a lock and key model in 1890, whereby the substrate fitted directly into the active site (Stryer, 1988). However, this model was found to be inaccurate for a number of enzymes. In 1958, Koshland proposed the idea of an induced fit mechanism of substrate binding. In the induced fit model the binding of a substrate to an enzyme causes a conformational change that aligns the catalytic groups in their correct orientations (Fersht, 1985). The induced fit model has been shown to be an accurate representation of substrate binding for many enzymes, for example, carboxypeptidase A (Lipscomb, 1983), and adenylate kinases (Schulz, 1992). An essential part of the induced fit model is enzyme flexibility. Control, catalytic conversion and product release may also require flexibility in the protein.

Many enzymes are characterised by fluctuating conformations, which are coupled to the binding and release of substrate. For some enzymes, including protein tyrosine phosphatases, the conformational change is restricted to the movement of a flexible loop that can be described as hinged loop movement. It has been found that upon substrate binding, the loop folds over the active site-substrate complex to promote catalysis. The crystal structure of the *Yersinia* protein tyrosine phosphatase was determined in both the unliganded and tungstate bound crystal forms. The binding of tungstate triggered a conformational change that swings an important catalytic residue by approximately 6 Å into the active site (Stuckey et al., 1994). A hinged loop movement is but one of the many functionally important dynamical processes that occurs in proteins.

The importance of conformational flexibility in the catalytic activity of dihydrofolate reductase has also been investigated by a number of researchers. Conformational flexibility, including subdomain rotation and alternate loop conformations, was shown to be important for both the transformation of the substrate to product and the regeneration of the enzyme (Miller and Benkovic, 1998). The importance of correlative enzyme motions on catalysis has also been studied (Bruice and Benkovic, 2000, and literature provided therein). As yet there is little direct evidence as to how enzymes use correlated motions in catalysis.

One potential source of information has come from studies on dihydrofolate reductase. Correlated motions have been found to occur over a distance of approximately 13 Å in the dihydrofolate reductase-folate complex, with motions in the βF,βG loop being linked to the active site (Faure et al., 1994). One interpretation of the data available for dihydrofolate reductase is that the correlated motions are acting to increase the frequency of barrier crossing through the transition state of the enzyme catalysed reaction (Bruice and Benkovic, 2000). Radkowicz and Brooks (2000) performed molecular dynamics simulations to further explore the link between catalysis and dynamics in dihydrofolate reductase. They found that the Michaelis complex exhibited extensive coupling between distant regions of the structure, as indicated by the presence of correlated motions. It was suggested that the coupled motions are probably necessary for the completion of the catalytic cycle. Furthermore, they found that mutations that caused a decrease in activity were located in the regions of the protein known to participate in highly coupled motions. This led them to suggest that the mutant enzymes were affecting catalysis by altering protein dynamics.

Protein flexibility has also been implicated in the efficiency of hydrogen tunneling in enzymes (Kohen and Klinman, 1999; Kohen et al., 1999; Kohen and Klinman, 2000). Bahnson et al. (1997) showed that hydrogen tunneling efficiency was reduced in a horse liver alcohol dehydrogenase mutant, due to an increase in the distance between the donor and acceptor carbons. This lead to the suggestion that that the flexibility in interdomain movement could potentially influence the catalytic rate, by reducing the hydrogen tunneling distance of the native enzyme. Later studies in the thermophilic alcohol dehydrogenase from *Bacillus stearothermophilus* supported this conclusion (Kohen et al., 1999). It was found that hydrogen tunneling made a significant contribution to catalysis at 65°C, and the tunneling efficiency decreased with decreasing temperature. These results lead to the conclusion that thermally excited enzyme fluctuations are involved in modulating the enzyme-catalysed hydride transfer reaction.

As discussed in the previous section, a transition in protein dynamics is observed around 200 K, below which only harmonic vibrational motions of the protein

remain. If protein function is dependent upon protein flexibility, a loss of activity might be expected below the transition temperature.

The relationship between the anharmonic motions observed above the transition temperature and protein function, has been investigated in a number of studies. Rasmussen et al. (1992) investigated the temperature dependency of inhibitor binding by crystalline ribonuclease-A. Ribonuclease-A did not bind either the substrate or the inhibitor, cytidine 2'-monophosphate, at 212 K, but bound rapidly to both at 228 K. Once bound at the higher temperature, the inhibitor could not be washed off after the enzyme was cooled to 212 K. It was suggested that thermal-driven collective atomic fluctuations in proteins, only present above the transition temperature, are essential for the rapid productive binding of large ligands.

A correlation between the photo-induced electron transfer and dynamic properties of the chromatophore membranes from *Rhodospirillum rubrum* was observed (Parak et al., 1980). The dynamics of the membrane protein chromatophores were investigated by the Mössbauer effect after incorporation of ^{57}Fe, and were shown to undergo a transition at approximately 170 K. The temperature dependence of the efficiency of the photo-induced electron transfer was also observed to undergo a transition at approximately 170 K.

Ferrand et al. (1993) studied the effect of temperature on the dynamics of bacteriorhodopsin in purple membranes, and a transition was observed at about 220 to 240 K, indicating the onset of anharmonic motions above this temperature. The function of bacteriorhodopsin can be divided into two parts; the excitation by light which results in the release of a proton outside the cell, and the relaxation of the system back to its initial state, with an associated conformational change. It has been found that the relaxation of the protein in the photocycle can be inhibited below 220 K. Therefore the dynamical transitions are strongly correlated with the relaxation of the protein to its initial state. The transition itself was suggested to be related to the membrane environment, with a 'fluid' membrane environment necessary for the large-amplitude (anharmonic) motions associated with the relaxation of the protein. Later studies on bacteriorhodopsin used hydrogen-deuterium labeling to study the dynamics of a specific region of the molecule near the active site, as compared to the global dynamics of the molecule as a whole

(Réat et al., 1998). The transition temperature for the specifically labeled active centre was approximately 220 K, while the transition temperature for the global dynamics was approximately 150 K. The active centre region was also found to be more rigid than the rest of the molecule above 260 K, due to a reduced effect of solvent melting. These results demonstrated how the global flexibility allows large conformational changes in the molecule, while the more rigid active site region allows stereo-specific selection of retinal conformations.

The temperature dependence of the activity of both mesophilic and thermophilic enzymes has been investigated over a wide temperature range, from approximately 190 to 360 K (More et al., 1995; Dunn, 1998; Daniel et al., 1998; Dunn et al., 2000). It was suggested that as thermophilic enzymes are less flexible than mesophilic enzymes at a given temperature, the dynamical transition might occur at a higher temperature than that observed for mesophilic enzymes. Therefore, if protein dynamics were required for activity, a transition in activity, corresponding to the transition in dynamics, would be seen at a higher temperature than in the mesophilic enzymes. Despite activity measurements being conducted at temperatures lower than the dynamic transition temperature of approximately 220 K, no transition in the Arrhenius plots has been detected, for either the thermophilic or mesophilic enzymes. This suggested that the rate-limiting step for these enzymes is independent of the fast anharmonic dynamics determined by neutron scattering techniques.

1.2.5 Techniques for Observing Protein Motion

A basic comprehension of the experimental techniques used to study protein dynamics, enables a greater understanding of the information obtained and the ability to critically compare results obtained from different techniques. A wide variety of experimental techniques are used to study protein dynamics. This section will give a brief overview of the more commonly used techniques, along with discussions of the applicability of each technique to particular enzymes and the dynamic information obtainable.

1.2.5.1 Mössbauer spectroscopy

Mössbauer spectroscopy is the recoil-free nuclear resonance of absorption of γ-rays. For resonance to occur, an overlap of the γ-ray spectrum for emission and absorption needs to occur. A nucleus of the source emits a γ-ray by transition from the excited state to the ground state, where the change in energy is the nuclear transition energy, E_0. The emitted γ-ray may be absorbed by another nucleus of the same kind in the sample, by transition from the ground state to the excited state (Gonser, 1975). When a nucleus emits or absorbs a γ-ray it recoils, which reduces the energy of the emitted γ-quantum relative to the nuclear transition energy, necessary to excite the absorbing nuclei. Mössbauer discovered that a recoil-free line exists at E_0, in the resonance absorption spectrum. A necessary condition for the Mössbauer effect is that the extent of motion of both the emitting and absorbing nuclei be limited.

The recoil-free fraction, or probability of a recoil-free event occurring, is given by the Lamb-Mössbauer factor:

$$f = \exp(-k^2\langle x^2\rangle)$$

where k is the magnitude of the wave vector of the γ-quantum, and $\langle x^2\rangle$ is the mean-square displacement of the particular nuclei (Parak et al., 1982). The Lamb-Mössbauer factor is a measure of the mean square vibrational amplitude of the resonating atom in the direction of observation, x. Unlike X-ray diffraction, there is no static disorder contribution to the Lamb-Mössbauer factor, and so only motion of the resonating nucleus affects the observed spectrum (Brooks et al., 1988). Also, only dynamical processes with a characteristic time comparable to or faster than τ_N, the lifetime of the Mössbauer nucleus, contribute to $\langle x^2\rangle$. Therefore, Mössbauer spectroscopy has an internal time threshold. Processes with a characteristic time comparable to τ_N increase the linewidth of the Mössbauer spectrum as a result of the Doppler effect, or give rise to additional broad lines (Parak et al., 1982). Mössbauer spectroscopy is therefore able to provide information on both the timescales and amplitudes of atomic motions.

Only certain nuclei can be studied by Mössbauer spectroscopy. The examination of the dynamics of proteins using this technique has only been performed on iron-containing proteins, for example, deoxymyoglobin (Parak et al., 1982),

oxymyoglobin (Keller and Debrunner, 1980), cytochrome *c* (Frolov et al., 1997), metmyoglobin (Bauminger et al., 1983), and ferritin (Cohen et al., 1981). In all of these studies, the natural isotopic mixture of iron had to be replaced with iron highly enriched in the Mössbauer 'active' isotope ^{57}Fe (Parak and Reinisch, 1986). Mössbauer spectroscopy of the iron nucleus in proteins allows the study of protein motions that are coupled to those of the iron nucleus. For ^{57}Fe, the timescales of the motions that contribute to the line shape of the observed spectrum are between approximately 1 and 100 ns. Mössbauer spectroscopy is useful for the study of protein dynamics as it is experimentally feasible to do measurements over a wide temperature range.

1.2.5.2 Fluorescence and phosphorescence measurements

When a molecule absorbs light it is excited to an upper singlet energy level, such as S_2, and rapidly goes to the lowest excited state, S_1, without emission of light. From S_1, the molecule may go to any of the rotational and vibrational energy levels of the ground state, S_0, either by fluorescence with the emission of a photon, or by internal conversion, which is a nonradiative process. A molecule may also go to the triplet state, T_1, by a nonradiative process referred to as intersystem crossing. From T_1, the molecule can return to S_0 by phosphorescence, a radiative process, or by nonradiative processes. Under appropriate conditions, S_1 and T_1 can also transfer their excitation energy to other molecules (Yguerabide, 1972). The lifetime of the molecule at S_1 may range from 10^{-8} to 10^{-10} s, depending on the chromophore. The lifetime of the T_1 excited state, involved in phosphorescence, has a comparatively long lifetime, ranging from 10^{-3} to 10^{-1} s, depending on the chromophore and the temperature (Käiväräinen, 1985). These processes are illustrated in Figure 1.2.

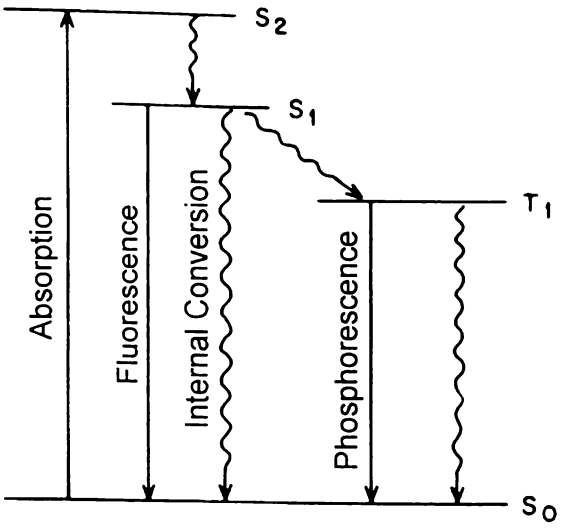

Figure 1.2. Energy level diagram of a chromophore. Straight and wavy arrows denote radiative and nonradiative processes, respectively. Adapted from Yguerabide, 1972.

Fluorescence spectroscopy provides a sensitive and versatile method for the study of protein structure and dynamics on a nanosecond timescale (Lakowicz, 1980). As well as steady-state fluorescence measurements, developments in the ability to generate and detect nanosecond light pulses, has allowed the measurement of the time dependence of fluorescence intensity following excitation (Käiväräinen, 1985). The important processes in fluorescence spectroscopy are characterised by the fluorescence spectrum, quantum yield, lifetime, and polarisation of fluorescence (Yguerabide, 1972). The fluorescent spectrum, quantum yield, and lifetime are dependent on the molecular structure of the chromophore, and are also sensitive to the environment. It is the sensitivity of these parameters to the environment that makes fluorescence spectroscopy useful in the study of protein dynamics. Another useful parameter that needs to be considered is the polarisation properties of the absorption and emission of light. A molecule absorbs plane-polarised light with maximum efficiency when the electric vector of the incident light wave vibrates along a certain direction relative to the molecule. The light is emitted from the molecule with maximum intensity also along a particular direction in the molecule. Therefore, light emitted in different directions is characterised by its intensity and also by its direction of polarisation. The spatial and polarisation properties of the emitted light allow the rotational motion of fluorescent molecules to be measured.

From the properties of fluorescence discussed above, there are several ways in which fluorescence spectroscopy can be used to monitor protein dynamics. The dependence of the fluorescence properties of a chromophore on its environment can be used to study the polarity of the active site, and to detect conformational changes that may occur, for example, on substrate binding. The transfer of the excitation energy from a donor to acceptor can be used to determine distances between particular sites in a protein molecule. The polarisation of the fluorescence can provide information on the size and flexibility of macromolecules in solution. The application of each of these variations of fluorescence spectroscopy will now be discussed in more detail.

As mentioned, when a chromophore is attached to a macromolecule, its fluorescence properties become dependent on the local macromolecular environment. The chromophore may be; intrinsic, such as a tryptophan residue, prosthetic, for example NADH, or an extrinsic fluorescent probe. When the molecule is excited, the transfer to an upper excited state takes between 10^{-14} to 10^{-15} s (Käiväräinen, 1985; Lakowicz, 1980). If this transition involves a major change in the electric dipole moment of the chromophore, the dipole field of the surroundings will not be at equilibrium and will undergo relaxation to a new equilibrium state. The relaxation time of this process is determined by the dynamic properties of the medium. The relaxation is accompanied by a change in the locations of the excited and ground energy levels, with a resulting shift (Stokes's shift) in the fluorescence spectrum relative to the absorption spectrum. The size of this shift is related to the change in dipole moment of the transition. The fluorescence spectrum of tryptophan is the most suited to the study of structural mobility of proteins, as the moment of indole transition in tryptophan is much larger than that for the other fluorescent amino acid residues, phenylalanine and tyrosine. The peak of the fluorescent spectrum due to the tryptophan residue, ν_c, is given by the ratio between the lifetime of the excited chromophore, τ_f, and the period of dipole relaxation, τ_p (Mazurenko, 1973):

$$\nu_c = \nu_\infty + \frac{(\nu_o - \nu_\infty)\,\tau_f}{(\tau_f + \tau_p)}$$

where ν_∞ is the value of ν_c if $\tau_p \ll \tau_f$, and ν_o is the value of ν_c if $\tau_p \gg \tau_f$.

Fluorescence energy transfer data can be used as a probe for changes in the local fluctuations of a protein molecule. If two fluorescent labels are associated with a protein, located 2 to 10 nm apart, a Förster-type resonance energy transfer (FRET) donor-acceptor pair can be formed (Somogyi and Damjanovich, 1988). The photon excitation energy, $h\nu$ (where h is Planck's constant and ν is the frequency in hertz), of the donor molecule can be transferred to the acceptor molecule by dipole-dipole interaction, and the acceptor can then relax through the emission of a photon, $h\nu'$, where $h\nu > h\nu'$. The transfer rate constant, k_t, can be expressed as:

$$k_t = dJn^{-4}k_eR^{-6}\kappa^2$$

where d is a constant, J is the spectral-overlap integral, n is the refractive index of the medium, R is the distance between the two chromophores, k_e is the rate constant of the donor emission, and κ^2 is a measure of the orientation of the electronic transition moments of the emitting state of the donor and the absorbing state of the acceptor. As can be seen, the rate of transfer between the donor and acceptor chromophores is dependent on the distance between them. By characterising the fluctuation of the relative motion of the two fluorescent probes, the relative fluctuation of the different parts of the protein can be determined (Somogyi and Damjanovich, 1988; Lakowicz et al., 1992; Bilderback et al., 1996; Haran et al., 1992). An extension of this method for use with systems with multiple fluorescent labels was developed by Somogyi et al. (2000), and shown to be just as effective in monitoring the change in intramolecular flexibility with temperature.

Fluorescence polarisation spectroscopy can lead to information about the rotational motion of a macromolecule, due to the spatial and polarisation properties of the emitted light. In general, the decay of fluorescence intensity of a system of rotating molecules is given by:

$$F(t) = r(t)e^{-t/\tau}$$

where F(t) is the fluorescent intensity after time, t, of light absorption, and r(t) characterises the rotational motion (Yguerabide, 1972). If a fluorescent probe is rigidly attached to a protein, the motion of the chromophore will be the same as the protein. Motion which results from local rotations of the label at its site of

attachment, or from rotations of different portions of the macromolecule with respect to each other, can also be studied by fluorescence polarisation techniques.

The arrangement of a fluorescence polarisation experiment is shown schematically in Figure 1.3.

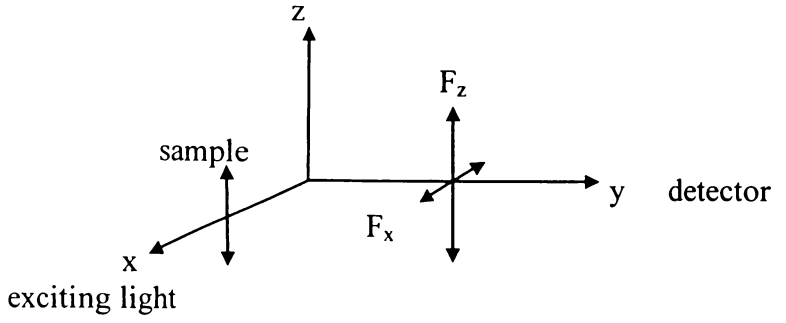

Figure 1.3. Coordinate axes for fluorescence polarization measurements. The exciting light travels along x and is polarised along z. The emitted light is detected along y through a polariser oriented either along z (F_z) or x (F_x). Adapted from Yguerabide, 1972.

The protein solution is excited by fast nanosecond pulses of polarised light, with the resulting fluorescent pulses detected through a polariser oriented first parallel to z, and then parallel to x. Two fluorescent decay curves, denoted $F_z(t)$ and $F_x(t)$, are obtained. The time dependence of these curves is determined by the lifetime of the fluorescent labels, and the rotational motion of the macromolecules (Yguerabide, 1972). The informative quantity obtained from this data is the anisotropy, A(t), defined by:

$$A(t) = \frac{F_z(t) - F_x(t)}{S(t)}$$

where S(t) is defined by:

$$S(t) = F_z(t) + 2F_x(t)$$

The anisotropy depends on the rotational motion of the molecule, and therefore on the rotational correlation time. As already mentioned, the motion of different portions of a molecule with respect to each other can also be detected by fluorescence polarisation. This motion is seen as a fast decaying component in the anisotropy versus time plot. For these studies, the lifetime of the fluorescent chromophore should be of the same order as the rotational correlation time of the motion being observed. If the fluorescence lifetime is much shorter, the rotational

motion will have little effect on the decay of fluorescence intensity (Lakowicz, 1980).

Phosphorescence has been used much less frequently than fluorescence. Rigid media are usually employed due to the normally efficient quenching of the triplet state in fluid solution by dissolved oxygen and other solvent-quenching processes (Saviotti and Galley, 1974). Due to the fact that aromatic amino acids are frequently buried within the globular structure of proteins, phosphorescence from proteins is obtainable in fluid solutions at temperatures where it cannot be observed from free chromophores (Saviotti and Galley, 1974). In the absence of quenching reactions, the phosphorescence lifetime of phosphorescent probes are dependent on the effective viscosity of the medium (Strambini and Gonnelli, 1985). For example, the intrinsic phosphorescence lifetimes of tryptophan residues in proteins reflects in part the local flexibility of the protein matrix. The high sensitivity of this technique, coupled to the long lifetime (millisecond to second) make this approach suitable to reveal distinct conformers of the macromolecule that persist for times longer than the phosphorescence lifetime (Shah and Ludescher, 1995; Cioni et al., 1994). The room temperature tryptophan phosphorescence lifetime has been shown to increase in some proteins following hydrogen-deuterium exchange. Fischer et al. (2000) used this property of phosphorescence to monitor hydrogen-deuterium exchange in *Escherichia coli* alkaline phosphatase as a function of time.

1.2.5.3 Nuclear magnetic resonance

Nuclear magnetic resonance (NMR) is an experimental technique that performs an essential role in the analysis of the internal motions of proteins. It is able to provide information about individual atoms, and is sensitive to both the magnitude and the timescale of the motion. A number of reviews have been written on the use of NMR to determine protein dynamics (Kay, 1997; Williams, 1989; Kay, 1998; Ishima and Torchia, 2000; Wand, 2001). NMR studies were initially limited to the study of molecules with a molecular mass of up to approximately 10 kDa (approximately 100 amino acids). The development of multidimensional, multinuclear solution NMR spectroscopy, and further methodological advances,

has significantly increased the molecular weight limitations previously imposed (Kay, 1997).

NMR parameters, such as nuclear spin-spin coupling constants and chemical shifts, are dependent upon the protein environment. In a protein molecule, different local conformations of the molecule exist, which are able to interconvert. If the interconversion is rapid on the NMR timescale of milliseconds, the NMR spectrum will record only a single, averaged spectrum, rather than separate spectra for each of the various discrete conformations. When the interconversion time in on the order of the NMR timescale or slower, the transition rates can be studied (Brooks et al., 1988). For example, the reorientation rates of the aromatic rings of the tyrosine and phenylalanine residues have been studied by NMR techniques (Brooks et al., 1988; Wagner and Wüthrich, 1978).

The dynamics of specific chemical groups or nuclei can also be determined from the dependence of relaxation parameters on their motion. The time of spin-lattice relaxation, T_1, and spin-spin relaxation, T_2, of magnetic moments of the nuclei, are dependent on the characteristic correlation time, τ, of their motion (Käiväräinen, 1985). The mobility of chemical groups in proteins may also be studied with the use of the Overhauser effect. The Overhauser effect is a result of suppressing the spin-spin interaction between the carbon nuclei, ^{13}C, and the protons of the macromolecule, owing to the saturation of the proton resonance lines by a strong radio-frequency (RF) field. An intensification of the ^{13}C resonance lines is seen. The magnitude of the effect depends on the frequencies of the interacting proton and carbon nuclei, and is therefore a measure of the motions of the molecule. The solution NMR methods for measuring ^{2}H, ^{13}C, and ^{15}N spin relaxation allows the characterisation of backbone and side chain dynamical properties of proteins on picosecond/nanosecond and microsecond/millisecond timescales (Palmer, 1997; Palmer et al., 2001).

1.2.5.4 Electron spin resonance

Electron spin resonance (ESR) enables the characterisation of molecules with unpaired electrons, for example, free radicals and some transition elements. ESR can be thought of as a similar technique to NMR, except that ESR primarily deals with the electron magnetic dipoles, while NMR deals with the nuclear magnetic

dipoles. Paramagnetic molecules possess a net electronic magnetic moment. When an external magnetic field is applied, the magnetic dipoles can align either parallel or antiparallel to the external field, with the former being the lowest energy state. Transitions between the two energy states will occur if the sample is irradiated with electromagnetic waves of the appropriate frequency, corresponding to the energy difference between the antiparallel and parallel states. In practice, the sample is exposed to a constant frequency of a microwave field, and an applied magnetic field is varied with an electromagnet until the resonance condition is satisfied, and transitions occur (Swartz et al., 1972).

Few biological molecules contain unpaired electrons. A common technique to overcome this problem in the application of ESR is the use of spin labels. The spin label contains unpaired electrons, is chemically stable, and is attached to the macromolecule of interest. A spin label ESR spectrum is extremely sensitive to the nature and rate of the motion that the label experiences. One of the more successful compounds used as spin labels to date are the nitroxides (Swartz et al., 1972).

The ESR spectra of all nitroxyl radicals are triplets. The width of the lines, and their location on the magnetic field axis, will depend on the averaged anisotropy of the g-factor, and on the hyperfine interaction between the magnetic moments of the lone electron and the nitrogen nucleus (Käiväräinen, 1985). The g-factor is the local magnetic field produced by the molecule that contains the unpaired electron (Franks, 1988). The nitroxide ESR spectra are very sensitive to the rate of its molecular rotation, covering a range of correlation times from 10^{-10}s, where a spectrum of three narrow lines of approximately equal width is observed, to 10^{-7}s, where a strongly immobilized spin label spectrum is observed. Therefore, if a spin label is rigidly attached to a particular part of a macromolecule, the dynamic motion of that region of the molecule may be studied by the observed parameters of the ESR spectrum (Morrisett, 1976). The tumbling of the protein in solution is too slow to have any significant effect on the spin label's spectrum, therefore the degree of immobilization, and hence the ESR spectrum, depends on the flexibility of the protein at the point of attachment.

1.2.5.5 X-ray diffraction

It is sometimes believed that X-ray crystallography is a static technique incapable of providing information about the dynamic properties of molecules. X-ray diffraction can in fact provide information about the amplitudes of the motions found in proteins. Discrete positions of electron density for the various atoms in a molecule are not observed in X-ray crystal structures. The electron density of any atom in a structure is a time average of the position of that atom in every unit cell in the crystal (static disorder), and also of the possible positions that the atom can sample during the diffraction experiment due to its motion (Ringe and Petsko, 1986).

For small molecule X-ray diffraction, detailed models have been introduced to take account of the anisotropic and anharmonic motions of the atoms, and then applied to high-resolution measurements. In protein crystallography, the available data is limited compared to the large number of parameters that have to be determined, and has made it necessary in most cases to assume that the atomic motions are isotropic and harmonic (Brooks et al., 1988). Based on this assumption the structure factor, F(Q), which is related to the measured intensity by $I(Q) = |F(Q)|^2$, is given by:

$$F(Q) = \sum_{j=1}^{N} f_j(Q) e^{iQ.\langle rj \rangle} e^{Wj(Q)}$$

where Q is the scattering vector, N is the number of atoms in the asymmetric unit of the crystal, and $\langle r_j \rangle$ is the average position of atom j, with atomic scattering factor, $f_j(Q)$, and Debye-Waller factor, $W_j(Q)$. The Debye-Waller factor is defined by:

$$W_j(Q) = -8/3\pi^2 \langle \Delta r_j^2 \rangle s^2 = -B_j s^2$$

where $s = |Q|/4\pi$. The quantity B_j is usually referred to as the temperature factor, which is directly related to the mean-square atomic fluctuations in the isotropic harmonic model.

In theory, temperature factors can then provide information on the motions of all heavy atoms in the molecule, due to their relationship to the mean-square displacement of the atom. In practice though, there is a difficulty in relating the

B-factors obtained from the protein structure refinement, to the motion of the atom. This is because as well as thermal motions, any static disorder in the crystal will also contribute to the calculated B-factors. For the protein myoglobin, the contribution of static disorder to the temperature factor was estimated by comparing the mean-square displacement calculated from the X-ray study, to the mean-square displacement of the iron atom determined from Mössbauer studies. The Mössbauer effect is not affected by static disorder, and so only dynamical processes contribute to the calculated mean-square displacement. The static disorder contribution to the mean-square displacement of the iron atom was determined to be approximately 0.08 Å. This indicated that the observed values from X-ray diffraction, which are on the order of approximately 0.4 to 0.5 Å, are dominated by the motional contribution (Brooks et al., 1988).

The technique of X-ray diffraction has been applied to the dynamic studies of a number of proteins, for example, lysozyme (Artymiuk et al., 1979). The effect of temperature on protein structure and dynamics has also been investigated by this technique, for example, with metmyoglobin (Frauenfelder et al., 1979; Frauenfelder et al., 1987), and ribonuclease-A (Tilton et al., 1992).

1.2.5.6 Neutron scattering and diffraction techniques

Neutron scattering studies are able to provide valuable information in the space- and time-dependency of the molecular motions in a protein sample in the range of 5 to 50 Å and 10^{-13} to 10^{-7} s, respectively. The main theory of neutron scattering is discussed in Section 3.4. The effect of hydration and temperature on the dynamics of a number of proteins has been studied by neutron scattering (Doster et al., 1989; Cusack and Doster, 1990; Loncharich and Brooks, 1990; Filabozzi et al., 1996; Zanotti et al., 1997).

Neutron diffraction of crystalline proteins is also a useful technique in the study of protein structure and dynamics (Kossiakoff, 1982, 1985 and 1986). Neutron diffraction is very similar to X-ray diffraction, in both the experimental methodology and the information that is obtained. However, neutron diffraction has the unique ability to locate the positions of the hydrogen or deuterium atoms in large molecules (Gutberlet et al., 2001). Neutron diffraction is also able to distinguish between hydrogen and deuterium atoms, as hydrogen is one of the few

atoms whose nucleus induces a phase change of 180° in the scattered neutrons. The position of a hydrogen atom is seen as a negative peak in the neutron density map, whereas positive peaks represent most other atoms.

Two applications of neutron diffraction have been used to study protein conformational dynamics. The first is the assignment of the configuration of terminal methyl groups. The methyl conformation has been used to study 'protein breathing', which is defined as the set of motions involving a transient local redistribution of the packing density in the interior or at the surface of the protein (Kossiakoff, 1985). From X-ray diffraction studies, it has been shown that proteins are typically more flexible at their surfaces than in their interior. The fact that the interior groups appear more ordered does not exclude the possibility that they undergo rapid reorientations. The presence of rapid motions in the protein interior has been confirmed by NMR studies, which showed the rapid rotation of terminal methyl groups (Lipari et al., 1982). The determination of methyl conformations by neutron diffraction allows the investigation of the forces imposed by the protein structure on the methyl group, and how these forces compete with the torsional forces of the side chain.

The second approach uses neutron diffraction combined with the hydrogen-deuterium (H/D) exchange technique (Kossiakoff, 1982). This technique is used to investigate the extent and nature of the inherent conformational fluctuations in a protein. The advantage of using neutron diffraction to detect exchange is that the location of the exchange site in the protein is known, and the exchange status of a particular site is easily characterised from inspection of the neutron density map.

1.3 Effect of Temperature on Catalysis

As with most chemical catalysts, the rate of an enzyme catalysed reaction increases with temperature (Copeland, 2000). The effect of temperature on catalysis is best shown by an Arrhenius plot, which is a plot of log v against 1/T, where v is the measured rate of the catalysed reaction, and T is the absolute temperature. To be able to interpret such a plot, it is necessary to understand the

reaction rate theories that it is derived from. In 1889 Svante Arrhenius suggested that the effect of temperature on a rate constant, k, could be described by:

$$\frac{d\ln k}{dT} = \frac{E_A}{RT^2}$$

where E_A is the energy of activation and R is the ideal gas constant. If E_A does not vary with temperature, this gives upon integration:

$$\ln k = -E_A/RT - \ln A$$

where ln A is the constant of integration. The Arrhenius equation has been shown by experiment to give a close approximation for the effect of temperature on the rate constant. Reaction rate theories were then developed to try and explain the temperature dependence of reaction rates (Moore, 1983).

For any chemical reaction, the step in which the "intermediate" with the highest free energy occurs determines the overall rate of the reaction. This high-energy intermediate is known as the transition state. The transition state theory states that the rate of any reaction at a given temperature is dependent only on the concentration of an energy-rich activated complex, which is in equilibrium with the ground state reactants (Creighton, 1993). According to this theory, all activated complexes break down at a rate given by $\kappa k_B T/h$, where k_B is the Boltzmann constant (the gas constant per molecule), h is Planck's constant, T is the absolute temperature, and κ is the transition coefficient which is assumed to be unity. Thus the reaction velocity constant, k, is given by:

$$k = \frac{\kappa k_B T K^*}{h}$$

where K* is the equilibrium constant between the activated complex and the unactivated molecules or reactants. The usual thermodynamic equations can be applied to this equilibrium, so that:

$$\Delta G^* = \Delta H - T\Delta S^* = -RT\ln K^*$$

$$\Rightarrow k = \frac{k_B T e^{-\Delta G^*/RT}}{h} = \frac{k_B T e^{-\Delta H^*/RT}\, e^{\Delta S^*/R}}{h}$$

where ΔG^*, ΔH^*, and ΔS^* represent the free energy , enthalpy, and entropy of activation, respectively. If it is assumed that ΔS^* does not vary with temperature, this gives the following relationship:

$$\frac{d\ln k}{dT} = \frac{1}{T} + \frac{\Delta H^*}{RT^2} = \frac{\Delta H^* + RT}{RT^2}$$

This is similar to the empirical Arrhenius equation, shown earlier:

$$\frac{d\ln k}{dT} = \frac{E_A}{RT^2}$$

The energy of activation of the Arrhenius theory and the enthalpy of activation from the theory of absolute reaction rates can be related as:

$$E_A = \Delta H^* + RT$$

It can be seen from the above equations that the rate constant, k, will decrease at low temperatures according to the activation energy, E_A. So a plot of log k against 1/T can be expected to give a linear graph with the slope related to the energy of activation (Dixon and Webb, 1979).

For enzyme catalysed reactions the measured rate and its relationship to the rate constant of the reaction may be quite complex. In the simplest case the enzyme reacts with the substrate with the formation of only a single intermediate. The rate of the enzyme catalysed reaction will then be a measure of the rate constant for the determining step in the reaction pathway. In many cases though there are in fact two or more intermediates involved in the reaction, and the measured rate of reaction will then be a complex function of several rate constants.

For enzyme catalysed reactions a linear fit to an Arrhenius plot is not always observed. Some departures from linearity are due to changes in experimental conditions (Dixon and Webb, 1979; Laidler and Peterman, 1979). For an enzyme to be optimally active, groups in the active site that are involved in substrate binding and catalysis must be in the correct ionisation state. Also groups involved in electrostatic interactions that help to maintain the enzyme in its active conformation must also be considered. If these groups have a significant heat of ionisation, the ionic state of the enzyme will vary with temperature. This means that the optimum pH and substrate binding affinity may change with temperature.

Significant distortions of Arrhenius plots can occur if rate measurements are made at a single substrate concentration, as changes in the Michaelis constant, K_M, and possible substrate inhibition will affect the observed temperature dependency of the reaction rate (Silvius et al., 1978). To avoid complications due to changes in K_M, the maximal rate of the reaction should be obtained by extrapolation of a Lineweaver-Burk or equivalent plot at each temperature.

Another experimental factor that may affect the enzyme rate of reaction is the change in solvent properties with temperature. For example the dielectric constant of the solution will change with temperature and may have an effect on the energy of activation of the reaction. The pH of any buffers present in the system will also vary with temperature and unless steps are taken to maintain the pH near the optimum a reduction in activity not due to temperature effects will be seen. Some enzyme reactions may be diffusion controlled, and in such cases the activity could decrease in proportion to increasing viscosity (as a function of 1/T) as the temperature is reduced (Douzou, 1974). But since few enzymes are diffusion limited, and as reaction rates usually drop faster with temperature than the viscosity increases, this is not usually a problem. For example, the enzyme xylanase was found to have a turnover number at 0°C of approximately one molecule of substrate converted every second per molecule of enzyme, with the rate of reaction decreasing by at least five orders of magnitude upon decreasing the assay temperature to –70°C (Dunn, 1998). In comparison, the increase in viscosity of a cryosolvent solution, for example, 40% ethylene glycol/20% methanol/40% water, was determined to increase only 28-fold over a similar temperature range (Douzou et al., 1976). Changes in solution conditions that affect the activity of enzymes that are more relevant to organic solvent-water solutions are discussed more thoroughly in Chapter Three.

Once the experimental artifacts have been minimised and corrected, there still remain departures from linearity in the Arrhenius plots for some enzyme catalysed reactions. A difficulty that is encountered in studying departures from linearity is establishing whether the plot contains an abrupt change of slope or discontinuity, or just a sharp bend or curvature (Londesborough, 1980; Bagnall and Wolfe,

1982). Usually the error in such experiments makes it impossible to distinguish between the two possible models.

As mentioned earlier the rate of an enzyme reaction may in fact be dependent upon several rate constants from the various steps in the reaction. A curve or bend in the Arrhenius plot may be seen as the various rate constants may have different enthalpies of activation or temperature dependencies (Londesborough and Varimo, 1979; Londesborough, 1980). It should be noted that when deriving the relationship between the rate constant and temperature it was assumed that the entropy of activation, ΔS^*, did not vary with temperature. This may not actually be true over a wide temperature range, and so a departure from linearity would be observed.

A break in an Arrhenius plot indicates a change in the enthalpy of activation for the reaction at the transition temperature. Various theories have been proposed to account for such discontinuities. From studies with the enzyme urease, Kistiakowsky and Lumry (1949) proposed that the sulfite used as a mild reducer caused reversible inactivation of the enzyme, which lead to a discontinuity in the Arrhenius plot. The plot gives two straight lines corresponding to when the enzyme is mainly in either the active or inactive form, with the difference in enthalpy of activation between the two slopes equal to the heat change of the conversion of one form to another. Maier et al. (1955) gave a similar proposal to explain the deviation from Arrhenius behaviour observed for phosphatase- and peroxidase-catalysed reactions, at low temperature. They suggested that a reversible equilibrium between active and inactive enzyme, due to an increase in intramolecular hydrogen bonding at low temperatures, was responsible for the discontinuity in behaviour. A variation to this theory is to assume that the enzyme exists in two forms of differing activities, which are in equilibrium with one another (Massey, 1953). A similar conclusion was reached from studies of the enzyme tryptophan synthase (Fan et al., 2000). The results indicated that the nonlinear Arrhenius plots were caused by a temperature-dependent conformational change that preceded the rate-limiting step in catalysis. Enzymes that utilise hydrogen tunneling as part of the catalytic mechanism are also not

expected to demonstrate linear Arrhenius plots (Kohen et al., 1999; Kohen and Klinman, 1998).

In the present study it is proposed that if at some temperature a particular dynamical aspect of the protein that is required for catalysis ceases, this will be reflected in the temperature dependence of the catalytic rate. The resulting cessation of activity will produce an obvious change of slope in any Arrhenius plot, as the enzyme is effectively being converted to an inactive form at the temperature at which the necessary motion ceases. It is thought that such a transition would be easily distinguishable from a possible curvature in the Arrhenius plot.

Chapter Two

Properties of Cryosolvents

2.1 Introduction

To enable the study of enzyme catalysis below 0°C, it is necessary to prevent the freezing that would occur in aqueous solutions. Therefore, in the current cryoenzymology and dynamic studies, cryosolvents are used for collecting solution data at subzero temperatures. Obviously, there is a difference between the solution properties of cryosolvents and aqueous solutions, which are the native environments for most enzymes. To determine what effects the cryosolvents are having on the measured enzyme properties, it is necessary to have an understanding of the properties of the cryosolvents themselves. For example, if a change in an enzyme's properties is seen at a particular temperature, it is not initially known if this reflects an intrinsic property of the enzyme, or an effect of the solvent. Studying the temperature effects on solvent properties, as well as on the enzyme, enables the distinction between protein-solvent interactions, and the inherent properties of the enzyme.

The purpose of this chapter is to investigate the change in cryosolvent properties with temperature, particularly phase changes, for example, melting and crystallisation. For the cryoenzymology and dynamic work, cryosolvents that remain homogeneous and fluid over the whole temperature range used are required. For cryosolvents that do undergo phase changes, it is important to know at what temperature this occurs, so that any potential influence on the results can be determined. This knowledge assists in choosing which cryosolvent to use over a particular temperature range, if phase changes in the solution are to be avoided.

I was involved in the DMTA experiments and most of the DSC experiments mentioned in this chapter. Other members of the research group conducted the X-ray scattering experiments and visual assessment of cryosolvents.

2.2 Properties of Cryosolvents

Cryosolvents are any solvent system that remains fluid at subzero temperatures. In this work, cryosolvents based on an aqueous system (≥ 20% water) with a miscible cosolvent are used. Commonly used cosolvents include: alcohols, for example methanol and ethanol; polyols, for example ethylene glycol and glycerol; and dimethylformamide(DMF) and dimethyl sulfoxide (DMSO). Although binary solvent systems are commonly used, for polyol-containing solutions, ternary solvent systems, made up of water, the polyol and an alcohol in various proportions, are used to reduce the high viscosity that is inherent in polyol-water binary systems (Douzou, 1977).

When miscible organic solvents are mixed with water they cause considerable perturbations of the physiochemical properties of water. The parameters that are modified by the presence of an organic solvent include the dielectric constant, the viscosity, and the ionic content, or dissociation of electrolytes. These parameters will be discussed below, as well as their dependence upon temperature.

The viscosity of a solution increases with decreasing temperature. This is important as it influences the rate of diffusion in solution and also because of technical problems associated with mixing viscous solutions. It has been suggested that the limiting value for the correct mixing of reactants by conventional techniques is 50 cP (Douzou, 1977). Generally alcohol and DMF-based cryosolvents have relatively low viscosities, and do not cause problems until near their freezing points. For example, the viscosity of a 70% methanol/water solution is 50 cP at –60°C, which gives a wide temperature range over which viscosity does not impede mixing (Douzou et al., 1976). It should be noted that as solutions approach their freezing point, the viscosity could increase dramatically, for example, for 70% methanol/30% water the viscosity increases to 280 cP at –80°C, five degrees above the freezing point (Douzou, 1971). DMSO solutions at low concentrations do not present any problems, but at concentrations greater than 50% (v/v), and at temperatures below –50°C, they become significantly viscous. Polyol-based cryosolvents have high viscosities even at relatively high temperatures; for example, a 50% (v/v) ethylene glycol/water solution has a viscosity greater than 100 cP at only –20°C (Douzou, 1971). For

this reason, as mentioned above, polyols are generally used in ternary solutions with an alcohol component to reduce the viscosity.

As stated earlier, the viscosity of a solution also affects diffusion. The effect of viscosity on diffusion is given by:

$$D = \frac{RT}{6\pi r N_A \eta}$$

where D is the diffusion coefficient of the diffusing species, R is the gas constant, T is the temperature, N_A is Avagadro's number, η is the viscosity of the solution, and r is the hydrodynamic radius of the diffusing species (Barrow, 1979). A high viscosity may cause problems with diffusion-limited enzymes, for example, triose phosphate isomerase. It has been suggested that the diffusion-controlled encounter frequency of an enzyme and a substrate is about 10^9 $M^{-1}s^{-1}$. The k_{cat}/K_M ratio of triose phosphate isomerase is between 10^8 and 10^9 $M^{-1}s^{-1}$, and so the reaction is limited by the rate of diffusion (Fersht, 1985).

The addition of organic solvents to water also causes changes to the dielectric constant. The dielectric constant influences electrostatic interactions, which are important in processes such as dissociation and solubility of molecules, and acid-base equilibria. The magnitude of the electrostatic force between two charged species, Q_1 and Q_2, separated by a distance, r, is given by Coulomb's Law as:

$$F = \frac{Q_1 Q_2}{4\pi\varepsilon_0\varepsilon_r r^2}$$

where ε_r is the dielectric constant of the medium, and ε_0 is the permittivity of a vacuum (Moore, 1983). As can be seen from the above equation, a high dielectric constant facilitates the separation of ions, as there is a reduced electrostatic force. The dielectric constant, also known as the electrical permittivity, is actually a measure of the interaction of atoms and molecules with an applied electric field. Water is a highly dipolar molecule, and the interaction of single molecules with the electric field is increased by the formation of extended structures due to hydrogen-bonding between the molecules. The dielectric constant of pure water at 20°C is 80. When organic solvents are added to water a decrease in the dielectric constant is generally seen, which increases with increasing organic solvent concentration. This can be thought of as a disruption of the oriented

structure of water by the organic solvent molecules. Different solvents affect the dielectric constant to different degrees; for example, methanol has a marked effect with increasing concentration, whereas DMF and polyols give a less pronounced effect. For DMSO, the dielectric constant for a 50% (v/v) solution at room temperature is 76, very close to the value of pure water (Travers and Douzou, 1974). This is quite different to most solvents, which usually cause a decrease in the dielectric constant of 10 to 30 units at a similar concentration. The variation in dielectric constant with temperature has been shown to increase with temperature according to the function:

$$\log D = a - bT$$

where a and b are empirical constants, and T is the absolute temperature (Akerlöf, 1932). Most of the mixed solvents become isodielectric with water far above their freezing points.

The ionic environment will also change, as the addition of organic solvent will affect the ionisation and solubility of solutes or electrolytes. The effect of organic solvents on proteins, which are also electrolytes, shall be discussed in the following chapter. The ionic strength of a solution is important as it influences electrostatic interactions. The effective interaction between a pair of ions is weakened as the ionic strength increases. This is due to the tendency of salts to cluster around any given ion of opposite charge, reducing the net field in the vicinity of the ion (Brooks et al., 1988). Neutral salts, such as sodium chloride and potassium chloride, are soluble to a concentration of approximately 0.1 M in cooled cryosolvents with an organic solvent composition of 50% (v/v) or greater. Higher ionic strengths can be obtained using potassium iodide, which is soluble up to concentrations of approximately 0.2 M (Fink and Geeves, 1979). If higher concentrations are used, 0.2 M to 3 M, a separation of the two phases can occur, with crystallisation of the aqueous phase (Douzou, 1977). It has been shown that strong electrolytes, such as sodium chloride and hydrochloric acid, are still completely dissociated at low temperatures in mixtures with high cosolvent concentrations.

For weak electrolytes, such as buffer salts, solubility is also a problem. Generally concentrations greater than 10 mM will precipitate as the temperature is lowered.

Two of the most commonly used buffers, phosphate and Tris, are the least soluble. At a concentration of 10 mM, phosphate buffer precipitates at –60°C in 70% (v/v) methanol, and in the presence of a high concentration of proteins or other solutes, can precipitate at higher temperatures. Phosphate can be replaced with cacodylate, which was found to be soluble over the whole temperature range in all the mixtures studied, up to a concentration of 0.1 M (Hui Bon Hoa and Douzou, 1973). Chloroacetate and acetate buffers also have a reasonable solubility in cryosolvents.

Unlike strong electrolytes, weak electrolytes are not completely dissociated, and the equilibrium position for dissociation will be shifted by the presence of the organic solvent. For buffers containing weak electrolytes, the acid-base equilibria will be shifted causing a shift in the pK_a of the buffer. The decreased dielectric constant, due to the addition of organic solvent, increases the amount of work required to separate ions, for example, to ionise an uncharged acid. This leads to a corresponding increase in pK_a values. However, it has been shown that the change in dissociation constant of an acid in two cryosolvents, with the same dielectric constant, was different. This indicates that although electrostatic forces may be involved, nonelectrostatic effects related to specific solvent compositions are also important (Douzou, 1971). Another factor may be that the dielectric constant of the microenvironment around the ions, may be different to that of the bulk dielectric constant measured for the solution.

For buffers in aqueous-organic solvent mixtures, the conventional pH scale is no longer appropriate, and so it is necessary to define a new scale with which to measure the 'pH'. The apparent pH, pa_H (also represented at pa_H* or pH*), which is -log $a^*(H^+)$, where $a^*(H^+)$ is the proton activity in the mixed solvent, is the most useful way of defining a new 'pH' scale. As the activity coefficient of the proton will vary with different solvent systems, each cryosolvent will have its own pa_H scale. The pa_H values vary with both temperature and cosolvent concentration.

There are several methods for measuring pa_H. A conventional pH meter with a glass electrode, equilibrated with the aqueous-organic solvent solution to be measured, can be used to give a direct estimate of pa_H. A modified electrode, in

which the electrolyte solution of the glass electrode is replaced with 0.1 M hydrochloric acid in the cryosolvent, gives a more accurate method for determining the pa_H at any temperature at which the cryosolvent is fluid. Another method, which is more indirect, uses the spectrophotometry of indicators to determine the proton activity at a particular temperature.

A substantial amount of work has previously been done on determining the effect of temperature and cosolvent on the dissociation constants of a variety of buffers (Douzou et al., 1976). For most buffer systems studied an increase in pa_H, between 0.1 to 0.3 pa_H units, was seen upon addition of varying amounts of different cosolvents. The change in dissociation with temperature in aqueous-organic solutions is similar to that in aqueous solutions, with a linear change with respect to the reciprocal of the absolute temperature. Both equimolar and non-equimolar buffers show the same behaviour, indicating that buffering capacity is maintained (Douzou, 1971; Douzou, 1977).

2.3 Differential Scanning Calorimetry

Differential scanning calorimetry (DSC) is a technique in which the difference in heat flow (power) to a sample and reference is monitored against time or temperature, while the temperature of the sample, in a specified atmosphere, is programmed. In heat flux DSC, the sample and reference are heated from the same source and the temperature difference, ΔT, is measured. The temperature difference is proportional to the difference in heat flow (from the furnace), between the two materials (Haines and Wilburn, 1995). The heat flux DSC measures the exothermic and endothermic reactions of the sample, and also heat capacity.

When heat is absorbed by a system (in this case the sample) under specified conditions, the heat capacity of the system changes. At constant pressure this is represented by a change in enthalpy, H. The amount of heat that is absorbed by an unreacting system in raising the temperature by 1 K at constant pressure is defined as the heat capacity at constant pressure, C_P, which is also a function of temperature.

$$C_P = (\partial H/\partial T)_P$$

If the heat capacity at constant pressure is known, the change in enthalpy with a change in temperature, T, at constant pressure can be calculated (Moore, 1983).

$$\Delta H = \int_{T1}^{T2} (\partial H/\partial T)_P dT = \int_{T1}^{T2} C_P.dT$$

For pure substances, changes such as fusion of a solid, or change of a solid from one crystal structure to another are called phase changes. These occur at a definite temperature and with a definite value of change of enthalpy, ΔH.

A first-order thermodynamic transition, such as fusion, results in a change in enthalpy, and results in a peak in the DSC curve. The area under the peak is proportional to the change in enthalpy. A second-order thermodynamic transition involves changes in properties such as heat capacity and compressibility, and does not involve changes in enthalpy (Andrews, 1971). These are shown in the DSC curve as a step in the baseline, and an increase ΔC_P. A glass transition resembles a second-order thermodynamic transition as it is also characterized by a shift in the baseline. At the glass transition temperature, T_g, the heat capacity of the sample increases as it becomes more flexible. However, unlike true second-order thermodynamic transitions, which always occur over a fixed, equilibrium temperature range, the value obtained for T_g always depends on the heating and cooling rates used in the DSC run. The glass transition is purely a kinetic or relaxation process that results when the supercooling of the liquid falls out of internal thermodynamic equilibrium as a result of a dramatic increase in structural relaxation times (Haines and Wilburn, 1995).

Sometimes an associated endotherm is also seen at the glass transition, as is shown in Figure 2.1, which is due to the enthalpy of relaxation. This is associated with the gradual approach of the non-equilibrium properties of the glass towards the extrapolated equilibrium value characteristic of the liquid (Hay, 1992). With aged glasses the endotherm increases progressively with the annealing time, as the enthalpy of the glass slowly approaches the extrapolated liquid value. The magnitude of the endotherm can also be affected by the relative rates of heating and cooling. For example, if a sample is cooled slowly and goes through the T_g at

say 80°C, and is then heated rapidly it may not transform until 85°C. The sample must absorb more energy to reach the enthalpy of the rubbery state, and results in an endotherm superimposed on the glass transition step (Haines and Wilburn, 1995).

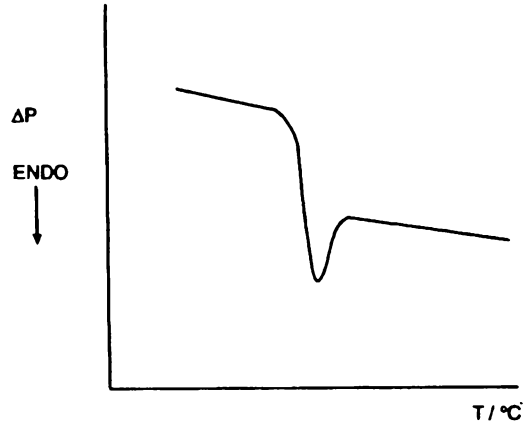

Figure 2.1. DSC curve showing an endotherm, proportional to the enthalpy of relaxation, superimposed on the shift in baseline, due to a change in heat capacity, at the glass transition.

2.4 Dynamic Mechanical Thermal Analysis

Dynamic mechanical thermal analysis (DMTA) is a technique that quantitatively measures the changes in the mechanical behaviour of a material, as a function of temperature, frequency, time, stress, or combinations of these parameters. Molecular motion and physical morphology determine the dynamic modulus (stiffness) and damping (loss).

If a sample is subjected to a force, it may behave in a variety of ways. Liquids will flow when a force is applied, and some solids may deform elastically, returning to their former shape and size when the force is removed. Other solids may behave viscoelastically, incorporating both flow and elastic deformations. When a stress is applied to a sample, the resulting deformation is measured by the strain, which is simply the deformation per unit dimension. For an elastic material the strain is proportional to the stress, the constant being the modulus. For example, the tensile, or Young's modulus is given by:

$$E = \sigma/\varepsilon$$

where E is the tensile modulus, ε is the tensile strain and σ is the normal tensile stress. For an ideal elastic material the deformations are reversible. If there is any viscoelasticity, however, the moduli become more complex and contain two parts. For example, the complex tensile modulus, E*, is given by:

$$E^* = E' + iE''$$

where E' is the real component, or storage modulus, E'' is the imaginary component, or loss modulus, and i is equal to $\sqrt{-1}$. The Argand diagram, in Figure 2.2, best shows the relationship between these quantities.

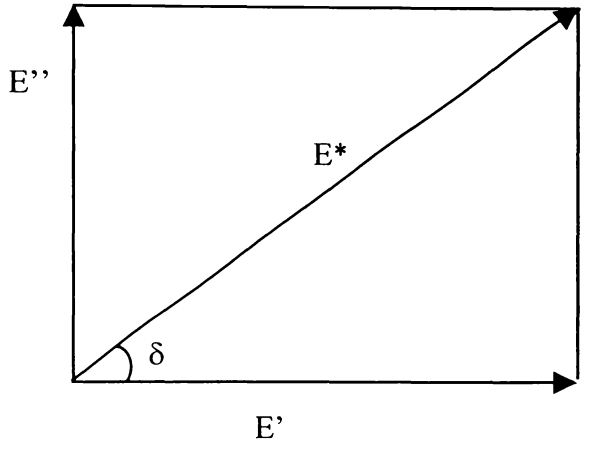

Figure 2.2. An Argand diagram showing the relationship between the storage modulus, E', and the loss modulus, E''.

The ratio of these two moduli gives the loss tangent, tan δ, which is given by:

$$\tan \delta = E''/E'$$

and is the ratio of the energy lost/energy stored per deformation cycle (Reading and Haines, 1995).

In DMTA a sinusoidal stress (σ) is applied to the sample, to produce a sinusoidal strain response (ε), which lags by some phase angle (δ) due to the viscoelastic behaviour of the sample. This is represented in Figure 2.3.

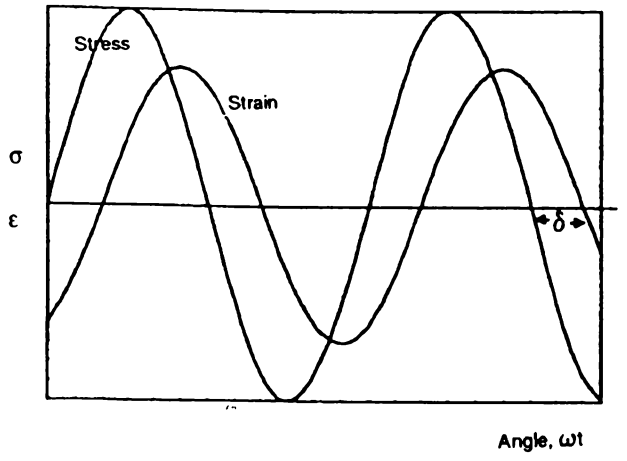

Figure 2.3. This diagram illustrates the sinusoidal stress (σ) with the strain response (ε), lagging by some phase angle (δ).

The values of the moduli will change with temperature as the molecular motions of the sample change. The tan δ exhibits a series of peaks as the temperature of the sample is increased, each peak corresponding to a specific relaxation process. Chain and side-chain motions of polymers and especially glass transitions will affect the moduli and tan δ. An increase in the frequency of the applied stress will show a shift of the moduli and tan δ to higher temperatures. The DMTA technique is a sensitive technique, particularly for determining glass transition temperatures, which give rise to a pronounced maximum in tan δ. For this reason it complements the DSC technique very well, where glass transitions are not as obvious.

2.5 Methods and Materials

2.5.1 Materials

For all cryosolvent solutions, the water was obtained from a Milli-Q (MQ) Water Purification System (Millipore). All solvents were of analytical grade and used without further purification, with the methanol supplied from BDH, the ethylene glycol supplied from Lancaster, and the glycerol obtained from FSA Lab Supplies. All deuterated reagents were obtained from Sigma. All solvent percentages are given by volume.

2.5.2 Differential Scanning Calorimetry

The differential scanning calorimetry (DSC) measurements were made using a Shimadzu DSC-60 differential scanning calorimeter, at the Thermal Methods Laboratory, Birkbeck College, London. The samples were sealed in 30 μl aluminium crucibles, with sample weights between 9 and 12 mg. An integrated device that is filled with liquid nitrogen cooled the samples to at least –140°C. Helium was used as a purge gas of the sample due to the low temperatures that were being used. All data were collected during heating at a standard rate of 10°C/minute. All solvent samples were prepared by individually dispensing each component to avoid errors due to changes in volume upon mixing. An empty crucible was used as the reference. Temperature calibration of the instrument was performed by the use of water and ammonium phosphate ($NH_4H_2PO_4$) standards, which are known to undergo reversible phase transitions at 0°C and –125°C, respectively. The peak area of the instrument was calibrated with an indium standard. In the DSC plots endothermic transitions give a downward 'peak', while exothermic transitions give an upward 'peak'.

The following hydrogenated solvents were run:

35% methanol/35% ethylene glycol/30% water;

40% methanol/40% ethylene glycol/20% water;

60% ethylene glycol/40% water;

70% ethylene glycol/30% water;

60% glycerol/40% water;

70% glycerol/30% water;

70% methanol/30% water;

and 70% methanol/10% ethylene glycol/20% water.

The following perdeuterated solvents were run:

40% CD_3OD/60% D_2O;

70% CD_3OD/30% D_2O;

40% DMSO/60% D_2O;

and 80% DMSO/20% D_2O.

Further cryosolvent samples were also run. The details can be found in the paper by Réat et al. (2000b), included in Appendix A.

2.5.3 DMTA

The dynamic mechanical thermal analysis measurements were carried out on a Rheometric Scientific DMTA MkIII analyser, at the Thermal Methods Laboratory, Birkbeck College, London. The samples were placed between stainless steel plates, which were then wrapped in aluminium foil to assist in sample retention between the plates. The samples are cooled to approximately -100°C, by liquid nitrogen gas, and then heated at a rate of 3°C/minute to approximately 100°C, with a sample taken every 4 seconds. The samples were generally placed in a small frame (clamp frame L, clamp C), with a length of 5 mm, width of 10 mm, and a thickness of 1 mm. A bending mode, with single cantilever geometry, was used to analyse the samples. A sinusoidal stress, with a frequency of 1 Hz, was applied to the sample.

The following solvent compositions were run:

35% methanol/35 % ethylene glycol/30% water;

70% methanol/10% ethylene glycol/20% water;

60% ethylene glycol/40% water;

and 70% methanol/30% water.

2.5.4 X-Ray Scattering

X-ray scattering experiments on the cryosolvents were carried out in Debye-Scherrer geometry on line 9.1 at the Daresbury synchrotron radiation source, UK, using a curved image-plate detector system. The samples were in standard 0.7 mm thin-walled glass capillary tubes. The presence of crystallisation was identified by the appearance of powder diffraction peaks. For full method details refer to the paper by Réat et al. (2000b), in Appendix A.

2.6 Results and Discussion

2.6.1 Initial Selection of Cryosolvents

A preliminary screening of a wide range of cryosolvents was conducted to determine their homogeneity and lack of phase separation at low temperatures (Réat et al, 2000b). A visual assessment of the cryosolvents was made to confirm the homogeneity of the solution to below –120°C. The cryosolvents that passed this initial assessment were then subjected to X-ray diffraction studies down to -160°C, to determine at what temperature, if detected, crystallisation occurred. Another important consideration is the viscosity of the solution as the temperature is decreased. It is important that the solution remains fluid enough to allow efficient mixing of the enzyme assays at the assay temperature. From these initial criteria, cryosolvents were chosen to then undergo further characterisation by DSC and DMTA.

2.6.2 Differential Scanning Calorimetry

Cryosolvents that exhibited no phase separation or crystallisation to below -120°C, and that maintained a low to moderate viscosity were selected for DSC studies, as detailed above. Cryosolvents based on methanol:ethylene glycol:water and methanol:glycerol:water, were the only solutions to satisfy these requirements. Variations on the methanol:ethylene glycol:water solvent ratios were studied by DSC (Réat et al., 2000b). These included: 70% methanol/30% water; 80% methanol/20% water; 75% methanol/5% ethylene glycol/20% water; 60% methanol/10% ethylene glycol/30% water; and 70% methanol/10% ethylene glycol/20% water. The resulting DSC curves can be found in the copy of the paper included in Appendix A. The majority of cryosolvents tested showed exothermic or endothermic changes characteristic of phase changes near -110°C. The only exception to this was 70% methanol/10% ethylene glycol/20%water, which was free of thermal transitions down to the lowest temperature measured, -160°C.

After this first series of experiments, the selection criteria was broadened to include cryosolvents that were homogeneous and relatively fluid to temperatures

as low as only -100°C. The cryosolvents that met this criteria include: 35% methanol/35% ethylene glycol/30% water; 40% methanol/40% ethylene glycol/20% water; 60% ethylene glycol/40% water; 70% ethylene glycol/30% water; 60% glycerol/40% water; and 70% glycerol/30% water (Daniel, personal communication). The DSC results for these cryosolvents are shown in Figures 2.4 to 2.9.

All of the cryosolvents exhibited an endothermic transition over the temperature range investigated. The binary glycerol/water solutions showed transitions near -100°C (Figure 2.8 and 2.9). Due to the shift in baseline that occurs at this transition, it is likely that this represents a glass transition. These results are in agreement with those of Chang and Baust (1991). They found that above 65% (w/w) glycerol, or approximately 60% (v/v), the solution could be readily vitrified during cooling and returned to the liquid state without experiencing devitrification, so that only glass transition thermal events occur.

The binary ethylene glycol/water solutions showed transitions near -120°C (Figure 2.6 and 2.7). The transitions observed near -50°C were not reproducible for the 70% ethylene glycol/30% water solution, and that observed for 60% ethylene glycol/40% water was due to ice formation on the outside of the sample pan. While the nature of the transitions seen at -120°C has not been conclusively determined, it may be that these also represent glass transitions in the solutions. Murthy (1998) conducted experiments into the characterisation of the equilibrium phase diagram for ethylene glycol/water solutions, and also studied the effect of composition on the temperature of the glass transition, T_g. The values for T_g were approximately -123°C and -121°C for 60% and 70% ethylene glycol, respectively.

The ternary solvent systems of methanol/ethylene glycol/water, exhibited endothermic transitions at lower temperatures than for the binary solutions (Figure 2.4 and 2.5). The temperatures of the transitions were approximately -134°C and -127°C for 35% methanol/35% ethylene glycol/30% water and 40% methanol/40% ethylene glycol/20% water, respectively.

The DSC results show that these cryosolvents can be used to at least -100°C without undergoing phase changes.

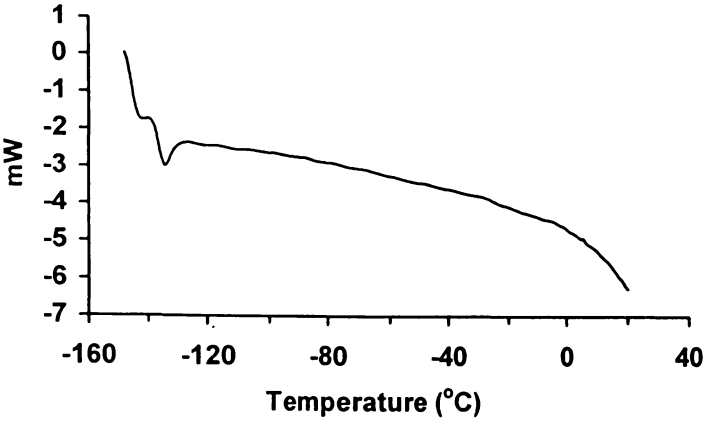

Figure 2.4. DSC curve for 35% methanol/35% ethylene glycol/30% water.

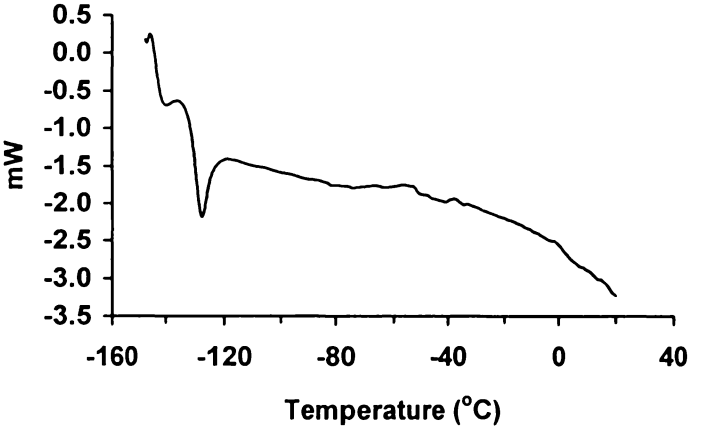

Figure 2.5. DSC curve for 40% methanol/40% ethylene glycol/20% water.

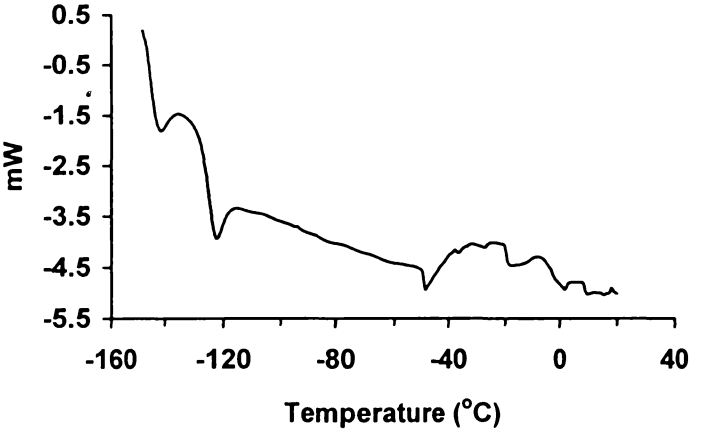

Figure 2.6. DSC curve for 60% ethylene glycol/40% water. The transitions observed near -50°C were due to ice formation on the outside of the sample pan.

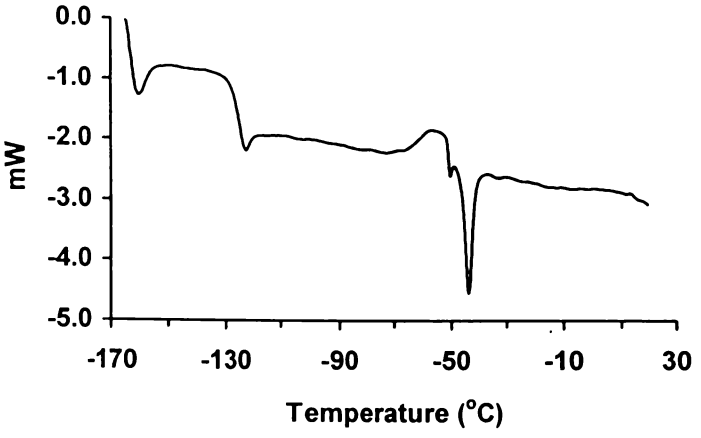

Figure 2.7. DSC curve for 70% ethylene glycol/30% water. The thermal transition observed near –50°C was found not to be reproducible, and should be disregarded.

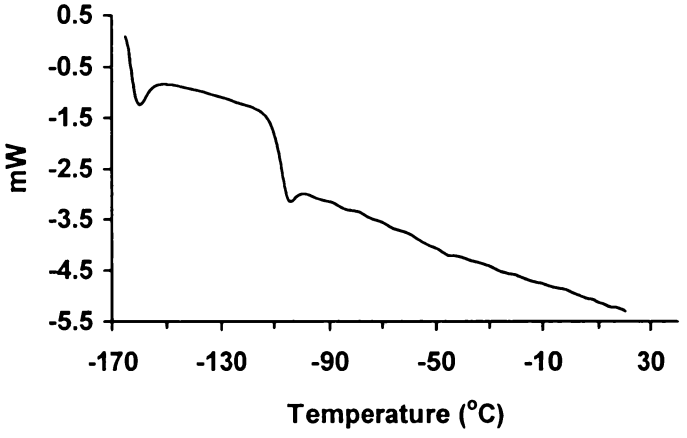

Figure 2.8. DSC curve for 60% glycerol/40% water.

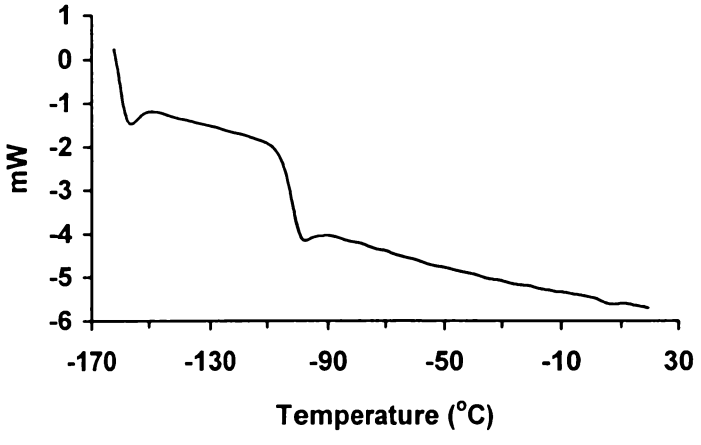

Figure 2.9. DSC curve for 70% glycerol/30% water.

A further group of cryosolvents was selected, due to their previous and continued use in the cryoenzymology and dynamic studies. Perdeuterated cryosolvents were run, as the use of perdeuterated solvents is required for the neutron scattering studies. The equivalent hydrogenated solvents were mostly run in the earlier DSC work by Réat et al. (2000b). The perdeuterated cryosolvents run were: 40% methanol/60% water; 70% methanol/30% water; 40% DMSO/60% water; and 80% DMSO/20% water. The hydrogenated solvents 70% methanol/10% ethylene glycol/20% water and 70% methanol/30% water were also run. The DSC results are shown in Figures 2.10 to 2.15.

For 40% deuterated methanol/60% D_2O, there is an endothermic peak at -100°C, followed by a broad endothermic transition at approximately -27°C (Figure 2.10). The broadness of the transition may be a reflection of inadequate sample sealing. There is also a potential glass transition near -115°C, which is seen as a small shift in the baseline. The 70% deuterated methanol/30% D_2O cryosolvent exhibited a double endothermic peak near -100°C, which is probably due to melting in the sample (Figure 2.11). There is no detectable glass transition before this temperature, as observed for the 40% deuterated methanol solution.

The DSC curve for 70% methanol/30% water is very similar to that obtained for the equivalent deuterated cryosolvent, with an endothermic transition observed near -100°C (Figure 2.14). In the initial series of DSC experiments, the endothermic transition for 70% methanol was observed near -110°C (Réat et al, 2000b). Takaizumi and Wakabayashi (1997) have determined the phase diagram for methanol/water solutions. While it is not directly applicable for the deuterated solutions, it provides a comparison for the observed transitions. The broad transition near -30°C for 40% deuterated methanol/water, corresponds to the temperature expected for melting of ice in the sample. The DSC curve of 70% methanol/10% ethylene glycol/20% water was identical to that obtained in the earlier study, with no thermal transitions observed down to the lowest temperature tested, in this case -150°C (Figure 2.15).

For 40% deuterated DMSO/60% D_2O, an endothermic transition is observed near -124°C, which may be due to a glass transition due to the shift in baseline, with the peak due to enthalpy of relaxation (Figure 2.12). A broad endothermic peak

near -27°C is then seen, which is probably due to melting in the sample. The DSC curve for 80% deuterated DMSO/20% D_2O is very similar, with an endothermic transition with a possible shift in baseline near -124°C, followed by a broad endothermic peak at -27°C. The glass transition temperatures for each composition agree with that given by Murthy (1998).

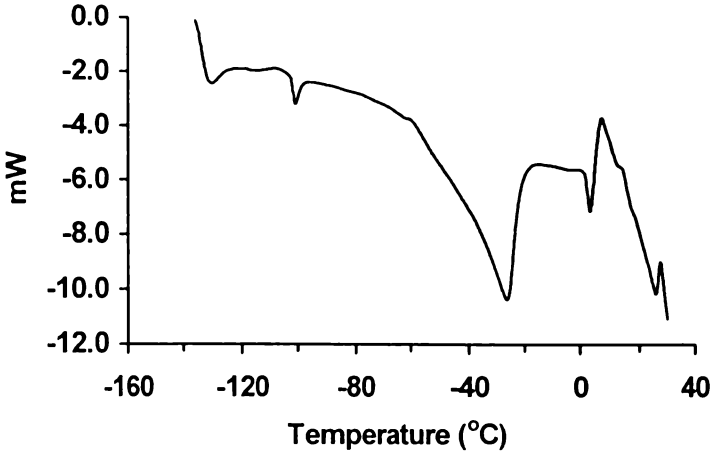

Figure 2.10. DSC curve for 40% deuterated methanol/60% D_2O. The broadness of the transition near –27°C may be due to inadequate sample sealing. The thermal transitions observed above 0°C are not reproducible.

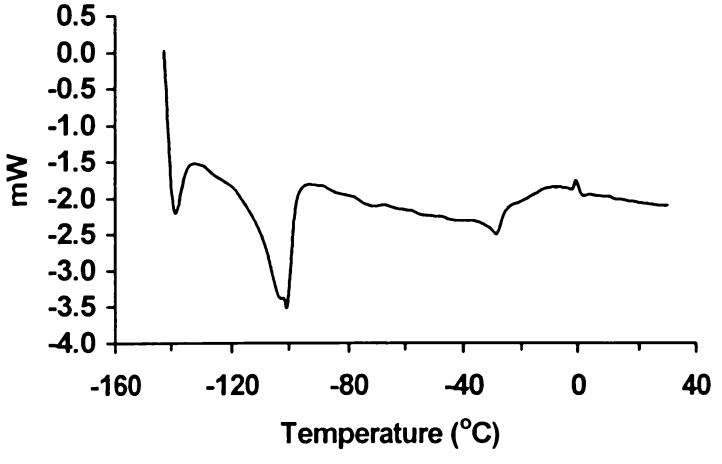

Figure 2.11. DSC curve for 70% deuterated methanol/30% D_2O.

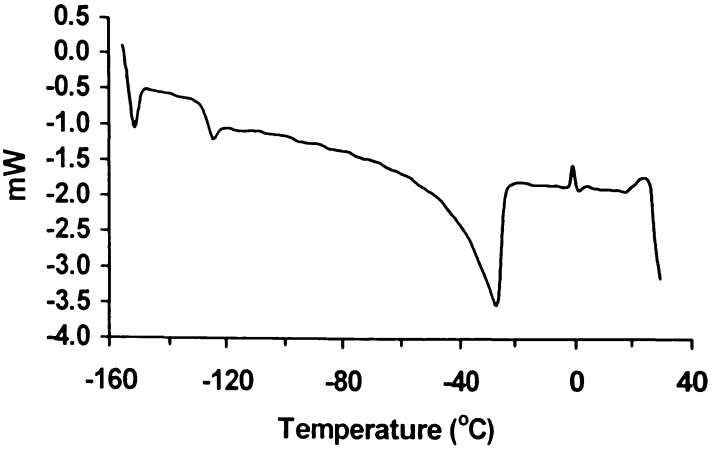

Figure 2.12. DSC curve for 40% deuterated DMSO/60% D_2O.

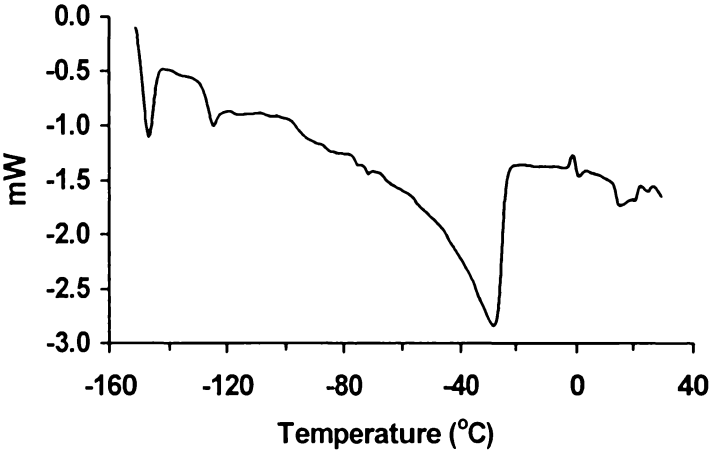

Figure 2.13. DSC curve for 80% deuterated DMSO/20% D_2O.

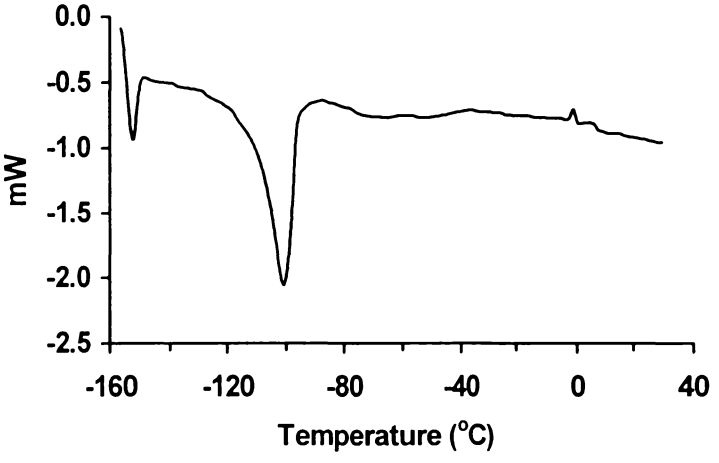

Figure 2.14. DSC curve for 70% methanol/30% water.

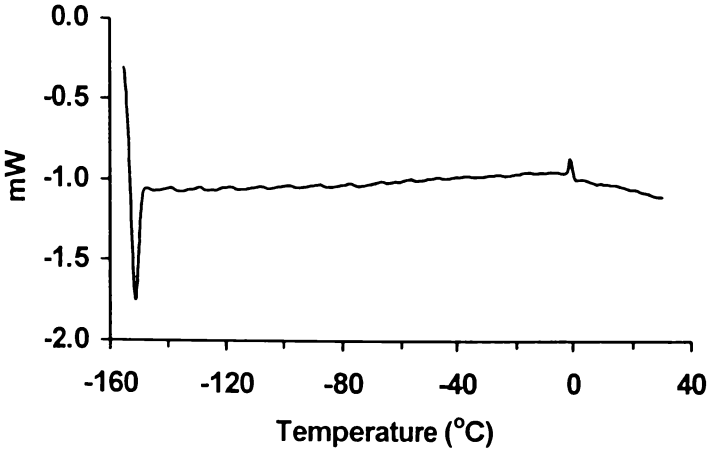

Figure 2.15. DSC curve for 70% methanol/10% ethylene glycol/20% water.

2.6.3 Dynamic Mechanical Thermal Analysis

Trials with this technique were conducted due to the relative ease with which glass transitions are observed compared to DSC. The greatest difficulty with this technique is the loading, or clamping, of liquid samples. The first attempts to address this difficulty involved the soaking of filter paper with the appropriate solution. Unfortunately, changes in composition due to differential evaporation of the solution components lead to inaccurate results. Also, it is unknown how the interaction of the solution components with the paper influences the results. The most recent approach, which seems more promising, is the placement of the sample between stainless steel plates, which are then wrapped in aluminium foil to help retain the sample and prevent evaporation. The plates can be pre-cooled to help prevent solvent evaporation.

Several cryosolvents were chosen that had been run on the DSC, and included: 35% methanol/35%ethylene glycol/30 %water; 60% ethylene glycol/40% water; 70% methanol/10% ethylene glycol/20% water; and 70% methanol/30% water. Initially, 35% methanol/35%ethylene glycol/30% water and 60% ethylene glycol/40% water were analysed after loading on to filter paper. The results are shown in Figures 2.16 and 2.17. As can be seen the transitions observed are very broad, which is most likely due to solvent evaporation causing changes in the composition. However, when the 35% methanol/35% ethylene glycol/30% water solution was placed between stainless steel plates and re-run, much sharper

transitions were observed, as shown in Figure 2.18. A sharp peak in tan δ is seen near -120°C.

The results for 70% methanol/10%ethylene glycol/20% water are shown in Figure 2.19. A large tan δ peak was seen near -145°C, but as the sample was not cooled further only part of the response is observed. When this is compared to the DSC curve, a peak is seen that coincides with the initial displacement of the trace, but is sharper and more intense than usual, and so confirms the DMTA data. Ideally the sample would be cooled to even lower temperatures to get an accurate measure of the transition that is occurring.

The 70% methanol/30% water cryosolvent also gave a large tan δ response, with the peak centered near -150°C (Figure 2.20). Further peaks are also seen near -100°C. The DSC plot shows a sharper and more intense initial displacement at -150°C than usual, which confirms the DMTA data. The peak near -100°C corresponds to the melting transition seen in the DSC curve at the same temperature.

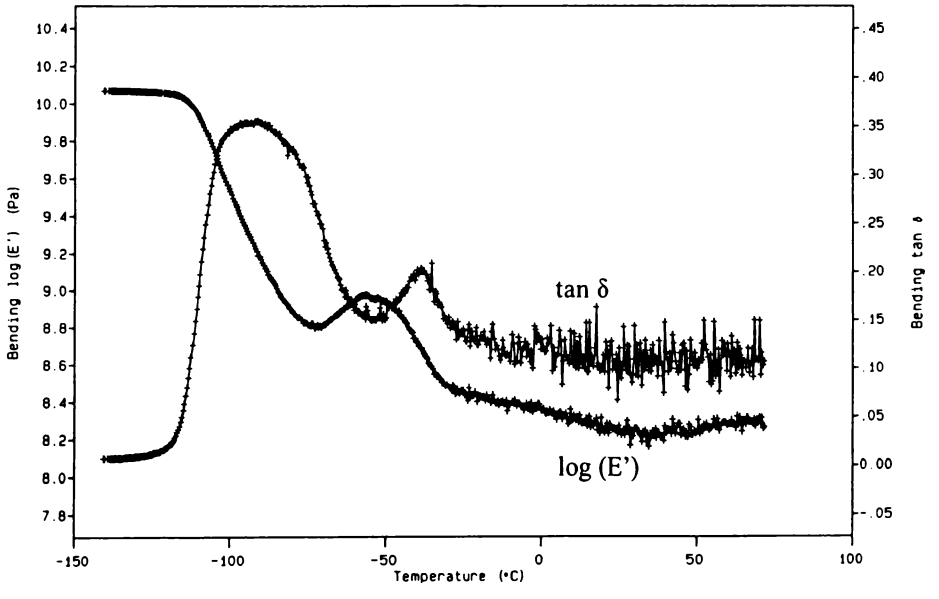

Figure 2.16. DMTA trace of 35% methanol/35% ethylene glycol/30% water loaded on to filter paper.

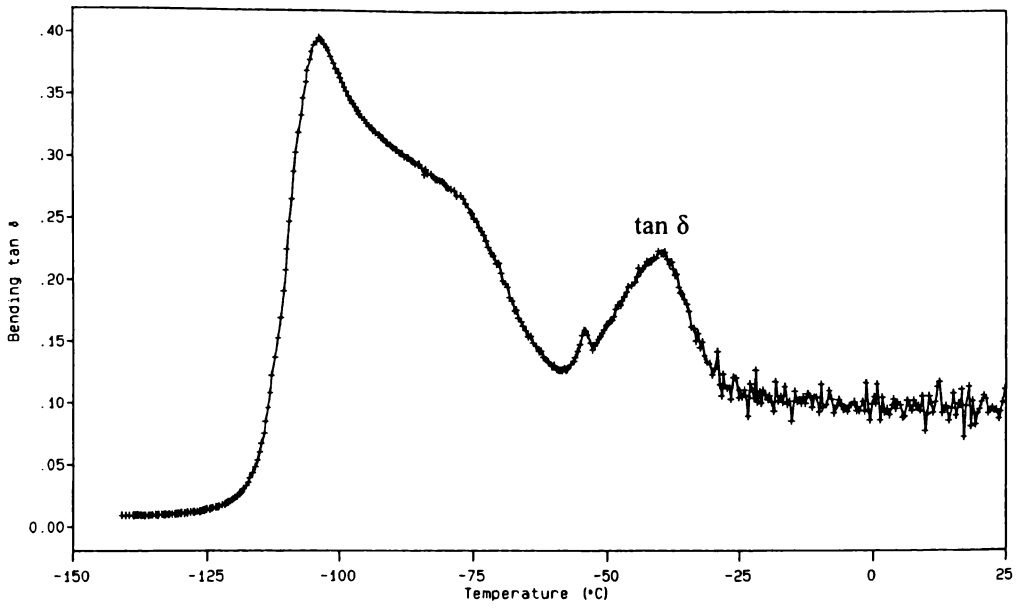

Figure 2.17. DMTA trace of 60% ethylene glycol/40% water loaded on to filter paper.

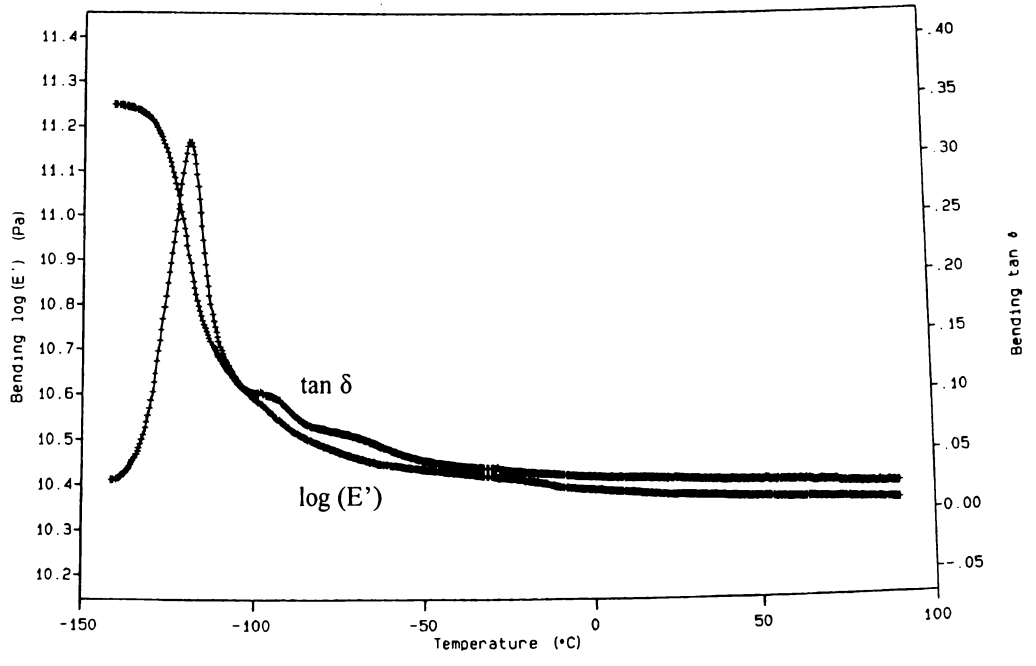

Figure 2.18. DMTA trace of 35% methanol/35% ethylene glycol/30% water loaded between stainless steel plates and wrapped in aluminium foil.

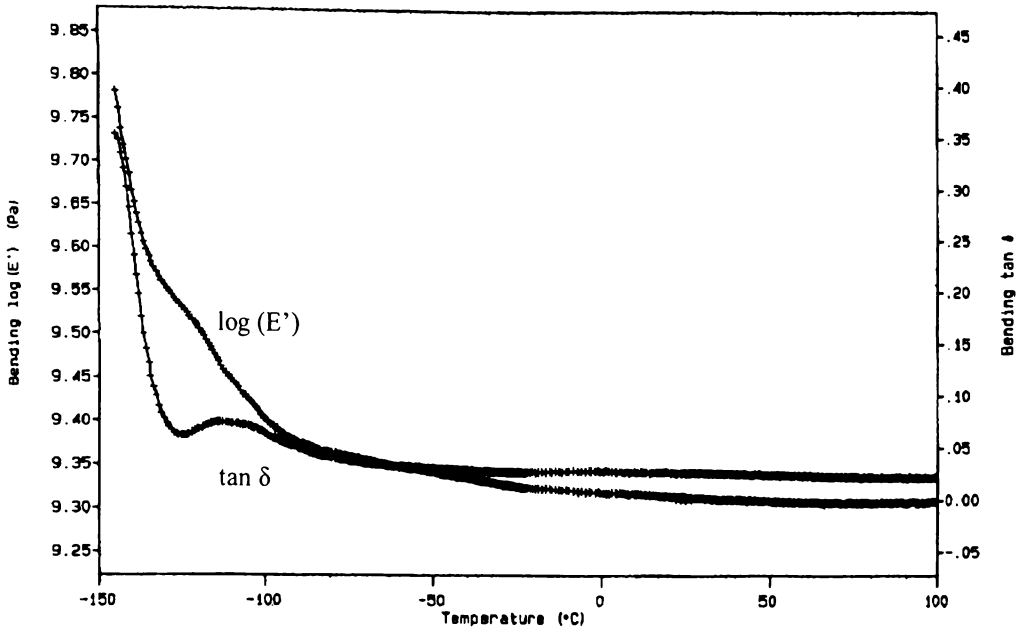

Figure 2.19. DMTA trace of 70% methanol/10% ethylene glycol/20% water loaded between stainless steel plates and wrapped in aluminium foil.

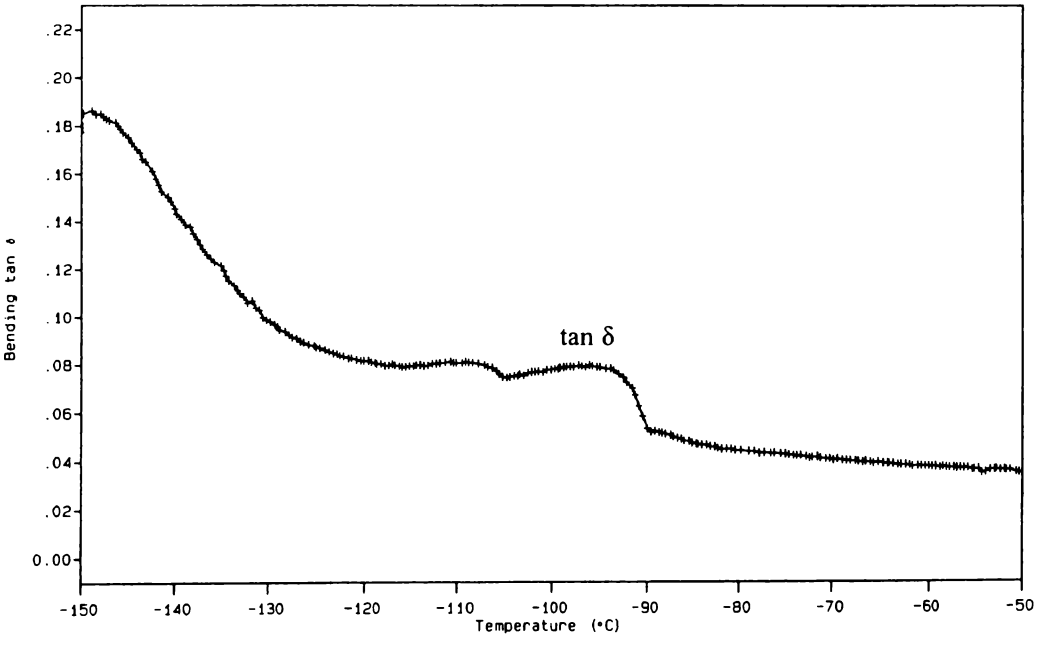

Figure 2.20. DMTA trace of 70% methanol/30% water loaded between stainless steel plates and wrapped in aluminium foil.

As the sample loading technique improved the results became more reliable, and agreed moderately well with the corresponding DSC curves. The DMTA technique provides support to the low temperature DSC results, where potential low temperature glass transitions are hidden by the initial displacement in the thermal analysis curve. The set-up of the DMTA also allows for greater ease of

sample cooling, thereby allowing low temperature transitions to be more fully characterised. To be able to determine the nature of the transitions observed by DMTA, it would be interesting to repeat the experiments with a range of frequencies for the applied sinusoidal stress. If the observed transitions reflect glass transitions, the peak of the tan δ would change with the applied frequency, whereas if it was a melting transition the tan δ would be independent of the frequency.

Chapter Three

Protein-Solvent Interactions

3.1 Introduction

Cryosolvents enable low temperature enzyme assays to be conducted, which provides a valuable tool for investigating the relationship between enzyme activity and dynamics. To be able to interpret the low temperature results correctly, it is necessary to investigate the interactions between the protein and cryosolvent solutions to know which effects are due to the effect of temperature on the solvent, which to the effect of temperature on the protein, and whether any effects are due to the influence of the solvent on the protein.

This chapter provides a look at the effect cryosolvents are having on the enzyme system, and the steps taken to ensure the validity of the low temperature work. The effect of cryosolvents on the dynamics and catalytic activity of enzymes is studied. This will enable the effect of temperature and solvent on the enzyme to be distinguished.

The effect of cryosolvents on enzyme dynamics was investigated by neutron scattering studies. For the neutron scattering experiments themselves, I was one of a group of researchers. The enzyme xylanase was used to investigate the effect of cryosolvents on the catalytic properties of the enzyme itself. DSC experiments were also performed on several protein-cryosolvent samples to allow further characterisation of these solutions.

3.2 Effect of Solvents on Proteins

3.2.1 General Considerations

In Chapter Two the potential change in solution properties caused by the addition of organic cosolvents to an aqueous enzyme solution were discussed. In this section the resulting changes in the enzyme itself will be discussed. The presence of cosolvents can affect the enzymes solubility, structure, stability, and catalytic

activity. These effects will also change with temperature as the properties of the cryosolvents and enzyme molecules change.

An initial concern is the solubility of proteins in cryosolvents. This is important for both the neutron scattering experiments and the related cryoenzymology studies of enzyme activity. For the neutron scattering studies of enzymes in cryosolvents, the protein needs to be in dissolved in solution to a final concentration of 50 to 100 mg/ml, as only thin samples are used. For the cryoenzymology work high enzyme concentrations, up to 1 mg/ml, are required for very low temperature (i.e. very low activity) assays in the cryosolvent. This enables the assay times to be reduced to a practical time period, even with the extremely slow enzymatic rates obtained at low temperatures. It is generally found that the solubility of proteins, as with other solutes, decreases as the cosolvent concentration increases, and that this effect becomes greater as the temperature is reduced. The addition of simple aliphatic alcohols, which are potential cryosolvents, induces the aggregation or precipitation of many proteins if they are at or near their isoelectric point. It has been shown though that neutral salts increase the solubility of proteins in aqueous-organic solutions in much the same way they do in water (Douzou, 1974). However, at higher concentrations of organic solvents and at lower temperatures (< 20°C), it was found that the solubility of proteins could not be significantly increased by the addition of neutral salts. At high organic solvent concentrations, the salts can then precipitate with the protein, as well as any buffers. Solubility is very dependent upon the protein itself, as some proteins remain readily soluble at high concentrations, even in the presence of high cosolvent concentration (up to 70%), and at very low temperatures (down to near –70°C). For example, the solubility of lysozyme in DMSO, ethylene glycol, and formamide, was found to be greater than 50 mg/ml (Chin et al., 1994). To maintain the enzyme concentration at a known constant level, a concentration must be found which is low enough to prevent precipitation at low temperatures.

The stability of proteins can also be affected. Some enzymes are stable at 0°C in high concentrations of cosolvent, while others are very unstable at such a high temperature. For example, the malic enzyme from the extreme thermoacidophilic

archaebacterium *Sulfolobus solfataricus* was found to be completely active in 50% DMF after a 24-hour incubation at 25°C (Guagliardi et al., 1989). In comparison, gradual loss of activity of α-chymotrypsin was observed at 25°C in both 65% DMSO and 70% methanol, but not if the temperature was reduced to below 10°C (Fink, 1973). The instability can sometimes be overcome by the synchronised addition of cosolvent and cooling, until the desired composition is obtained. This approach was used for the cryoenzymology trials with myokinase, which was found to be unstable in the presence of organic cosolvents at temperatures near 0°C (results not shown). Incubating the enzyme in the cryosolvent at 0°C or lower must be used to check the stability of that enzyme in a particular cryosolvent: aliquots can be assayed periodically to check for a possible decrease in the activity. A decrease in activity in the cryosolvent compared to an aqueous solution is commonly seen, and it is important to show by the above procedure that this apparent inhibition does not increase with time, and that it is fully reversible by dilution of the cosolvent. Otherwise, it could indicate the progressive denaturation of the enzyme, slowed down by the low temperature, in the cryosolvent (Douzou, 1977). A decrease in protein stability in cryosolvents has also been shown by a decrease in the temperature required for thermal denaturation.

A factor closely related to stability, is the effect of cosolvents, and also low temperatures, on the conformation of the enzyme. Conformational stability is an important factor in determining enzyme activity. To be fully active, the correct conformation needs to be maintained so that key residues in the active site are correctly positioned. The variations in solution properties brought about by the addition of an organic solvent can all potentially lead to changes in the protein conformation. For example, as the temperature is reduced the dielectric constant of the solution increases, which means that the polar interactions will be strengthened, and that hydrophobic interactions will be weakened (Douzou, 1971). This change in the relative force of various interactions could lead to a change in enzyme structure. The addition of acetonitrile to an aqueous solution of lysozyme was suggested to weaken the hydrophobic interaction and to strengthen the peptide-peptide hydrogen bond. In confirmation of this, the conformation of

lysozyme was found to change to a helix-rich form above acetonitrile concentrations of 40% (Gekko et al., 1998).

For oligomeric proteins, changes in the state of association may occur due to the presence of the cosolvent, and also due to the low temperatures. For the protein D-amino-acid-oxidase, apparent activation was seen when its normal dimers dissociated into monomers (Douzou, 1974). More minor conformational changes have been observed with proteins in weakly protic solvents, and involved an increase in helical content. This was probably related to the decreased hydrogen-bonding capacity of the mixed solution compared to water, and increased electrostatic repulsive interactions between charges on the protein molecule due to the reduced dielectric constant (Douzou, 1974). An extensive conformational transition of lysozyme has been detected in lysozyme solutions upon the addition of particular organic solvents. A transition of the polypeptide backbone from a predominantly α-helical to increased random coiled and β-sheet structures, as well as unorthodox protein secondary structures, was seen upon addition of the organic cosolvents. This produced a significant increase in viscosity due to the subsequent short-lived inter-chain contacts leading to an entanglement of the system as a whole (Arêas et al., 1996; Arêas et al., 1999).

Since any transition from the native to denatured state in a non-aqueous solvent is usually an endothermic process, a decrease in temperature should favour the native form or conformation (Douzou, 1971). It is also thought that the disruption of the native conformation observed at room temperature, could possibly be reversed at subzero temperatures (Singer, 1962). Studies with synthetic polypeptides in aqueous-organic solutions showed that they undergo a random coil $\leftrightarrow$ helix transition at low temperatures, and that they can also be dissolved in the helical state at low temperatures (Douzou, 1971).

To be able to assess possible conformational changes, the methods used must be relatively sensitive to be able to detect subtle and localised changes from the native conformation. The more sensitive methods include ultraviolet and visible absorption, optical rotatory dispersion, and circular dichroism. Possibly the most sensitive test of structural integrity is the catalytic properties of the enzyme.

The remaining factor to be considered is the effect of organic cosolvents on enzyme catalysis. Most enzymes retain some catalytic activity when dissolved in aqueous-organic solvents at low temperatures. The cosolvent has been shown to both increase and decrease enzyme activity, relative to aqueous conditions depending on the enzyme. In most cases though, the addition of an organic solvent causes inhibition of activity, which is reversible by dilution. The effects of the cosolvent on the catalytic properties of the enzyme can be determined by studying the effects on the kinetic parameters as a function of cosolvent concentration (Fink and Geeves, 1979; Travers and Barman, 1995). For example, if the reaction is a hydrolysis reaction, a decrease in V_{max} with decreasing water concentration may be expected. In some cases a decreased rate is observed due to the cosolvent exerting a negative effect on substrate binding, due to a hydrophobic partitioning effect on the substrate (Fink and Geeves, 1979; Maurel, 1978; Ryu and Dordick, 1992; Wescott and Klibanov, 1994; Kvittingen, 1994). This results in an exponential increase in K_M with cosolvent concentration, and so a plot of log K_M versus cosolvent concentration should be linear.

Studies with inhibitor binding can also be done to ensure that the inhibition involves the binding step of the enzyme-catalysed reaction. Inhibition by the cosolvent could be competitive if the solvent molecules bind at or near the active site, and may be seen as curvature in log K_M versus cosolvent concentration plots, if the inhibition is significant. Non-competitive inhibition could also be seen if solvent molecules bind to the enzyme at a site distant from the active site, thereby influencing its structure.

As with buffers, the 'pK_a' of essential ionising groups at the active site can be affected by the presence of the cosolvent. Changes in the relative acidity of groups in the enzyme can cause the optimal pH to change, and so pa_H-activity curves should be determined so that the pa_H can be adjusted to an appropriate value to give optimal activity. It has been observed with many enzymes that unless the substrate is a polyelectrolyte, the pa_H dependence is similar to that in aqueous solution. A possible explanation to account for the absence of the expected perturbations was that the hydration shell surrounding the protein might not be significantly disturbed by the presence of the cosolvent. Therefore, the

environment around the key ionisable catalytic groups in the cryosolvent may be similar to that in the aqueous environment. The groups in the active site have sufficient enthalpies of ionisation that changes in temperature may also cause a change in their ionisation.

Once the ionic strength, proton activity, and dielectric constant of the aqueous-organic solution are optimised for enzyme activity, changes in the ionisation of the enzyme and substrate that may interfere with activity should be minimised. But even though these parameters are optimised, an intrinsic effect of the cosolvent commonly still remains, and in most cases is inhibitory. This is probably due to the fact that although these bulk macroscopic properties of the solution are optimised, they may be significantly different to the microscopic properties of the solution surrounding the enzyme and substrate. From neutron scattering studies of protein solutions, we have found that the dynamics of the protein solutions were independent of the solution composition, despite the use of solvents with different melting points (Réat et al., 2000a). A possible explanation is that the solvent shell of the enzyme may be qualitatively similar in all of the solvents, despite very different bulk-solution compositions.

The dielectric constant is a parameter that highlights such discrepancies. Theoretical treatments have shown that the energy of activation of a reaction can be influenced by the dielectric constant, and also by changes in the dielectric with temperature, influencing the Arrhenius frequency factor, A. But selective solvation of a solute by the solvent would diminish such an effect, and such deviations between theory and experiment have been commonly seen in a number of chemical reactions (Douzou, 1977). For reactions of small molecules in methanol/water solutions with a high cosolvent composition, deviations of the reaction rates towards those of pure water were seen. A direct comparison of these results to those of enzyme-catalysed reactions is difficult though, as enzymatic reactions are occurring on the surface of a macromolecule, with an unknown dielectric constant. A more relevant study was performed on the effect of solvents of varying dielectric constant, on the kinetic parameters of three enzymes, each with different interactions involved in enzyme-substrate complex formation (Maurel, 1978). Reactions involving electrostatic interactions in

substrate binding were expected to be affected more strongly by changes in dielectric constant, as they are theoretically more sensitive to variations in the dielectric constant. Instead, they found that with the enzyme systems studied, electrostatic interactions were apparently not affected by the dielectric constant.

3.2.2 Effect of Solvents on Protein Dynamics

A number of studies have shown that the environment surrounding a protein may play a role in the observed dynamics of proteins. In this study we are particularly interested in the effect of solvent environments, the most common of which is water. The binding of water to proteins produces a sigmoidal adsorption isotherm (e.g. Rupley et al., 1983; Careri et al., 1979; Rupley and Careri, 1991). Below 0.05 to 0.1 *h* (where *h* is the grams of water bound per gram of protein) water interacts primarily with the ionisable groups in the protein. Between 0.1 to 0.25 *h* water binds to the polar sites on the protein molecule. Above 0.25 *h* water condenses onto the weakest binding sites of the protein surface to complete the process, and then at sufficiently high water contents, the system is approximately equivalent to that of the solution. The adsorption isotherms for proteins suspended in organic solvents have also been determined. After conversion to a basis of thermodynamic water activity (a_w), the adsorption isotherms were compared to those known for proteins equilibrated with water from a gas phase. At low water contents, with a_w less than about 0.4, similar adsorption isotherms were found for proteins in each solvent studied and in the gas phase. However, at higher a_w values, significant differences between the isotherms were seen (Halling, 1990).

The importance of hydration with respect to enzyme activity has been investigated by the use of hydrated powders. For example, studies of lysozyme powders equilibrated with water in air have shown that catalysis occurs at a hydration level of approximately 0.2 *h*, which is well below monolayer water coverage (Careri et al., 1980).

Hydration effects on enzyme activity in organic solvents have also been studied. The transesterification activity of subtilisin Carlsberg in tetrahydrofuran was found to increase after the addition of less than 1% (v/v) water to the organic solvent (Affleck et al., 1992b). However, whereas earlier studies looked at the

effect of water concentration in the organic solvent on activity, as with the above study, it was later found that a more accurate parameter was that of the water bound to the enzyme itself (Zaks and Klibanov, 1988). A simple correlation between the percentage of water present and activity is not seen, as the water is distributed between several different phases. The water may be bound to the enzyme molecules, dissolved in the organic liquid phase, or adsorbed to other solid components. It is generally accepted that the thermodynamic water activity is the most useful in determining the influence of water on enzymes in organic media, as it determines the equilibrium distribution of water between the various phases (Partridge et al., 1998; Bell et al., 1995). As mentioned earlier, it is found that the amount of water bound to a protein is essentially equivalent in solvents with the same a_w (Halling, 1990).

The relationship between a_w and enzymatic activity was investigated by Partridge et al. (1998), for the enzyme subtilisin Carlsberg. They found that the catalytic rate profiles showed the same dependence on a_w for assasys conducted in cyclohexane, dichloromethane and acetonitrile. A sudden sharp rise in catalytic activity was seen to occur at an a_w of 0.55. A similar dependence on a_w was observed for the condensation reaction of β-glucosidases from almonds and *Fusarium oxysporum*. An a_w of approximately 0.53 was needed to achieve a detectable level of activity (Tsitsimpikou et al., 1996). An a_w of 0.5 corresponds to an enzyme hydration of approximately 0.12 *h* (Rupley and Careri, 1991; Hallling, 1990). However, lipases have been shown to retain activity at a greatly reduced water activity, as low as 0.0001 for the lipase from *Rhizomucor meihei* (Valivety et al., 1992a and 1992b). The ability of a_w to correctly predict the onset of enzymatic activity is not always so reliable. For example, it was found that a_w was not able to correctly predict the critical hydration level for activity of the enzyme laccase in polar solvents (Bell et al., 1997). It was suggested that polar solvents, such as acetonitrile and acetone, have a direct effect on the enzyme, as well as competing for water.

In the current work, the lowest water concentration in any of the various cryosolvents used was 20% (v/v). This is to ensure that the enzymes were hydrated sufficiently for activity. The highest cosolvent concentrations used in

the cryoenzymology work were 60% (v/v) DMSO and 70% (v/v) methanol, which correspond to water activity values of approximately 0.45 and 0.63, respectively, based upon the calculations of Bell et al. (1997). It is difficult to calculate how much water is bound to a particular enzyme at these levels, and this will probably be enzyme and solvent dependent. However, from the studies detailed above, it appears that this is an adequate level of water activity for enzymatic activity. Also, the fact that activity is easily detected in these cryosolvents for a range of enzymes suggests that the enzymes are indeed sufficiently hydrated.

The relationship between water and protein dynamics has been shown by a number of hydration studies, using various techniques (Smith et al., 1987; Partridge et al., 1998; Zanotti et al., 1997; Diehl et al., 1997; Zanotti et al., 1999; Perez et al., 1999; Careri et al., 1986; Krupyanskii et al., 1982). The effect of hydration on proteins embedded in lipid (hydrophobic) membranes has also been investigated (Fitter et al., 1996; Ferrand et al., 1993). Lysozyme has been shown to be inactive in the absence of minimal hydration (Careri et al., 1980; Rupley et al., 1983). From related NMR measurements of exchangeability of the main chain amide hydrogens (Poole and Finney, 1983), and from measurements of the rate of exchange of labile hydrogens (Schinkel et al., 1985), it is suggested that a hydration-related increase in conformational flexibility is necessary for activity. Measurements of the Rayleigh scattering of Mössbauer radiation, which monitors the average motional properties of the protein, were used to investigate the dynamic consequences of hydration for myoglobin (Krupyanskii et al., 1982). It was found that at low hydration levels (37% relative humidity, approximately 0.1 *h*), the mean square displacement, $\langle x^2 \rangle$, showed no motion at temperatures up to 300 K. However, for myoglobin hydrated at a relative humidity of 94%, an increase of the dynamic amplitudes was seen near 220-240 K. An increase in dynamic amplitudes was also found in subsequent work on lysozyme powders (Smith et al., 1987), and qualitatively similar results have been observed by more recent neutron scattering studies on hydrated myoglobin, lysozyme, parvalbumin, and α-amylase (Diehl et al., 1997; Perez et al., 1999; Zanotti et al., 1997; Fitter, 1999). At room temperature, it was shown that hydrated myoglobin and lysozyme exhibit a more pronounced quasielastic spectrum due to diffusive motions, which was suggested to be due to modification of the amplitude, but not the timescale, of

the fast protein motions (Diehl et al., 1997). A later study suggested that upon hydration from dry powder to monolayer coverage, the surface side-chains acquire the possibility to diffuse locally, and then upon further hydration the main effect is to improve the rate of these motions. In the solution state the motions then increase in amplitude compared to the fully hydrated powder, and have a shorter average relaxation time than for proteins with monolayer coverage of water (Perez et al., 1999).

From the above studies it is clear that hydration is necessary for the activation of anharmonic vibrational and diffusive motions on picosecond timescales. Water has been called the "lubricant of life" because of the role it appears to play in promoting fast protein conformational fluctuations (Barron et al., 1997). A number of studies have suggested various mechanisms by which water, and solvents in general, are able to influence and affect protein dynamics. One suggestion is related to the effect of solvent dielectric on electrostatic interactions. For example, from studies with chymotrypsin, it was suggested that the increased flexibility observed upon protein hydration may in part be due to the reduced interaction of charged and/or polar residues, due to dielectric screening caused by water forming clusters on the protein surface (Bone, 1987). Dielectric screening by water was also suggested to be the cause of coupling between enzyme hydration and flexibility for the enzyme subtilisin Carlsberg suspended in tetrahydrofuran and acetonitrile (Affleck et al., 1992b; Schmitke et al., 1996). The dynamics of α-chymotrypsin in a variety of essentially dry organic solvents, ranging in dielectric constant from 72 to 1.9, were determined by electron paramagnetic resonance (EPR) spectroscopy (Affleck et al., 1992a). It was found that the mobility of two spin-labeled amino acids decreased with decreasing dielectric constant, consistent with changes in the electrostatic force between charged residues. Solvent molecules can also in principle affect protein dynamics by modifying the effective potential surface of the protein, or they could have more direct dynamic effects as a result of collisions between solvent molecules and the protein atoms (Brooks and Karplus, 1989; van Gunsteren and Karplus; 1982; Smith et al., 1990). Frictional damping can result from intramolecular anharmonicities, protein-protein interactions for powder samples, and from the surrounding solvent (Smith et al., 1990; Smith, 1991).

The electrical interaction of the hydration water and the protein has been suggested as another mechanism to account for the coupling of protein and solvent interactions. The temperature dependency of the dielectric relaxation rate of 'free' water and of water adsorbed to myoglobin crystals was studied using microwave measurements (Singh et al., 1981). It was found that the dielectric relaxation rate of the adsorbed water is nearly identical to the temperature dependence of the conformational fluctuation rate of the protein, as observed by the Mössbauer effect. The fluctuating electric field of the hydration water, arising from dipole reorientation, might interact with the fluctuating electric field of the protein charged groups, thereby causing the observed correlation in dynamics.

As mentioned in Chapter One, proteins have been observed to undergo a dynamical transition to greater flexibility above 170-230 K, which is sometimes referred to as the glass transition. A number of studies have suggested that the surrounding solvent may play a role in causing the observed dynamical transition. The biphasic behaviour of the average mean-square displacement of ribonuclease-A, was attributed to the coupling between the structure and the dynamics of the solvent shell and the protein (Tilton et al., 1992). Parak et al. (1982) performed Mössbauer studies over a wide range of temperatures, on both ^{57}Fe of deoxygenated myoglobin crystals and on $K_4{}^{57}(Fe(CN)_6$ dissolved in the water of metmyoglobin crystals. The temperature dependence of the calculated mean-square displacement of the iron atom in both the protein and water solution was shown to be similar. A model was proposed in which the temperature dependence of the protein dynamics is governed by a mechanical friction constant. The mechanical friction constant has contributions from crystal water, as well as the interior of the protein. Therefore, although the protein dynamics depend on the structure of the protein itself, they are strongly influenced by the surrounding water.

Studies by Iben et al. (1989) also showed the influence of solvent in the dynamic transition of proteins. Measurements on the infrared stretching frequencies of CO bound to myoglobin indicated that the dynamic behaviour of the protein is correlated with a glass transition in the surrounding solvent. Also, in a recent molecular dynamics analysis of hydrated myoglobin, solvent mobility was found

to be a dominant factor in determining protein fluctuations above 180 K (Vitkup et al., 2000). The involvement of hydrogen-bonding interactions between the hydration water and the protein in the observed dynamical transition has been suggested in a number of studies (Demmel et al., 1997; Diehl et al., 1997; Fitter, 1999).

Several studies have made use of environmental changes to determine the correlation between solvent and the dynamic transition of the protein. By placing proteins in a room temperature glass, such as trehalose, the transition to anharmonic dynamics was not observed, even up to room temperature (Cordone et al., 1999). It was found that the constraints imposed by the trehalose matrix have a much greater effect on the quasidiffusive motions detected by neutron scattering, as opposed to motions in the core of the protein (Hagen et al., 1995; Gottfried et al., 1996; Hagen et al., 1996).

Although the above studies show a significant influence of the solvent on the dynamical transition of proteins, the dependence on the protein structure itself has also been demonstrated. The conformational dynamics within the complex between Zn-substituted cytochrome *c* peroxidase and cytochrome *c* was studied by fluorescence quenching (Nocek et al., 1991). To examine whether the observed transition in dynamics was 'slaved' to the solvent, the temperature dependence of the quenching rate constant of the complex was studied in a range of ethylene glycol-water solvents. It was found that the midpoint and the width of the transition were largely independent of the solvent composition, indicating that the transition in dynamics is an intrinsic phenomenon of the complex. A comparison of the temperature dependence of the Mössbauer spectra of oxymyoglobin in aqueous solution with that of metmyoglobin crystals was performed by Keller and Debrunner (1980). A near identity in the conformational contribution to the mean-square displacement was found. This suggests that the conformational fluctuations occur independently of the matrix, and are thus an intrinsic property of the protein.

3.3 Xylanase Mechanism

The thermophilic xylanase used in these studies was obtained from an *E.coli* clone containing the gene from *Thermotoga* sp. strain FjSS3-B.1. Strain FjSS3-B.1 was enriched from an intertidal hot spring in Fiji and is an extremely thermophilic anaerobic eubacterium, which grows optimally at 80°C (Simpson et al., 1991). The recombinant enzyme is a single subunit enzyme with a molecular mass of 40.5 kDa as determined from the DNA sequence (Saul et al., 1995).

Glycosyl hydrolases have been classified into families based upon conserved amino acid sequence similarities in the catalytic domains, with over 70 different families being classified so far (Henrissat, 1991; Henrissat and Davies, 1997; Gilkes et al., 1991; Henrissat and Bairoch, 1993). These sequences are available through a web-site that gives updated listings of these family members, as well as information on the identities of important amino acid residues (http://afmb.cnrs-mrs.fr/~pedro/CAZY/db.html). A further grouping has also been suggested, as the three-dimensional structures have been determined for representatives from the various families. A 'clan' is a group of families that are thought to have a common ancestry, and have significant similarities in tertiary structure, as well as conservation of the catalytic residues and catalytic mechanism (Henrissat and Bairoch, 1996). The xylanase from strain FjSS3-B.1 belongs to family 10 of glycosyl hydrolases.

Xylanases are one of the many enzymes involved in the enzymatic degradation of xylan. The xylanase used in this study is an endo-β-1,4-xylanase (EC 3.2.1.8), which cleaves the internal β-1,4-glycosidic linkages of the heteroxylan backbone, with retention of configuration at the anomeric carbon. Retaining β-glycosyl hydrolases may adopt a wide variety of folding motifs, but the catalytic mechanism is similar. Koshland (1953) first proposed that the retention of anomeric configuration worked via a double-displacement mechanism involving an enzyme nucleophile. Evidence suggests that a covalent glycosyl-enzyme intermediate is formed and then released via oxocarbenium-ion-like transition states (Sinnott, 1990).

Two carboxyl groups are the key catalytic residues, and are only approximately 5.5 Å apart for retaining β-glycosidases. One carboxyl serves as the catalytic nucleophile, forming a covalent glycosyl-enzyme intermediate. The second carboxyl group provides acid/base assistance, functioning initially as a general acid catalyst to protonate the glycosidic oxygen of the scissile bond, concomitant with bond cleavage. In the second step of the reaction the carboxyl group acts as a base catalyst by deprotonating the incoming water molecule, which attacks at the anomeric center and displaces the sugar (Sinnott, 1990; Zechel and Withers, 2000; White and Rose, 1997; Withers, 2001). The mechanism for retaining glycosyl hydrolases is illustrated in Figure 3.1. Substrate cleavage is defined to occur between binding sites −1 and +1, with the negative side representing the non-reducing end of the substrate (Davies et al., 1997).

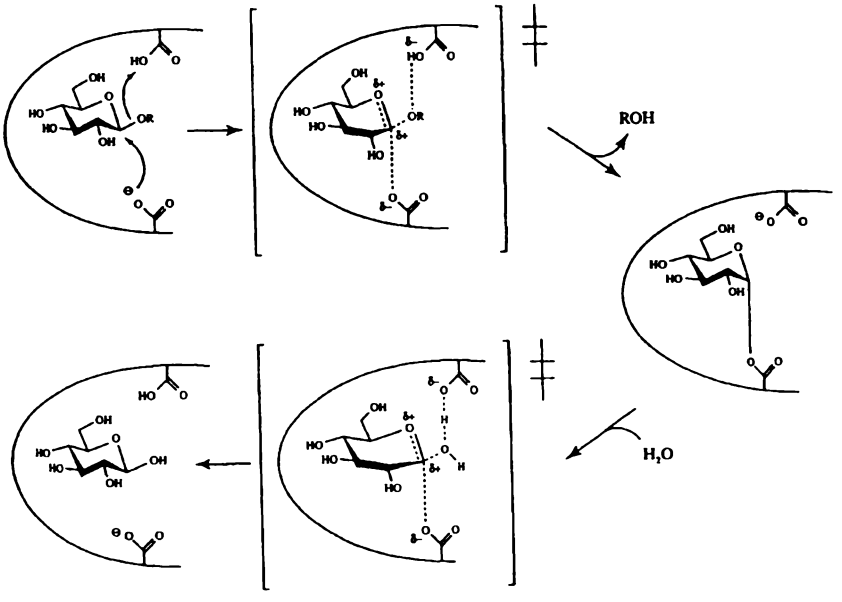

Figure 3.1. Mechanism of action of retaining β-glycosyl hydrolases. The symbol ‡ denotes the transition states in the reaction, and ROH represents the leaving aglycone. Reproduced from Ly and Withers, 1999.

The overall structure of family 10 xylanases consists of an 8-fold β/α-barrel. The active site is an open cleft, with two conserved glutamate residues acting as the catalytic nucleophile and acid/base catalyst (Jenkins et al., 1995). The enzyme-substrate interactions include both hydrogen bonding between the carbohydrate ring oxygens and hydroxyls and polar residues on the protein, as well as hydrophobic interactions between the xylose rings and aromatic side chains (Lo Leggio et al., 2000). The polar aromatic residues around the active site are highly

conserved, as well as a line-up of negative charges within the cleft (Natesh et al., 1999). A suggestion has been made that the active site of a retaining β-glycosidase is of a largely structurally static nature, while being electronically dynamic. The enzyme is thought of as providing a pre-organised cavity in which the substrate can optimally undergo binding rearrangement, due to the positioning of functional groups. Therefore, very little change is needed in the enzyme structure during catalysis, while substantial conformational changes in the substrate take place (Zechel and Withers, 2000; Withers, 2001).

In all known structures, the length of the active site cleft is approximately 30 Å long, suggesting the presence of 6 to maybe 7 subsites. From subsite mapping studies on the endo-β-1,4-xylanase from *Crytococcus albidus*, it was shown that the subsite-binding energies are highest for subsites –2 and +2 (Biely et al., 1981a). Lo Leggio et al. (2000) determined the structure of the complex between a catalytically compromised *Pseudomonas fluorescens* xylanase A and xylopentaose. They found the loss of accessible surface area at individual subsites on binding xylopentaose paralleled earlier results from measurements of subsite binding energies, that showed decreasing binding energy on going from subsite +2 to +4. They also concluded that the xylosyl residue at subsite –1 is distorted and pulled toward the catalytic residues, causing the glycosidic bond to be strained, leading to the formation of the enzyme-substrate covalent intermediate.

Retaining glycosyl hydrolases are known to also display transglycosylation reactions (Armand et al., 1996; Moreau et al., 1994; Hays et al., 1998). This is also seen in the activity of family 10 xylanases on xylooligosaccharides. At low substrate concentrations the enzymes appear to be strictly hydrolytic, but at higher substrate concentrations substantial transferase activities can be observed. The fact that transglycosylation activity with family 10 enzymes is only observed at high substrate concentrations, can be explained by poor ligand recognition at the plus subsites (Ntarima et al., 2000). The mechanism of substrate digestion by the endo-β-1,4-xylanase of *Cryptococcus albidus* was investigated by Biely et al. (1981b). Xylobiose was shown to be a poor substrate for hydrolysis, agreeing with their earlier work that subsites +1 and –1 have low affinity for xylosyl units. For xylotriose, xylotetraose and xylopentaose, the bond cleavage frequencies were

found to be concentration dependent. At high substrate concentration, reactions such as xylosyl and xylobiosyl transfer occurred and resulted in formation of products larger than the starting substrate. Xylose and xylobiose were found to enter the reaction pathway as glycosyl acceptors. The results also showed that the enzyme-glycosyl intermediates effective in the transfer reactions were formed from the non-reducing end units of the oligosaccharides.

Glycosyl transfer reactions are also observed with activity on synthetic substrates (Biely et al., 1980; Biely et al., 1997). The reaction rate shows a sigmoidal dependence on substrate concentration. At higher substrate concentrations the enzymes catalyse the degradation of the substrate by a complex reaction pathway involving a series of glycosyl transfer reactions followed by hydrolysis (Biely et al., 1997). The xylanase from *Cryptococcus albidus* was shown to be unable to catalyse simple hydrolysis of the substrate phenyl-xyloside, even at low substrate concentrations, suggesting that any degradation mechanism involved transglycosylation reactions, with xylobiose as the dominant product (Biely et al., 1980). In this case aryl xylosides are better substrates for glycosyl transfer than for hydrolysis.

As the Thermotoga xylanase is being studied in alcohol-based cryosolvents, a particular mention should be made of the complication that can arise for hydrolytic enzymes in these solutions. Many retaining glycosidases will transfer glycosyl residues to low molecular weight alcohols such as methanol, as well as to water (Sinnott, 1990; Fink and Geeves, 1979). An alcoholysis reaction catalysed by β-galactosidase was first described in 1912 (Wallenfels and Malhotra, 1961). Another example is the direct transglycosylation reaction between xylan and octanol, catalysed by xylanase from *Aureobasidium pullulans*, used to produce octyl β-D-xylobioside (Matsumura et al., 1999). In cases where these reactions occur, the interpretation of the effect of the cosolvent on the catalytic parameters is somewhat more complicated if the rate-determining step involves the attack of water. If there is no specific binding site for the alcohol, then a linear relationship between cosolvent concentration and the increased rate should result. This is due to the fact that alcohols are usually more effective attacking agents because of their better nucleophilicity. The increased rate brought about by the alcohol,

however, can also lead to a change in the rate-determining step (Fink and Geeves, 1979).

3.4 Theory of Neutron Scattering

The properties of neutrons make them a unique tool for studying the dynamical properties of proteins and cryosolvents on the nanosecond to picosecond timescale. Compared with the quanta used in other radiation scattering techniques, neutrons have a large rest mass, m. For a neutron with a de Broglie wavelength λ_o, the neutron velocity and energy are given by:

$$v_o = \frac{h}{m\lambda_o} \quad \text{and} \quad E_o = \frac{h^2}{2m\lambda_o^2}$$

where v_o is the velocity, E_o is the energy and h is Planck's constant (Middendorf, 1984). A neutron produced from a typical source possesses a wavelength of a few Å, and will therefore have energy of a few meV. This means that a neutron with a wavelength of a few Å, which allows the study of protein features on the scale of interatomic distances, has an energy very similar to that required to excite molecular motions. Thus the energy and momentum exchanged between the neutron and the protein can be significant fractions of the values possessed by the incident neutron. This allows the unique ability to energy-analyse the intensity at each scattering angle, and therefore to obtain time- and space-dependent information on the molecular motions in the protein sample (Smith, 1991). For comparison, if X-rays with a wavelength of a few Å are considered, the corresponding energy is given by:

$$E = \frac{hc}{\lambda}$$

where c is the speed of light (Tipler, 1991). The energy of the X-rays will be several orders of magnitude greater than the energy required to excite molecular motions in the sample, and also the energy of a neutron with a similar wavelength.

Neutron energies have been given in meV, but it should be noted that the following energy units can be used:

$$1 \text{ THz} = 1 \text{ ps}^{-1} = 4.13 \text{ meV} = 33.35 \text{ cm}^{-1} = 48.02 \text{ K}.$$

The units of cm^{-1} are simply used as a convenient energy measure, defined as shown, without any reference to optical spectroscopy (Middendorf et al., 1984).

Neutrons interact with molecules primarily by a neutron-nuclear interaction. The 'scattering efficiency' of neutrons by different elements and isotopes, varies irregularly through the periodic table (Shapiro and Shirane, 1991). This means that unlike X-ray studies, a light element, such as hydrogen, can contribute to the scattering from molecules just as much as a heavier element. The scattering from a single atom can be characterised by a single parameter, the scattering length, b. The total scattering cross section, σ, from a single stationary atom is given by $4\pi|b|^2$. However, the value of b depends on the nuclear spin. A neutron has a spin ½, and can interact with a nucleus of spin i in states of total spin $i + ½$ or $i - ½$. The scattering length is different for each of these processes. In a sample, the nuclear spin orientation of the atoms will be randomly distributed.

Two types of scattering will therefore be seen, one due to the average scattering length, $\bar{b}$, (averaged for isotope distribution, nuclear spin distribution etc.), and one due to fluctuations from the average, $b-\bar{b}$. Coherent scattering arises from the average scattering amplitude, $\bar{b}$, and can give interference effects due to correlations in the positions of different atoms. The deviations from the average, $b-\bar{b}$, are randomly distributed so do not produce interference effects, but give incoherent scattering. The intensity of incoherent scattering is determined by self-correlations in the atomic positions (Smith, 1991).

For a protein, the largest cross-section is due to incoherent scattering from hydrogen atoms. The incoherent cross section for hydrogen is 80 barns (1 barn is 10^{-24} cm^2), which is an order of magnitude greater than any other atom found in proteins (Engelman et al., 1984). Consequently the incoherent scattering from hydrogen is a significant component of the neutron scattering from proteins. In proteins hydrogen atoms are uniformly distributed over the macromolecule, and so neutron scattering leads to a global view of protein dynamics.

In a neutron scattering experiment, the incident and scattered neutrons are described by waves with wave vectors k and k', respectively, with the resulting scattering wave vector $q = k-k'$. This can be represented by the following diagram, where θ is the scattering angle.

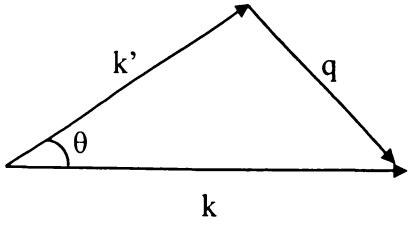

The change in energy and momentum is given by $\hbar q = \hbar(k-k')$ and $\hbar\omega = E-E'$, respectively, where $k = 2\pi/\lambda$, $\hbar = h/2\pi$, ω is the exchange of energy with the sample, and E and E' are the initial and final energy of the scattered neutron, respectively (Middendorf et al., 1984). A useful relationship between the energy and the momentum transferred, which is essentially an expression of the conservation of energy, is given by:

$$\hbar\omega = E-E' = \frac{\hbar^2}{2m}(k^2-k'^2)$$

(Lovesey, 1984). Wave vector and energy changes in the ranges [$0.01 < q\ (Å^{-1}) < 30$] and [$1\ \mu eV < \hbar\omega < 1$ eV] are readily measurable in available spectrometers.

If incoherent scattering is considered, which is the dominant form of scattering from proteins due to the hydrogen atoms, the scattering profile can be divided into three regions. These are the elastic, quasielastic, and inelastic regions. Inelastic scattering is due to the exchange of energy with vibrational modes in the molecule. Quasielastic scattering is the result of stochastic motions, such as intramolecular barrier crossing events and overdamped vibrational modes. Elastic scattering occurs when there is no exchange of energy between the neutrons and the sample. Generally, the more confined the atom is, the more intense its elastic scattering (Smith, 1991).

In the neutron scattering studies carried out on the enzyme cryosolvent solutions, the elastic scattering intensity was used as an indication of the protein dynamics at various temperatures. The quantity measured is the incoherent dynamic structure factor, $S(q,\omega=0)$, which is the space-time Fourier transform of the self-correlation function $G_s(r,t)$ which describes the correlation of the position, r, of an atom at time zero with the position of the same atom at time t (Cusack and Doster, 1990). For systems in which only harmonic vibrational motion is present, the elastic scattering follows the relationship that ln S(q,0) is proportional to q^2. If a

dynamical transition occurs involving the appearance of anharmonic motion, such as diffusion, a sharp decrease in the elastic intensity S(q,0) is seen at the temperature at which the transition occurs. For the neutron scattering experiments conducted the elastic scattering was used to calculate the average dynamical mean-square displacement, $\langle u^2 \rangle$, of the protein. A sharp decrease in the elastic intensity will be shown as an increase in $\langle u^2 \rangle$.

The measurement of momentum and energy transfers between the incident neutrons and the protein sample can be performed in various ways. The energy resolution of the spectrometers is an important characteristic in neutron scattering experiments. As the resolution is finite, the elastic peak is not a perfectly sharp line but has a characteristic width. The resolution is given as the full width half maximum (FWHM). The width of the peak, or resolution, is important as it determines the longest timescale of motions detectable by the instrument. Motions which are slower that those detectable will lead to quasielastic broadening of the elastic peak, which will be negligible compared to the characteristic instrumental elastic peak width (Smith, 1991). For example, the instruments IN6 and IN16 at the Institut Laue-Langevin (ILL) have energy resolutions of 50 meV and 1 meV, respectively (Ibel, 1994). This means that only motions faster than approximately 100 ps can contribute to the scattering from IN6, and motions faster than approximately 5 ns contribute to the scattering from IN16. This in turn determines the timescale of the motions that contribute to the average dynamical mean-square displacement calculated from each instrument.

3.5 Methods and Materials

3.5.1 Neutron Scattering

The experiments were performed on the thermophilic xylanase from Thermotoga sp. strain FjSS3-B.1 in a dry powder, in D_2O, and in single-phase water-solvent mixtures consisting of 40% CD_3OD/60% D_2O, 70% CD_3OD/30% D_2O, 40% DMSO/60% D_2O, and 80% DMSO/20% D_2O (all solvent percentages are given by volume). The equivalent mixed solvent solutions in the absence of protein were also examined.

The dynamic neutron scattering measurements were performed on the IN6 time-of-flight spectrometer at the Institut Laue-Langevin, Grenoble. The incident neutron wavelength was 5.12 Å, with an energy resolution of 50 μeV. All data were collected with the sample holder oriented at 135° relative to the incident beam. The samples were contained in aluminium flat-plate cells of 0.7 mm thickness for the protein-cryosolvent and 2 mm thickness for the cryosolvent solutions. The following protein solutions were run (with their measured transmission in parentheses): 68 mg/ml xylanase in 70% CD_3OD/30% D_2O (0.89); 68 mg.ml xylanase in 40% CD_3OD/60% D_2O (0.88); 51 mg/ml xylanase in 80% DMSO/20% D_2O (0.87); 68 mg/ml xylanase in 40% DMSO/60% D_2O (0.90); 100 mg/ml dry powder xylanase (0.98); and 100 mg/ml xylanase in D_2O (0.90). The dry powder was prepared by freeze drying and then holding at 100 milliTorr for 2 days at 200°C. The following perdeuterated solvents were run: 70% CD_3OD/30% D_2O (0.80); 40% CD_3OD/ 60% D_2O (0.79); 80% DMSO/20% D_2O (0.80); 40% DMSO/60% D_2O (0.86); and pure D_2O (0.82).

Samples were first cooled to 110 K and then heated up to 300 K in steps of 10 K. Raw data were corrected in identical fashion. The elastic intensity was determined by integrating the detector counts over the energy range of the instrumental resolution. The detectors were calibrated by normalizing with respect to a vanadium sample. The cell scattering was subtracted, taking into account attenuation of the singly scattered beam. Finally, the scattering was normalized with respect to that at the lowest measured temperature, 110 K.

At the end of each experiment, the activity of the enzyme preparation was checked to ensure that the enzyme was stable under the experimental conditions. Full activity was recovered confirming that no denaturation of the enzyme sample had occurred.

3.5.2 Differential Scanning Calorimetry

The DSC measurements were made using a Shimadzu DSC-60 differential scanning calorimeter, at the Thermal Methods Laboratory, Birkbeck College, London. The samples were sealed in 30 μl aluminium crucibles, with sample weights of approximately 10 mg. Helium was used as the purge gas of the

sample. All data were collected during heating at a standard rate of 10°C/minute. An empty crucible was used as the reference. The instrument was calibrated with respect to temperature with water and ammonium phosphate ($NH_4H_2PO_4$), which undergo a reversible phase transition at 0°C and –125°C, respectively. The peak area of the instrument was calibrated with an indium standard. As mentioned earlier, endothermic transitions are shown as a downward 'peak', while exothermic transitions are shown as an upward 'peak'.

Protein samples in various perdeuterated solvents were run. To prevent hydrogen-deuterium exchange occurring between the protein and the solvents, the protein samples were previously exchanged with deuterium. The protein samples were twice dissolved in D_2O (10 mg/ml), and then freeze-dried. To ensure exchange had reached equilibrium, the samples were left at room temperature for at least 12 hours. The following protein samples, all at 30 mg/ml, were run: xylanase in 40% CD_3OD/ 60% D_2O; xylanase in 70% CD_3OD/ 30% D_2O, xylanase in 40% DMSO/ 60% D_2O; and xylanase in 80% DMSO/D_2O. A glutamate dehydrogenase protein sample (60 mg/ml) was also run in the hydrogenated solvent 70% methanol/ 30% water.

3.5.3 Xylanase Methods

3.5.3.1 Xylanase assay

Xylanase was assayed by measuring the release of nitrophenol from *o*-nitrophenyl-β-D-xylopyranoside. The enzyme was routinely assayed in a reaction mixture containing 10 mM *o*-nitrophenyl-β-D-xylopyranoside, 10 mM sodium acetate/acetic acid buffer, pH 5.5, and enzyme, with a total assay volume of 100 µl. The reaction was stopped by the addition of 500 µl of ice-cold 1 M sodium carbonate, and the assays put on ice for at least two minutes. The absorbance at 420 nm was then read in plastic cuvettes.

For assays in cryosolvents, sodium acetate/acetic acid buffers giving a final pa_H of approximately 5.3 to 5.5, at the assay temperature, were used. The pH of the appropriate aqueous buffer at 20°C was determined from data compiled by Douzou and colleagues (1976). The assays were started by the addition of enzyme. For enzyme assays at 0°C the tubes were incubated on ice, for other

temperatures the assays were kept in insulated containers in fridges or freezers. Some assays below 0°C were incubated in a cooled methanol bath at the appropriate temperature. The assays were stopped by the addition of 500 µl of 3:5:2 (v/v) ethanolamine/DMSO/water, pre-cooled to below the assay temperature. The stopped assays were incubated at the assay temperature for at least 30 minutes to ensure complete cessation of activity, before being gradually warmed to room temperature.

3.5.3.2 HPLC determination of reaction products

The reaction products were determined by high-performance anion-exchange chromatography with pulsed amperometric detection (HPAE-PAD) (Dionex). A CarboPac PA1 Analytical (4 x 250 mm) column and guard (4 x 50 mm) column were used. All buffers were prepared with MQ water and certified 50% (w/w) sodium hydroxide (Fisher Scientific), purged with helium gas to remove dissolved carbon dioxide. The column was equilibrated with 20 mM sodium hydroxide. The eluent was kept at 20 mM sodium hydroxide for the first five minutes, followed by a linear gradient to 200 mM sodium hydroxide over ten minutes, and then maintained at this concentration for five minutes. A linear gradient from 200 mM to 20 mM sodium hydroxide was then run over five minutes, with conditions maintained at the lower concentration for a further ten minutes to ensure all compounds were eluted. A 50 µl sample was taken to fill a 25 µl sample loop. The sample was loaded at one minute through the gradient programme. Standards dissolved in MQ water and samples from various enzyme assays were run. Most samples were loaded directly unless previously diluted with MQ water to reduce the organic solvent concentration.

3.5.3.3 Electrospray mass spectrometry of reaction products

All electrospray mass spectrometry (ES-MS) measurements were carried out on a VG Platform II mass spectrometer (Fisons/Micromass) equipped with an electrospray interface. The samples were run under standard conditions with an injection volume of 10 µl, nitrogen gas as the drying agent, and methanol as the carrier solvent, at a flow rate of 0.02 ml/minute. Positive ion scans were run, with a cone voltage of 160 V. Data was collected for approximately one minute, at a scan rate of 1.5 seconds/scan, and then averaged to give the final relative peak

intensities. Sodium chloride was added to the samples, to improve the signal to noise ratio of the samples (Skinner and Manley-Harris, personal communication). The assay samples were injected directly without removal of the enzyme, as it did not interfere in the spectrum. When a time course of the reaction was performed, it was assumed that the reaction would cease upon injection in to the ES-MS, obviating the need for a stopping reagent.

3.6 Results

3.6.1 Effect of Solvents on Protein Dynamics

The effect of varying solution composition on the picosecond time-scale dynamics of the enzyme xylanase was investigated by dynamic neutron scattering (Réat et al., 2000a). The enzyme xylanase was chosen, because a significant amount of cryoenzymology work had previously been done with this enzyme (Dunn, 1998; Dunn et al., 2000). A summary of the main experimental results shall be given here, with full details and figures available in the attached paper (Appendix B).

The dynamic neutron scattering experiments were performed on dry xylanase powder, xylanase in D_2O, xylanase in 40%/60% and 80%/20% deuterated DMSO/D_2O, and xylanase in 40%/60% and 70%/30% CD_3OD/D_2O. The corresponding perdeuterated solvents were also analysed. As mentioned earlier, only motions faster than 100 ps contribute to the calculated mean-square displacement of the atoms.

For the dry powder sample only a small increase in the cross section-weighted average mean-square displacement, $\langle u^2 \rangle$, with temperature over the range examined (100 K to 300 K) was seen. The major component of this $\langle u^2 \rangle$ is expected to be due to small-amplitude, solid-like, vibrational dynamics. The possibility of a small contribution from anharmonic motions cannot be excluded. A marked transition in the neutron scattering data was not observed for this sample, as obtained with previous work on other enzymes (Ferrand et al., 1993).

The general shape of the integrated elastic intensity, $S_{INT}(T)$, for the xylanase in D_2O resembled that for the pure D_2O sample. A gradual decrease with temperature was seen from 110 K to 280 K, with a sharp transition occurring due

to melting of the solution. At the transition point there is a strongly nonlinear increase of $\langle u^2 \rangle$ with temperature, which is consistent with the activation of anharmonic picosecond dynamics. The transition is seen to be less steep and begin at a slightly lower temperature (approximately 270 K) for the xylanase in D_2O sample, compared to the pure D_2O sample (approximately 280 K). This suggests that the protein acts to depress the freezing point of the solution.

The dynamic behaviour for both the enzyme-cryosolvent and pure cryosolvent samples is different compared to the D_2O samples. For the cryosolvent samples the decrease of $S_{INT}(T)$ with temperature is much more gradual. The dynamics of the protein solutions approximately follow that of the pure solvents. In the protein-cryosolvent solutions, large-amplitude anharmonic dynamics are activated at significantly lower temperatures than in the protein-D_2O sample, as observed from a plot of $\langle u^2 \rangle$ versus temperature. The $\langle u^2 \rangle$ data in the four protein-cryosolvent systems are essentially identical, with the activation of anharmonic motion seen near 230 K. The increase of $\langle u^2 \rangle$ with temperature is much more gradual, resembling that observed with hydrated protein powders (Doster et al., 1989).

From DSC and synchrotron X-ray diffraction measurements, it was confirmed that the melting temperatures of the perdueterated cryosolvents agreed with published results for the equivalent hydrogenated solvents (Douzou et al., 1976; Weast, 1974). The melting temperature was found to be between 170-190 K for the 70% CD_3OD/30% D_2O cryosolvent, and near 235 K for the remaining cryosolvents. Therefore, for three of the four enzyme-cryosolvent samples, the dynamical transition is seen to occur at approximately the same temperature as their phase transition. However, for the enzyme in 70% CD_3OD/D_2O, no activation of anharmonic motion is observed near the highest melting point of 190 K, but occurs at the higher temperature of approximately 230-235 K. There is therefore remarkably little difference in the picosecond dynamics of the enzyme-cryosolvent samples, despite greatly different compositions, water contents and highest melting points.

These results show that for various protein-solvent samples the dynamic transition is strongly coupled to the melting of pure water, but is relatively invariant in

cryosolvents of differing compositions and melting points. As already mentioned, the transition itself is also more gradual in the protein-cryosolvent solutions than in the D_2O samples. It would therefore be interesting to see how the dynamic behaviour varied with cosolvent concentration, and if there was a change to the sharp D_2O transition behaviour at a particular cosolvent concentration.

3.6.2 DSC Studies of Enzyme-Cryosolvent Solutions

The effect of high protein concentrations on the phase transitions of cryosolvents was investigated by DSC. The resulting DSC curves for deuterated xylanase in various perdeuterated cryosolvents are shown in Figures 3.2 to 3.5. The cryosolvents chosen were the same as those used in the neutron scattering studies of xylanase-cryosolvent solutions. The DSC curve obtained for glutamate dehydrogenase in the hydrogenated solvent 70% methanol/30% water is shown in Figure 3.6. The DSC curves obtained for the corresponding straight cryosolvents are also shown to enable easy comparison. Only the relative positions of the thermal transitions should be compared, as the thermograms have not been normalised with respect to sample weight.

For xylanase in 40% CD_3OD/60% D_2O there is a broad exothermic peak at -110°C, followed by a sharp endothermic peak at –100°C (Figure 3.2). These transitions are probably due to crystallisation followed by melting as the temperature is increased. It is interesting to note that the beginning of the exothermic transition coincides with a potential glass transition at –115°C in the pure cryosolvent sample. An endothermic transition near –100°C is also seen in the DSC curve of the straight cryosolvent. There is also a broad endothermic transition seen near –28°C, which is also observed in the DSC curve for 40% CD_3OD/60% D_2O, and is probably due to melting of the sample. The broadness of the transition may be due to inadequate sample sealing, and should probably be resealed to confirm this.

For xylanase in 70% CD_3OD/D_2O there is a potential glass transition at –115°C, seen as a small shift in the baseline, followed by an endothermic peak near -101°C, which is probably due to melting of the sample (Figure 3.3). A potential glass transition was not observed for the pure cryosolvent sample, although DSC does not easily detect such transitions. The endothermic peak at –101°C was

reflected in the pure solvent sample, although a double endothermic peak was observed. The equivalent hydrogenated solvent 70% CH_3OH/H_2O gave a similar DSC curve in the presence of glutamate dehydrogenase, even though the protein concentration was double that of the xylanase solution (Figure 3.6). A double endothermic peak was observed near -100°C, which again is probably due to melting in the sample. A broad endothermic transition for the hydrogenated cryosolvent was also observed at a similar temperature of -101°C.

For xylanase in 40% deuterated DMSO/60% D_2O there is an endothermic peak at -120°C, which may have an associated shift in baseline. This is followed by a broad endothermic transition at -28°C, which is probably due to melting in the sample (Figure 3.4). The DSC curve for the pure cryosolvent is very similar, with only the initial endothermic transition observed at a slightly lower temperature of -124°C. The two endothermic peaks observed for the protein-cryosolvent sample are known to be reversible, as they were still detected after a further cool/heat cycle of the sample.

For xylanase in 80% deuterated DMSO/20% D_2O an endothermic transition was seen at –121°C, again at a slightly higher temperature than the corresponding transition in the pure cryosolvent DSC curve (Figure 3.5). There is also a potential change in heat capacity, as shown by a shift in the baseline, near -100°C. It is difficult to know if a similar transition is present in the pure cryosolvent sample, as the baseline is very noisy around this temperature. A broad endothermic transition is also observed, with the peak centered at –20°C. The temperature of this transition is significantly different to that observed for 80% deuterated DMSO/20% D_2O, where the peak of the transition is at a lower temperature of –27°C.

Overall, the thermal transitions occurred at essentially the same temperature for the protein-cryosolvent samples as the corresponding straight cryosolvent solutions. This is in agreement with X-ray diffraction experiments, where the addition of glutamate dehydrogenase (60 mg/ml) was found not to affect the crystallisation or phase separation of the various cryosolvents (Réat et al., 2000b). The only exception was for 50% acetone/30% ethanediol/20% water, where the presence of protein eliminated the slight crystallisation observed at approximately

–125°C. This is interesting, as one of the few significant changes observed upon addition of protein was the appearance of an exothermic transition most likely due to crystallisation in the sample, for 40% CD_3OD/D_2O. The other significant change observed was the shift of a broad endothermic transition from near –27°C to near –20°C for 80% deuterated DMSO/20% D_2O upon addition of enzyme. It might be worthwhile to repeat the sample to ensure this result is reproducible, as this effect was not seen for any of the other cryosolvent compositions.

It would be interesting to further characterise the protein-cryosolvent solutions by the DMTA technique, as it is able to detect glass transitions more easily. This would perhaps allow more subtle changes in thermal properties to be detected.

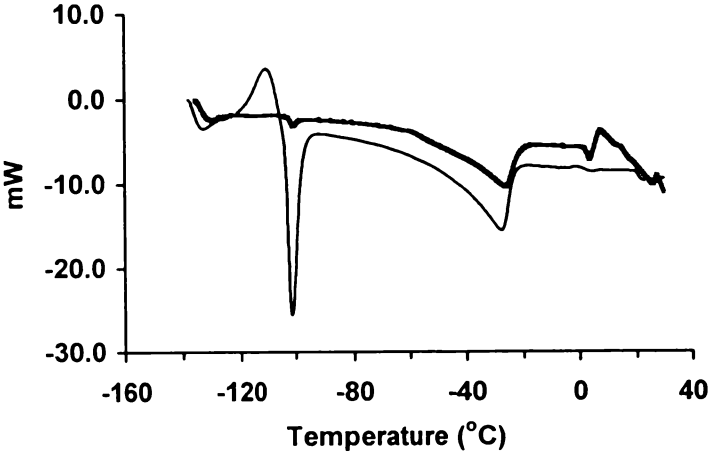

Figure 3.2. DSC curve for xylanase dissolved in 40% CD_3OD/60% D_2O to a final concentration of 30 mg/ml and for 40% CD_3OD/D_2O as a comparison (thicker line).

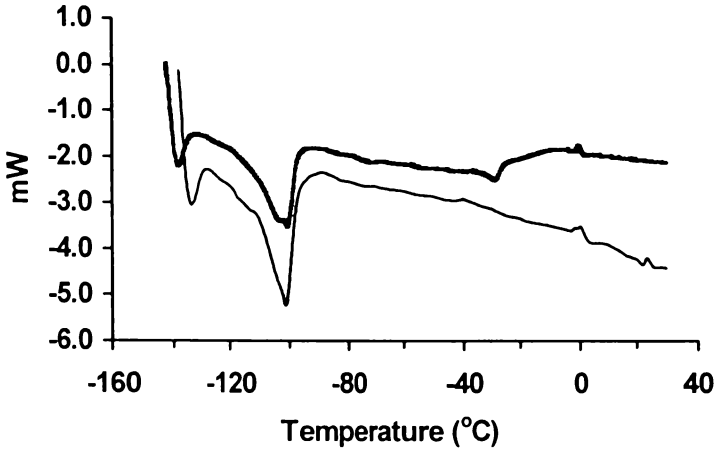

Figure 3.3. DSC curve for xylanase dissolved in 70% CD_3OD/30% D_2O to a final concentration of 30 mg/ml and for 70% CD_3OD/D_2O as a comparison (thicker line).

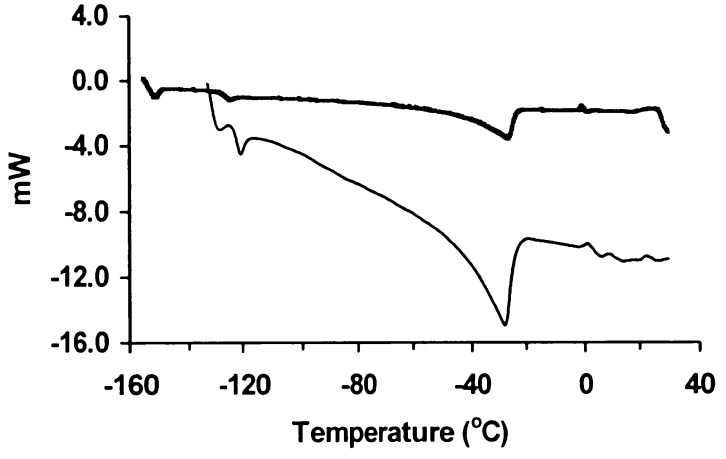

Figure 3.4. DSC curve for xylanase dissolved in 40% deuterated DMSO/60% D_2O to a final concentration of 30 mg/ml and for 40% deuterated DMSO/60% D_2O as a comparison (thicker line).

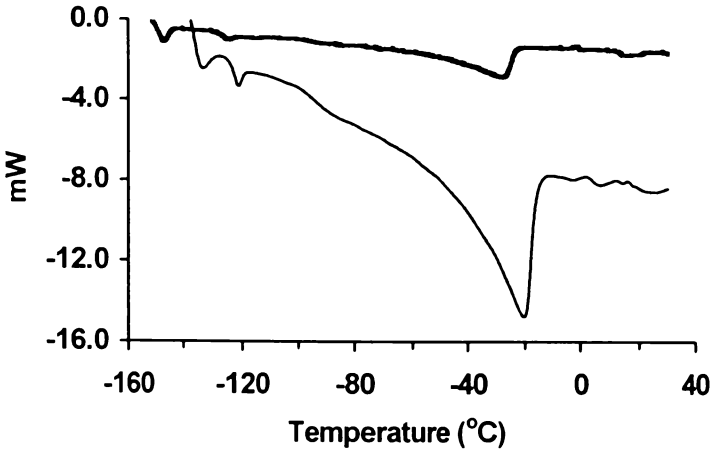

Figure 3.5. DSC curve for xylanase dissolved in 80% deuterated DMSO/20% D_2O to a final concentration of 30 mg/ml and for 80% deuterated DMSO/20% D_2O as a comparison (thicker line).

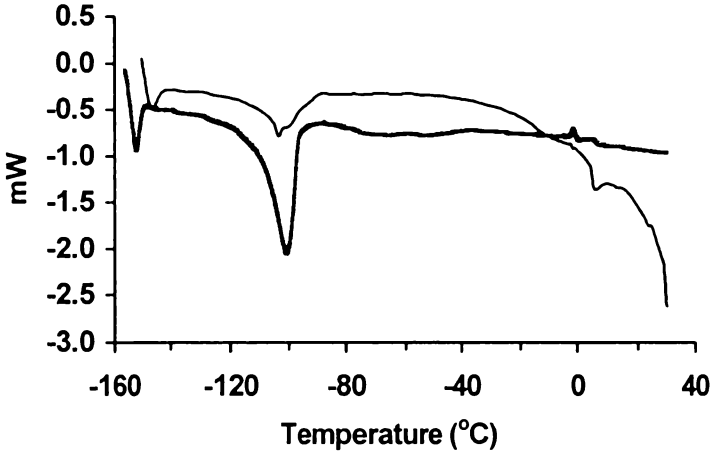

Figure 3.6. DSC curve for glutamate dehydrogenase dissolved in 70% CH_3OH/30% H_2O to a final concentration of 60 mg/ml and for 70% CH_3OH/30% H_2O as a comparison (thicker line).

3.6.3 Effect of Solvents on Xylanase

Since it was found that the protein dynamics were significantly different in cryosolvent as compared to aqueous conditions, it was decided to investigate further the effect of solvents on enzyme activity. The effect of increasing methanol concentration on xylanase activity was investigated. It was thought that a change in the picosecond dynamics with solution composition might be reflected in the activity data. The stability of xylanase in the cryosolvents used in the above neutron scattering work was also determined.

3.6.3.1 Stability of xylanase in cryosolvents

The stability of xylanase in the various cryosolvents used in the neutron scattering experiments was investigated. From previous studies, it was shown that no significant loss of activity occurs when the enzyme is incubated at 0°C in the various cryosolvents over a 12 hour period (Dunn, 1998). This is important for the neutron scattering experiments, as it demonstrates that the protein is stable in the cryosolvents, even after the relatively long data collection times required. In this work, the stability of xylanase in the cryosolvents was determined at higher temperatures to enable potential differences to be distinguished.

For stability determinations at 50°C, the enzyme in the appropriate cryosolvent was incubated in small diameter plastic tubes, covered with parafilm, in a total volume of 200 µl. At the required time intervals tubes were removed from the 50°C water bath and put on ice. Aliquots were then removed and assayed for remaining activity at 80°C by the routine assay method. A similar procedure was used to determine the stability of xylanase in 40% DMSO/60% H_2O, as evaporation of the sample was not significant. However, when stability assays were conducted at 60°C in 40% methanol/60% H_2O, the samples had to be sealed in glass capillary tubes to prevent evaporation. The capillaries were filled with 50 µl samples, and completely immersed in an oil bath at the required temperature. The capillaries were put on ice at the appropriate time intervals. A 10 µl aliquot was then taken and assayed for remaining activity. The percentage remaining activity is relative to a zero time sample, taken before the enzyme-cryosolvent solutions were heated at the required temperature. The results are shown in Figures 3.7 to 3.9.

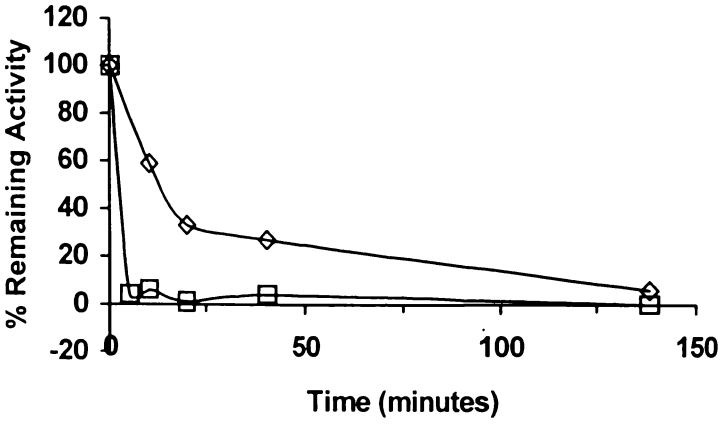

Figure 3.7. Xylanase stability in 70% methanol/30% water (◇) and 80% DMSO/20% water (□) at 50°C.

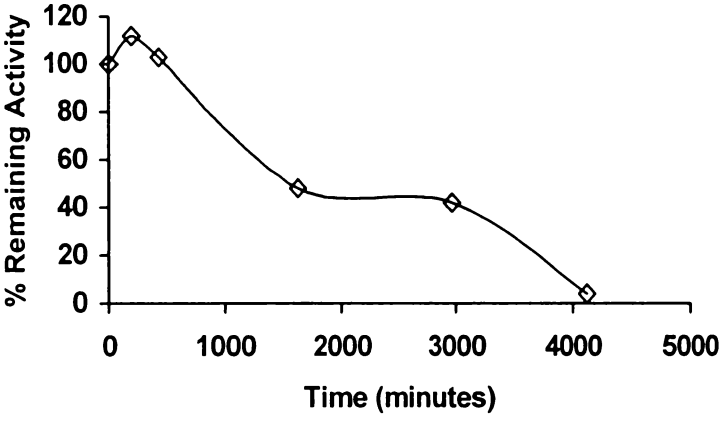

Figure 3.8. Xylanase stability in 40% methanol/60% water at 60°C.

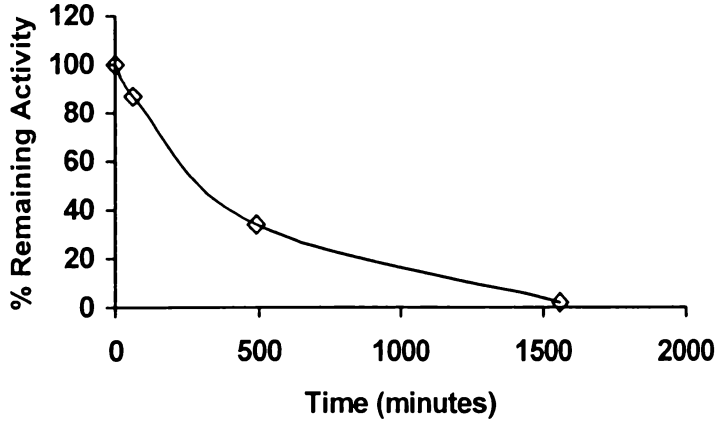

Figure 3.9. Xylanase stability in 40% DMSO/60% water at 80°C.

For all of the above temperatures, an aqueous enzyme control showed no loss of activity during the time of incubation. This agrees with the reported half-life of xylanase in water, which is found to be greater than 20 hours at 95°C (Thompson,

personal communication). The half-lives were calculated to be approximately: 20 minutes at 50°C in 70% methanol/30% water; less than two minutes at 50°C in 80% DMSO/20% water; 18 hours at 60°C in 40% methanol/60% water; and 6 hours at 80°C in 40% DMSO/60% water. It is clear that as the cosolvent concentration increases, the xylanase stability decreases. The enzyme also appears to exhibit greater stability in methanol-based cryosolvents compared to DMSO-based cryosolvents. The temperature dependence of solution properties would be different for each of the cryosolvents, and may account for some of the variation in stability observed at higher temperatures.

Another possibility is that the solvent may be perturbing the shell of molecules closest to the protein thereby potentially destabilising the enzyme. As the stability results vary with cryosolvent composition, it suggests that the solvent shell may be different for each of the samples. There is some evidence that non-water solvent molecules do interact with the protein surface directly (Ringe, 1995; Lehmann et al., 1985; Lehmann and Stansfield, 1989). However, from the similarity in the dynamic neutron scattering results for the various xylanase-cryosolvent solutions, it was suggested that perhaps the solvent shell is qualitatively similar for each of the cryosolvents (Réat et al., 2000a).

3.6.3.2 Effect on catalytic properties

The effect of increasing methanol concentration on the catalytic properties of xylanase was investigated. This work was conducted using the chromogenic substrate *o*-nitrophenyl-β-D-xylopyranoside (ONP-xylose). Lineweaver-Burke plots of the data were graphed to ensure that Michaelis-Menten kinetics was followed. The kinetic parameters, K_M and V_{max}, were determined from Direct Linear plots of the data. The results are presented in Tables 3.1 to 3.2, and plotted in Figures 3.10 to 3.11. The V_{max} values are expressed as percentage activity values in the data shown in Table 3.2, and as log (percentage activity) values in Figure 3.11.

Table 3.1. Effect of temperature and solution composition on the K_M (mM) values for *o*-nitrophenyl-β-D-xylopyranoside of xylanase.

	Temperature (°C)				
Solution Composition (v/v)	**-22**	**0**	**8**	**15**	**30**
100% Water		0.41	0.35	1.1[a]	1.05
2% Methanol		3.2	2.23	2.25	1.0
5% Methanol		3.51	3.36	2.8	2.1
10% Methanol		3.13	2.35	4.8	3.8
15% Methanol		3.15	2.09		6.5
20% Methanol		3.7	6		12
30% Methanol	1.96	3.78			16
40% Methanol	2.17	7.5	12.15		29.6
50% Methanol	4.84	7.8			21.8
70% Methanol	15.57	21.5	16		
80% Methanol	25.2	23.77			

Table 3.2. Effect of temperature and solution composition on Vmax for *o*-nitrophenyl-β-D-xylopyranoside of xylanase. V_{max} is expressed as percentage activity values, where 100% activity corresponds to 0.56 μmole/min/mg.

	Temperature (°C)		
Solution Composition (v/v)	**0**	**8**	**30**
100% Water	100	169	1778
2% Methanol	245	398	1659
5% Methanol	257	549	2290
10% Methanol	257	489	3467
15% Methanol	223	478	4570
20% Methanol	275	724	8128
30% Methanol	251		6309
40% Methanol	281	776	7244
50% Methanol	251		4786
70% Methanol	234	616	5128
80% Methanol	266		

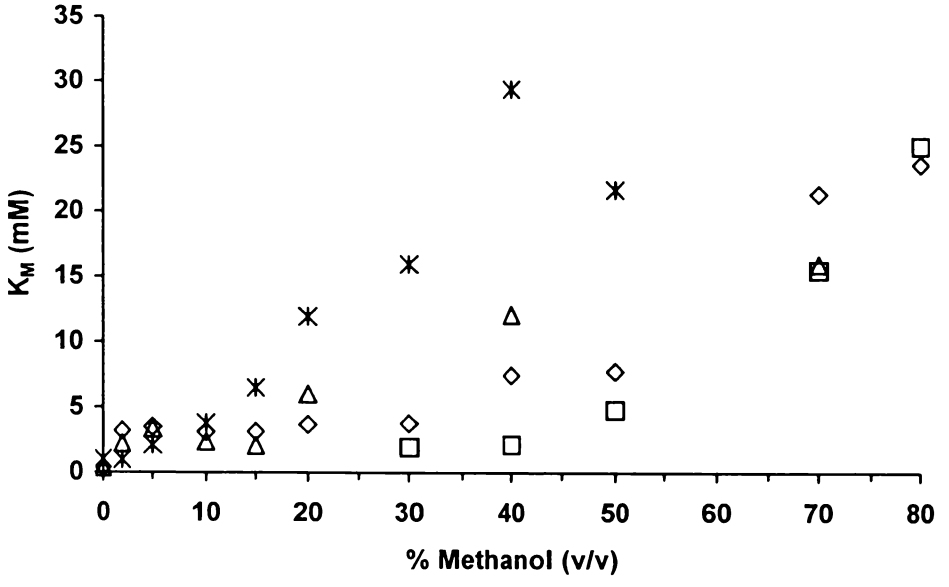

Figure 3.10. Effect of methanol concentration on the K_M (mM) for *o*-nitrophenyl-β-D-xylopyranoside of xylanase at –22°C (□), 0°C (◇), 8°C (△) and 30°C (∗).

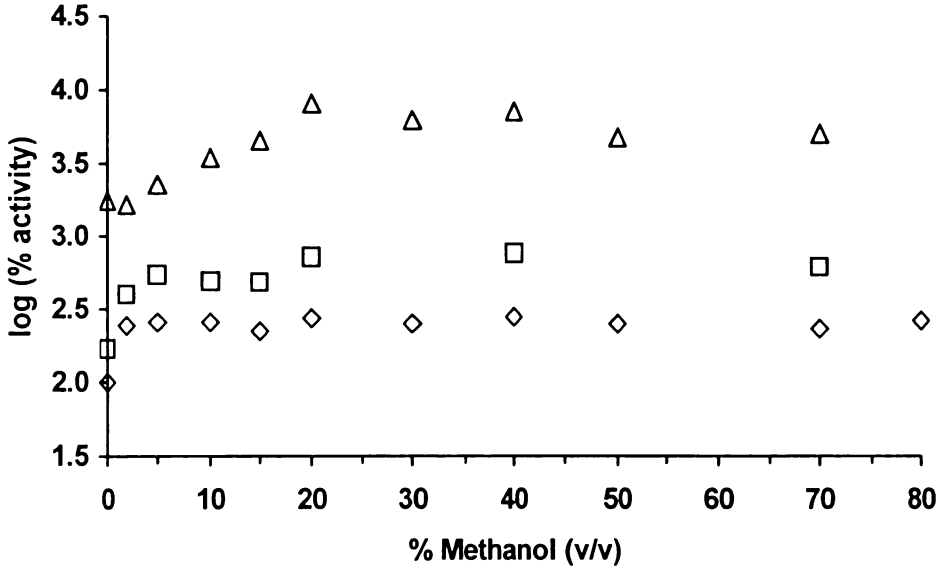

Figure 3.11. Effect of methanol concentration on the activity of xylanase for *o*-nitrophenyl-β-D-xylopyranoside, at 0°C (◇), 8°C (□) and 30°C (△). The activity is expressed as the percentage residual activity corresponding to activity in aqueous solution at 0°C. 100% activity corresponds to 0.56 μmole/min/mg.

From the data several trends can be seen in the effect of solution composition on K_M. As the organic solvent concentration increases, the K_M value increases. However, the change in K_M value with methanol concentration does not exhibit the same behaviour at each temperature. The K_M values display biphasic behaviour, with the transition point occurring at lower methanol concentrations

with increasing temperature. For example, at –22°C the transition in behaviour occurs between 40% to 50% methanol, whereas at 8°C the transition occurs between 15% to 20% methanol. This varying effect with temperature could be due to changes in the solution properties being temperature dependent.

A possible explanation for the general trend of increasing K_M values with methanol concentration could be due to the organic cosolvent exerting a negative effect on substrate binding. This is probably due to a hydrophobic partitioning effect, with the substrate having a reduced affinity for the active site compared to the aqueous system. Such an effect is predicted to result in an exponential increase in K_M values, so that plots of log K_M versus cosolvent concentration are linear (Fink and Geeves, 1979). Obviously, such an effect will be complicated if other factors are contributing to the changes in substrate affinity. When the data for 30°C is plotted as log K_M versus methanol percentage, a linear relationship is observed up to a concentration of 20% to 30%, as shown in Figure 3.12. The data does not follow this relationship at higher methanol concentrations. This may be due to the enzyme not being fully saturated with substrate under these conditions. However, such a relationship is not seen with the 0°C data, also graphed in Figure 3.12. This could be due to the complication that more than one factor is contributing to the observed changes in substrate affinity.

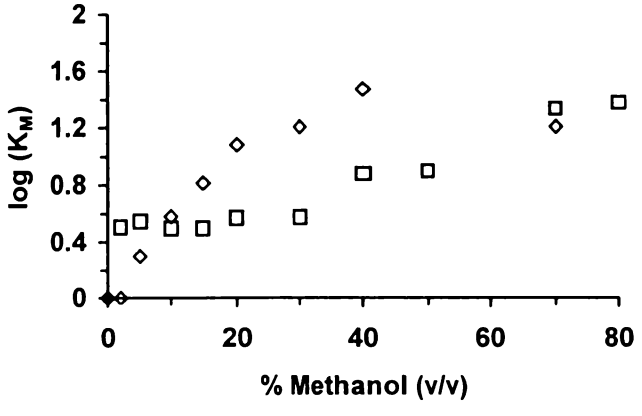

Figure 3.12. Plot of log K_M (mM) versus methanol concentration for xylanase at 0°C (□) and 30°C (◇).

There is also a general trend towards higher K_M values with increasing temperature. Some of the data is graphed in Figure 3.13 to illustrate this trend. The increase in K_M values is particularly evident for methanol concentrations of

15% and higher. However, for methanol concentrations of 5% and lower, excluding the aqueous solution, the K_M values actually decrease with temperature, and at 10% methanol they remain approximately equal with temperature. The cause of the change in K_M behaviour from low to high methanol concentrations is unknown. A change in K_M values with temperature can be due to several reasons, and is not specific to organic solvent-water solutions. A change in temperature could produce a change in the state of ionisation of groups on the enzyme, modifying the affinity for the substrate due to a change in structure of the enzyme, or the ionisation of catalytic residues involved in substrate binding. An increase in the apparent Michaelis-Menten constant has also been observed with a number of other enzymes, including the muscle-type lactate dehydrogenase (Somero, 1995).

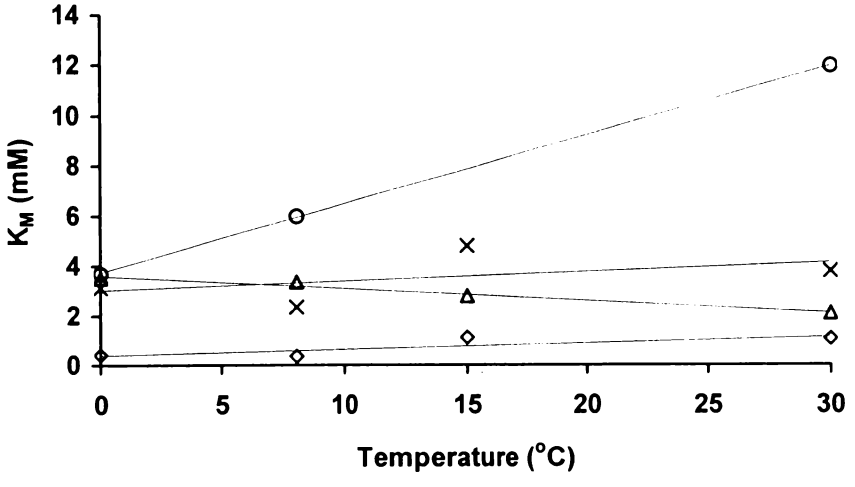

Figure 3.13. Effect of temperature on the K_M (mM) for *o*-nitrophenyl-β-D-xylopyranoside of xylanase, with a methanol concentration of 0% (◇), 5% (△), 10% (×) and 20% (○).

The effect of methanol concentration on V_{max} is subtler than that for the K_M values. At 0°C and 8°C the Vmax shows an initial increase in value from the aqueous solution to 2% methanol, after which it remains essentially constant. At the higher temperature of 30°C, a more gradual increase in V_{max} values with methanol concentration is seen. The expected trend towards a greater catalytic rate with increasing temperature is also observed. These trends are illustrated in Figure 3.11. A change in the reaction rate with cosolvent concentration could be due to several reasons. Most of the effects caused by the presence of organic solvents, as discussed in the introduction, would be expected to lead to a decrease

in activity. It would seem unlikely that a change in, for example, the enzyme structure would lead to a more efficient catalyst. Two possibilities that could lead to an increase in V_{max} are that either the rate-determining step of the reaction is changing, or a change in mechanism is occurring upon addition of methanol to the enzyme assay.

From the above results, a change in the temperature dependence of the K_M values is seen at approximately 5% methanol, and an increase in the V_{max} values is seen at only 2% methanol. From the dynamic neutron scattering results on the protein-cryosolvent solutions, a change in dynamic behaviour was seen on moving from the D_2O-protein solution to the cryosolvent-protein solutions. It may be that either of the observed effects on the catalytic properties is related to a change in the dynamics of the enzyme upon addition of methanol. If this is so, it suggests that only 2% to 5% methanol is required to cause a change in the dynamic properties of the enzyme.

3.6.3.3 Effect on reaction mechanism

From the results of the effect of methanol concentration on the catalytic properties of the reaction of xylanase on *o*-nitrophenyl-β-D-xylopyranoside, it was decided to investigate the effect of methanol on the reaction mechanism. From the reaction mechanism proposed for aryl-xylosides of other enzymes, as well as the possibility of glycosyl transfer to the methanol, it was expected that multiple reaction products would be formed. The reaction products of xylanase activity in both cryosolvents and aqueous solution were determined by a combination of HPAE-PAD and ES-MS.

Initially, the products formed from xylanase activity in aqueous solution and in a 10% methanol solution, at 0°C, were compared qualitatively by HPAE-PAD. Three new unidentified peaks were seen in the chromatogram of the 10% methanol assay. A time course of the reaction was then performed to ensure that the observed peaks were actually products, and not artifacts due to the inclusion of methanol in the reaction. The three peaks were seen to increase in intensity with time, suggesting that they were in fact new products of the reaction. An overlay of the early part of the chromatograms is shown in Figure 3.14, with the relevant peaks occurring at 2, 2.7, and 4.1 minutes. The detection of new products in the

10% methanol assay indicated that methanol was probably involved in the reaction mechanism, either as a new substrate or by changing the reaction pathway. The products of the reaction in both aqueous solution and in the presence of methanol cosolvent were then characterised.

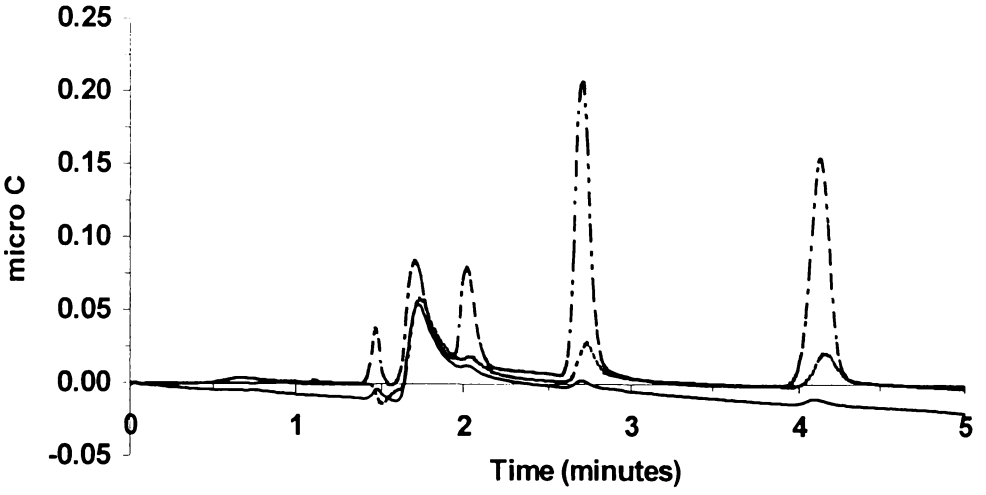

Figure 3.14. Time course of xylanase activity in 10% methanol on *o*-nitrophenyl-β-D-xylopyranoside at 0°C, as determined by ES-MS. The overlaid chromatograms are for the following assay times: 1 minute (—), 35 minutes (....), and 270 minutes (..-..-).

Reactions were followed by the production of *o*-nitrophenol (absorbance at 420 nm), but neither HPAE-PAD nor ES-MS was able to resolve this compound. Variations in cone voltage and ion mode with the ES-MS failed to enable detection of the standard *o*-nitrophenol. The production of xylose was also difficult to quantify, due to high background levels in the chromatogram of the ONP-xylose control when detected by HPAE-PAD. This may be due to degradation of the substrate in the alkaline conditions of the eluent buffers, as opposed to high contaminating levels of xylose in the substrate. This is supported by the ES-MS results, as when a similar sample was analysed only insignificant amounts of xylose were observed.

When a 0°C aqueous assay sample was analysed by HPAE-PAD, xylobiose and xylotriose were detected as reaction products, as well as remaining substrate ONP-xylose. A significant peak due to xylose was also detected. When a similar sample was run on the ES-MS the following compounds were detected: ONP-xylose, xylobiose, xylotriose, ONP-xylobiose, and ONP-xylotriose. The ES-MS

and HPAE-PAD results for the aqueous xylanase assays are shown in Figures 3.15 and 3.16, respectively. The peaks in the HPAE-PAD chromatogram were identified by standards run under similar conditions. A number of standards were run to help identify the compounds detected by ES-MS, the results are shown in Table 3.3. For the products where a standard was unavailable, the calculated *m/z* values were used as identification based upon the expected behaviour of these molecules. The compounds identified in the ES-MS of the aqueous assay sample are shown in Table 3.4.

Table 3.3. ES-MS results of standards run in positive ion mode.

Compound	MW	*m/z*	Ion
Xylose	150	173.8	$[Xyl{\cdot}Na^+]^+$
		323.6	$[2Xyl{\cdot}Na^+]^+$
Methyl xylose	164.2	187.8	$[MeXyl{\cdot}Na^+]^+$
		351.3	$[2MeXyl{\cdot}Na^+]^+$
ONP-xylose	271.2	294.4	$[ONPXyl{\cdot}Na^+]^+$
		565.2	$[2ONPXyl{\cdot}Na^+]^+$
Xylobiose	282	305.6	$[Xyl_2{\cdot}Na^+]^+$

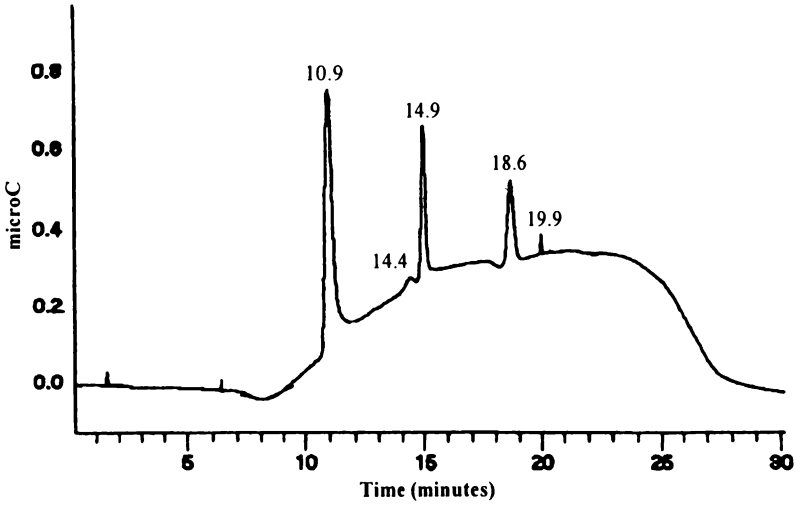

Figure 3.15. HPAE-PAD chromatogram obtained for an aqueous xylanase assay, conducted at 0°C, with *o*-nitrophenyl-β-D-xylopyranoside as the substrate. The peaks identified in order of increasing retention time are: xylose, ONP-xylose, xylobiose, xylotriose, and xylotetraose.

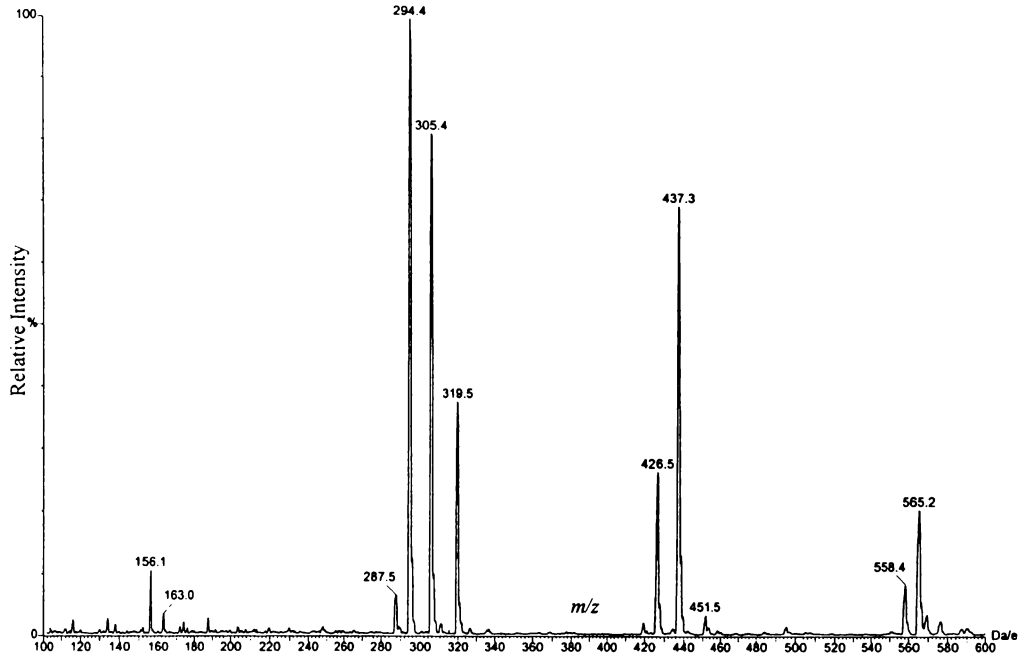

Figure 3.16. Positive ion ES-MS spectrum of xylanase reaction products from an aqueous assay at 0°C. The molecular ions with a *m/z* value of 319.5 and 451.5 are contaminants from a previous sample.

The fact that peaks corresponding to ONP-xylobiose and ONP-xylotriose were not seen in the HPAE-PAD chromatogram, could be due to the degradation of these compounds to xylobiose and xylotriose, respectively. When a time course of the reaction was performed, ONP-xylobiose was initially detected, with xylobiose and xylotriose becoming the main reaction products, as seen in Figure 3.16. If higher xylooligosaccharides were produced, they would not have been detected due to the *m/z* range being examined. From the initial production of ONP-xylobiose and the absence of xylose as a product, it seems likely that xylanase is degrading the ONP-xylose substrate by a transglycosylation reaction as the first step. This would agree with the mechanism of degradation for aryl-xylosides found for other family 10 xylanases (Biely et al., 1997; Biely et al., 1980).

From the results it is impossible to know the exact reaction pathway, but it is known that glycosyl transfer reactions occur to produce larger oligosaccharides than the starting substrate. The initial series of reactions are probably as shown below.

$$\text{ONP-Xyl} + \text{ONP-Xyl} \rightarrow \text{NPh} + \text{ONP-Xyl}_2$$

$$\text{ONP-Xyl} + \text{ONP-Xyl}_2 \rightarrow \text{NPh} + \text{ONP-Xyl}_3$$

Where ONP-Xyl, NPh, ONP-Xyl_2 and ONP-Xyl_3 stand for *o*-nitrophenyl-β-D-xyloside, *o*-nitrophenol, *o*-nitrophenyl-β-D-xylobiose and *o*-nitrophenyl-β-D-xylotriose, respectively. The ONP-Xyl_2 and ONP-Xyl_3 formed, as well higher aryl-xylooligosaccharides not shown, could then be hydrolysed to give xylobiose and xylotriose, also detected in the assay reaction. It is also possible that the xylooligosaccharides formed, which are hydrolysable by the enzyme, could serve as glycosyl donors with further substrate molecules acting as the acceptors. These reactions are shown below.

$$\text{ONP-Xyl}_2 \rightarrow \text{NPh} + \text{Xyl}_2$$

$$\text{ONP-Xyl}_3 \rightarrow \text{NPh} + \text{Xyl}_3$$

$$\text{ONP-Xyl} + \text{Xyl}_3 \rightarrow \text{Xyl}_2 + \text{ONP-Xyl}_2$$

Table 3.4. Xylanase aqueous assay products assigned from positive ion ES-MS.

m/z	Ion	Compound
294.4	$[ONPXyl{\cdot}Na^+]^+$	ONP-xylose
305.4	$[Xyl_2{\cdot}Na^+]^+$	Xylobiose
426.6	$[ONPXyl_2{\cdot}Na^+]^+$	ONP-xylobiose
437.3	$[Xyl_3{\cdot}Na^+]^+$	Xylotriose
558.4	$[ONPXyl_3{\cdot}Na^+]^+$	ONP-Xylotriose
565.2	$[2ONPXyl{\cdot}Na^+]^+$	ONP-Xylose

When the same assay was run in the presence of methanol new products were detected, as mentioned above. It is known that glycosyl transfer to alcohols occurs, with the alcohol acting as the attacking nucleophile of the covalent enzyme-saccharide intermediate instead of water. In this case the end products would be methylated saccharides. When a standard of methyl-β-D-xylopyranoside (Me-Xyl) was run on the HPAE-PAD, the resulting peak on the chromatogram eluted at the same time as the earliest new product peak. The remaining unidentified products of the chromatogram were hypothesised to be methyl-xylobiose and methyl-xylotriose. To confirm the identity of these products, as well as to detect other assay products, samples were analysed by ES-MS. The assigned compounds are shown in Table 3.5. As can be seen, molecular ions with the appropriate *m/z* values for methyl-xylobiose and methyl-xylotriose are

identified, supporting the identification of these compounds as the new products in the presence of methanol. The following products were detected by ES-MS: ONP-xylose, ONP-xylobiose, ONP-xylotriose, methyl-xylose, methyl-xylobiose, methyl-xylotriose, xylobiose, and xylotriose. As with the aqueous assays, the first product to reach a detectable level was ONP-xylobiose, with a *m/z* value of approximately 426. The main product of the reaction was methyl-xylobiose. A series of ES-MS results are given in Figures 3.17 to 3.19, which show the production of various products with time, for an assay run at 0°C in 20% methanol.

When the methanol content of the assay was varied the amount of methylated products formed, as detected by HPAE-PAD, was seen to increase qualitatively with the methanol concentration. Also the amount of methyl-xylotriose produced was seen to decrease with both assay time and methanol concentration. It may be that this product was further degraded, therefore never accumulating in the assay reaction.

Due to the large number of products formed in the reaction, it is difficult to propose a detailed reaction pathway from these results. Some further trials were conducted to try and eliminate some reaction possibilities. When an aqueous enzyme assay was conducted at 0°C, in the presence of either methyl-xylose (4 mg/ml) or methyl-xylose and xylose (both at 4 mg/ml), no reaction was seen to occur as analysed by HPAE-PAD. Also, the inclusion of 10% methanol with methyl-xylose (4 mg/ml) did not lead to any reaction. However, when an aqueous assay was conducted at 0°C on ONP-xylose with the inclusion of methyl-xylose (4 mg/ml), the production of methyl-xylobiose was detected by HPAE-PAD, suggesting that methyl-xylose can be involved in further reactions, leading to incorporation into new products.

From these results, it is likely that the enzyme reaction on ONP-xylose in the presence of methanol proceeds initially via the same glycosyl transfer reactions as for aqueous assays, with the later reactions involving either water or methanol as the attacking nucleophile. These reactions are summarized below.

$$\text{ONP-Xyl} + \text{ONP-Xyl} \rightarrow \text{NPh} + \text{ONP-Xyl}_2$$

$$\text{ONP-Xyl} + \text{ONP-Xyl}_2 \rightarrow \text{NPh} + \text{ONP-Xyl}_3$$

$$ONP\text{-}Xyl_2 + H_2O \rightarrow NPh + Xyl_2$$

$$ONP\text{-}Xyl_2 + MeOH \rightarrow NPh + Me\text{-}Xyl_2$$

$$ONP\text{-}Xyl_3 + MeOH \rightarrow NPh + Me\text{-}Xyl_3$$

$$ONP\text{-}Xyl + Xyl_3 \rightarrow Xyl_2 + ONP\text{-}Xyl_2$$

$$Me\text{-}Xyl + Xyl_3 \rightarrow Xyl_2 + Me\text{-}Xyl_2$$

The low concentration of methyl-xylotriose may be due to further degradation of this product. It is not known from these results what is the preferred bond of cleavage for this substrate. The suggested reactions below assume that the scissile bond is the first glycosidic linkage from the reducing end of the substrate.

$$Me\text{-}Xyl_3 + H_2O \rightarrow Me\text{-}Xyl + Xyl_2$$

$$Me\text{-}Xyl_3 + MeOH \rightarrow Me\text{-}Xyl + Me\text{-}Xyl_2$$

The cleavage of methyl-xylotriose at the first glycosidic linkage would lead to the small production of xylose observed, as well as the dominance of methyl-xylobiose as a final reaction product. The reactions shown above for the mechanism of xylanase action in the presence of methanol are just a subset of the potential degradation pathways, but do highlight the main reactions expected.

Table 3.5. Xylanase assay products assigned from positive ion ES-MS, for assays conducted in the presence of the cosolvent methanol.

m/z	Ion	Compound
187.8	$[MeXyl{\cdot}Na^+]^+$	Methyl-xylose
294.4	$[ONPXyl{\cdot}Na^+]^+$	ONP-xylose
305.4	$[Xyl_2{\cdot}Na^+]^+$	Xylobiose
319.5	$[MeXyl_2{\cdot}Na^+]^+$	Methyl-xylobiose
426.6	$[ONPXyl_2{\cdot}Na^+]^+$	ONP-xylobiose
437.3	$[Xyl_3{\cdot}Na^+]^+$	Xylotriose
451.3	$[MeXyl_3{\cdot}Na^+]^+$	Methyl-xylotriose
558.4	$[ONPXyl_3{\cdot}Na^+]^+$	ONP-Xylotriose
565.2	$[2ONPXyl{\cdot}Na^+]^+$	ONP-Xylose

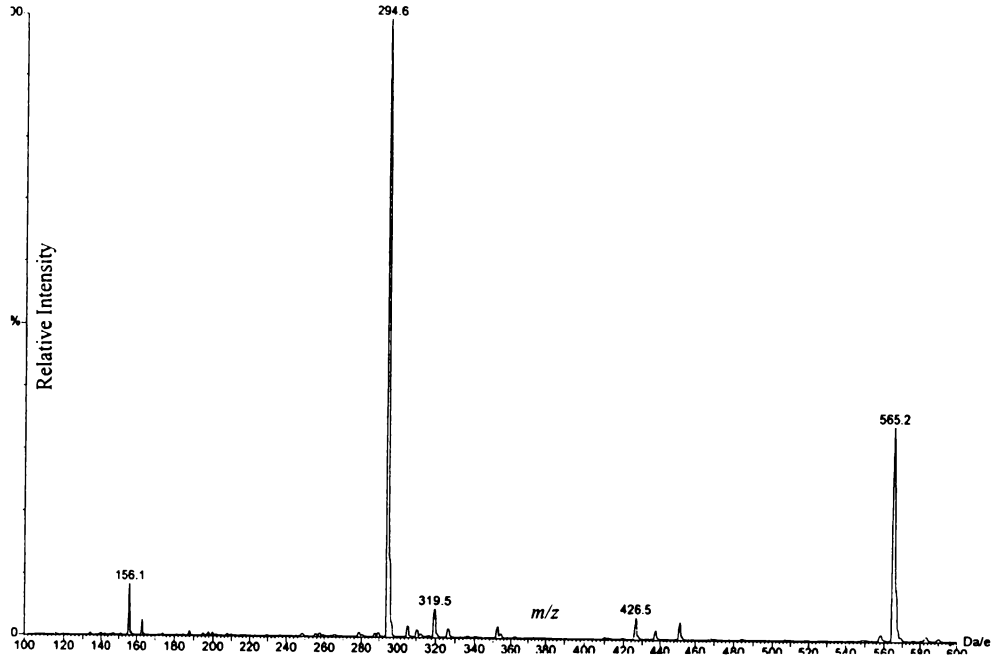

Figure 3.17. Positive ion ES-MS of xylanase reaction products from an assay in 20% methanol, run for approximately 5 minutes.

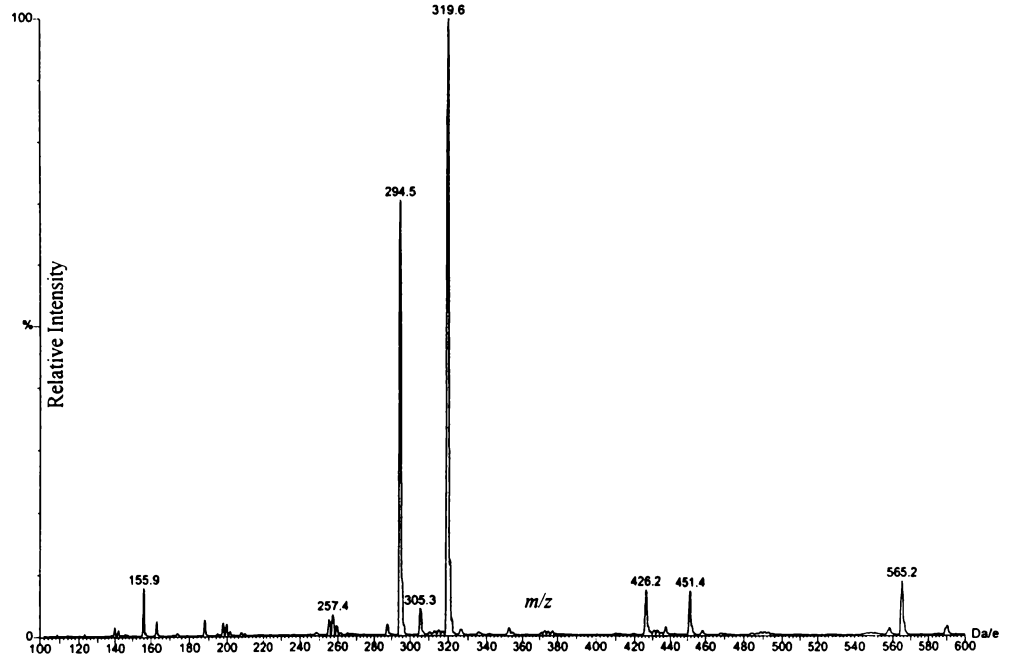

Figure 3.18. Positive ion ES-MS of xylanase reaction products from an assay in 20% methanol, run for approximately 20 minutes.

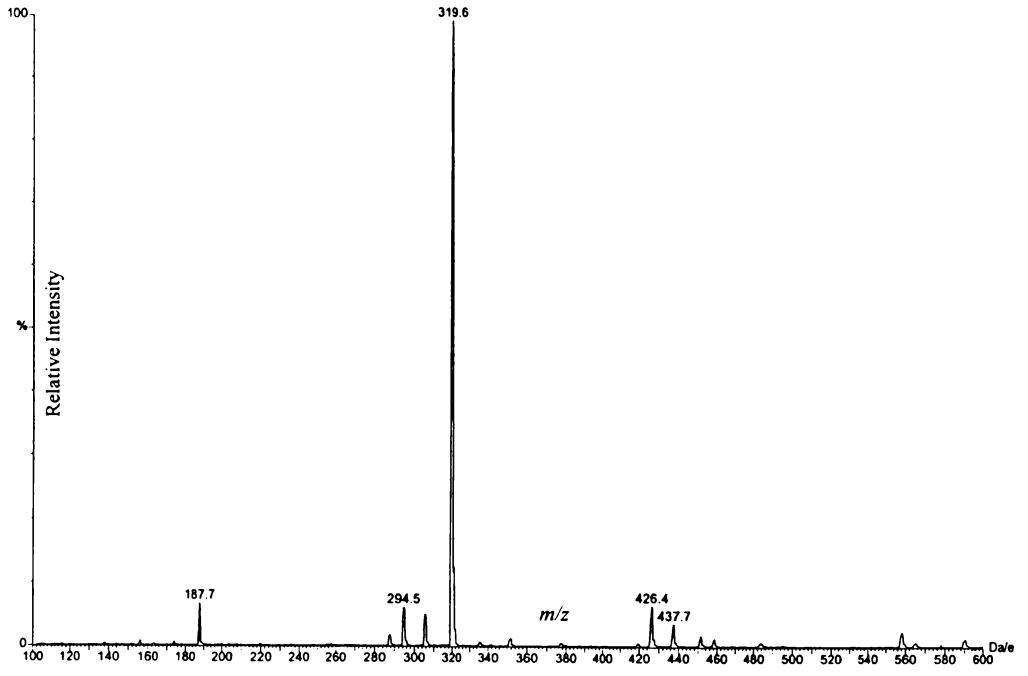

Figure 3.19. Positive ion ES-MS of xylanase reaction products from an assay in 20% methanol, run for approximately 45 minutes.

A summary of the reaction pathways for xylanase activity on ONP-xylose in both aqueous and methanol/water solutions is shown in Figures 3.20 and 3.21. By comparing the proposed reaction pathways, it is easy to see why ONP-xylobiose is the first product to be detected for both assay conditions. The aqueous reaction pathway clearly illustrates the potential dominance of xylobiose and xylotriose as final reaction products. The potential dominance of methyl-xylobiose as a final product for assays conducted in the presence of methanol is also shown.

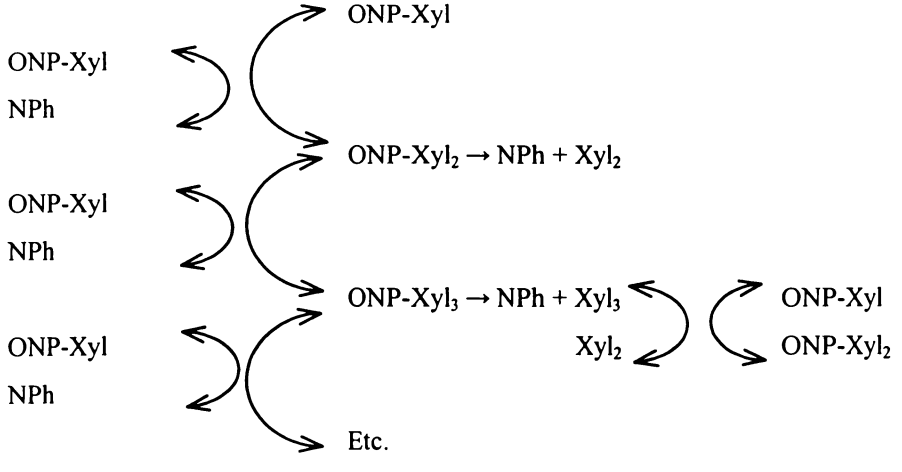

Figure 3.20. Summary of proposed reaction pathway for activity of xylanase on *o*-nitrophenyl-β-D-xylopyranoside in aqueous solution.

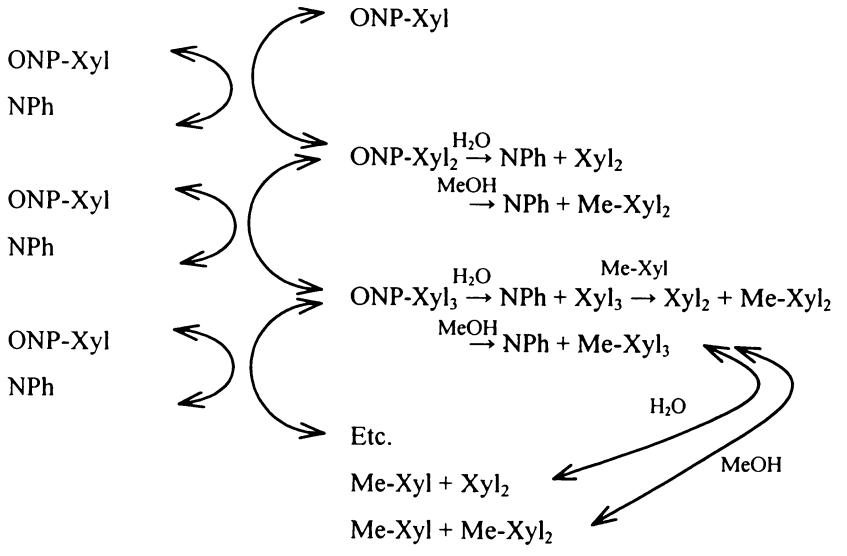

Figure 3.21. Summary of proposed reaction pathway for activity of xylanase on *o*-nitrophenyl-β-D-xylopyranoside in the presence of the cosolvent methanol.

From the above results, it is clear that new products are formed when xylanase assays are conducted in the presence of methanol. This is due to a change in the reaction pathway for the substrate *o*-nitrophenyl-β-D-xylopyranoside, with methanol probably acting as a competing nucleophile with water for the covalent xylosyl-enzyme intermediate. However, the catalytic mechanism of xylanase may not be changed, with the rate-determining step of the reaction being unaltered. For the xylanase from *Bacillus circulans*, it is found that the glycosylation step is rate limiting with all known synthetic substrates (Lawson et al., 1997). Therefore, as the methanol is not involved until the deglycosylation step, it is likely that the rate-determining step is unchanged. This is further supported by the fact that the energy of activation is the same for xylanase assays conducted in both methanol- and DMSO-based cryosolvents (Dunn, 1998). DMSO is not able to accept transfer of a glycosyl residue, and therefore the products of a xylanase reaction in the presence of DMSO should be the same as those for an aqueous assay. When a xylanase assay was conducted in 60% (v/v) DMSO, the products were the same as those for an aqueous assay, as determined by HPAE-PAD (result not shown). The ES-MS spectrum of a xylanase assay run in 20% DMSO, at 0°C, is shown in Figure 3.22. The products detected were the same as those for an aqueous assay sample, and are ONP-xylose, xylobiose, xylotriose, and ONP-xylobiose. Only an insignificant amount of ONP-xylotriose was seen, as the assays was run for a long time and this product can be further degraded. It can be seen from the ES-MS

spectrum that xylobiose and xylotriose become the dominating reaction products. Therefore, the increase in rate seen upon addition of even relatively low concentrations of methanol to the xylanase assay may be due to a combination of factors. These include a potential change in reaction mechanism, a change in the rate-determining step, or possibly a change in the dynamic properties of the enzyme, leading to greater activity.

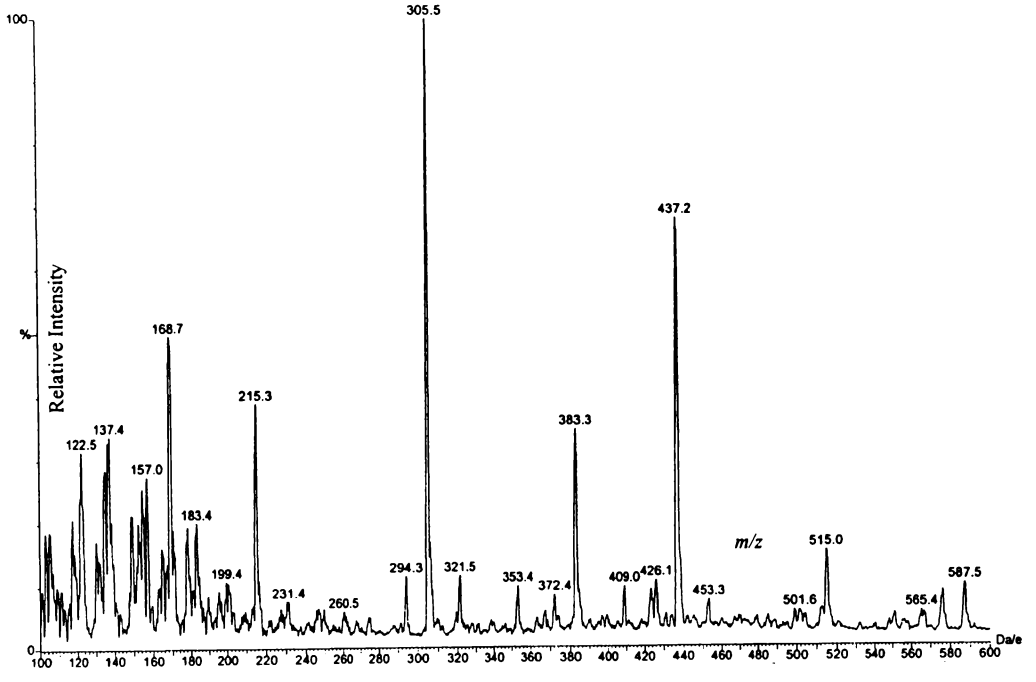

Figure 3.22. Positive ion ES-MS of xylanase reaction products from an assay in 20% DMSO, at 0°C, run for approximately one hour.

Chapter Four

Cryoenzymology Trials

4.1 Introduction

A key part of this research included the cryoenzymology studies of various enzymes. The ability to assay enzymes over a wide temperature range, especially at low temperatures, is essential to enable useful comparisons between the activity data and the protein dynamic measurements. As mentioned previously, cryosolvents are used for collecting solution data at subzero temperatures. A number of very comprehensive reviews have been written on cryoenzymology and the use of cryosolvents, for example, by Douzou (1971, 1977, 1977, 1980), by Fink and Geeves (1979) and by Travers and Barman (1995). A detailed coverage of cryosolvent properties and the effect of cryosolvents on enzymes are given in Chapter Two and Chapter Three, respectively.

There are several factors to be considered when choosing enzymes for the low temperature work. The enzyme must be stable in the various cryosolvents to enable enzyme activity to be accurately determined. The enzyme should also be soluble in the chosen cryosolvent, as an effective means of decreasing the assay time at extremely low temperatures is to increase the protein concentration. It is also preferable to choose an enzyme that has a relatively high turnover number. However, the most significant factor in determining whether an enzyme will be suitable for low temperature assays is the temperature dependence of the reaction. For example, an Arrhenius plot of hypothetical reactions, each with a different energy of activation, is shown in Figure 4.1. As can be seen, the reaction rate decreases more steeply with temperature as the energy of activation of the reaction increases. Due to the magnitude of this effect, it is more likely to be the limiting factor when attempting to measure enzyme activity to as low a temperature as possible. A more minor consideration was to find a suitable single subunit, low molecular weight enzyme. This was to enable the ease of potential computer simulation studies.

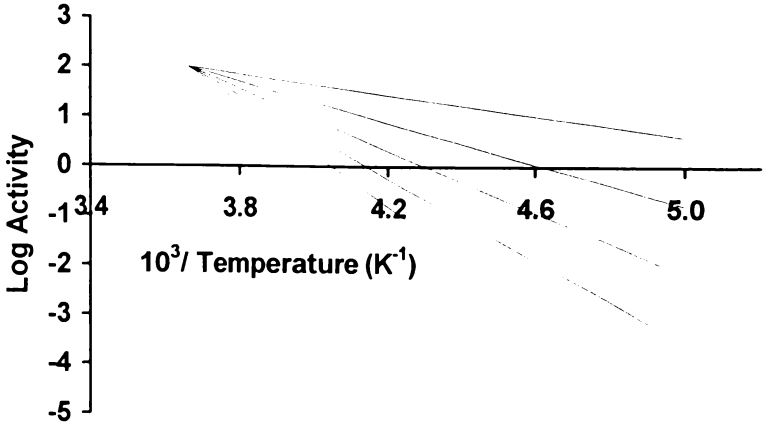

Figure 4.1. Arrhenius plot for hypothetical reactions with increasing energy of activation. From top to bottom the lines correspond to energy of activation values of: 20, 40, 60, 80, and 100 kJ/mol.

Initially, thermophilic proteins were chosen as potential enzymes for the cryoenzymology studies (More et al., 1995; Dunn, 1998). This was due to the fact that, as well as having enhanced thermal stability, thermophilic enzymes have been shown to have an increased stability against denaturation by other factors, including resistance to denaturation by organic solvents (Owusu and Cowan, 1989; Guagliardi et al., 1989; Cowan, 1997). However, the thermophilic xylanase and glutamate dehydrogenase studied were found to have relatively high energies of activation in cryosolvents (Dunn, 1998). This meant that enzyme activity could only be determined down to –70°C due to practical limitations.

Another reason for initially choosing to work with thermophilic enzymes is the decreased probability for cold denaturation. The temperature profiles of the free energy of stabilisation for thermophilic enzymes are different to those of mesophilic enzymes. From the available data it appears that the temperature profile is either shifted to higher temperatures or flattened, leading to a higher denaturation temperature (Jaenicke et al., 1996). Because of this flattening effect, thermophilic enzymes do not exhibit cold denaturation as a common feature (Jaenicke, 1991). Cold-induced unfolding is a highly reversible process that occurs for both single-subunit and multi-subunit enzymes, and appears to be a general feature of globular proteins (Privalov, 1990; Franks, 1995). Cold denaturation has thermodynamic characteristics opposite to those of heat

denaturation, with the process proceeding with heat release and a decrease in entropy.

The purpose of this chapter was to trial various enzymes to determine whether they had the necessary characteristics, as detailed above, for extremely low temperature activity measurements. Low temperature cryoenzymology studies were then conducted with the most suitable enzymes, the results of which are presented in the following chapter.

4.2 Methods and Materials

4.2.1 Materials

Alkaline phosphatase from calf intestine was obtained from Boehringer Mannheim as a suspension in 50% glycerol. The xylanase from the thermophilic bacterium Rt8B.4, genus *Caldicellulosiruptor*, was obtained from an *Escherichia coli* clone containing the plasmid pNZ2012, and stored in the Thermophile Culture Collection as TG 632 (Dwivedi et al., 1996).

All solvents, such as methanol, DMSO and ethylene glycol, as well as all reagents were of analytical grade. The lowest grade of water used was reverse osmosis (RO) purified water. In most cases the water was obtained from a Milli-Q (MQ) Water Purification System (Millipore).

4.2.2 General Cryoenzymology Techniques

Some general techniques were applied to all assays carried out in cryosolvents at low temperatures. A variety of methods were used to incubate the assays at the appropriate temperature. For assays at 0°C, an equilibrated water-ice bath was used. For assays above -50°C, freezers kept at the required temperature were used, with the assays stored in insulated containers to minimize fluctuations in temperature when the door was opened. Assays at –50°C were incubated in a methanol bath cooled by a Flexi Cool Immersion Cooler (FTS Systems). At -70°C, assays were either stored in a deep freeze or placed in a cryostat. Assays below -70°C were mostly run in the cryostat, with only a few assays at –80°C to -90°C being stored in the cooled methanol bath. For assays down to -70°C, a

transportable methanol bath was used to transport the samples or to pre-cool assays before incubating in the freezer. Below this temperature a propanol bath was used, as it remains fluid to a lower temperature. The methanol and propanol were cooled by the addition of liquid nitrogen. All temperatures were checked with a thermocouple thermometer (Digi Sense, Cole Palmer).

To prepare an enzyme solution in a cryosolvent, several steps were taken to ensure the stability of the enzyme. The enzyme was first dissolved in the aqueous component, and cooled on ice. The solvent component was cooled separately on ice, before gradual addition to the enzyme solution. The solution was constantly stirred to prevent a higher concentration of solvent from forming. The cryosolvent enzyme solutions were prepared immediately prior to use to minimise the exposure of the enzyme to the cryosolvent.

The cryostat was constructed based upon a design by Douzou (1974). The cryostat relies simply on liquid nitrogen as a source of cold nitrogen gas, which is then heated to the required temperature before passing over the samples. A temperature probe placed near the samples controls the heating of the nitrogen gas. A separate heating device placed in the liquid nitrogen, was manually controlled to adjust the flow rate of nitrogen through the cryostat. Stable temperatures as low as $-110^{\circ}C$ could easily be obtained. In all cases, sample temperature was directly and independently monitored with a temperature probe.

4.2.3 Xylanase Methods

4.2.3.1 Partial purification of Rt8B.4 Xylanase

A freeze dried culture of the *E. coli* clone TG 632 was reconstituted in Luria Broth (LB), and grown in LB medium containing 100 μg/ml ampicillin at $37^{\circ}C$, until the stationary phase was reached, as monitored by the optical density at 650 nm. The cells were harvested by centrifugation with a JA14 rotor for 20 minutes at 8,000 *g*. The cells were then washed and resuspended in 10 mM MOPS buffer, pH 7.0, followed by sonication for 5 minutes. The majority of the *E. coli* proteins were then removed by heat treatment at $70^{\circ}C$ for 1½ hours, followed by centrifugation at 9,000 g for 20 minutes. The supernatant was retained and kept frozen until required for use.

4.2.3.2 Dinitrosalicylic acid assay

Initial xylanase assays were conducted by measuring the reducing sugars released from xylan, and quantified with dinitrosalicylic acid (DNSA), on a method based on that of Sumner (1921). A stock oatspelts xylan solution of 6% (w/v), was prepared by boiling the xylan in water for 10 minutes, cooling to room temperature, and then centrifuged for 5 minutes with a bench top centrifuge to remove insoluble particles (Beckman Microfuge E, 15,900 *g*). The reaction mixture typically contained 180 µl stock xylan solution and 20 µl enzyme solution. The reaction was stopped by the addition of 400 µl ice-cold DNSA reagent. The solution was then boiled for 6 minutes and cooled to room temperature, and the absorbance at 575 nm read. The xylose equivalents were determined from a xylose standard curve, obtained by identical treatment as the assays. One unit of enzyme activity is defined as the number of µmoles of xylose equivalents released per minute.

The DNSA reagent is prepared by adding the following reagents: 6.8 g dinitrosalicylic acid (Sigma), 1.35 g phenol, 0.34 g sodium sulfite (anhydrous), 6.8 g sodium hydroxide, and 136.5 g potassium sodium tartrate, to distilled water to a final volume of 500 ml. The solution is then filtered through a 0.2 µm membrane filter.

4.2.3.3 Chromogenic Substrate Assay

The activity of the Rt8B.4 xylanase on *o*-nitrophenyl-β-D-xylopyranoside was tested. The reaction mixture contained 10 mM *o*-nitrophenyl-β-D-xylopyranoside and enzyme, to a final volume of 100 µl. The reaction was stopped by the addition of 500 µl 1 M ice-cold sodium carbonate and the absorbance at 420 nm, due to *o*-nitrophenol release, was read. Control tubes containing all reagents, except for the enzyme, were also run to account for natural degradation of the substrate.

4.2.4 Alkaline Phosphatase Methods

4.2.4.1 *p*-Nitrophenyl–β-D-phosphate assay

Alkaline phosphatase activity was assayed continuously by measuring the release of nitrophenol from *p*-nitrophenyl-β-D-phosphate, at 37°C. The reaction mixture contained 1 mM *p*-nitrophenyl-β-D-phosphate, diethanolamine HCl buffer, pH 9.7, in a total volume of 600 µl. The reaction was started by the addition of enzyme, and the initial rate calculated from the increase of absorbance at 410nm due to *p*-nitrophenol release.

Qualitative assays were conducted for the initial cryosolvent trials. The production of the yellow coloured product was detected visually, and the time required to detect product was recorded.

4.2.4.2 4-Methylumbelliferyl-phosphate assay

Alkaline phosphatase activity was determined by measuring the fluorescence due to release of 4-methylumbelliferone from 4-methylumbelliferyl-phosphate. The enzyme was assayed in the cryosolvent 70% methanol/10% ethylene glycol/20% water. The reaction mixture contained the appropriate volume of solvents, diethanolamine HCl buffer, pH 9.7, 0.5 mM 4-methylumbelliferyl-phosphate, and enzyme to give a final assay volume of 100 µl. When undiluted enzyme was used, the glycerol component was treated as part of the ethylene glycol fraction. For assays below 0°C, the assay components were pre-cooled to 10°C below the assay temperature, and the assay started by the addition of substrate dissolved in the cryosolvent, followed by warming to the assay temperature.

The assays were stopped by the addition of 400 µl of 1 M NaOH in 80% methanol, which was cooled to below the assay temperature. After addition of the stopping reagent, the assays were held at the assay temperature for at least half an hour to ensure complete cessation of activity, before being warmed to room temperature. For the determination of 4-methylumbelliferone, 100 µl of the stopped assay was added to 2 ml of water, and the fluorescence measured in a quartz cuvette with an excitation wavelength of 360 nm, an emission wavelength of 440 nm, and a slit width of 10 nm for each wavelength. The fluorescence was read using the Perkin Elmer Luminescence Spectrometer LS 50B. For assays with

substantial activity, only 10 µl of the stopped assay was taken, with the difference in volume made up with MQ water.

At each temperature, three assays were run, each stopped at a different time interval. A control tube with no enzyme was also included to account for the background fluorescence of the reagents.

4.3 Results and Discussion

4.3.1 Cryoenzymology Trials with Rt8B.4 Xylanase

This enzyme was chosen for study due to its reportedly low energy of activation (Daniel, personal communication). The partially purified enzyme was used in all the trials.

4.3.1.1 Selection of cryosolvent

Trials were conducted to find the cryosolvent in which the enzyme was stable and the most active. Three cryosolvents were tested initially, these were: 70% methanol/30% water, 65% methanol/15% ethylene glycol/20% water, and 60% DMSO/20% ethylene glycol/20% water. The stability of xylanase in each of these cryosolvents was tested at 0°C. Aliquots were removed at the appropriate times, and assayed for remaining activity at 60°C in aqueous solution against oatspelts xylan. After 24 hours the remaining activity of xylanase in 70% methanol/30% water and 65% methanol/15% ethylene glycol/20% water had not dropped significantly. However, in 60% DMSO/20% ethylene glycol/20% water, the xylanase had lost half its activity in approximately one hour. From this it was decided to continue the trials with the methanol based cryosolvents.

4.3.1.2 Selection of assay method

As the enzyme is active against oatspelts xylan in aqueous solution, it was chosen as the first substrate to be tested. The partially purified enzyme had an activity of 170 units/ml against oatspelts xylan at 60°C. The effect of organic solvents on the response of the DNSA assay was checked to ensure it was a reliable method for xylanase assays in cryosolvents. As can be seen from the standard curve (Figure 4.2), the addition of organic solvents to the standards does not have a significant

effect on the response of the assay. The effect of increasing methanol concentration on xylanase activity on oatspelts xylan was determined. At 10% methanol, only 10% activity is obtained as compared to aqueous assays (results not shown). This may be due to a problem with xylan solubility with increasing methanol, as a significant precipitate is seen at 50% methanol. It is unlikely that methanol is interfering in the colour development, as xylose standards give a comparable absorbance reading in the presence of methanol. Due to the significant reduction in activity on xylan at even 10% methanol, a different substrate was needed.

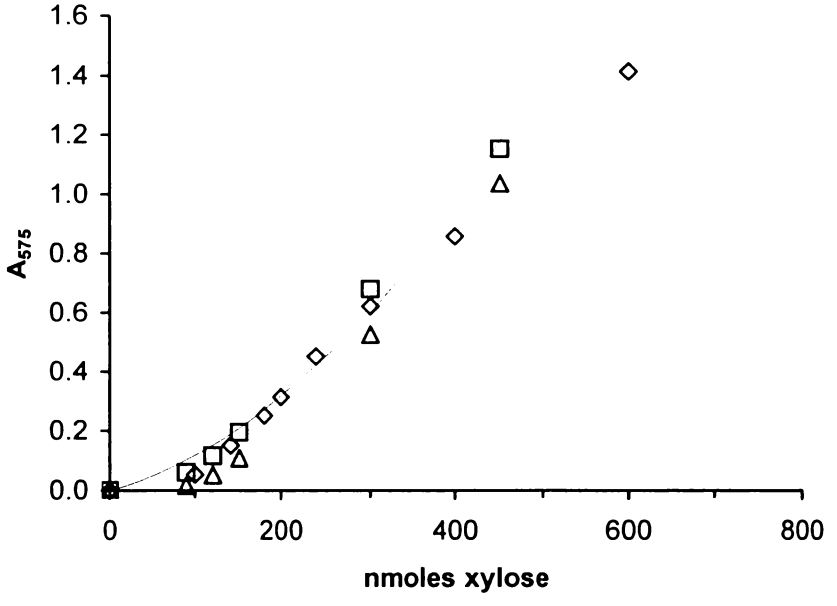

Figure 4.2. Standard curve for xylose by DNSA assay method. Standards prepared in water (◊); 25% methanol (Δ); 25% ethylene glycol (□).

An alternative was the use of the chromogenic substrate *o*-nitrophenyl-β-D-xylopyranoside. Aqueous assays run at 60°C showed that the enzyme was active against this substrate. The partially purified enzyme had an activity of 1.3 units/ml at 60°C, which is significantly reduced from the activity seen on oatspelts xylan. The temperature dependence of xylanase activity on *o*-nitrophenyl-β-D-xylopyranoside was then determined in aqueous and 70% methanol conditions. The energy of activation was calculated to be 47 $kJmol^{-1}$ from an Arrhenius plot of the data, as shown in Figure 4.3. This is significantly higher than the energy of activation for activity on oatspelts xylan, which was determined to be 34 $kJmol^{-1}$.

This means that the activity on *o*-nitrophenyl-β-D-xylopyranoside would be expected to drop at least five orders of magnitude from 0°C to −100°C. With the partially purified enzyme, this would require an assay time of approximately 700 days to be able to detect activity. Even if the enzyme was further purified and concentrated, it is likely the assay time would remain impractical. Due to the combination of reduced specific activity and increased energy of activation with *o*-nitrophenyl-β-D-xylopyranoside, it is an unsuitable substrate for the cryoenzymology work. As these quick trials did not determine a suitable cyroenzymology substrate for the xylanase, it was decided not to continue work with this enzyme. A suitable substrate for cryoenzymology studies with this enzyme may be found after further trials.

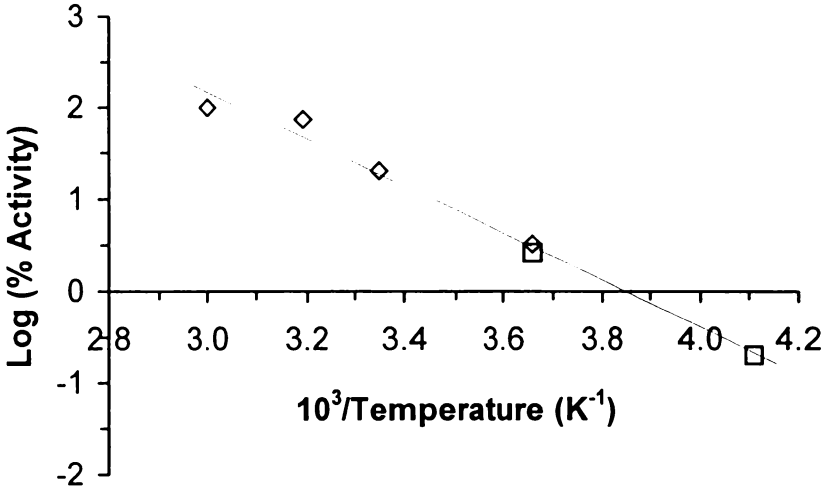

Figure 4.3. Arhenius plot showing effect of temperature on activity (expressed as the percentage residual activity corresponding to activity in aqueous solution at 60°C) for xylanase in 100% water (◊) and 70% methanol (□).

4.3.2 Cryoenzymology Trials with Alkaline Phosphatase

4.3.2.1 Selection of cryosolvent

An initial test group of cryosolvents was chosen based upon their ability to remain homogeneous to low temperatures, and with a consideration of the viscosity. From these, the cryosolvent in which alkaline phosphatase had the greatest activity was selected. The initial cryosolvents chosen were 70% methanol/10%

ethylene glycol, 60% DMSO, 70% DMF/10% ethylene glycol, 70% methoxyethanol/10% ethylene glycol, 35% methoxyethanol/35% acetone/10% ethylene glycol and 50% acetone/25% ethylene glycol, with the remaining volume made up with water. The assays were performed at 0°C with *p*-nitrophenyl-β-D-phosphate (1 mM) as the substrate, and the activity measured qualitatively with the visual detection of yellow coloured product. The two best cryosolvents with respect to alkaline phosphatase activity were 70% methanol/10% ethylene glycol and 50% acetone/25% ethylene glycol, which both gave a tenth of the activity of the aqueous assays (results not shown). A quick trial of the effect of substrate concentration on alkaline phosphatase activity was performed in the two best cryosolvents. A concentration range from 0.5 mM to 5.0 mM gave no apparent change in rate, suggesting that the concentration used in the assay was not rate limiting. Qualitative assays were then run at -30°C and -70°C to see how temperature affected the activity, and if there were any differences between the solvents. The time to visually detect the production of product in the 50% acetone/25% ethylene glycol cryosolvent was longer than that for the 70% methanol/10% ethylene glycol cryosolvent. From this result it was decided to continue the low temperature studies in 70% methanol/10% ethylene glycol, as the assays could be run with a shorter incubation time.

4.3.2.2 Selection of assay method for low temperature assays

Trials were conducted to find the most sensitive method for the determination of activity at low temperatures in cryosolvent. The first method that was investigated involved the use of the chromogenic substrate *p*-nitrophenyl-β-D-phosphate, with the absorbance at 420 nm being measured. This method is very simple, and was used in the initial cryosolvent trials. Experiments with the fluorescent substrate 4-methylumbelliferyl-phosphate were then conducted to see if an increase in assay sensitivity could be obtained.

As it was impossible to measure enzyme activity continuously at low temperatures, an appropriate stopping reagent was required. Alkaline stopping reagents were tested, as both potential assay methods give a greater sensitivity if the final solution is alkaline. The fluorescence of the product 4-methylumbelliferone is greatest around pH 10 (Goodwin and Kavanagh, 1950).

Two stopping reagents were tested, 3:5:2 (v/v) ethanolamine:DMSO:water and 1 M NaOH in 80% methanol The ability of 3:5:2 (v/v) ethanolamine:DMSO:water to stop activity was effective down to temperatures as low as -70°C. Below this temperature the stopping reagent became too viscous to allow thorough mixing with the assay reagents, which caused an erroneously high activity reading as the assays were warmed. As well as this, a control in which the stopping reagent was added to the assay before the enzyme showed significant activity at high enzyme concentrations. When similar controls were conducted with 1 M NaOH in 80% methanol, no activity was detected, and the solution was less viscous at low temperatures. Because of this, it was decided to continue the low temperature assays with this reagent.

The sensitivity of the fluorescent detection of 4-methylumbelliferone in the presence of stopping reagent was determined. The standards were prepared by adding 400 µl of 1 M NaOH in 80% methanol to 100 µl of 4-methylumbelliferone (dissolved in methanol). A 100 µl aliquot of the resulting solution was then added to 2 ml MQ water, and the fluorescence measured. The resulting standard curve is shown in Figure 4.4. The slight difference in composition between the standards and the assay samples should not cause significant changes in the response, and any changes in background fluorescence should be accounted for by the reagent control.

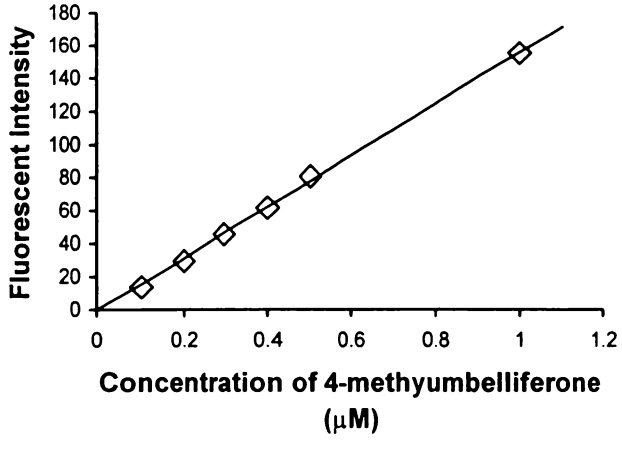

Figure 4.4 Standard curve for 4-methylumbelliferone detection. The fluorescence of the standards was measured with an excitation wavelength of 360 nm and an emission wavelength of 440 nm.

From the standard curve it can be seen that as little as 1 μM 4-methylumbelliferone can be detected in a 100 μl assay, which corresponds to 100 picomoles. In comparison, the sensitivity of the *p*-nitrophenyl-phosphate assay is approximately 700 picomoles, assuming an absorbance of 0.02 in a final volume of 600 μl, with an extinction coefficient for the product of 18,000 $lmol^{-1}cm^{-1}$ (John, 1992). The fluorescent method is almost an order of magnitude more sensitive than the detection of *p*-nitrophenol. When equivalent enzyme assays were run for each of the assay methods, the fluorescent method was able to detect activity with ten-fold less enzyme than the *p*-nitrophenol assay (results not shown), enabling substantial reduction in assay time.

As a sensitive assay method was determined that allowed the detection of low levels of enzyme activity, this enzyme was suitable for low temperature enzyme assays. The results of the cryoenzymology studies are given in the following chapter.

Chapter Five

Effect of Temperature on Proteins

This chapter consists of the published paper on the low temperature enzyme activity determinations. My contribution to this work involved the low temperature cryoenzymology experiments with the enzyme alkaline phosphatase, as well as assistance in the construction of the cryostat.

Enzyme Activity Down to –100°C

J. M. Bragger, R. V. Dunn, and R.M. Daniel

Biochimica et Biophysica Acta 1480 (2000) 278-282

Department of Biological Sciences, University of Waikato, Private Bag 3105, Hamilton, New Zealand

Key words: Alkaline phosphatase; Catalase; Cryoenzymology; Cryosolvent; Exobiology; Protein dynamics.

Correspondence to: R.M. Daniel, Dept. Biological Sciences, University of Waikato, Private Bag 3105, Hamilton, New Zealand

Tel + 64 - 7 - 838 4213

Fax + 64 - 7 - 838 4324

Email : r.daniel@waikato.ac.nz

Summary

The activities of two enzymes, beef liver catalase [E.C. 1.11.1.6] and calf intestine alkaline phosphatase [E.C. 3.1.3.1], have been measured down to –97°C and -100°C, respectively. Enzyme activity has not previously been measured at such low temperatures. For catalase, the cryosolvents used were methanol:ethylene glycol:water (70:10:20) and DMSO:ethylene glycol:water (60:20:20). For alkaline phosphatase, methanol:ethylene glycol:water (70:10:20) was used. All of the Arrhenius plots were linear over the whole of the temperature range examined. Since the lowest temperatures at which activity was measured are well below the dynamic transition observed for proteins the results indicate that the motions which cease below the dynamic transition are not essential for enzyme activity. In all cases the use of cryosolvent led to substantial increases in Arrhenius activation energies, and this imposed practical limitations on the measurement of enzyme activity below –100°C. At even lower temperatures enzyme activity may be limited by the effect of solvent fluidity on substrate/product diffusion, but overall there is no evidence that any intrinsic enzyme property imposes a lower temperature limit for enzyme activity.

Introduction

Low temperature studies of enzymes can provide useful information in a number of areas [1-3]. They allow correlation of enzyme activity with biophysical studies of protein dynamics, the determination of the effect of organic solvents on enzyme reactions without risk of denaturation, and, since enzyme activity is a prerequisite for life, could conceivably set a lower temperature limit for life.

A variety of biophysical studies have shown a temperature-dependent transition in the dynamic behaviour of hydrated proteins, involving cessation of anharmonic motion below the transition temperature, which is in the range –40°C to -75°C. Much of this work has been done on myoglobin using Mossbauer spectroscopy [4-6], neutron scattering [7,8], or X-ray crystallography [9] of hydrated crystals, powders, or frozen solutions. Similar results have been found in X-ray crystallographic studies of ribonuclease A [10] and in Mossbauer [11] and neutron scattering [12] studies of membrane proteins. Because of the dependence of protein function on dynamics it is expected that function will cease below this dynamic transition [13] Some protein functions have been observed to cease with the loss of equilibrium anharmonic dynamics as the protein is cooled through the dynamic transition. Among these are electron tunnelling in *Rhodospirullum rubrum* chromatophores [11], some elements of the photocycle of bacteriorhodopsin in hydrated membranes of *Halobacterium salinarum* [12], and ligand binding in ribonuclease A crystals [14]. However, enzyme activity, one of the most important protein functions, has rarely been measured below -55°C, and the only report of activity below -80°C is for glutamate dehydrogenase [15]. Since most dynamic transitions observed to date occur in the temperature range -45°C to -75°C, there is relatively little evidence so far on any general effect the dynamic transition in proteins may have on enzyme catalytic activity. The dynamic transition observed for glutamate dehydrogenase in solution [at –45°C over picosecond timescales] did not correlate with any loss of enzyme activity, which was measured down to –85°C [16, 17]. The situation is somewhat complicated by recent evidence suggesting that the temperature at which the dynamic transition is observed may be timescale dependant: it has been found that for the same enzyme cryosolutions the dynamic transition is observed at progressively lower

temperatures as neutron spectrometers with progressively longer timescale resolutions are used [16].

We report here measurements of enzyme activity down to -100°C. This is the lowest temperature at which enzyme activity has been measured. The work has been facilitated by the use of a cryosolvent, which is fluid and free of phase changes, to well below –100°C [18]. The enzymes studied are catalase to -97°C, and alkaline phosphatase to –100°C.

Methods and materials

The properties of the methanol/ethylene glycol cryosolvent are described by Réat et al. [18], and those of the DMSO/ethylene glycol cryosolvent are described by Douzou et al. [19].

Catalase was obtained from Boehringer Mannheim as an aqueous suspension from beef liver. A 'killed' control, included in all experiments, was prepared by pre-mixing enzyme and methanol at 20°C and leaving overnight. No detectable activity remained after this time.

The hydrogen peroxide substrate was diluted in cryosolvent (pre-cooled to -70°C), and included in all assays and controls at a final concentration of 750 mM.

Incubations were performed in small volumes (100 ul – 120 ul) in closed, round-bottomed tubes for efficient heat transfer and to allow mixing. Direct temperature measurements were made using duplicate tubes. Substrate and enzyme were pre-cooled to 10 degrees colder than the incubation temperature, then rapidly mixed and transferred to the incubation temperature, and timing started.

Phosphate buffer was added to a final concentration of 10 mM in all assays from a 500 mM stock pH adjusted at room temperature.

The reactions were stopped by the addition of sodium azide to a final concentration of 30 mM. The sodium azide was dissolved in cryosolvent and pre-cooled. After the addition of azide the reactions were left at the incubation temperature for 20 minutes to ensure that inhibition had taken place. An equal volume of 2 M HCl (in cryosolvent, and cooled to the incubation temperature)

was added just before the tubes were warmed to room temperature. The stopped reactions were diluted with water and the remaining hydrogen peroxide determined from the absorbance at 240nm by comparison with standard hydrogen peroxide. When DMSO was used as a cryosolvent, the remaining hydrogen peroxide was measured by the o-danisidine method [20].

Each enzyme assay was run over several time periods.

Alkaline phosphatase from calf intestine was obtained from Boehringer Mannheim as a suspension in 50% glycerol. It was assayed in methanol:ethylene glycol:water (70:10:20) by measuring the fluorescence due to 4-methylumbelliferone release from 4-methylumbelliferyl-phosphate (0.5 mM). Diethanolamine HCl buffer, pH_{20} 9.7, was added to give a final assay volume of 100 ul. When undiluted enzyme was used, the glycerol component was treated as part of the ethylene glycol fraction. The assay components were pre-cooled to 10 degrees below the assay temperature, and the reaction started by the rapid addition of substrate dissolved in the cryosolvent, and warming to the assay temperature. The assays were stopped by the addition of 400 ul of 1 M NaOH in 80 % (v/v) methanol, which was pre-cooled to below the assay temperature. Once stopped, the assays were held at the assay temperature for at least half an hour to ensure complete cessation of activity, before being gradually warmed to room temperature. For determination of 4-methylumbelliferone 100 ul of the stopped assay was added to 2ml of water, and fluorescence measured with an excitation wavelength of 360nm, and an emission wavelength of 440nm.

At each temperature three assays were run, each stopped after a different time interval. A control tube with no enzyme was also included to account for any background fluorescence of the reagents.

Above $-70^{\circ}C$ a variety of cooling baths and insulated boxes in deep freezes were used for the temperature control of enzyme assays. Below $-70^{\circ}C$ a simplified version of the cryostat described by Douzou [1] was used to maintain enzyme reaction temperatures. For all assays, direct temperature measurements using a thermocouple were made in duplicate assay tubes.

Results

For all enzyme assays a number of control experiments (See Methods and Materials) were carried out to ensure that the activity measured was enzymic, and that any change in activity with temperature was not due to denaturation, substrate limitation, or to pH effects. The full activity of the enzymes could be recovered after incubation in the cryosolvents at the temperatures used. Neither of the enzymes studied showed any evidence for cold denaturation [21]. This is perhaps surprising given the very low temperatures and that the cryosolvents might be expected to have a tendency to denature the enzymes, but the results are consistent with those found for a variety of other enzymes studied well below 0°C [eg 2, 3, 15, 22-24].

Catalase

In buffer at +20°C and +2°C catalase showed optimum activity around pH_{20}6.5, but with little change in activity over the pH_{20} range 5.5 to 7.5. There was a fall in activity below pH_{20} 5.0 and above 9.0. For assays at -50°C, -60°C and -70°C in methanol:ethylene glycol:water (70:10:20), the rate of activity was the same at each temperature whether the phosphate buffer (included at 10 mM in the assay) was at pH 6.0, 7.0, 8.0 or 9.0 at room temperature. The activity fell by 50% if buffer adjusted to pH_{20} 5.0 was used.

Arrhenius plots for catalase were derived using methanol:ethylene glycol:water (70:10:20) and DMSO:ethylene glycol:water (60:20:20) as cryosolvents (Fig. 5.1). Above -40°C methanol interfered with the assay for peroxide. Activity was measured from +40°C to -70°C in DMSO/ethylene glycol, and from –40°C to -97°C in methanol/ethylene glycol. There was no evidence of deviation from linearity in the Arrhenius plots (Fig. 5.1). The Arrhenius activation energy (Ea) for catalase was 15 kJ/mol in buffer (data not shown), 48 kJ/mol in DMSO/ethylene glycol and 60 kJ/mol in methanol/ethylene glycol. This considerable increase in the Arrhenius activation energy in the presence of cryosolvent, together with lower reaction rates, made it impractical to measure the activity below -100°C, despite the very high turnover number for this reaction at

room temperature (Table 5.1). The variation in the Arrhenius activation energies in different solvents is not uncommon and may be due to effects of solvent on the enzyme structure, or on the reaction catalysed [eg 23, 24]

Table 5.1. Turnover numbers of catalase in cryosolvents.

Solvent	Temperature (°C)	Turnover number (s^{-1})
10 mM phosphate buffer, pH_{20} 6.5	+20	1.9×10^5
	+2	7 x 104
60% DMSO/20% ethylene glycol	+20	1916
	+2	447
	-50	10
70% methanol/10% ethylene glycol	-50	2.5
	-90	0.038
	-97	0.0032

Alkaline Phosphatase

Using methanol:ethylene glycol:water (70:10:20) as the cryosolvent, the activity of alkaline phosphatase was measured down to -100°C (Fig. 5.1). Due to the slow enzymatic rates at low temperatures these points show some scatter, but there is no evidence for any significant deviation from linearity of the Arrhenius plot and a line of best fit gives an Arrhenius activation energy of 55 $kJmol^{-1}$. This is somewhat higher than the Arrhenius activation energy of 41 $kJmol^{-1}$, obtained for alkaline phosphatase in aqueous solution [25].

A

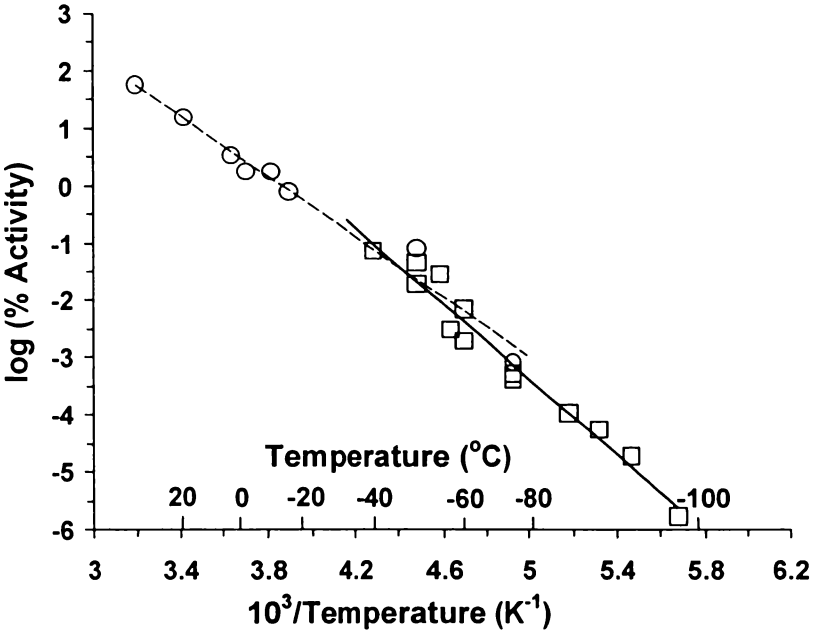

B

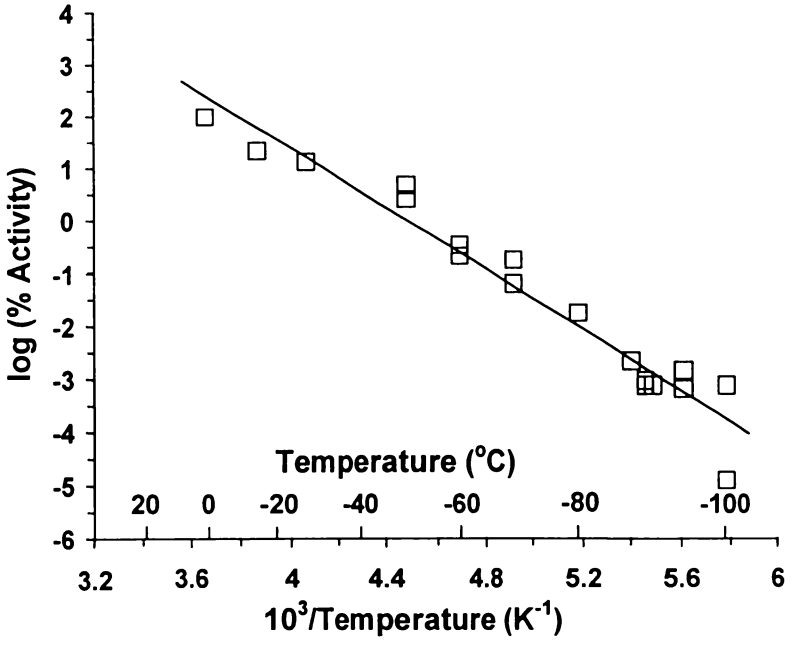

Figure 5.1. Arrhenius plots of catalase and alkaline phosphatase. (A) Effect of temperature on the activity of catalase in DMSO/ethylene glycol/water (60/20/20) (○), and methanol/ethylene glycol/water (70/10/20) (□). (B) Effect of temperature on the activity of alkaline phosphatase in methanol/ethylene glycol/water (70/10/20) (□).

Discussion

There are a variety of factors that can affect enzyme activity at very low temperature [1-3, 15]. Most will lower activity, although for discontinuous assays failure to stop a reaction before warming to room temperature for determination of substrate or product levels will lead to erroneously high rates. The various control experiments in this study, and the practice of carrying out assays over several time intervals, indicate that the changes in activity were due to the effect of temperature on the rate limiting step of the enzyme reaction, and not to factors such as cryosolvent-induced pH changes, buffer temperature coefficients, Km changes, substrate insolubility, non-enzymic catalysis, or ineffectively stopped reactions. This conclusion tends to be supported by the absence of deviations in the Arrhenius plots.

The finding that these two different enzymes display linear Arrhenius plots down to below –95°C, well below the temperature at which dynamic transitions have been commonly observed in proteins [4-13], supports the conclusion [16,17] that such transitions have no effect on the catalytic activity of soluble, multisubunit enzymes. Results from a similar study carried out on xylanase suggest that single subunit enzymes are also unaffected by the observed dynamic transition, although activity measurements were only made down to –70°C [22].

The main practical difficulties in measuring enzyme activities at even lower temperatures are likely to be the mixing of high viscosity cryosolvents, and in maintaining incubations below -100°C for the long assay periods necessary because of the low activity of most enzymes in cryosolvents at these temperatures.

There is no evidence for any intrinsic lower temperature limit for enzyme activity. We do not know whether there is a lower temperature limit for enzyme activity above absolute zero. It seems reasonable to expect that an extrinsic limiting factor will be the necessity for a fluid medium to allow substrate and product movement. We do not observe enzyme activity in frozen mixtures at -40°C, even at enzyme concentrations and incubation periods sufficient to detect less than 5% of the expected activity (Dunn and Daniel, unpublished observations). At very low temperature enzyme and substrate solubility, and the decreased rates of activity at the solvent/water ratios necessary to maintain the fluidity of any cryosolvent, may

conceivably become limiting, although some enzymes exhibit activity in anhydrous solvents [26]. Currently there is no evidence that low temperatures will affect the enzyme-associated water molecules in such a way as to prevent activity.

We believe the work has implications for life at low temperatures. The use of cryosolvents has the combined effect of reducing enzyme activity and increasing the Arrhenius activation energy. The result has been enzyme activities at -90°C, which are between 5 and 7 orders of magnitude lower than at 20°C. Thus the turnover rate for catalase of more than 10^5 sec^{-1} at 20°C falls to 10 sec^{-1} in DMSO/ethylene glycol at -50°C and to 2.3 min^{-1} in methanol/ethylene glycol at -90°C (Table 5.1). But in a fluid medium that did not increase the Arrhenius activation energy or slow the reaction, the rate of reaction for catalase would fall less than 200-fold from +20°C to -100°C. However for alkaline phosphatase (and most other enzymes) the Arrhenius activation energy is higher than for catalase, so that at 40 kJ/mol the rate of reaction will decease from that at room temperature by more than 10^4-fold at –90°C. Nevertheless, in the presence of a suitable fluid, there seems no obvious reason to regard cessation of enzyme activity as a factor limiting the emergence or survival of life at very low temperatures.

Acknowledgments

We thank the Royal Society of New Zealand for the award of a James Cook Fellowship to RMD.

References

[1] Douzou, P. (1974) Methods Biochem. Anal. 22, 401-512.

[2] Douzou, P. (1977) Adv. Enzymol. 45, 157-272.

[3] Fink, A.L. and Geeves, M.A. (1979) Methods Enzymol. 63, 336-370.

[4] Keller, H., and Debrunner, P.G. (1980) Phys. Rev. Lett. 45, 68-74.

[5] Parak F., Knapp E.W. and Kucheida, D.(1982) J. Mol. Biol. 161, 177-194.

[6] Knapp, E.W., Fischer S.F. and Parak, F. (1982) J. Phys. Chem. 86, 5042-5047.

[7] Doster, W., Cusack, S.C. and Petry, W. (1989.) Nature 337, 754-756.

[8] Cusack, S. and Doster, W. (1990) Biophys. J. 58, 243-251.

[9] Frauenfelder, H., Petsko, G.A. and Tsernoglou, D. (1979) Nature 280, 558-563.

[10] Tilton, R.F., Dewan, J.C. and Petsko, G.A. (1992) Biochemistry 31, 2469-2481.

[11] Parak, F., Frolov, E.N., Kononenko, A.A., Mossbauer, R.L., Goldonskii, V.I. and Rubin, A.G. (1980) FEBS Lett. 117, 368-372.

[12] Ferrand, M., Dianoux, A.J., Petry, W., and Zaccai, G. (1993) Proc. Natl. Acad. Sci. U.S.A. 90, 9668-9672.

[13] Brooks, C.L., Karplus, M. and Pettitt, B.M. (1988) Proteins: A theoretical perspective of dynamics, structure, and thermodynamics, John Wiley, New York

[14] Rassmussen, B.F., Stock, A.M., Ringe, D. and Petsko, G.A. (1992) Nature 357, 523-424.

[15] More, R., Daniel, R.M.,and H.H. Petach. (1996) Biochem. J. 305, 17-20.

[16] Daniel, R.M., Finney, J.L., Reat, V., Dunn, R., Ferrand, M. and Smith, J.C. (1999) Biophys. J. 77, 2184-2190.

[17] Daniel, R.M., Smith, J.C., Ferrand, M., Hery, S., Dunn, R. and Finney, J.L. (1998) Biophys. J. 75, 2504-2507.

[18] Réat, V., Finney, J.C., Steer, A., Roberts, M.A., Smith, J., Petersen, M., and Daniel, R.M. (2000) J. Biochem. Biophys. Meth. 42, 97-103.

[19] Douzou, P., Hui Bon Hoa, G., Maurel, P. and Travers, F., In Handbook of Biochemistry and Molecular Biology Vol 1, 3rd Edn (G.D. Fasman, ed.), pp 520-539,CRC Press, Ohio, USA.

[20] Raabo, E. and Terkildsen, T.C. (1960) Scand. J. Clinical Lab. Invest. 12, 402-405.

[21] Privalov, P.L. (1990) CRC Crit. Rev. Biochem. 25, 281-305.

[22] Dunn, R., Réat, V., Finney, J., Smith, J. and Daniel, R.M. (2000) Biochem. J. 346, 355-358.

[23] Compton, P.D., Coll, R.J. and Fink, A.L. (1986) J. Biol. Chem. 261, 1248-1252.

[24] Travers, F. and Barman, T. (1995) Biochimie 77, 937-948.

[25] Fernley, H.N. and Walker, P.G. (1965) Biochem. J. 97, 95-103.

[26] Zaks, A. and Klibanov, A.M. (1984) Science 224, 1249-1251.

Chapter Six

Protein Dynamics

6.1 Introduction

A key part of this work was to investigate the relationship between protein dynamics and catalytic activity. Therefore, to complement the cryoenzymology research, protein dynamic studies over a comparable temperature range were also undertaken. The protein dynamics were determined by neutron scattering experiments, carried out at the Institut Laue-Langevin (ILL) in Grenoble, France.

The dynamic studies focused on two areas of research. The first was the investigation of the timescale dependence of a dynamic transition, previously observed with glutamate dehydrogenase solutions (Daniel et al., 1998; Daniel et al., 1999). The second area of research was the presence of dynamic transitions in a xylanase-cryosolvent solution (Dunn et al., 2000). The cryosolvent chosen was the same as that used for the low temperature xylanase activity determinations, which ensured that the activity and dynamic data were obtained from similar enzyme preparations.

The purpose of this chapter is to provide an overall summary of the main results from the dynamic studies detailed above. A complete discussion of this work in relation to the data presented in other parts of the thesis is given in Chapter Seven. The published papers are contained in the Appendix, and provide details not covered here (Daniel et al., 1999; Dunn et al., 2000).

6.2 Methods and Materials

Full details of the experimental methods can be found in the attached papers in the Appendix.

6.2.1 Materials

The glutamate dehydrogenase is from *Thermococcus zilligii* strain AN1, and was purified, assayed, and prepared for neutron scattering as described elsewhere (Hudson et al., 1993; More et al., 1996; Daniel et al., 1998). The xylanase was obtained from an *Escherichia coli* clone, containing the gene from the thermophilic bacterium, *Thermotoga maritima* strain FjSS3-B.1 (Saul et al., 1995; Bergquist et al., 2000). Both enzymes were assayed after each neutron scattering experiment to ensure that no denaturation had taken place.

6.2.2 Neutron Scattering

The dynamic neutron scattering experiments were performed on the IN6 time-of-flight spectrometer and the IN16 backscattering spectrometer at the Institut Laue-Langevin, Grenoble. The incident neutron wavelengths were 5.12Å and 6.28Å, on IN6 and IN16, respectively. All data were collected with the sample holder oriented at 135° relative to the incident beam. Raw data on the two instruments were corrected in an identical manner. The elastic intensity was determined by integrating the detector counts over the energy range of the instrumental resolution. The detectors were calibrated by normalizing with respect to a standard vanadium sample. The cell scattering was subtracted, taking into account the attenuation of the singly scattered beam. Finally, the scattering was normalized with respect to the scattering at the lowest measured temperature, and to the lowest wavevector, q.

For glutamate dehydrogenase two samples were run, one on IN6 with 100 mg/ml enzyme in 70% (v/v) CD_3OD/D_2O, and the other on IN16 with 56 mg/ml enzyme in 70% (v/v) CD_3OD/D_2O. The samples were contained in aluminium flat-plate cells with a path length of 0.3 mm for IN6 and 0.5 mm for IN16. The measured sample transmissions were 0.92 and 0.85 for the IN6 and IN16 sample, respectively. For xylanase, the sample was run on IN6 and consisted of 68 mg/ml enzyme in 70% (v/v) CD_3OD/D_2O. The sample was contained in an aluminium flat-plate cell with a path length of 0.7mm, and had a measured transmission of 0.891.

The energy resolution of IN6 is 50 μeV, whereas that of IN16 is 1 μeV. This allows the determination of the average dynamical mean-square displacements of the enzyme protons over timescales of up to approximately 100 ps for IN6, and 5 ns for IN16.

6.3 Results and Discussion

6.3.1 Xylanase Dynamics

The measured scattering contains a contribution from the protein hydrogen atoms, and also a contribution from self-coherent scattering from the solvent. The incoherent scattering from hydrogen atoms, due to self-correlations in their dynamics, is a significant component of the neutron scattering from proteins. As the hydrogen atoms are uniformly distributed over the protein molecule, the technique gives a global view of protein dynamics (Smith, 1991). The scattering data obtained is presented as the average mean square displacement, $\langle u^2 \rangle$, as a function of temperature (refer to attached paper in Appendix D and Figure 5.1).

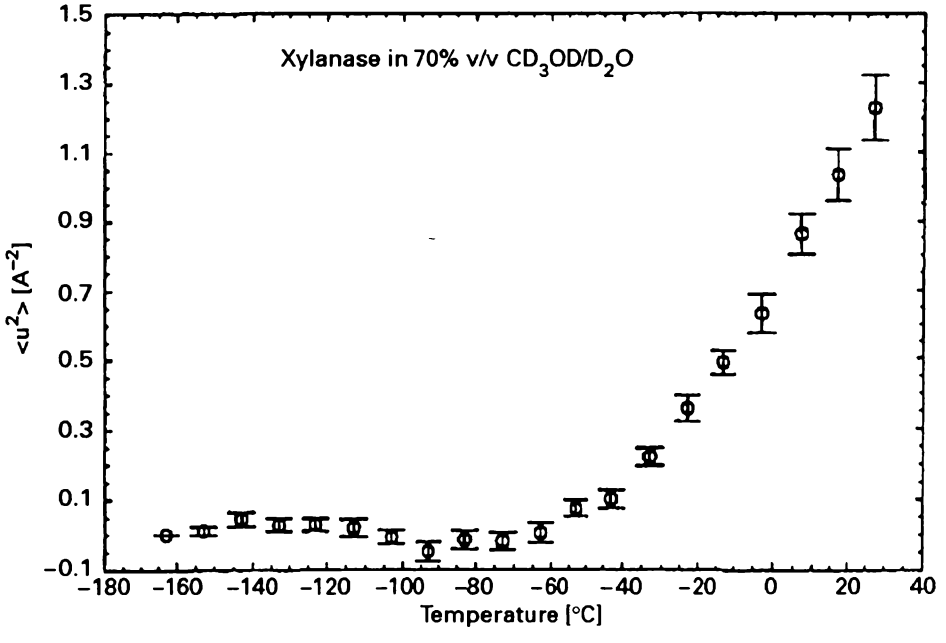

Figure 6.1. Effect of temperature on the dynamics of xylanase in 70% (v/v) CD_3OD/30% D_2O, as measured by neutron scattering.

For temperatures ≤ -70°C, $\langle u^2 \rangle$ was found to remain at zero within experimental error. Any small increase over this temperature range due to harmonic vibrations is likely to remain below the experimental error. At approximately –50°C, a

dynamic transition was observed, at which the $\langle u^2 \rangle$ begins to rise rapidly. This indicates the activation of anharmonic dynamics on a picosecond timescale.

The effect of temperature on the activity of xylanase in both hydrogenated and fully deuterated cryosolvent, of identical composition to that of the dynamic studies, was determined over the temperature range of 10°C to –70°C (Dunn, 1998; Dunn et al., 2000). From the similarity of the data, it does not appear that the catalytic activity is affected by the use of deuterated solvents. The Arrhenius plots of the activity data were found to be essentially linear over the temperature range investigated. This indicates that the rate-limiting step remains the same, and suggests that the catalytic mechanism is unchanged, as the temperature is lowered. The effect of solvents on the catalytic mechanism was also investigated, as detailed in Chapter Three. Although not a comprehensive analysis, it indicated that the catalytic mechanism was the same, despite the appearance of new reaction products when the xylanase assays were conducted in the presence of methanol.

6.3.2 Time-Scale Dependence of the Dynamic Transition

From initial work on the parallel study of activity and dynamics of glutamate dehydrogenase, it was found that activity showed no deviation in Arrhenius behaviour through the dynamical transition (Daniel et al., 1998). These results indicated that there was a range of temperatures (approximately 190 to 220 K) at which glutamate dehydrogenase activity does not require anharmonic motions taking place on the picosecond timescale. To further address the dependence of activity on motions of a particular time scale, the temperature dependence of glutamate dehydrogenase activity was compared to the dynamics of the enzyme solution on two different timescales. The experiments were performed on glutamate dehydrogenase dissolved in 70% (v/v) CD_3OD/D_2O, in which the enzyme is known to be stable and active.

From the elastic incoherent scattering intensities obtained on IN6 and IN16, the $\langle u^2 \rangle$ was determined and plotted as a function of temperature (refer to the attached paper in Appendix C and Figure 5.2). There was found to be a clear timescale dependence of the dynamic transitions observed in the protein sample. The onset of anharmonic motion occurs at approximately 140 K for motions faster than 5 ns

(IN16) and at approximately 220 K for motions faster than 100 ps (IN6). There were also additional inflexions in the IN16 data at approximately 185 K, 210 K, and 280 K. If the inflexions in the $\langle u^2 \rangle$ are defined as "dynamical transitions", then the IN16 data shows the presence of four dynamical transitions in the sample. The three highest-temperature transitions do not correspond to transitions from harmonic to anharmonic behaviour, but rather to modification of the anharmonic behaviour itself.

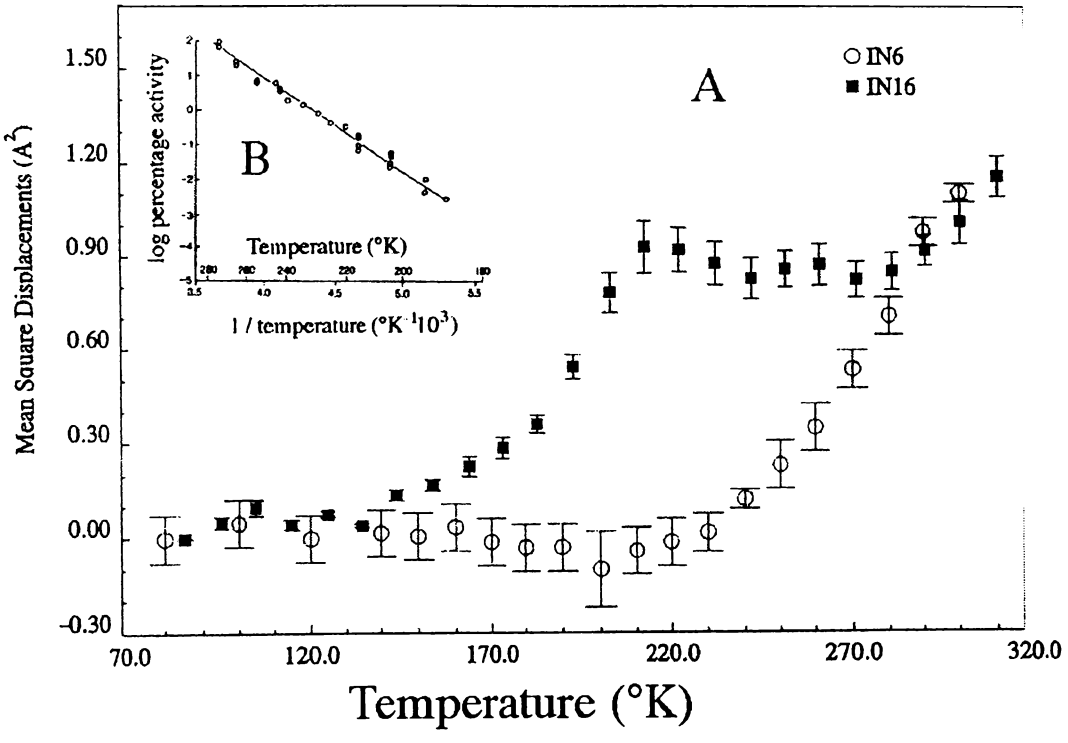

Figure 6.2. Effect of temperature on the enzyme activity (inset, B), and the dynamics as measured by neutron scattering, of glutamate dehydrogenase in 70% (v/v) CD_3OD/30% D_2O.

To investigate whether any of the various transitions are coupled with changes in solvent behaviour, a number of supplementary experiments were performed. These included DSC and X-ray diffraction studies of both the pure cryosolvents and the enzyme-cryosolvent solutions. It is suggested that the DSC phase transition observed at 170 K and the discontinuity observed at 185 K in the IN16 $\langle u^2 \rangle$ temperature profile are associated with the melting of one component of the cryosolvent. However, no features are found in either the X-ray or DSC results that accompany either of the dynamic transitions observed at 140 K or at 210 K (Daniel et al., 1999). It was therefore concluded that the transitions occurring at

these two temperatures are not correlated with detectable structural or thermodynamic changes in the cryosolvent.

To verify the dynamic nature of the transitions, further experiments were conducted to detect associated changes in the quasielastic scattering on IN16. Quasielastic scattering, which is visible as a broadening under the elastic peak, arises from the presence of nonvibrational motion in the sample (Bee, 1988). The presence of qualitative changes in the quasielastic scattering confirmed the dynamic origin of the transitions observed in the IN16 $\langle u^2 \rangle$ data.

Further discussion of these results can be found in the following chapter.

Chapter Seven

Final Discussion

The aim of this research was to investigate the relationship between enzyme catalytic activity and protein flexibility. The effect of temperature on both global protein dynamics and catalytic activity was determined, by utilising cryoenzymology and neutron scattering techniques, respectively. The direct comparison of these results, conducted on similar enzyme preparations, was used as a probe of the relationship between these two properties.

To enable solution studies at subzero temperatures, it was necessary to use cryosolvents with a miscible organic solvent component. This leads to the complication that the organic solvent may perturb the enzyme, affecting both enzyme dynamics and activity. To enable the distinction between protein-solvent interactions and the inherent properties of the enzyme, the temperature effects on solvent properties were also characterised by DSC, neutron scattering, and X-ray scattering techniques. Initial trials with the DMTA technique were also conducted, as it is relatively easy to detect glass transitions of the cryosolvents with this method. Cryosolvents that remain fluid and homogeneous over the required temperature range were preferred.

A number of studies have shown that the environment surrounding a protein may play a role in its observed dynamics (Iben et al., 1989; Vitkup et al., 2000; Fitter et al., 1999). The effect of varying solution composition on the picosecond timescale dynamics of the enzyme xylanase was investigated by dynamic neutron scattering (Réat et al., 2000a). The results indicate a significant effect of the solvent, as the picosecond fluctuations of the protein solution largely followed that of the corresponding pure cryosolvent solution. The results also indicate that for various protein-solvent samples the dynamic transition is strongly coupled to the melting of pure water, but is relatively invariant in cryosolvents of different compositions and melting points. One possible explanation for this observed insensitivity of the dynamic transition to cryosolvent composition is that the

structure of the solvent shell surrounding the protein is qualitatively similar in all of the cryosolvents but different from pure water.

The effect of cryosolvents on xylanase stability was shown to vary with solvent composition. A possible mechanism for this effect is that the solvent perturbs the shell of molecules closest to the protein, thereby destabilising the enzyme. If this were an accurate model, it would suggest that perhaps the solvent shells surrounding the protein are not identical in each of the cryosolvents, as suggested from the neutron scattering data. An alternative explanation for the observed insensitivity of the dynamic transition to cryosolvent composition was provided, which suggested that the onset of anharmonic protein motion takes place at a temperature, determined either by the solvent or by the protein, depending on which component has the higher transition temperature. This suggestion is in agreement with the molecular dynamics simulation results of hydrated myoglobin by Vitkup et al. (2000). It would be interesting to see how variations in cosolvent composition affect the dynamic behaviour, and if there was a change to the pure water behaviour at a particular cosolvent concentration.

As well as stability measurements, the effect of solvents on the catalytic properties of xylanase was studied. Although not a crucial part of the overall research, it does allow further insight into the potential effects cryosolvents have on the enzymes studied. It also ensures that the results obtained from protein-cryosolvent solution studies are applicable to aqueous solutions. It was shown that as the organic solvent concentration increased the K_M values increased. A change in the temperature dependence of the K_M values was also observed, and was seen at approximately 5% methanol. General trends from the effect of methanol concentration on V_{max} values were not as obvious, and tended to vary with temperature. However, increases in catalytic rate were observed after the addition of only 2% methanol.

Due to the observed change in catalytic properties for xylanase upon addition of methanol, the effect of cosolvent concentration on the reaction mechanism was investigated. Although not a comprehensive study, it did show the production of new reaction products when assays were conducted in the presence of methanol. This is most likely due to a glycosyl transfer reaction to the methanol, as such

reactions are known to occur with hydrolytic enzymes (Sinnott, 1990; Matsumura et al., 1999). Even though new products are formed, the rate-limiting step of the enzyme reaction may still be the same in both aqueous and cryosolvent solution. From studies with the xylanase from *Bacillus circulans*, it was found that the glycosylation step is rate limiting with all known synthetic substrates (Lawson et al., 1997). Therefore, as the methanol does not enter the reaction pathway until the deglycosylation step, it is likely that the rate-determining step is the same, despite the better nucleophilic characteristics of methanol compared to water. This is supported by the fact that the energy of activation for the reaction is the same for xylanase assays conducted in both methanol- and DMSO-based cryosolvents (Dunn, 1998). These results do not affect the conclusions drawn from the Arrhenius plot data for xylanase, since we are looking for cessation of activity at a particular temperature due to dynamic changes in the enzyme. Therefore, even if the rate-limiting step of the reaction changes in cryosolvents as compared to aqueous solution, we are more concerned with whether activity is still present over the temperature range investigated.

Comparisons between the temperature dependence of the activity and dynamic data allow the relationship between fast, picosecond motions, and enzyme activity to be determined, as mentioned above. The slowest step in the catalytic cycle of an enzyme is the rate-determining step. The enzyme-catalysed reaction is also accompanied by substrate binding, product release, and protein rearrangement steps, any one of which can be rate limiting for enzymes (Kohen and Klinman, 1998). If it is assumed that a single rate-determining step determines the overall rate of reaction, the time scale of this step can be expressed as the reciprocal of the turnover number. For the xylanase, the timescale of the rate-determining step is approximately 1 s at 0°C, and increases by at least three orders of magnitude at -50°C. As discussed earlier, the mechanism of xylanase involves multiple steps (Zechel et al., 1998), including rapid equilibration of reaction intermediates, with each step possibly relying on one or more dynamical modes on the second/millisecond timescale, at –50°C. Therefore, any catalytically relevant motions occurring in the enzyme at low temperatures are significantly slower than the picosecond motions detected by neutron scattering.

The absence of a transition in the activity data corresponding to the observed transition in the dynamic data suggests that anharmonic picosecond motions are not necessary for xylanase activity over the temperature range of –50°C to –70°C. Therefore, anharmonic fast motions, as detected by neutron scattering, may not necessarily be coupled to the slower motions required for barrier-crossing transitions along the reaction pathway. It should be noted that due to the level of sensitivity in the neutron scattering experiments, anharmonic motions activated in a more localised region, for example the active site, may still be present but undetectable.

As previously mentioned, it was suggested that the active site region of a retaining β-glycosidase is of a largely structurally static nature, while being electronically dynamic, with little change in enzyme structure required during catalysis (Zechel and Withers, 2000; Withers, 2001). Therefore, the lack of correlation between the picosecond dynamics and activity may be due to the enzyme requiring minimal flexibility for catalysis. However, an independence of catalytic activity on anharmonic picosecond dynamics was also observed for glutamate dehydrogenase (Daniel et al., 1998). The activity of catalase and alkaline phosphatase has been shown to exhibit no deviations in Arrhenius behaviour down to near –100°C (Bragger et al., 2000). This is significantly below the temperature at which the dynamic transition has been observed in a number of proteins. Therefore, while no dynamic studies have been performed on these enzymes specifically, they do support the observation of an independence of activity on fast anharmonic motions.

The next step in determining the correlation between activity and dynamics would involve the specific study of the dynamics of the active site region, as opposed to the global dynamics. Also, to determine which motions are needed for activity, it is necessary to study protein dynamics over a range of time scales.

From the dynamic results for the glutamate dehydrogenase-cryosolvent solutions, it can be seen that a shift of the lowest transition temperature to lower temperatures occurs as the timescale probed increases from approximately picoseconds to nanaoseconds. As the same enzyme preparation is used for both the IN16 and IN6 experiments, it allows this kind of trend to be easily observed.

These results suggest that the temperature dependence of the transition in average protein motions is time scale dependent. Therefore, the lowest dynamical transition temperature for the present system can be seen to be heavily dependent upon the instrument timescale, rather than occurring at a fixed temperature. Likhtenshtein et al. (2000) showed a similar observation from studies with labelled serum albumins. They found that the general tendency with increasing temperature was as follows: the lower the value of the characteristic frequency of the method, the lower the temperature at which the label mobility can be monitored.

The timescale dependence of the dynamic transition temperature can be explained by the anharmonic motions slowing, with motions over a given time scale progressively being replaced by slower motions, as the temperature is reduced. This qualitative effect is consistent with a description of the dynamics associated with the lowest temperature transition as an essentially activated process, involving an energy-barrier crossing event.

The internal molecular motions of bacteriorhodopsin in the purple membrane have also been studied over a range of time scales (Fitter et al., 1997). Quasielastic incoherent neutron scattering was used to determine the internal motions over a range of temperatures. There data showed a dynamical transition between 180 K and 220 K for all motions resolved at time scales ranging from 0.1 to a few hundred picoseconds. Whereas below the transition temperature the motions were found to be purely vibrational, above the transition temperature they were found to be mainly diffusive in nature. They mention that one description of the dynamical transition, using mean-square displacements as a function of temperature, suggests that the required volume or the jump distances of the motions are decreasing with decreasing temperature. Such an interpretation was given in a study by Andreani et al. (1995) on the enzyme superoxide dismutase. But they report that the approach of relating decreasing quasielastic scattering components to decreasing "amplitudes" of the motions is only one possible interpretation. Another interpretation, in agreement with our interpretation of the timescale dependence of the transition, is that the motions become slower with decreasing temperature. This is based upon the model first proposed by

Frauenfelder and coworkers (1979), that diffusive motions are related to "barrier crossing" between conformational substates.

Despite the present study, and other work, it is still not clear what the effect of decreasing temperature is on motions over a variety of time scales. Detailed dynamic studies are needed of specifically labelled regions over a range of time scales.

Appendix A

My contribution to this work included preliminary stability work with the xylanase and alkaline phosphatase, assistance with the low temperature characterisation of the various cryosolvent solutions, and a share of the manuscript preparation.

ELSEVIER J. Biochem. Biophys. Methods 42 (2000) 97–103

JOURNAL OF biochemical and biophysical methods

www.elsevier.com/locate/jbbm

Cryosolvents useful for protein and enzyme studies below −100°C

Valerie Réat[a,1], John L. Finney[a], Andrew Steer[a], Mark A. Roberts[b], Jeremy Smith[c], Rachel Dunn[d], Michelle Peterson[d], Roy Daniel[d,*]

[a]*Department of Physics and Astronomy, University College London, London WC1E, 6BT, UK*
[b]*CLRC Daresbury Laboratory, Daresbury, Warrington WA4 4AD, UK*
[c]*Lehrstuhl für Biocomputing, IWR, Universität Heidelberg, Im Neuenheimer Feld 368, D-69120 Heidelberg, Germany*
[d]*Department of Biological Sciences, University of Waikato, Hamilton, New Zealand*

Received 2 August 1999; accepted 23 September 1999

Abstract

For the study of protein structure, dynamics, and function, at very low temperatures it is desirable to use cryosolvents that resist phase separation and crystallisation. We have examined these properties in a variety of cryosolvents. Using visual and X-ray diffraction criteria, methanol:ethanediol (70%:10%), methanol:glycerol (70%:10%), acetone:methoxyethanol:ethanediol (35%:35%:10%), dimethylformamide:ethanediol (70%:10%), dimethylformamide (80%), methoxyethanol (80%), and methoxyethanol:ethanediol (70%:10%) were all found to be free of phase-changes down to at least −160°C. The least viscous of these, methanol:ethanediol (70%:10%), was miscible down to −125°C and showed no exo or endothermic transitions when examined using DSC. It is therefore potentially particularly suitable for very low temperature cryoenzymology.

Keywords: Cryosolvent; Cryoenzymology; Methanol; Phase change; X-ray diffraction; DSC

*Corresponding author. Tel.: +64-7-838-4213; fax: +64-7-838-4324.
E-mail address: r.daniel@waikato.ac.nz (R. Daniel)
[1]Present address: Institute Laue-Langevin, BP156, 38042, Grenoble Cedex 9, France.

0165-022X/00/$ – see front matter
PII: S0165-022X(99)00053-6

1. Introduction

The study of proteins at low temperatures has a number of advantages. Functions are slowed and thus easier to study and motions are reduced. Furthermore, the use of low temperatures increases the range over which studies of the effect of temperature on proteins can be carried out. For enzymes, assay at low temperatures slows the reaction, facilitating the study of mechanisms and extending the use of temperature as a tool to study enzyme structure, function, and dynamics. Most such studies require a fluid (solvent) medium, and thus below 0°C this work requires the use of compatible cryosolvents, and a corresponding knowledge of their properties. The work of Douzou and others [1–4] has provided an excellent and thorough coverage of cryosolvent properties (as well as many other aspects of cryoenzymology), in some cases down to − 100°C. But to date there is little information on the properties of potential cryosolvents below − 100°C, other than the documented fact that most cryosolvents currently in use undergo phase separation above that temperature [2].

As part of a research programme to measure enzyme activity at temperatures extending to below the temperature at which discontinuities in the dynamic behaviour of proteins have been observed [5,6], we have sought cryosolvents useful below − 100°C. We have investigated a variety of solvents containing at least 20% water for their ability to resist phase separation and crystallisation of one or more of their components, visually and by X-ray diffraction to − 160°C. A number have been examined for the effect of protein on phase separation, and for their effect on enzyme stability. Some of the cryosolvents have also been subjected to DSC. Use of some of these cryosolvents will allow the study of proteins, including enzyme assays, in a homogeneous medium to below − 125°C.

2. Materials and methods

All solvent percentages are by volume. Preliminary assessment of cryosolvents for any signs of phase separation was carried out visually on 2 ml volumes in 16 mm diameter closed glass tubes immersed in a stirred *n*-propanol bath cooled with liquid nitrogen. The tubes were equilibrated for at least 30 min at various set temperatures down to − 125°C, below which stirring the *n*-propanol bath became difficult.

X-ray scattering experiments on the cryosolvents, and solvent plus enzyme, were carried out down to − 160°C in Debye-Scherrer geometry on line 9.1 at the Daresbury synchrotron radiation source, UK, using a curved image-plate detector system. The cryosolvents were in standard 0.7 mm thin-walled glass capillary tubes. The cooling rate was 120°C/h and the warming rate 360°/h. The scattering from the samples was observed on both cooling and warming at a number of intermediate temperatures. The presence of crystallisation was identified by the appearance of powder diffraction peaks. Where no crystallisation was observed, the changes to the measured diffraction patterns were as would be expected from a liquid or glass on reducing the temperature. Samples were also examined visually during image plate changes, down to − 160°C, for any

increase in optical opacity which would have indicated possible changes such as crystallisation or phase separation.

X-ray diffraction work was also carried out on some solvents in the presence of 60 mg ml^{-1} of the glutamate dehydrogenase from *Thermococcus zilligii* strain AN1 [7], since some applications of the cryosolvents will involve the use of high protein concentrations. This glutamate dehydrogenase was chosen because although it is a large complex enzyme, it is a very soluble, stable enzyme, which is resistant to denaturation by cryosolvents (see [5,6] and Dunn and Daniel, unpublished observations).

Differential scanning calorimetry measurements were made using a Shimadzu DSC-50 differential scanning calorimeter. Samples were sealed in 50 μl aluminium crucibles (sample weights between 25 and 40 mg) and cooled down using a flowing nitrogen atmosphere. All data were collected during heating at a standard rate of 10°C/min.

The effect of the cryosolvents on enzyme stability was assessed by incubating the enzyme in the cryosolvent at 0°C, and withdrawing 20 μl aliquots at various time intervals. These aliquots were injected directly into 1.5 ml volumes of the appropriate enzyme assay mixture containing substrate and buffer, and the activity remaining determined by assay at 30°C. The β-glucosidase was from *Caldicellosiruptor saccharolyticum* strain Tp8, cloned and expressed in *E. coli*, and prepared and assayed as described [8]. The xylanase was from *Thermotoga maritima* strain FjSS3B1, cloned and expressed in *E. coli*, and prepared and assayed as described [9]. Both these enzymes are from extreme thermophiles, and the key purification step is a simple heat treatment which denatures and precipitates the less stable cellular proteins of the *E. coli* host. They have been used here to provide a stable single subunit enzyme (xylanase) and a stable multisubunit enzyme (β-glucosidase) The alkaline phosphatase (dimeric) and the esterase (single subunit) are from mesophilic sources and may be expected to be less stable in cryosolvents; they were supplied by Boehringer Mannheim (Auckland, NZ) and Sigma (St. Louis, Mo. USA) respectively. These were assayed by following the hydrolysis of *p*-nitrophenyl phosphate and *p*-nitrophenyl butyrate, respectively (see Ref. [8]).

3. Results and discussion

3.1. Cryosolvent homogeneity

During preliminary visual screening of a wide variety of potential cryosolvents we found none with a water content above 20% that would resist phase separation below − 120°C. We have not examined cryosolvents with less than 20% water.

Of a variety of cryosolvents tested in a preliminary test-tube screening, of those which were binary mixtures, i.e. single solvents mixed in different proportions with water, only dimethylformamide (DMF) (80%) and methoxyethanol (80%) resisted phase separation and crystallisation below − 120°C by visual and X-ray diffraction criteria. However, the addition of ethanediol (and glycerol) to methanol, and ethanediol to acetone, to form 3-component cryosolvents, prevented phase separation and crystallisation in these solvents also. The further addition of methoxyethanol to the acetone:ethanediol mixture

Table 1
Aqueous cryosolvents remaining homogenous below − 120°C. Cryosolvents were assessed for homogeneity visually, and for absence of crystallisation by X-ray diffraction, down to − 160°C

Cryosolvent (%)[a]	Homogenous/no crystallisation to	Viscosity at	
		− 105°C	− 125°C
Methanol:ethanediol (70:10)	< − 160°C	+ + +	+
Methanol:glycerol (70:10)	< − 160°C	+ + +	+
Acetone:ethanediol (50:30)	− 125°C	+ +	−
Acetone:methoxyethanol:ethanediol (35:35:10)	< − 160°C	+ (+)	−
DMF:ethanediol (70:10)	< − 160°C	+	−
DMF (80)	< − 160°C	+	−
Methoxyethanol (80)	< − 160°C	+	−
Methoxyethanol:ethanediol (70:10)	< − 160°C	−	−

[a] All cryosolvents contain 20% H_2O.
+ + + = readily miscible, + + = miscible, + = very viscous, − = solid.

eliminated the phase transition apparent just below − 125°C. The cryosolvents found to remain homogenous below − 120°C are arranged in Table 1 in order of increasing viscosity.

In addition to the cryosolvents shown in Table 1, different proportions of these components (including increased proportions of H_2O) and other cryosolvents were also tested visually. Among the single solvents tested in this way, with H_2O, were acetone, acetonitrile, allyl alcohol, DMSO, ethanol, methanol, *n*-propanol, and tetrahydrofuran. Among the three or four phase systems (including H_2O) tested were, acetone:methoxyethanol, acetone:glycerol, acetonitrile:ethanediol, allyl alcohol:ethanediol, *n*-butanol:ethanediol, methylacetate:acetone, methylacetate:acetone:ethanediol, methylacetate:ethanediol, *n*-propanol:ethanediol, DMSO:acetone, tetrahydrofuran:ethanediol. All of these systems contained 20–40% H_2O. All either exhibited phase separation above − 120°C, or were appreciably more viscous than similar mixtures listed in Table 1. They were therefore not subjected to X-ray or DSC measurements.

X-ray diffraction measurements were also carried out on cryosolvent containing dissolved (60 mg ml^{-1}) glutamate dehydrogenase. The solvents comprised 70% methanol:10% ethanediol, 70% methanol:10% glycerol, 50% acetone:30% ethanediol, and 70% DMF:10% ethanediol. No phase separation or crystallisation was seen at any temperature tested, i.e., the results were the same as for the cryosolvents alone except in the case of 50% acetone:30% ethanediol where the presence of the protein eliminated the slight crystallisation observed at about − 125°C

3.2. Differential scanning calorimetry

Although several cryosolvents remained homogenous below − 120°C (Table 1), the methanol:ethanediol and methanol:glycerol cryosolvents were the least viscous, and were the only ones which could be mixed below − 125°C. The former, and variants of it, were examined using DSC (Fig. 1). Alone, both 70% and 80% methanol exhibit exo-

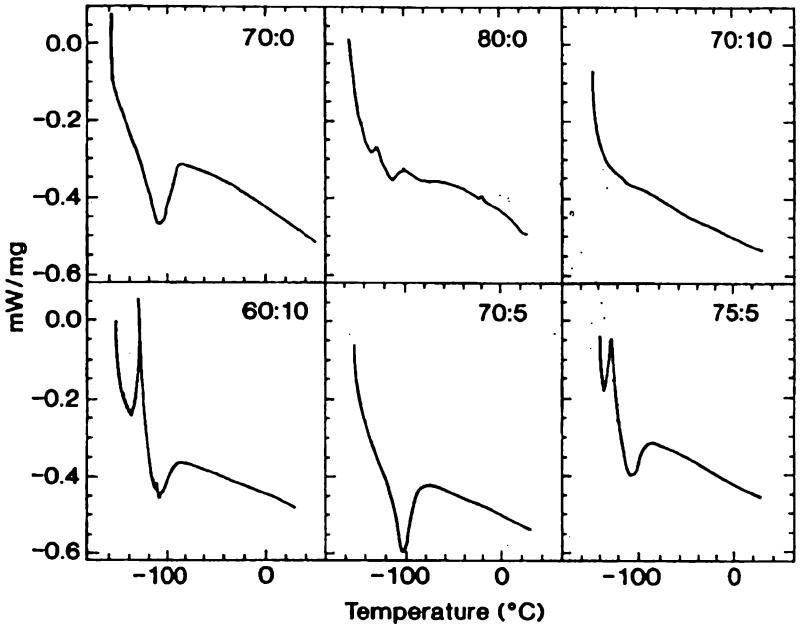

Fig. 1. Differential scanning calorimetry of methanol cryosolvents. The figure shows the effect of different ethanediol and water concentrations on the differential scanning calorimetry plot of methanol. The numbers given are the percentages of methanol and ethanediol respectively, with the balance being water.

or endothermic changes characteristic of phase transitions at about −110°C, although the increase in concentration to 80% methanol has reduced the size of the transition. The presence of 5% ethanediol is insufficient to abolish the transition even with 75% methanol, and 10% is ineffective with 60% methanol. Within the constraint of maintaining a 20% water content in the cryosolvent, of the various mixtures of methanol and ethanediol tried here, 70% methanol:10% ethanediol seems optimal. It is clearly free of phase transitions, with no significant exo or endothermic transitions observable down to the lowest temperature tested, −160°C. Mixtures containing higher concentrations of ethanediol (e.g. methanol:ethanediol, 65:15%) were also free of transitions but were substantially more viscous. The molar ratios of the 70:10% mixture are 1 (water):1.56 (methanol):0.16 (ethanediol). Attempts to gain a similar result using less methanol, or less ethanediol were unsuccessful. These DSC results are fully consistent with assessments of homogeneity made visually.

3.3. Cryosolvent effect on enzyme stability

An essential requirement of a cryosolvent is that it is compatible with protein and enzyme stability. The data in Table 2 compares the stability at 0°C of several enzymes in cryosolvents obtained by incubating them in cryosolvent and determining residual activity. Our experience suggests that enzymes that will withstand exposure to

Table 2
Stability of four enzymes at 0°C in various cryosolvents. Figures are for percentage activity remaining after enzymes are exposed to cryosolvent for 1 and 3 h; assays for remaining activity contain < 1% residual cryosolvent

Cryosolvent (%)	β-glucosidase 1 and (3) h	Xylanase 1 and (3) h	Alkaline Phosphatase 1 and (3) h	Esterase 1 and (3) h
Control (H_2O)	100 (100)	100 (100)	100 (100)	100 (100)
Methanol/Ethanediol (70:10)	92 (63)	77 (87)	118 (116)	2 (16)
Methanol/Glycerol (70:10)	88 (83)	97 (77)	117 (110)	2 (16)
Acetone/Ethanediol (50:30)	87 (83)	81 (89)	99 (101)	5 (15)
Acetone/Methoxyethanol/Ethanediol (35:35:10)	90 (85)	92 (105)	114 (87)	69 (66)
DMF/Ethanediol (70:10)	83 (73)	65 (37)	116 (63)	10 (19)
DMF (80)	81 (75)	25 (22)	23 (26)	27 (24)
Methoxyethanol (80)	83 (84)	116 (105)	128 (93)	54 (45)
Methanol (70)	78 (73)	90 (87)	147 (88)	38 (24)
Methanol (80)	73 (63)	119 (96)	65 (55)	23 (14)

cryosolvent at 0°C will not succumb to cold denaturation as the temperature is lowered, but will instead be even more stable at lower temperatures. There are few obvious systematic trends in the data. Most of the cryosolvents seem to have a destabilising effect on some enzymes, and not on others, with the extent depending upon the enzyme/cryosolvent pairing. The presence of ethanediol does not have a consistently stabilising effect. For the enzymes investigated here, DMF seems to be the most destabilising cryosolvent. Methoxyethanol, whose use in a cryosolvent mixture we have not seen described elsewhere, seems to have a stabilising effect on the enzymes tested, and may have applications when other cryosolvents are too destabilising. On the basis of the data here it seems that the methanol/ethanediol (70%:10%) cryosolvent is, on average, not significantly more destabilising at 0°C than any other cryosolvent tested.

4. Simplified description

The work described here has found cryosolvents in which enzymes and proteins can be studied in a homogeneous (phase-change-free) medium down to temperatures lower than previously reported. Use of 70% methanol:10% ethanediol (20% water) as a cryosolvent will allow such studies down to at least − 160°C. The solvent is sufficiently fluid to allow mixing down to at least − 125°C, so that enzyme assays, ligand binding studies, and other functional studies are possible down to this temperature. Use of 70% methanol:10% glycerol (20% water) would also appear to be satisfactory, and several other of the cryosolvents described here, including acetone:ethanediol (50:30%), acetone:methoxyethanol:ethanediol (35:35:10%), DMF:ethanediol (70:10%), DMF (80%), methoxyethanol (80%), and methoxyethanol:ethanediol (70:10%) may be useful under particular circumstances.

Acknowledgements

We thank the Royal Society of New Zealand for the award of a James Cook Fellowship to RMD:Also, the UK Engineering and Physical Sciences Research Council (EPSRC) for funding of the image-plate camera development (grant GR/K57916), the Council for the Central Laboratories of the Research Councils (CCLRC) for access to the Daresbury Synchrotron Source, and the University of London Intercollegiate Research Service on Thermal Analysis for the DSC measurements.

References

[1] Douzou P. The use of subzero temperatures in biochemistry: slow reactions. Methods Biochem Anal 1974;22:401–512.
[2] Douzou P, Hui-Bon-Hoa G, Maurel P, Travers F. Physical chemical data for mixed solvents used in low temperature biochemistry. In: Fasman GD, editor, 3rd ed, Handbook of biochemistry and molecular biology, vol. 1, Ohio, USA: CRC Press, 1976, pp. 520–39.
[3] Douzou P. Enzymology at subzero temperatures. Adv Enzymol 1977;45:157–272.
[4] Fink AL, Geeves MA. Cryocnzymology: The study of enzyme catalysis at subzero temperatures. Methods Enzymol 1979;63:336–70.
[5] More N, Daniel RM, Petach HH. The effect of low temperatures on enzyme activity. Biochem J 1995;305:17–20.
[6] Daniel RM, Smith JC, Ferrand M, Hery S, Dunn R, Finney JL. Enzyme activity below the dynamical transition at 220 K. Biophys J 1998;75:2504–7.
[7] Hudson RC, Ruttersmith LD, Daniel RM. Glutamate dehydrogenase from the extremely thermophilic archaebacterial isolate AN1. Biochim Biophys Acta 1993;102:244–50.
[8] Plant AR, Oliver JE, Patchett L M, Daniel RM, Morgan HW. Stability and substrate specificity of a β-glucosidase from the thermophilic bacterium Tp8 cloned into *E. coli*. Arch Biochem Biophys 1988;262:181–8.
[9] Thompson D, Fernandez R, Mateo C, Cowan DA, Guisan J, Daniel RM. Degradation and denaturation of stable enzymes. Prog Biotech 1998;15:349–52.

Appendix B

My contribution to this work included all the xylanase activity and stability determinations in the various cryosolvents. I also assisted in the preparation and placement of the samples for the neutron scattering experiments, and shared in the manuscript preparation.

Solvent dependence of dynamic transitions in protein solutions

Valerie Réat*†, Rachel Dunn‡, Michel Ferrand†, John L. Finney*, Roy M. Daniel‡, and Jeremy C. Smith§¶

*Department of Physics and Astronomy, University College London, Gower Street, London WCIE, 6BT, England; §Lehrstuhl für Biocomputing, Interdisziplinäres Zentrum für Wissenschaftliches Recken, Universität Heidelberg, Im Neuenheimer Feld 368, D-69120 Heidelberg, Germany; ‡Department of Biological Sciences, University of Waikato, Hamilton, New Zealand; and †Institut Laue-Langevin, BP156, 38042 Grenoble Cedex 9, France

Edited by Hans Frauenfelder, Los Alamos National Laboratory, Los Alamos, NM, and approved June 27, 2000 (received for review March 3, 2000)

A transition as a function of increasing temperature from harmonic to anharmonic dynamics has been observed in globular proteins by using spectroscopic, scattering, and computer simulation techniques. We present here results of a dynamic neutron scattering analysis of the solvent dependence of the picosecond-time scale dynamic transition behavior of solutions of a simple single-subunit enzyme, xylanase. The protein is examined in powder form, in D_2O, and in four two-component perdeuterated single-phase cryosolvents in which it is active and stable. The scattering profiles of the mixed solvent systems in the absence of protein are also determined. The general features of the dynamic transition behavior of the protein solutions follow those of the solvents. The dynamic transition in all of the mixed cryosolvent–protein systems is much more gradual than in pure D_2O, consistent with a distribution of energy barriers. The differences between the dynamic behaviors of the various cryosolvent protein solutions themselves are remarkably small. The results are consistent with a picture in which the picosecond-time scale atomic dynamics respond strongly to melting of pure water solvent but are relatively invariant in cryosolvents of differing compositions and melting points.

X-ray diffraction, dynamic neutron scattering, and various spectroscopies have demonstrated a quantitative change in the nature of internal motions of proteins, at ≈200–220 K (1–8). Below this transition, the internal motions are essentially harmonic whereas above it anharmonic dynamics contribute and, at physiological temperatures, dominate the internal fluctuations. The anharmonic motions may involve confined continuous diffusion (6, 9) and/or jump diffusion between potential energy wells associated with "conformational substates" of slightly different structure in which proteins are trapped below the transition (2, 10–12).

Correlations have been made between some protein functions (such as ligand binding, electron transfer, and proton pumping) and the presence of equilibrium anharmonic motion (8, 13–17). Recent x-ray diffraction work on carbon monoxy-myoglobin showed that, below 180 K, photodissociated ligands migrate to specific sites within an internal cavity of an essentially immobilized, frozen protein, from which they subsequently rebind by thermally activated barrier crossing (18). On photodissociation above 180 K, ligands escape from the distal pocket, aided by protein fluctuations that transiently open exit channels.

The increased flexibility conferred by anharmonic dynamics may indeed be required for some proteins to rearrange their structures to achieve functional configurations. However, the forms and time scales of the anharmonic motions required for function are in general unknown. In particular, it was recently shown that, in cases of enzyme activity in a cryosolvent, the rate-limiting step is independent of the ≈220 K dynamic transition (19, 20). Furthermore, it was demonstrated that dynamic transition temperatures in a cryosolvent solution of glutamate dehydrogenase are strongly dependent on the time scale of the motions involved (21).

To further understand the nature of dynamic transitions in proteins, it is particularly important to characterize solvent effects. Solvent can in principle affect protein dynamics by modifying the effective potential surface of the protein and/or by frictional damping (22, 23). Solvent viscosity is known to influence fast, diffusion-limited reaction rates in, for example, ligand binding to myoglobin (24). Changes in the structure and internal dynamics of proteins as a function of solvent conditions at physiological temperatures have been found by using several experimental techniques. In the absence of minimal hydration, lysozyme does not function (25), and related NMR measurements of exchangeability of the main chain amide hydrogens suggest a hydration-related increase in conformational flexibility of the protein (26), which may be coupled to (probably small) Raman-detected conformational changes that appear to be necessary before activity (26, 27). Rayleigh scattering of Mössbauer radiation demonstrated an increase of dynamic amplitudes on hydration of myoglobin (28). This increase was also found in subsequent neutron work on lysozyme powders (29), and qualitatively similar results have been found in more recent neutron work on parvalbumin, lysozyme, myoglobin, and the bovine pancreatic trypsin inhibitor (23, 30–33).

It is clear from the above and other work that solvent affects protein dynamics at physiological temperatures. Therefore, a solvent dependence of the dynamic transition might be expected. Indeed, measurements on CO binding to myoglobin indicate that dynamic behavior of the protein is correlated with a glass transition in the surrounding solvent (34, 35), and a recent molecular dynamics analysis of hydrated myoglobin also indicates a major solvent role in protein dynamic transition behavior (36). Several recent neutron studies have been made of environmental effects on the dynamic transition in proteins. These studies indicate that gross changes in the environment, such as dehydration or trehalose embedding, can abolish the transition (14, 37, 38).

Here, we examine how modification of the composition of the solvent affects dynamic transition behavior by using neutron scattering, which provides a means of directly probing atomic fluctuations in protein solutions (32, 39). The dynamic information is obtained from the elastic scattering, which can be used to derive the cross section-weighted average mean-square displacement $\langle u^2 \rangle$ of the atoms in the solution. The $\langle u^2 \rangle$ contains contributions from all motions resolvable by the instrument used, which in the present experiments corresponds to those faster than ≈100 ps. It is found that, in pure water, the dynamics reflect melting but are invariant in cryosolvents of strongly different composition and phase transition behavior.

This paper was submitted directly (Track II) to the PNAS office.

Abbreviation: DSC, differential scanning calorimetry.

¶To whom reprint requests should be addressed. E-mail: biocomputing@iwr.uni-heidelberg.de.

The publication costs of this article were defrayed in part by page charge payment. This article must therefore be hereby marked "*advertisement*" in accordance with 18 U.S.C. §1734 solely to indicate this fact.

Methods

The experiments were performed on a thermophilic xylanase enzyme in a dry powder, in D_2O, and in single-phase water-solvent mixtures consisting of 40% CD_3OD/60% D_2O, 70% CD_3OD/30% D_2O, 40% DMSO/60% D_2O, and 80% DMSO/20% D_2O (all solvent percentages are by volume). The corresponding mixed solvent solutions in the absence of protein were also examined. These cryosolvents were chosen because they are all well-characterized and maintain enzyme activity. The xylanase was chosen because it is a relatively simple, single subunit enzyme that is stable under all of the experimental conditions used in this work and active down to at least 190 K. The enzyme was purified and assayed as described elsewhere (19, 20). For the 40% CD_3OD/60% D_2O and 70% CD_3OD/30% D_2O solvents, xylanase activity data exist (40, 41). As found in previous work (20), all of the xylanase activity was recovered at the end of the present experiments, confirming that the enzyme is stable under all of the experimental conditions used here.

The dynamic neutron scattering measurements were performed on the IN6 time-of-flight spectrometer at the Institut Laue-Langevin, Grenoble. The incident neutron wavelength was 5.12 Å, and energy resolutionwas 50 μeV. All data were collected with the sample holder oriented at 135° relative to the incident beam. The samples were contained in aluminum flat-plate cells of 0.7 mm thickness for the protein–cryosolvent and 2 mm thickness for the cryosolvent solutions. The following protein samples were run (with their measured transmissions in parentheses): 68 mg/ml xylanase in 70% CD_3OD/30% D_2O (0.89); 68 mg/ml xylanase in 40% CD_3OD/60% D_2O (0.88); 51 mg/ml xylanase in 80% DMSO/20% D_2O (0.87); 68 mg/ml xylanase in 40% DMSO/60% D_2O (0.90); 100 mg/ml dry powder xylanase (0.98); and 100 mg/ml xylanase in D_2O (0.90).

The dry powder was prepared by freeze drying and then holding at 100 milliTorr for 2 days at 200°C. The following perdeuterated solvents were run: 70% CD_3OD/30% D_2O (0.80); 40% CD_3OD/60% D_2O (0.79); 80% DMSO/20% D_2O (0.80); 40% DMSO/60% D_2O (0.86); and pure D_2O (0.82).

Samples were first cooled to 110 K and then heated back up to 300 K in steps of 10 K. Raw data were corrected in identical fashion. The elastic intensity was determined by integrating the detector counts over the energy range of the instrumental resolution. The detectors were calibrated by normalizing with respect to a standard vanadium sample. The cell scattering was subtracted, taking into account attenuation of the singly scattered beam. Finally, the scattering was normalized with respect to that at the lowest measured temperature, 110 K.

The quantity measured in neutron scattering is the dynamic structure factor, $S(\mathbf{q},\omega)$, which is a function of the scattering wave vector $\mathbf{q}$ and the energy transfer ω (32, 29). $S(\mathbf{q},\omega)$ has two components: incoherent (which arises from self-correlations in the atomic positions) and coherent (which arises from self- and cross-correlations in the atomic positions). The incoherent scattering cross section (scattering power) for hydrogen is an order of magnitude greater than any other cross section in biological systems. Therefore, the hydrogen incoherent scattering dominates the signal from the protein. Because hydrogens are evenly distributed in a protein, the protein scattering gives a global view of the protein motions. To maximize the contribution from the protein motions under controlled conditions, the present experiments were performed by using fully deuterated solvents and hydrogen/deuterium exchanged proteins (twice dissolved in D_2O and freeze-dried). This deuteration procedure serves to ensure that the solvent is fully deuterated (and not partially hydrogenated by exchange of hydrogen from the enzyme) and that no change in the deuteration of the enzyme or solvent occurs during the experiment. The consequent partial deuteration of the enzyme is limited to the exchangeable hydrogens, which means that the hydrogens left are essentially all in the protein. Knowledge of the isotopic scattering cross sections and isotopic compositions of the samples then indicates that, for the protein solutions, about 50% of the scattering is incoherent and 50% coherent. Seventy-five percent of the incoherent scattering originates from the protein, because of the strong hydrogen contribution. Therefore, 25% originates from the solvent atoms and will influence the observed profile in a manner depending on the solvent dynamics and the region of $\mathbf{q},\omega$ space examined.

The isotopic coherent scattering cross sections and protein solution sample composition indicate that most of the coherent scattering originates from the solvent. The self-coherent contribution to this, which is strongest in the low q regime considered here (below 1 $Å^{-1}$), is dynamic and identical in form to the incoherent scattering from the same atom (the amplitude is not identical because it is weighted by the coherent cross section) (39). In addition, there is a contribution originating from cross-correlations (i.e., distance distributions). The intramolecular "Bragg" part of this contribution lies at q values higher than those considered here. However, a structural "small-angle" scattering contribution can also exist in the same q-range as the self-coherent and incoherent scattering. The small-angle scattering can be distinguished from the dynamic self-coherent scattering by its q-dependence. To remove the temperature-independent small-angle scattering, the scattering profiles were normalized with respect to the intensities measured at 110 K. For the protein solution samples examined here, there was no evidence for additional temperature-dependent, small-angle coherent scattering.

We define $\langle u_L^2 \rangle$ as the mean-square displacement of the Lth atom, where the brackets indicate an ensemble-average. If $\mathbf{q}^2\langle u_L^2 \rangle < 1$, the elastic incoherent scattering is given by (39)

$$S_{\text{inc}}(\mathbf{q},\omega = 0,T) = \sum_L b_L^{\text{inc}}\, e^{-\frac{1}{3}\mathbf{q}^2\langle u_L^2\rangle}, \qquad [1]$$

where b_L is the scattering length of atom L. Assuming a uniform mean-square displacement $\langle u^2 \rangle$, this $\langle u^2 \rangle$ can be accessed by performing a plot of $\ln S(\mathbf{q},\omega = 0,T)$ vs. $\mathbf{q}^2$ and taking the limiting slope as $\mathbf{q} \to 0$ at each temperature. In the present work, the $\langle u^2 \rangle$ thus determined is equal to $(\langle u^2 \rangle_T - \langle u^2 \rangle_{110})$, where $\langle u^2 \rangle_{110}$ is the absolute mean-square displacement at 110 K. $\langle u^2 \rangle$ is analogous to that obtained by x-ray crystallographic temperature factor analysis except that it is molecule averaged, time resolved, and purely dynamic, i.e., without a static disorder contribution.

We introduce here the integrated elastic intensity $S_{\text{INT}}(T)$, obtained by summing $S(\mathbf{q},\omega = 0,T)$ over a range of small q values. $S_{\text{INT}}(T)$ provides a qualitative guide of dynamic transition behavior, with good counting statistical accuracy, and it is especially useful in cases where the $\ln S(\mathbf{q},\omega = 0,T)$ vs. $\mathbf{q}^2$ plots are too noisy to extract meaningful $\langle u^2 \rangle$ data, such as was found for the pure solvent samples in the present work. The improved statistics are obtained by integrating over a range of q chosen to lie in the dynamic scattering region, i.e., the straight-line regions in the $\ln S(\mathbf{q},\omega = 0,T)$ vs. $\mathbf{q}^2$ plots ($0.35 < q < 1.03$ $Å^{-1}$ in Fig. 2). The approximate physical sense of $S_{\text{INT}}(T)$ can be appreciated by expanding the exponential in Eq. 1 to first order, integrating over q, and averaging over the atoms. One then obtains that $S_{\text{INT}}(T) \propto -\langle u^2 \rangle$.

In certain pure solvent systems, significant temperature-dependent small-angle coherent scattering was found (see *Results*). The pure solvent $S_{\text{INT}}(T)$ should therefore be considered only as an approximate guide to the dynamic transition behavior of the pure solvent systems studied. Moreover, relatively poor counting statistics were obtained for the pure solvent samples, due in part to the absence of strongly scattering hydrogens,

rendering impossible the extraction of statistically significant mean-square displacements for these samples.

Structural and Thermodynamic Measurements on the Solvents. X-ray scattering experiments on the cryosolvents were carried out down to 110 K in Debye-Scherrer geometry on line 9.1 at the Daresbury Synchrotron Radiation Source (Daresbury, U.K.) using a curved image-plate detector system (41). The cryosolvents were in standard 0.7-mm, thin-walled glass capillary tubes. The cooling rate of 120 K/h was similar to that used in the neutron experiments, and the warming rate was 360 K/h. The scattering from the samples was observed on both cooling and warming at a number of intermediate temperatures. The presence of crystallization was identified by the appearance of powder diffraction peaks. Where no crystallization was observed, the changes to measured diffraction patterns were as would be expected from a liquid or glass on changing the temperature. Samples were also examined visually during image plate changes down to 110 K for any change in optical opacity that would have indicated possible changes, such as crystallization or phase separation. Differential scanning calorimetry (DSC) measurements were made by using a Shimadzu DSC-50 differential scanning calorimeter. Samples were sealed in 50 μl aluminum crucibles (sample weights between 25 and 40 mg) and cooled down by using a flowing nitrogen atmosphere. All data were collected in heating at a standard rate of 10 K/min (42).

Results

Dynamic Neutron Scattering. In Fig. 1 are presented $S_{INT}(T)$ for the samples. For the protein samples, it was possible to fit the data to straight lines in semilog plots of ln $S(q,\omega = 0,T)$ vs. q^2 (an example of such a fit is given in Fig. 2) so as to obtain corresponding mean-square displacement data, which are shown in Fig. 3. The dry powder $S_{INT}(T)$ profile in Fig. 1*A* shows only a relatively small decrease, with temperature over the range examined (from 110 K to 300 K), and there is a correspondingly small increase in $\langle u^2 \rangle$ in the data in Fig. 3*A*. The major component of this $\langle u^2 \rangle$ is expected to be due to small-amplitude, solid-like, vibrational dynamics, the physical nature of which has been explored (43) although one cannot rule out the existence of a small anharmonic contribution. The profile indicates that, in dehydrated powder form, xylanase does not possess a marked transition in the neutron scattering data, consistent with previous work on other proteins (14, 15, 28).

For the pure D_2O sample in Fig. 1*A*, there is a significant decrease with temperature from 110 K to 280 K, without any clear transition but with a gradual increase in curvature. The profile is again consistent with predominantly vibrational fluctuations, but of larger amplitude than in the dry protein powder. Between 280 K and 290 K, there is a sharp transition occurring slightly above the thermodynamic melting point, the latter being at 277 K. This strongly nonlinear increase of $\langle u^2 \rangle$ with T is consistent with the activation of anharmonic picosecond dynamics.

The general form of $S_{INT}(T)$ for xylanase in D_2O resembles that of the pure D_2O, again with a sharp transition associated with melting of the solution. Fig. 3*A* indicates that the melting transition in the xylanase/D_2O system is associated with an 8-fold increase in the mean-square displacement over the temperature range 270–290 K. In Fig. 1*A*, the drop starts earlier and is less steep than that of D_2O, indicating that the transition in the protein solution is slightly more gradual and begins at a slightly lower temperature (≈270 K). This suggests that the protein acts to depress the dynamic transition temperature. Experiments performed on glutamate dehydrogenase and myoglobin in D_2O (not shown) produced results similar to the present xylanase work.

A phenomenon seen in all of the systems is that, below the transition, $S_{INT}(T)$ is higher for xylanase solution than for the

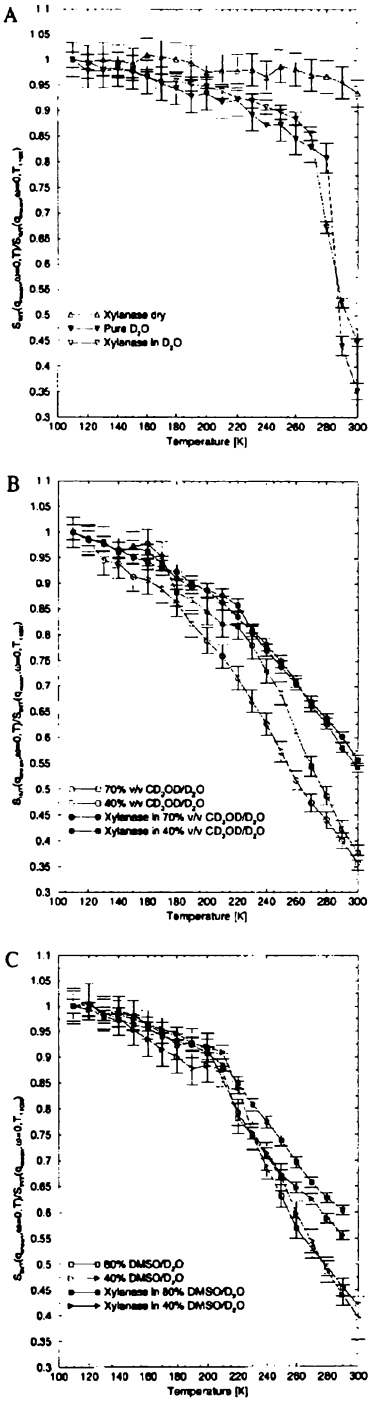

Fig. 1. Normalized integrated elastic intensity. The q integration range is 0.35 $Å^{-1} < q < 1.03$ $Å^{-1}$ and $q_{mean} = 0.66$ $Å^{-1}$. (*A*) Xylanase powder, pure D_2O, and xylanase in D_2O. (*B*) 40% CD_3OD/60% D_2O solvent, 70% CD_3OD/30% D_2O solvent, xylanase in 40% CD_3OD/60% D_2O, and xylanase in 70% CD_3OD/30% D_2O. (*C*) 40% DMSO/60% D_2O, 80% DMSO/20% D_2O, xylanase in 40% DMSO/60% D_2O, and xylanase in 80% DMSO/20% D_2O.

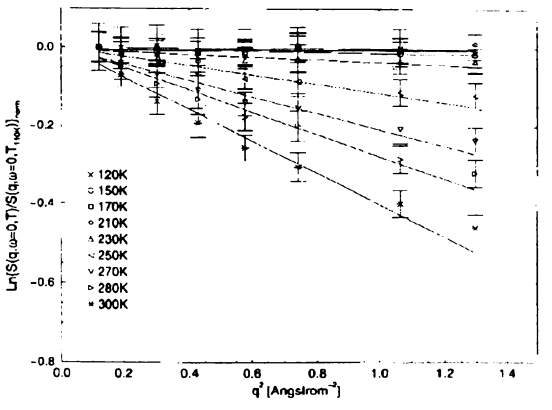

Fig. 2. Ln S(q,0) vs. q^2 plot for xylanase in 70% CD_3OD/D_2O.

corresponding pure solvent. This indicates that, in the protein solution, the atomic fluctuations are decreased relative to those in the pure solvent. This may reflect the relatively high packing of the protein interior, which might lead to restricted vibrational

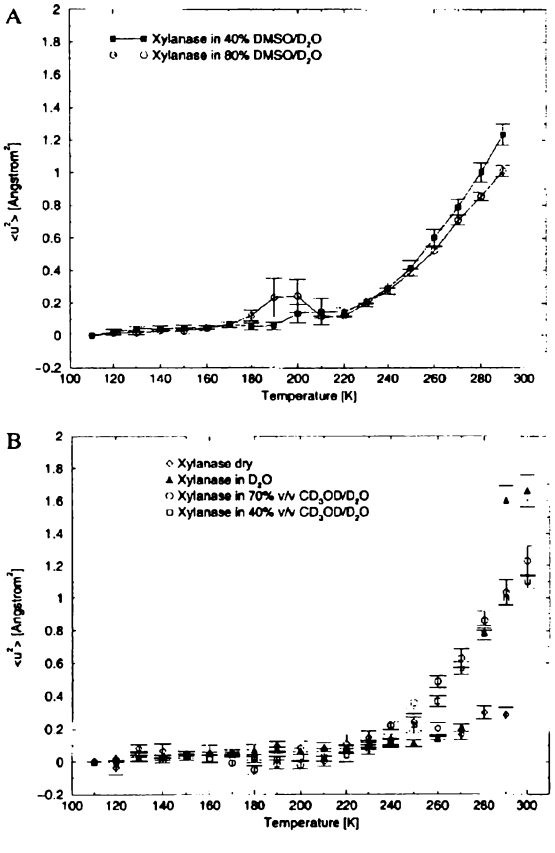

Fig. 3. Mean-square displacement vs. temperature for (*A*) xylanase that is dry, in D_2O, in 40% CD_3OD/D_2O, and in 70% CD_3OD/D_2O. (*B*) Xylanase in 40% DMSO/60% D_2O and in 80% DMSO/20% D_2O.

Table 1. Thermodynamic and stability data

Solvent	Solvent melting temperature, K	Half-life of xylanase in solvent
70% CH_3OH/30% H_2O	188	20 min at 50°C
40% CH_3OH/60% H_2O	233	18 h at 60°C
80% DMSO/20% H_2O	235	<2 min at 50°C
40% DMSO/60% H_2O	232	6 h at 80°C

The stability data were taken at temperatures well above that at which the present experiments were performed. The half-lives at the temperatures used in the present neutron work are very much longer than those given here. The half-life of xylanase in water is >20 h at 95°C.

motion relative to in-bulk solvent. Furthermore, the amplitude of the vibrational modes of the solvent molecules could be reduced by interaction with the protein.

The decrease of $S_{INT}(T)$ with T in all four enzyme–cryosolvent systems and the corresponding pure solvents (Fig. 1 *B* and *C*) is much more gradual than in the D_2O samples. To a first approximation, the dynamics of the protein solutions follow that of the pure solvents. $S_{INT}(T)$ decreases continually over the whole temperature range examined. For some of the samples, unevenness in $S_{INT}(T)$ is seen at low temperatures (below 220 K). This is likely to be related to the thermodynamic and structural phase transitions in these samples discussed in the next section; some contamination from small-angle scattering cannot be ruled out. Apart from this contamination, no clear inflection points in $S_{INT}(T)$ are visible for the pure CD_3OD/D_2O samples whereas for the DMSO samples a change of slope is seen at ≈200–220 K.

The dynamic transition behavior of the protein–cryosolvent solutions is clearly visible in the $\langle u^2 \rangle$ vs. T plots in Fig. 3. In the protein–cryosolvent solutions, large-amplitude anharmonic dynamics are activated at significantly lower temperatures than in the protein/D_2O sample, and the increase of $\langle u^2 \rangle$ with T is much more gradual, resembling that seen in hydrated protein powders (7). The $\langle u^2 \rangle$ data in the four cryosolvent–protein systems are virtually identical.

Structural and Thermodynamic Properties of the Solvents. Published melting temperatures in the hydrogenated mixed solvents (44, 45) and data on the enzyme stability in the mixed solvents are given in Table 1. Three of the four solvents melt in the range 232–235 K whereas the 70% CH_3OH remains liquid to below 190 K.

The DSC and synchrotron x-ray diffraction measurements were performed to provide additional structural and confirmatory thermodynamic information on the perdeuterated pure solvents. Both methods were used to indicate the presence of phase changes, whereas the diffraction data additionally probed structural effects as evidenced by the appearance of Bragg peaks, using heating/cooling rates closely similar to those used in the neutron experiments. The DSC indicated that the melting temperature is at 170–190 K for the 70% CD_3OD/30% D_2O sample and ≈235 K for the 40% CD_3OD/60% D_2O sample, consistent with the above published results.

All solvents showed noticeable Bragg scattering at low temperatures at $q > 0.8$ Å^{-1}. For the 70% CD_3OD/30% D_2O sample, this was visible at temperatures below 190 K, whereas the 40% CD_3OD/60% D_2O solution exhibited Bragg diffraction at 220 K but not 245 K (intermediate temperatures were not examined). These results are consistent with the above published melting temperatures and our DSC measurements. The 40% CD_3OD/60% D_2O sample also exhibited small-angle x-ray scattering at very low q (0.34 Å^{-1}) at 160–180 K, suggesting some long-range periodicity accompanying the formation of microcrystallites at these temperatures in this sample. The above Bragg scattering is consistent with the $S_{INT}(T)$ data in Fig. 1*B*, which shows nonsmooth behavior

below 235 K for the 40% CD_3OD/60% D_2O sample but smooth behavior in the 70% sample. The nonsmooth behavior may be due to dynamic effects accompanying structural phase transitions or due to contamination of $S_{INT}(T)$ by low-q diffraction in the sample. The x-ray data for both the 80% and 40% DMSO solvents showed complex solid-state phase behavior between 170 K and 210 K, which, for the 80% sample, could be related to the uneven $S_{INT}(T)$ and the peak in $\langle u^2 \rangle$ at 190 K and 200 K seen in Fig. 3*B*. The final melting temperature was between ≈230–245 K for both these samples, again consistent with the results of refs. 44 and 45.

Discussion

A number of investigations strongly suggest that the intrinsic anharmonicity of the protein potential surface will be modulated by qualitative changes in solvation conditions (see, for example, refs. 14, 16, 22–33, and 37). The present results indicate a large effect of solvent on dynamic transition behavior by showing that the fast picosecond fluctuations of concentrated protein solutions largely follow those of the corresponding pure solvents.

The compositional inhomogeneity of the mixed solvents may play a role in the nonlinear increase of $\langle u^2 \rangle$ in the protein–cryosolvent systems being much more gradual than in D_2O (Fig. 3). This $\langle u^2 \rangle$ behavior is consistent with the presence of a distribution of energy barriers, with successively higher barriers being crossed on the picosecond time scale with increasing temperature. This is in contrast to the abruptness of the transition in D_2O, which indicates a more cooperative dynamic transition, associated with the melting point. The cooperativity may in principle involve both the ice–water structural transition and associated whole-molecule diffusion.

The results also indicate that, in solutions of proteins in markedly different cryosolvents, similar picosecond dynamic transition behavior is seen. The $\langle u^2 \rangle$ data for xylanase in all four cryosolvents are closely similar, with onset of anharmonicity seen at ≈230 K (Fig. 3). This is around the highest melting points of three of the four cryosolvents which are at 232–235 K. Therefore, the dynamical transition behavior of these three samples occurs at about the same temperature as their phase transition. However, although the highest melting point for 70% CD_3OD/30% D_2O is below 190 K, no associated activation of the picosecond dynamics is seen close to this temperature in the corresponding protein solution. The 230–235 K transition does remain, although perhaps at a slightly lower temperature than for xylanase in 40% CD_3OD/60% D_2O. Remarkably, then, there is little difference in the temperature dependence of the picosecond dynamics of protein–cryosolvent samples here that contain very different proportions of the mixed solvents and water contents and have very different highest melting points. Melting of the 70% CD_3OD/30% D_2O solvent system has no measurable effect on the fast dynamics. The present results also raise the interesting question as to how the dynamics will vary as the proportion of CD_3OD (or DMSO) is decreased, i.e., whether there is a (perhaps narrow) concentration range where a "switch" to the sharp D_2O transition behavior takes place.

Structural effects that might be related to the presently observed dynamic insensitivity to cryosolvent composition would be interesting to investigate. One possible explanation might be that the structure of the solvent shell of the enzyme may be qualitatively similar in all of the cryosolvents but different from pure water. What limited evidence we do have from crystallographic studies in mixed solvents suggests that the non-water solvent molecules do interact with certain parts of the protein surface directly (46–49). However, although xylanase is active in all of the cryosolvent mixtures used here, the mixtures do destabilize the protein relative to water, and they do so to differing degrees (See Table 1). Therefore, if the effect of a solvent on stability is mediated in part by perturbing the shell of molecules closest to the protein, then these stability results would indicate that the composition of the solvent shell is not similar in each sample.

Another possibility, suggested by a referee and consistent with the present and other data, is that the onset of the anharmonic protein motion takes place at a temperature, determined either by the solvent or by the protein, being governed by the component having the higher transition temperature. According to this scenario, the solvent would drive the transition in the pure D_2O solution whereas the protein would drive it in the 70% CD_3OD/30% H_2O system, for which in the absence of protein the solvent melts at about 190 K whereas the onset of anharmonicity is seen at ≈230–240 K. For the other mixed solvent systems, the protein and solvent transition temperatures would essentially coincide. This explanation is consistent with molecular dynamics simulations of isolated myoglobin, for which an intrinsic protein dynamic transition was seen at ≈220 K (50) and is also in agreement with the "protein cold/solvent hot" and "protein hot/solvent cold" results in the recent molecular dynamics simulations of hydrated myoglobin by Vitkup *et al.* (36).

In the future, it will be important to determine the time scale dependence of the solvent influence on dynamic transition behavior. Although it is shown here that the phase transition behavior of xylanase in 70% CD_3OD/30% D_2O is decoupled from the picosecond dynamic transition behavior, it is likely to be coupled to slower motions. Furthermore, because the time scale accessed in the present experiments is also well sampled with modern computer power in molecular dynamics simulation, this computational technique can in principle be used to obtain a detailed decomposition of the dynamic transition behavior revealed here.

We thank the Institut Laue Langevin (Grenoble) for access to neutron beam facilities, the United Kingdom Engineering and Physical Sciences Research Council for access to the Daresbury Synchrotron Radiation Source, the University of London Intercollegiate Thermal Analysis Research Service for facilitating the DSC measurements, and C. Monk and D. Thompson for assistance with enzyme preparation. For part of this work, R.M.D. was supported by a James Cook fellowship from the Royal Society of New Zealand, and V.R. was a European Union-funded Marie Curie Research Fellow.

1. Parak, F. & Formanek, H. (1971) *Acta Crystallogr. A* **27**, 573–578.
2. Frauenfelder, H., Petsko, G. A. & Tsernoglou, D. (1979) *Nature (London)* **280**, 558–563.
3. Keller, H. & Debrunner, P. G. (1980) *Phys. Rev. Lett.* **45**, 67–68.
4. Parak, F., Frolov, E. N., Mossbauer, R. L. & Goldanskii, V. I. (1981) *J. Mol. Biol.* **145**, 825–833.
5. Cohen, S. G., Bauminger, E. R., Nowik, I., Ofer, S. & Yariv, J. (1981) *Phys. Rev. Lett.* **46**, 1244–1248.
6. Knapp, E. W., Fischer, S. F. & Parak, F. (1982) *J. Phys. Chem.* **86**, 5042–5047.
7. Doster, W., Cusack, S. & Petry, W. (1989) *Nature (London)* **337**, 754–756.
8. Rassmussen, B. F., Stock, A. M., Ringe, D. & Petsko, G. A. (1992) *Nature (London)* **357**, 423–424.
9. Kneller, G. R. & Smith, J. C. (1994) *J. Mol. Biol.* **242**, 181–185.
10. Elber, R. & Karplus, M. (1987) *Science* **235**, 318–321.
11. Lamy, A., Souaille, M. & Smith, J. C. (1996) *Biopolymers* **39**, 471–478.
12. Frauenfelder, H., Sligar, S. & Wolynes, P. (1991) *Science* **254**, 1598–1603.
13. Parak, F., Frolov, E. N., Kononenko, A. A., Mossbauer, R. L., Goldanskii V. I. & Rubin, A. B. (1980) *FEBS Lett.* **117**, 368–372.
14. Ferrand, M., Dianoux, A. J., Petry, W. & G. Zaccai. (1993) *Proc. Natl. Acad. Sci. USA* **90**, 9668–9672.
15. Fitter, J., Lechner, R. E. & Dencher, N. (1997) *Biophys. J.* **73**, 2126–2137.
16. Lehnert, U., Réat, V., Weil, M., Zaccai, G. & Pfister, C. (1998) *Biophys. J.* 1945–1952.
17. Ding, X., Rasmussen, B. F., Petsko, G. A. & Ringe, D. (1994) *Biochemistry* **33**, 9285–9293.

18. Ostermann, A., Waschipky, R., Parak, F. G. & Nienhaus, G. U. (2000) *Nature (London)* **404**, 205–208.
19. Daniel, R. M., Smith, J. C., Ferrand, M., Hery, S., Dunn, R. & Finney, J. L. (1998) *Biophys. J.* **75**, 2504–2507.
20. Dunn, R. V., Réat, V., Finney, J. L., Ferrand, M., Smith, J. C. & Daniel, R. M. (2000) *Biochem. J.* **346**, 355–358.
21. Daniel, R. M., Finney, J. L., Réat, V., Dunn, R., Ferrand, M. & Smith, J. C. (1999) *Biophys. J.* **77**, 2184–2190.
22. Brooks, C. L., III, & Karplus, M. (1989) *J. Mol. Biol.* **208**, 159–181.
23. Smith, J. C., Cusack, S., Tidor, B. & Karplus, M. (1990) *J. Chem. Phys.* **93**, 2974.
24. Frauenfelder, H. (1989) *Nature (London)* **338**, 623–624.
25. Rupley, J. A., Gratton, E. & Careri, G. (1983) *Trends Biochem.* **8**, 18–22.
26. Poole, P. L. & Finney, J. L. (1983) *Int. J. Biol. Macromol.* **5**, 308–310.
27. Poole, P. L. & Finney, J. L (1985) *J. Biosci.* **8**, Suppl., 25–35.
28. Krupyanskii, Y. U. F, Parak, F., Goldanskii, V. I., Mossbauer, R. L, Gaubman, E. E., Engelmann, H. & Suzdalev, I. P. (1982) *Z. Naturforsch. C* **37**, 57–62.
29. Smith, J. C., Cusack, S., Poole, P. L. & Finney, J. L. (1987) *J. Biomol. Struct. Dyn.* **4**, 583–588.
30. Zanotti, J.-M., Bellissent-Funel, M.-C. & Parello, J. (1999) *Biophys. J.* **76**, 2390–2411.
31. Perez, J., Zanotti, J.-M. & Durand, D. (1999) *Biophys. J.* **77**, 454–469.
32. Smith, J. C. (1991) *Q. Rev. Biophys.* **24**, 227–291.
33. Diehl, M., Doster, W. & Schober, H. (1997) *Biophys. J.* **73**, 2726–2732.
34. Iben, I. E., Braunstein, D., Doster, W., Frauenfelder, H., Hong, M. K., Johnson, J. B., Luck, S., Ormos, P., Schulte, A., Steinbach, P. J., *et al.* (1989) *Phys. Rev. Lett.* **62**, 1916–1919.
35. Meyer, E. (1994) *Biophys. J.* **70**, 862–873.
36. Vitkup, D., Ringe, D., Petsko, G. A. & Karplus, M. (2000) *Nat. Struct. Biol.* **7**, 34–38.
37. Fitter, J. (1999) *Biophys. J.* **76**, 1034–1042.
38. Cordone, L., Ferrand, M., Vitrano, E. & Zaccai, G. (1999) *Biophys. J.* **76**, 1043–1047.
39. Lovesey, S. W. (1984) *Theory of Neutron Scattering from Condensed Matter* (Clarendon, Oxford).
40. Dunn, R. V. (1998) M. Sc. thesis (Univ. of Waikato, Hamilton, New Zealand).
41. Roberts, M. A., Finney, J. L. & Bushnell-Wye, G. (1998) *Mater. Sci. Forum* **278**, 318–322.
42. Réat, V., Finney, J. L., Steer, A., Roberts, M. A., Smith, J. C., Dunn, R., Petersen, M. & Daniel, R. M. (2000) *J. Biochem. Biophys. Methods* **42**, 97–103.
43. Melchers, B., Knapp, E. W., Parak, F., Cordone, L., Cupane, A. & Leone, M. (1996) *Biophys. J.* **70**, 2092–2099.
44. Douzou, P., Hui Bon Hoa, G., Maurel, P. & Travers, F. (1976) in *Handbook of Biochemistry and Molecular Biology*, ed. Fasman, G. D. (CRC, Boca Raton, FL), 3rd Ed., Vol. 1, pp. 520–539.
45. Weast, R. C., ed. (1974) *Handbook of Chemistry and Physics* (CRC, Boca Raton, FL), 55th Ed.
46. Bouquiere, J. P., Finney, J. L. & Lehmann, M. S. (1993) *J. Chem. Soc. Faraday Trans.* **89**, 2701–2705.
47. Lehmann, M. S., Mason, S. A. & McIntyre, G. J. (1985) *Biochemistry* **24**, 5862–5869.
48. Lehmann, M. S. & Stansfield, R. F. D. (1989) *Biochemistry* **28**, 7028–7033.
49. Ringe. D. (1995) *Curr. Opin. Struct. Biol.* **5**, 825–829.
50. Smith, J. C., Kuczera K. & Karplus, M. (1990) *Proc. Natl. Acad. Sci. USA* **87**, 1601–1605.

Appendix C

My contribution to this work included all the enzymology, including the determination of the temperature dependence of glutamate dehydrogenase activity in perdeuterated cryosolvents, and a share in the preparation of the manuscript. The glutamate dehydrogenase enzymology studies were conducted as part of my Masters research.

2184 Biophysical Journal Volume 77 October 1999 2184–2190

Enzyme Dynamics and Activity: Time-Scale Dependence of Dynamical Transitions in Glutamate Dehydrogenase Solution

Roy M. Daniel,* John L. Finney,# Valérie Réat,# Rachel Dunn,* Michel Ferrand,§ and Jeremy C. Smith¶
*Department of Biological Sciences, The University of Waikato, Hamilton, New Zealand; #Department of Physics and Astronomy, University College London, London WC1E 6BT, England; §Institut Laue Langevin, 38042 Grenoble Cedex 9, France; and ¶SBPM/DBCM, CEA-Saclay, 91191 Gif-sur-Yvette Cedex, France, and Lehrstuhl für Biocomputing, IWR, Universität Heidelberg, D-69120 Heidelberg, Germany

ABSTRACT We have examined the temperature dependence of motions in a cryosolution of the enzyme glutamate dehydrogenase (GDH) and compared these with activity. Dynamic neutron scattering was performed with two instruments of different energy resolution, permitting the separate determination of the average dynamical mean square displacements on the sub-~100 ps and sub-~5 ns time scales. The results demonstrate a marked dependence on the time scale of the temperature profile of the mean square displacement. The lowest temperature at which anharmonic motion is observed is heavily dependent on the time window of the instrument used to observe the dynamics. Several dynamical transitions (inflexions of the mean squared displacement) are observed in the slower dynamics. Comparison with the temperature profile of the activity of the enzyme in the same solvent reveals dynamical transitions that have no effect on GDH function.

INTRODUCTION

It is generally accepted that enzymes require internal flexibility for catalytic activity (e.g., Frauenfelder, 1989). However, which motions are required is not yet well understood. Of particular interest is the role in activity of the fast (e.g., picosecond and nanosecond time scale) structural fluctuations that are probed by molecular dynamics simulations. An important question is whether these fast motions are coupled to the structural changes associated with the catalytic rate-limiting step, which itself may take place on time scales several orders of magnitude slower. One important question that can be and has been addressed is whether the fast motions need to be anharmonic for protein function. This might be the case if, for example, picosecond-nanosecond motions involve rearrangements of the protein that are required to permit slow dynamics across the highest-energy reaction barrier.

In this context it is of interest that a variety of techniques have shown a temperature-dependent transition in the dynamic behavior of hydrated proteins at ~200–220K, involving cessation of anharmonic motion below this temperature. Much of this work has been done on myoglobin with Mossbauer spectroscopy (Keller and Debrunner, 1980; Parak et al., 1982; Knapp et al., 1982), neutron scattering (Doster et al., 1989; Cusack and Doster, 1990), or x-ray crystallography (Frauenfelder et al., 1979) of hydrated crystals, powders, or frozen solutions, but similar results have been found in x-ray crystallographic studies of ribonuclease A (Tilton et al., 1992) and in Mossbauer (Parak et al., 1980) and neutron scattering (Ferrand et al., 1993) studies of membrane proteins. Some protein functions have been observed to cease with the loss of equilibrium anharmonic dynamics as the protein is cooled through the dynamic transition. Among these are electron tunneling in *Rhodospirullum rubrum* chromatophores (Parak et al., 1980), some elements of the photocycle of bacteriorhodopsin in hydrated membranes of *Halobacterium salinarum* (Ferrand et al., 1993), and ligand binding/release in ribonuclease A crystals (Rassmussen et al., 1992).

Motions in proteins are known to exist over a range of time scales. An important remaining issue then is the time scale dependence of the dynamical transition. Whether there is a time scale dependence depends on the nature of the underlying potential surface. The first parallel studies of enzyme activity and dynamics, using glutamate dehydrogenase (GDH) in a cryosolution, probed picosecond time scale motions. The results showed no deviation from Arrhenius behavior through the dynamical transition (Daniel et al., 1998). These results indicate that there is a range of temperatures (190–220K) at which the enzyme rate-limiting step does not require, and is not affected by, anharmonic motions taking place on the picosecond time scale.

To further address the time scale problem we have performed here a study comparing the temperature dependence of the activity of GDH with the dynamics of the enzyme solution on two different time scales, determined by neutron scattering. The experiments make use of the different energy resolutions of two neutron scattering spectrometers: IN16 and IN6 at the Institut Laue-Langevin reactor in Grenoble. Whereas IN6 probes motions on time scales faster than ~100 ps, those detected by IN16 extend to ~5 ns. The experiments were performed over a temperature range extending through the previously observed dynamic transition, in a 70% v/v methanol/water cryosolvent in which the enzyme is active and stable.

Received for publication 27 April 1999 and in final form 13 July 1999.
Address reprint requests to Dr. R. M. Daniel, Department of Biological Sciences, University of Waikato, Hamilton, New Zealand. Tel.: +64-7-838-4213; Fax: +64-7-838-4324; E-mail: r.daniel@waikato.ac.nz.

0006-3495/99/10/2184/07 $2.00

Glutamate dehydrogenase is a key enzyme of central metabolism. It catalyzes the reversible conversion of 2-ketoglutarate, ammonia, and reduced nicotinamide adenine dinucleotide phosphate (NADP) to glutamate and oxidized NADP. The reaction is complex and has multiple steps. Kinetic analysis of this enzyme (Hudson and Daniel, 1995) suggests the reaction proceeds by a sequential, steady-state, random mechanism. At the growth temperature of the source organism, *Thermococcus zilligii* strain AN1, ~350K, the turnover number of the enzyme is ~1500 s^{-1}. In fully deuterated cryosolvent at 220K the turnover number is ~0.01 s^{-1}. For comparison, the turnover number of lysozyme at room temperature is 0.5 s^{-1}. The turnover number of course applies to the rate-limiting step, and given the complexity of the reaction and the necessary rapid equilibration of intermediates, some reaction steps will be very much faster.

The results demonstrate a marked dependence on time scale of the temperature profile of the mean square displacements. The dynamical transitions occurring within the temperature range for which enzyme activity was measured have no significant effect on function.

MATERIALS AND METHODS

The glutamate dehydrogenase is from *Thermococcus* strain AN1 (now known as *T. zilligii* strain AN1) (DSM 2770) and was purified, assayed, and prepared for neutron scattering as described elsewhere (Hudson et al., 1993; More et al., 1996; Daniel et al., 1998). Temperature-activity determinations were carried out in hydrogenated cryosolvent: isolated determinations carried out in the perdeuterated (completely deuterated) cryosolvent used for the neutron scattering experiments, at various temperatures, showed that Arrhenius behavior (apparent activation energy) was unaffected. At the completion of each neutron scattering experiment the activity was assayed to ensure that no denaturation had occurred.

The dynamic neutron scattering measurements were performed on the IN6 time-of-flight spectrometer and on the IN16 backscattering spectrometer at the Institut Laue-Langevin, Grenoble. The incident neutron wavelengths were 5.12 Å on IN6 and 6.28 Å on IN16. All data were collected with the sample holder oriented at 135° relative to the incident beam. The samples were contained in aluminum flat-plate cells, of 0.3-mm and 0.5-mm path lengths on IN6 and IN16 respectively.

Two samples were run: 1) on IN6, 100 mg ml^{-1} of enzyme in 70% v/v CD_3OD/D_2O solvent, and 2) on IN16, 56 mg ml^{-1} of enzyme in 70% v/v CD_3OD/D_2O solvent. The samples were cooled to 80K then heated progressively to 320K over 16–24 h. The measured transmissions were 0.92 for the IN6 sample and 0.85 for the IN16 sample. Raw data on the two instruments were corrected in identical fashion. The elastic intensity was determined by integrating the detector counts over the energy range of the instrumental resolution. The detectors were calibrated by normalizing with respect to a standard vanadium sample. The cell scattering was subtracted, taking into account attenuation of the singly scattered beam. Finally, the scattering was normalized with respect to the scattering at the lowest measured temperature, 80K, and to the lowest wavevector, q.

The elastic incoherent scattering intensity $S_{inc}(q, \omega = 0)$ (where q is the magnitude of the scattering wave vector and ω is the energy transfer) was used to obtain $\langle u^2 \rangle$ by using the relationship $\ln S_{inc}(q, \omega = 0) = -\langle u^2 \rangle q^2/3$, which is valid in the regime $q^2 \langle u^2 \rangle / 3 < 1$. $\langle u^2 \rangle$ was thus obtained by fitting a straight line to a semilog plot of $S(q, \omega = 0)$ versus q^2 in the linear regime, which was found at $0.12\ Å^{-2} < q^2 < 1.07\ Å^{-2}$ and $0.10\ Å^{-2} < q^2 < 1.13\ Å^{-2}$ in the IN6 and IN16 experiments, respectively. The linear regime was found to be well separated from the Bragg scattering of the solution, which was found at $1.4\ Å^{-1} < q < 2.0\ Å^{-1}$, and no evidence was found for a low-q protein-protein interaction peak. As the scattering was normalized with respect to the 80K intensities, the $\langle u^2 \rangle$ determined is equal to $(\langle u^2 \rangle_T - \langle u^2 \rangle_{80})$, where $\langle u^2 \rangle_T$ is the absolute mean square displacement at temperature T. In practice, the measured $\langle u^2 \rangle$ corresponds to the H atoms, the scattering cross section of which is strongly dominant. For the samples used on IN16 and IN6, 70% and 80% of the incoherent signal are due to the enzyme, respectively. The $\langle u^2 \rangle$ values obtained for these samples are therefore dominated by the enzyme motions. The energy resolution of IN16 is 1 μeV, whereas that of IN6 is 50 μeV. The inverses of these energy resolutions correspond to times of 5 ns and 100 ps, respectively.

The quasielastic scattering experiment was run on IN16, using 60 mg ml^{-1} of enzyme in 70% v/v CD_3OD/D_2O solvent. Data were collected during heating from 80K, using the same proceedure as for the elastic scans, and during cooling from 320K over 16–24 h. No statistically significant differences were observed between the two sets of data. Data were corrected by normalization of the detectors with vanadium and subtraction of the empty cell scattering.

X-ray scattering experiments on the solvent and solvent plus enzyme were carried out on line 9.1 at the Daresbury synchrotron radiation source, using a curved image-plate detector system. Enzyme concentrations and cooling and heating rates were chosen to match those used in the neutron scattering experiments. Differential scanning calorimetry measurements were made on samples of the same concentrations during both cooling and heating, but with higher rates of temperature change (10°/min).

RESULTS AND DISCUSSION

The elastic incoherent scattering intensities obtained on IN6 and IN16 for a range of temperatures are shown in Fig. 1. The fitted straight lines were used to plot $\langle u^2 \rangle$ versus temperature in Fig. 2. The upward inflexion of the $\langle u^2 \rangle$ from $\langle u^2 \rangle \sim 0$ in Fig. 2 indicates the onset of anharmonic dynamics as the temperature is increased. There is a clear indication from Fig. 2 of a time scale dependence of this dynamical transition. The onset of anharmonic motion occurs at ~140K on IN16 (motions <~5 ns) and at ~220K on IN6 (<~100 ps). In addition to the dynamical transition at ~140K, there are inflexions in the IN16 $\langle u^2 \rangle$ at ~185K, ~210K, and ~280K. If one defines a "dynamical transition" as an inflexion in $\langle u^2 \rangle$, then the IN16 profile demonstrates the presence of four dynamical transitions in the sample. The three highest-temperature transitions do not correspond to transitions from anharmonic to harmonic behavior, but rather to modification of the anharmonic behavior itself.

To investigate whether any of the various transitions in Fig. 2 are coupled with changes in solvent behavior, a number of supplementary experiments were performed. Differential scanning calorimetry (DSC) indicated the presence of one thermodynamic phase transition, at 180K in the pure cryosolvent and 170K in the enzyme/cryosolvent solution. No qualitative differences in behavior were seen when the data were gathered during heating rather than cooling. The associated exothermic change is 2.5 times smaller for the enzyme/cryosolvent system. Synchrotron x-ray diffraction experiments indicate that the 180K transition in the pure cryosolvent is associated with the melting of one crystalline phase. However, the x-ray diffraction patterns obtained from the enzyme/cryosolvent system showed no detectable crystallization at any temperature down to

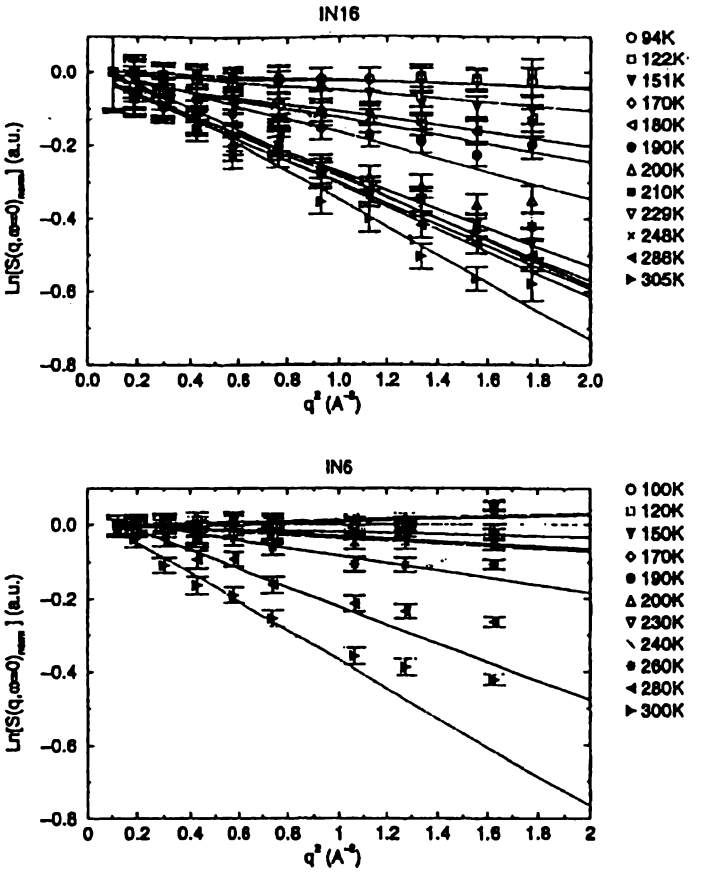

FIGURE 1 Variation of the logarithm of the elastic incoherent scattering of glutamate dehydrogenase in CD_3OD/D_2O (70:30), $S(q,\omega = 0)$, normalized to 80K, as a function of q^2. The IN6 spectrometer has an energy resolution corresponding approximately to motions faster than 10^{-10} s (Daniel et al., 1998), and the IN16 spectrometer an energy resolution corresponding to motions faster than 5×10^{-9} s.

110K. In contrast, crystallization was visible in neutron scattering in the enzyme/solvent system at 170K, as evidenced by the appearance of Bragg diffraction at $Q > 1.4$ $Å^{-1}$. Moreover, the neutron peaks were found at the same d-spacing as those appearing in the 70% methanol/water x-ray diffraction pattern at 180K. The differences between the neutron and x-ray diffraction results may be related to differences in the sample sizes, which are a few microliters for the x-ray experiments, ~50 μl for the DSC, and a few milliliters for the neutron scattering. It is therefore possible that the DSC phase transition at 170K and the discontinuity observed at 185K in the temperature profile of the IN16 $\langle u^2 \rangle$ are associated with the melting of one component of the cryosolvent. However, no features are found in either the x-ray or DSC results that accompany either of the dynamical transitions at 140K or at 210K. We therefore conclude that these two transitions are not correlated with detectable structural or thermodynamic changes in the cryosolvent.

To verify the dynamic origin of the observed transitions, additional experiments were performed to detect associated changes in quasielastic neutron scattering on IN16. Quasielastic scattering, which is visible as a broadening under the elastic peak, arises from the presence of nonvibrational motion in the sample, such as jump or continuous diffusion (Bee, 1988). In favorable cases quasielastic scattering can be analyzed to give details on the geometries and time scales of the contributing motions. Here, however, the counting statistics were found to be insufficient for such an analysis. Rather, the presence of a qualitative change in the quasielastic scattering was used to confirm that the origin of the IN16 scattering changes in Fig. 2 are indeed dynamic. Measured spectra are presented in Fig. 3. At 130K the form of the spectrum is essentially that of the vanadium control. As vanadium is a pure elastic scatterer, this indicates that no quasielastic scattering and hence no diffusive dynamics are present. Quasielastic scattering appears between 130K and 170, and intensifies between 170K and 190K and again between 190K and 210K. These results are consistent with the positions of the dynamical transitions in the IN16 $\langle u^2 \rangle$ data in Fig. 2. From 225K to 290K little change is seen in the quasielastic spectrum, again consistent with the behavior of $\langle u^2 \rangle$ in Fig. 2. The quasielastic scattering data confirm the IN16 $\langle u^2 \rangle$ transitions at ~140K, ~210K, and ~280K as arising from changes in the anharmonic motion in the enzyme.

In previous work on a number of proteins (Keller and Debrunner, 1980; Parak et al., 1982; Knapp et al., 1982;

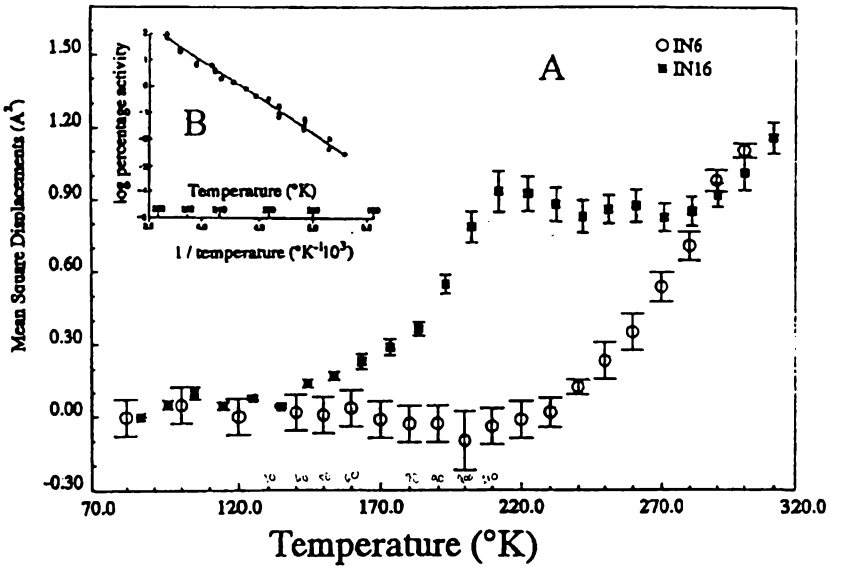

FIGURE 2 Effect of temperature on the enzyme activity (*inset, B*), and the dynamics as measured by neutron scattering, of glutamate dehydrogenase in CD_3OD/D_2O (70:30). Neutron scattering data are from Fig. 1. Enzyme activity data are from More et al. (1996).

Doster et al., 1989; Cusack and Doster, 1990; Frauenfelder et al., 1979; Tilton et al., 1992; Parak et al., 1980; Ferrand et al., 1993), a dynamical transition was observed at various temperatures between 170 and 230K. Moreover, although the different techniques used have sometimes covered different time scales, comparison between them, and with activity, has been hampered by the use of different proteins in a variety of physical states. In the experiments presented here, the use of a consistent method on a single preparation reveals a shift of the lowest transition temperature to lower temperatures as the time scale probed increases from approximately picoseconds to approximately nanoseconds. This effect was also seen on the same preparation in preliminary measurements using the IRIS spectrometer at the ISIS spallation neutron source in Oxford, which has an energy resolution intermediate between that of IN16 and IN6, and resolves motions on the <500-ps time scale. The lowest IRIS transition was found at an intermediate temperature, between 150K and 180K (Finney and Daniel, 1998).

Given the direct nature of neutron scattering as a determinant of global protein motions (Smith, 1991) (as compared with Mossbauer spectroscopy, which examines Fe dynamics, and x-ray crystallography, which gives time-averaged displacements and includes static disorder), the conclusion that the temperature dependence of the transition in average protein motions is time scale dependent can be considered to be relatively robust. The lowest dynamical transition temperature for the present system can therefore be seen to be heavily dependent upon the instrument time scale, rather than occurring at a fixed temperature. As the temperature is lowered, the anharmonic motions slow down, moving from fast to slow time windows. This qualitative effect is consistent with a description of the dynamics associated with the lowest transition as essentially activated, i.e., as involving energy-barrier crossing. A remaining question is therefore whether at time scales longer than nanoseconds the lowest dynamical transition will be found below 140K, and correspondingly at time scales significantly shorter than 10^{-11} s it will be found above 220K. Within the framework of an activated process, the recent simulation evidence for the lowering of the dynamical transition temperature in a viral capsid protein upon ligand binding (Phelps et al., 1998) could be interpreted as the ligand leading to a decrease in the effective associated energy barrier.

The amplitude of the slower motions (IN16) remains essentially unchanged from 210K to 280K. This surprising result is consistent with an effective square-well potential over this temperature range. Also of interest is the apparent coincidence (to within experimental error) of the IN6 and IN16 data points above 280K. This coincidence between the $\langle u^2 \rangle$ values above 280K would indicate that the contribution to the overall motion at these higher temperatures from motions on the time scales intermediate between IN6 and IN16 is very small; i.e., these intermediate time scale motions have risen to a peak at ~210K (observable by subtracting IN6 $\langle u^2 \rangle$ values from IN16 $\langle u^2 \rangle$ values) and decline steadily to a low value at ~280K. This is consistent with the conclusion (above) that the dynamic transition is heavily dependent upon the time scale window of the instrument used to observe dynamics, with motion over a given time scale progressively replaced by slower motions as the temperature is lowered. However, it is possible that the IN16 values are affected by systematic error at high values of $\langle u^2 \rangle$, possibly associated with the relatively low corresponding elastic counting intensities. Therefore, the approximately constant $\langle u^2 \rangle$ between 220K and 280K and the coincidence of the IN6 and IN16 data above 280K merit

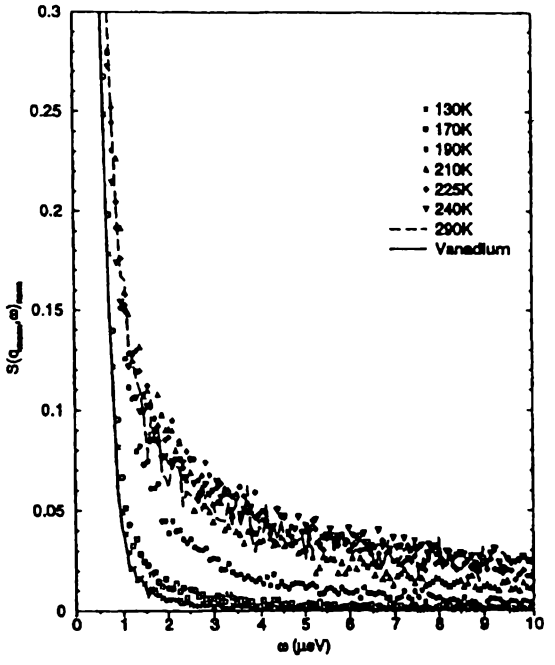

FIGURE 3 IN16 dynamic structure factor of glutamate dehydrogenase in CD_3OD/D_2O (70:30) over a range of temperatures. Data averaged over angles corresponding to the q range over which the data fit in Fig. 2 were linear, i.e., $0.10 < q < 1.13$ Å^{-1}. Spectra were normalized to 1 for zero energy transfer to visualize the variation in shape of the quasielastic intensity.

further confirmation. Experimental errors are also probably responsible for the absence of a detectable $\langle u^2 \rangle$ at temperatures below the lowest dynamical transition on both instruments: small-amplitude vibrational motions are active in the protein at these temperatures. In parallel measurements on low hydration samples of GDH, the better statistics of the data possible in the absence of excess solvent showed a clear, steady rise in $\langle u^2 \rangle$ from the lowest temperature measured.

The inset to Fig. 2 shows that enzyme activity in the cryosolvent used in the neutron scattering experiments exhibits no deviation in Arrhenius behavior down to the lowest temperature at which activity could be measured, 185K. Three of the dynamical transitions visible in Fig. 2 occur at temperatures significantly above 185K: those at 210K and 280K on IN16 and at 220K on IN6. Therefore, these apparent changes in dynamic behavior have no visible affect on activity. Whether the remaining transitions at lower temperatures (140K and 185K on IN16) involve the activation of dynamics required for function is unknown.

In considering the significance of the above results it is important to assess whether enzyme structure/activity in the cryosolvent is likely to be similar to that in a physiological solvent. Many studies of protein dynamics have been carried out on hydrated crystals or powders, and there is evidence that, given a hydration of >0.2 g H_2O/g protein, many protein properties are close to those in solution (Rupley and Careri, 1991). The present measurements were carried out under conditions where enzyme activity can be accurately measured. Given the relatively small effect of cryosolvent on the activity of the enzyme and the low water activity in the interior of a cell, the physical and functional properties of the enzyme in the 70% methanol cryosolvent are likely to be at least as close to those of the in vivo enzyme as are those dissolved in dilute buffer or as hydrated powders. The solvent has little influence on activity or stability under the experimental conditions used here. The reaction rate in cryosolvent is about half the rate in buffer. K_m values are somewhat lower, but these effects are relatively small and with appropriate precautions do not affect activity determinations (More et al., 1996). The viscosity of the cryosolvent rises by ~200-fold between 273K and 188K (Weast, 1974), but the decrease in reaction velocity is very much greater than this, so that activity does not approach diffusion limitation. Full activity was found to be recoverable after the neutron beam experiments. However, solvent properties will be expected to influence the dynamical properties examined here. An example of this is given in the recent work on myoglobin in trehalose, where the protein was found to remain approximately harmonic up to room temperature (Cordone et al., 1999). The dynamical transitions examined here might be expected to change with the properties of the solvent. Work is in progress to examine this point.

The present results may not be representative of all proteins. Neutron experiments performed on bacteriorhodopsin (an insoluble, integral membrane protein) in hydrated membranes of *Halobacterium salinarum* have not detected a time dependence of the dynamical transitions (Réat et al., 1997). Whether the present findings will be generalized to other (water) soluble enzyme classes under the same environmental conditions remains to be seen. The GDH used here is a large, hexameric enzyme from an archeal extreme thermophile. It is a good subject for work of this type, being stable and active in the cryosolvent over a very wide temperature range, as well as being very soluble. There is no evidence that such enzymes in general have systematic differences of structure or function from mesophilic or non-archeal organisms; i.e., the differences between mesophilic and thermophilic enzymes, and between archeal and bacterial enzymes are no greater than the differences found within each group (Daniel et al., 1997). Specific studies on this GDH, including those on Arrhenius behavior, have shown that it is no more different from other GDHs than these are from one another (Hudson and Daniel, 1993, 1995; Hudson et al., 1993; More et al., 1996), and GDHs are not atypical of soluble multisubunit enzymes. We currently have no reason to believe that the results reported here will not apply to this class of enzymes and possibly also to simpler soluble enzymes. A variety of enzymes, including xylanase, catalase, alkaline phosphatase (Dunn, Bragger, and Daniel, unpublished observations), β-glucosidase, and β-galactosidase (More et al., 1996) do exhibit straight Ar-

rhenius plots to below 200K, well below the picosecond dynamical transition temperature for GDH.

The work described here is the first determination of the global dynamics of an active enzyme over a range of time scales, measured under similar conditions. It seems likely from the present and earlier work (Daniel et al., 1998) that anharmonic fast (ps) time scale motions are not required at all temperatures for the enzyme rate-limiting step. Therefore, anharmonic fast motions are not necessarily coupled to the much slower motions describing transitions along the enzyme reaction coordinate. However, the neutron technique used here reveals average dynamics, and it is conceivable that functionally important fast motions may occur locally in the protein at the active site, at levels below the noise in Fig. 2.

Glutamate dehydrogenase is a multisubunit enzyme catalyzing the interconversion of five reactants by a rather complex mechanism (Hudson and Daniel, 1993, 1995). Therefore, it is not feasible to relate the global dynamics we have described here to elements in the structure critical to function or to the rate-limiting step. Clearly more needs to be done in combining techniques with which the dynamical transitions can be studied. Further work is required to examine the intramolecular localization of functionally important motions. It is encouraging in this respect to see that site-specific labeling studies have recently been shown to be successful in dynamic neutron scattering studies on proteins (Lehnert et al., 1998; Réat et al., 1998). Moreover, techniques sensitive to local dynamics, such as optical spectroscopy, can also provide useful information (Di Pace et al., 1992; Melchers et al., 1996). The availability of the crystal structure of GDH may also help future work in this regard. It is of interest to note that the crystallographic study of a related GDH provided evidence for a large relative movement of the two domains between which the active site is located, during the catalytic cycle (Baker et al., 1997).

The results of further investigations can be expected to improve our understanding of the relationships between protein activity, flexibility, and stability. For example, there is a commonly held view that stability is inversely related to activity because molecular flexibility is required for activity, but excessive flexibility tends to be destabilizing (see Daniel et al., 1997). The recent engineering of subtilisin to withstand 100°C with full retention of activity may indicate that this principle is not general (Vandenbrug et al., 1998). Alternatively, a more careful distinction may need to be made between the flexibility required for activity (which may be local or restricted to particular time scales) and that which is likely to affect stability (which is possibly global). Clearly, a complete understanding of this and related problems will require continued investigation into the forms, amplitudes, and time scales of motions involved in enzyme catalysis.

We thank the Institut Laue-Langevin (Grenoble, France) and the ISIS facility (Didcot, UK) for access to neutron beam facilities, C. Monk for assistance with enzyme preparation, the Royal Society of New Zealand for the award of a James Cook Fellowship to RMD, and The European Community for the award of a postdoctoral fellowship to VR (contract no. ERBFMBICT975595).

REFERENCES

Baker, P. J., M. L. Waugh, X. G. Wang, T. J. Stillman, A. P. Turnbull, P. C. Engel, and D. W. Rice. 1997. Determinants of substrate specificity in the superfamily of amino acid dehydrogenases. *Biochemistry.* 36: 16105–16109.

Bee, M. 1988. Quasielastic neutron scattering. Adam Hilger, Bristol, U.K.

Cordone, L., M. Ferrand, E. Vitrano, and G. Zaccai. 1999. Harmonic behavior of trehalose-coated carbon-monoxy-myoglobin at high temperature. *Biophys. J.* 76:1043–1047.

Cusack, S., and W. Doster. 1990. Temperature dependence of the low frequency dynamics of myoglobin. *Biophys. J.* 58:243–251.

Daniel, R. M., M. Dines, and H. H. Petach. 1997. The denaturation and degradation of stable enzymes at high temperatures. *Biochem. J.* 317: 1–11.

Daniel, R. M., J. C. Smith, M. Ferrand, S. Hery, R. Dunn, and J. L. Finney. 1998. Enzyme activity below the dynamical transition at 220K. *Biophys. J.* 75:2504–2507.

Di Pace, A., A. Cupane, M. Leone, E. Vitrano, and L. Cordone. 1992. Protein dynamics. Vibrational coupling, spectral broadening mechanisms, and anharmonicity effects in carbonmonoxy heme proteins studied by the temperature dependence of the Soret band lineshape. *Biophys. J.* 63:475–484.

Doster, W., S. C. Cusack, and W. Petry. 1989. Dynamical transition of myoglobin revealed by inelastic neutron scattering. *Nature.* 337: 754–756.

Ferrand, M., A. J. Dianoux, W. Petry, and G. Zaccai. 1993. Thermal motions and function of bacteriorhodopsin in purple membranes: effects of temperature and hydration studied by neutron scattering. *Proc. Natl. Acad. Sci. USA.* 90:9668–9672.

Finney, J. L., and R. M. Daniel. 1998. ISIS Experimental Report RB8790. Rutherford Appleton Laboratory, Chilton, Didcot, Oxon, England.

Frauenfelder, H. 1989. New looks at protein motions. *Nature.* 338: 623–624.

Frauenfelder, H., G. A. Petsko, and D. Tsernoglou. 1979. Temperature-dependent x-ray diffraction as a probe of protein structural dynamics. *Nature.* 280:558–563.

Hudson, R. D.,R. D.R. C. and R. M. Daniel. 1993. L-Glutamate dehydrogenase: distribution, properties and mechanism. *Comp. Biochem. Physiol.* 106:767–792.

Hudson, R. C., and R. M. Daniel. 1995. Steady state kinetics of the glutamate dehydrogenase from an archaebacterial extreme thermophile, isolate AN1. *Biochim. Biophys. Acta.* 1250:60–68.

Hudson, R. C., L. D. Ruttersmith, and R. M. Daniel. 1993. Glutamate dehydrogenase from the extremely thermophilic archaebacterial isolate, AN1. *Biochim. Biophys. Acta.* 1202:244–250.

Keller, H., and P. G. Debrunner. 1980. Evidence for conformational and diffusional mean square displacements in frozen aqueous solution of myoglobin. *Phys. Rev. Lett.* 45:68–67.

Knapp, E. W., S. F. Fischer, and F. Parak. 1982. Protein dynamics from Mossbauer spectra: the temperature dependence. *J. Phys. Chem.* 86: 5042–5047.

Lehnert, U., V. Réat, M. Weik, G. Zaccai, and C. Pfister. 1998. Thermal motions in bacteriorhodopsin at different hydration levels studied by neutron scattering: correlation with kinetics and light-induced conformational changes. *Biophys. J.* 75:1945–1952.

Melchers, B., E. W. Knapp, F. Parak, L. Cordone, A. Cupane, and M. Leone. 1996. Structural fluctuations of myoglobin from normal-modes, Mossbauer, Raman, and absorption spectroscopy. *Biophys. J.* 70: 2092–2099.

More, R., R. M. Daniel, and H. H. Petach. 1996. The effect of low temperatures on enzyme activity. *Biochem. J.* 305:17–20.

Parak, F., E. N. Frolov, A. A. Kononenko, R. L. Mossbauer, V. I. Goldonskii, and A. G. Rubin. 1980. Evidence for a correlation between the photo induced electron transfer and dynamic properties of the chromatophore membranes from *Rhodospirillum rubrum*. *FEBS Lett.* 117: 368–372.

Parak, F., E. W. Knapp, and D. Kucheida. 1982. Protein dynamics: Mossbauer spectroscopy on deoxymyoglobin crystals. *J. Mol. Biol.* 161: 177–194.

Phelps, D. K., P. J. Rossky, and C. B. Post. 1998. Influence of antiviral compound on the temperature dependence of viral protein flexibility and packing. *J. Mol. Biol.* 276:331–337.

Rassmussen, B. F., A. M. Stock, D. Ringe, and G. A. Petsko. 1992. Crystalline ribonuclease A loses function below the dynamical transition at 220K. *Nature.* 357:523–424.

Réat, V., H. Patzelt, M. Ferrand, C. Pfister, D. Oesterhelt, and G. Zaccai. 1998. Dynamics of different functional parts of bacteriorhodopsin: H-2H labelling and neutron scattering. *Proc. Natl. Acad. Sci. USA.* 95: 4970–4975.

Réat, V., G. Zaccai, M. Ferrand, and C. Pfister. 1997. Functional dynamics in purple membrane. *In* Biological Macromolecular Dynamics. S. Cusack, H. Buttner, M. Ferrand, P. Langan, and P. Timmins, editors. Adenine Press, Schenectady, NY. 117–122.

Rupley, J. A., and G. Careri. 1991. Protein hydration and function. *Adv. Protein Chem.* 41:37–172.

Smith, J. C. 1991. Protein dynamics: comparison of simulation with inelastic neutron scattering experiments. *Q. Rev. Biophys.* 25:227–293.

Tilton, R. F., J. C. Dewan, and G. A. Petsko. 1992. Effects of temperature on protein structure and dynamics: x-ray crystallographic studies of the protein ribonuclease A at nine different temperatures from 98 to 320 K. *Biochemistry.* 31:2469–2481.

Vandenbrug, B., G. Vriend, O. R. Veltman, and V. G. H. Eijsink. 1998. Engineering an enzyme to resist boiling. *Proc. Natl. Acad. Sci. USA.* 95:2056–2060.

Weast, R. C., editor. 1974. Handbook of Chemistry and Physics, 55th Ed. CRC Press, Cleveland, OH.

Appendix D

My contribution to this work included all the enzymology, including the determination of the temperature dependence of xylanase activity in both hydrogenated and perdeuterated cryosolvents. I took the lead role in writing this paper. The xylanase cryoenzymology studies were conducted mostly as part of my Masters research.

Biochem. J. (2000) 348, 355–358 (Printed in Great Britain) 355

Enzyme activity and dynamics: xylanase activity in the absence of fast anharmonic dynamics

Rachel V. DUNN*, Valerie RÉAT†, John FINNEY†, Michel FERRAND‡, Jeremy C. SMITH§ and Roy M. DANIEL*[1]

*Department of Biological Sciences, University of Waikato, Hamilton, New Zealand, †Department of Physics and Astronomy, University College London, Gower Street, London, WC1E 6BT, U.K., ‡Institut Laue Langevin, 156X, Avenue des Martyrs, 38042 Grenoble Cedex 9, France, and §Lehrstuhl für Biocomputing, IWR, Universität Heidelberg, Im Neuenheimer Feld 368, D-69120 Heidelberg, Germany

The activity and dynamics of a simple, single subunit enzyme, the xylanase from *Thermotoga maritima* strain Fj SS3B.1 have been measured under similar conditions, from −70 to +10 °C. The internal motions of the enzyme, as evidenced by neutron scattering, undergo a sharp transition within this temperature range; they show no evidence for picosecond-timescale anharmonic behaviour (e.g. local diffusive motions or jumps between alternative conformations) at temperatures below −50 °C, whereas these motions are strongly activated at higher temperatures. The activity follows Arrhenius behaviour over the whole of the temperature range investigated, −70 to +10 °C. The results indicate that a temperature range exists over which the enzyme rate-limiting step is independent of fast anharmonic dynamics.

Key words: cryoenzymology, neutron scattering, thermophile.

INTRODUCTION

There is good evidence that most, if not all, enzymes require molecular flexibility for function, as is implicit in the concept of induced fit [1–5]. The most direct evidence is the large conformational changes which crystallographic studies show accompany substrate binding and/or product release in some enzymes [6,7], and on a smaller scale the changes in covalent bond lengths that occur during catalysis [8]. More general evidence arises from a variety of studies of enzymes from extreme thermophiles that show them to be, at any given temperature, less flexible and less active than enzymes from mesophiles [9–13].

Proteins exhibit a variety of internal motions, that cover a wide range of amplitudes (0.01–100 Å) and timescales (10^{-15} to > 1 s) [1,2]. Which of these are essential for enzymatic activity, and how these motions couple to each other is not yet known. While it is evident that many of the motions involved in enzyme flexibility must occur over shorter timescales than those of the enzyme rate-limiting step, the nature of the dynamic changes required for catalysis is unclear: for example, whether they are local or global, fast or slow. One possibility is that fast, small-amplitude fluctuations of single atoms and amino-acid side-chains, on the picosecond (10^{-11} s) and sub-Angstrom time and length scales, are essential to other motions that occur on longer length scales, such as relative motions of domains, and on physiological timescales. The shorter motions may therefore be coupled to the longer ones, serving as the 'lubricant' that makes the latter possible. This idea is consistent with results that indicate that the temperature dependence of the fast hydrogen mean-square displacements in hydrated myoglobin, as obtained by neutron scattering, resembles that derived by Mossbauer spectroscopy, which detects motions of the iron atom in the haem group on slower timescales down to 10^{-7} s. Both techniques provided evidence for a dynamical transition in myoglobin, at about −50 to −70 °C [14–16]. Below this, the protein is relatively solid-like, exhibiting only vibrational, harmonic motion, and above this more liquid-like, anharmonic motion is seen, indicating increased flexibility of the protein. The anharmonic motion involves the activation of non-vibrational random motion, such as jumps between closely-related conformations or diffusive motion of groups of atoms in effective cages [17]. The similarity in the temperature dependence obtained with the two techniques lead to the suggestion that the picosecond fluctuations observed with neutron scattering could couple to the haem group, and were likely to be an important factor in the slower motions resolved in the Mossbauer spectrum [14].

The dynamical transition has now been observed with a number of biophysical techniques [14–16,18–22], and some protein functions including ligand binding have been shown to cease at temperatures below the transition [21,23,24]. The implication of this is that flexibility at the active site is required for efficient substrate binding and/or protein function. This, and the interdependence of the fast and slow motions, is consistent with the idea that the fast anharmonic motions are required for enzyme activity. If this were the case we might expect that an enzyme would not exhibit catalytic activity below the transition temperature, where these motions are absent. However, it has recently been shown that glutamate dehydrogenase, a large multisubunit enzyme, catalysing a complex reaction, is active below the dynamical transition (as evidenced by the cessation of picosecond timescale anharmonic motions) at −50 °C [22]. However, it is not clear whether this applies to all enzymes, and in particular whether it applies to simple, single-subunit enzymes, for which intersubunit motions play no role. In the present work this question is addressed. We report here the result of the concomitant determination of the activity and dynamics of a single-subunit enzyme, a xylanase, catalysing a relatively simple hydrolytic reaction. The activity determinations were carried out over the temperature range of +10 to −70 °C, in a 70% (v/v) methanol cryosolvent. The dynamics were determined in the same solvent by elastic neutron scattering, giving the average dynamical mean square displacement in the solution over time-

[1] To whom correspondence should be addressed (e-mail r.daniel@waikato.ac.nz).

scales of up to approx. 100 ps. The results thus enable the direct correlation of xylanase activity with fast dynamics over a wide temperature range. It is found that a temperature range exists in which the enzyme rate-limiting step is independent of the fast anharmonic dynamics.

EXPERIMENTAL

Materials

The xylanase was obtained from an *Escherichia coli* clone containing the gene from the extremely thermophilic bacterium, *Thermotoga maritima* strain FjSS3-B.1 [25,26]. The *E. coli* clone was grown on Luria broth media, with 50 mg/l ampicillin for the initial inoculum, at pH 7.0. It was grown as a batch-fed culture, in a 10 l fermenter at 28 °C. Xylanase production was induced at the end of the logarithmic growth phase by raising the temperature to 38 °C. Further nutrients were also added at the time of induction. The cells were then harvested at the end of the second logarithmic growth phase (approx. 12–18 h after induction). The xylanase was purified as described by Bergquist et al. [26]. The cells were concentrated by hollow fibre filtration, collected by centrifugation at 15000 *g* and washed, recentrifuged, and resuspended in Bis-Tris buffer at pH 7.0. The solution was then taken through two freeze–thaw cycles to help lyse the cells, followed by sonication for 15 min, on ice. The cell debris was removed by centrifugation at 15000 *g* for 30 min. DNase is added to the supernatant, and the solution stirred for 3 h at 37 °C. The supernatant was heat treated at 75 °C for 30 min, and allowed to stand at 4 °C for 2–3 days, to ensure complete precipitation of the denatured protein. The resulting precipitate was removed by centrifugation at 15000 *g* for 60 min. Ammonium sulphate was then added to a concentration of 1 M. The protein solution was loaded onto Phenyl Sepharose, and the xylanase eluted by a single-step gradient to water. The ammonium sulphate was removed from the eluted xylanase by filtration on an Amicon ultrafiltration cell, with a YM3 membrane and equilibrated with Bis-Tris buffer at pH 6.7 to a salt concentration of approx. 20 mM in the same ultrafiltration cell. The protein solution was then loaded on to Fast Flow Q-Sepharose, and eluted with 150 mM NaCl in Bis-Tris buffer at pH 6.7. The eluted xylanase was then dialysed against 10 mM Mes buffer at pH 5.3, loaded on to high load S-Sepharose column, and eluted with a linear gradient of 1–100 mM NaCl. From a 10 l fermenter culture, approx. 100 mg of purified xylanase was obtained.

Assays

Xylanase activity was routinely assayed by measuring the release of nitrophenol from *o*-nitrophenyl-β-D-xyloside at 80 °C, for 10 min. The reaction mixture contained 10 mM *o*-nitrophenyl-β-D-xyloside, 0.1 M sodium acetate/acetic acid buffer, pH_{80} 5.5, and 0.14–5 μg of enzyme, in a total assay volume of 100 μl. The reaction was stopped by the addition of 500 μl of ice-cold 1 M sodium carbonate, and the absorbance at 420 nm read.

In the cryosolvent, 70% (v/v) methanol, assays were carried out at temperatures of 10 °C and below. Sodium acetate/acetic acid buffers, giving a final pK_{a_m} of approx. 5.4 at the assay temperature, were used [27]. The total assay volume was 100 μl, with the enzyme solution and 0.1 M sodium acetate/acetic acid buffer making up 30% of this. The substrate, *o*-nitrophenyl-β-D-xyloside, was dissolved in the miscible organic solvent. The assays were started by the addition of the enzyme, cooled to the assay temperature. For assay temperatures below 0 °C, the enzyme was dissolved in the cryosolvent to prevent freezing upon addition to the cooled assay solution.

The reaction was stopped by the addition of 500 μl of precooled ethanolamine/DMSO/water (3:5:2; by vol.). At temperatures between 0 °C and −50 °C, the assays were cooled to at least 10 °C below the assay temperature before the addition of the stopping reagent. For assays at −50 °C and below, the assay tubes were immersed in liquid nitrogen to ensure efficient stopping of activity. The assay tubes were allowed to gradually warm, after thorough mixing with the stopping reagent below the assay temperature. The absorbance at 420 nm was read once the assays had warmed to room temperature. Control measurements were made in the absence of enzyme to account for any background absorbance of the substrate and solvents.

For the corresponding deuterated solvent assays, deuterium oxide replaced water, and CD_3OD replaced CH_3OH, throughout. The pD of the buffer solution was checked with a conventional pH meter, calibrated with aqueous buffers, using the relationship $pD = pH_{(meter)} + 0.4$ units [28].

For assay temperatures above −60 °C, a methanol bath cooled by a Flexi Cool Immersion Cooler (FTS Systems) was used. For −70 °C an ultra deep freeze was used to incubate the assays.

Neutron scattering

The dynamic neutron scattering measurements were carried out on the IN6 time-of-flight spectrometer at the Institut Laue-Langevin, Grenoble. The energy resolution of IN6 is 50 μeV, which allows determination of the average dynamical mean-square displacements of the enzyme protons over timescales of up to approx. 100 ps. To minimize the contribution of the solvent to the scattering, fully deuterated solvents were used. Exchange of labile enzyme protons was carried out by twice dissolving the xylanase in warm D_2O and freeze-drying to ensure no exchange took place during neutron scattering. The samples were contained in aluminium flat plate cells of 0.7 mm thickness, and were oriented at 135° with respect to the incident neutron beam. The incident neutron wavelength was 5.12 Å. The sample consisted of 68 mg/ml xylanase in 70% (v/v) CD_3OD/D_2O cryosolvent.

The sample was cooled to −163 °C and then heated progressively, with elastic scan data measurements taken at temperature intervals of 10° or 20° up to 30 °C. The measured transmission was 0.891. Raw data were corrected to determine the elastic intensity by integrating the detector counts over the energy range of the instrumental resolution. The detectors were calibrated by normalizing with respect to a standard vanadium sample. The cell scattering was subtracted, taking into account the attenuation of the singly scattered beam. Finally, the scattering was normalized with respect to the scattering at the lowest measured temperature, −163 °C.

The measured scattering contains a contribution from the protein hydrogen atoms, and also a contribution of similar magnitude from self-coherent scattering from the solvent. The mean-square displacement derived is therefore approximately equivalent to averaging over the elastic scattering from both the solvent and protein. The incoherent scattering from hydrogen atoms, due to self-correlations in their dynamics, is a significant component of the neutron scattering from proteins. As the hydrogen atoms are uniformly distributed over the macromolecule, the technique gives a global view of protein dynamics [29]. The elastic scattering intensity $S(q, \omega = 0)$ (where q is the magnitude of the scattering wave vector, and ω is the energy transfer) is then used to obtain the average mean square displacement $\langle u^2 \rangle$, using the relationship $\ln S(q, \omega = 0) = -\langle u^2 \rangle q^2/3$, which is valid in the regime $q^2\langle u^2 \rangle/3 < 1$. $\langle u^2 \rangle$ was thus obtained by fitting a straight line to a semi-log plot of $S(q, \omega = 0)$

versus q^2 in the linear regime which was found at $0.12 < q^2 < 1.06$. As the scattering is normalised with respect to the -163 °C intensities, the $\langle u^2 \rangle$ determined is equal to $(\langle u^2 \rangle_T - \langle u^2 \rangle_{-163})$, where $\langle u^2 \rangle_T$ is the absolute mean-square displacement at temperature T. The $\langle u^2 \rangle$ obtained by dynamic neutron scattering is purely dynamical and, unlike crystallographic atomic displacements, does not contain a static disorder contribution.

RESULTS AND DISCUSSION

To ensure valid measurement of activity at low temperatures in cryosolvent, a number of preliminary experiments were carried out. The stability of the xylanase in the 70% methanol cryosolvent was determined by incubation in the cryosolvent at 0 °C over a 12-h period, with aliquots removed and assayed at various time intervals. The remaining activity, assayed at 80 °C in an aqueous buffer, showed no significant decrease over the 12-h period, and was the same as that obtained for xylanase not exposed to the cryosolvent.

To ensure that substrate did not become limiting, K_m and V_{max} determinations were carried out in cryosolvent at temperatures down to -30 °C. As found for other enzymes [30] the K_m decreased with temperature (results not shown).

Figure 1 shows the effect of temperature on xylanase activity in both hydrogenated and fully deuterated cryosolvent, over the temperature range of $+10$ to -70 °C. From the similarity of the data, it does not appear that the catalytic activity of xylanase is significantly affected by deuterated solvents. The Arrhenius plots are essentially linear for both the hydrogenated and deuterated cryosolvents. This indicates that the rate-limiting step remains the same, and suggests that the catalytic mechanism is unchanged, as the temperature is lowered. As the temperature is reduced from 0 °C to -70 °C the activity declines by about 5 orders of magnitude. In comparison, the viscosity of the cryosolvent declines by less than 2 orders of magnitude. As the diffusion coefficient of a solute is inversely proportional to the viscosity of the solution, this implies that the activity of the xylanase is not likely to be diffusion limited at any temperature studied here.

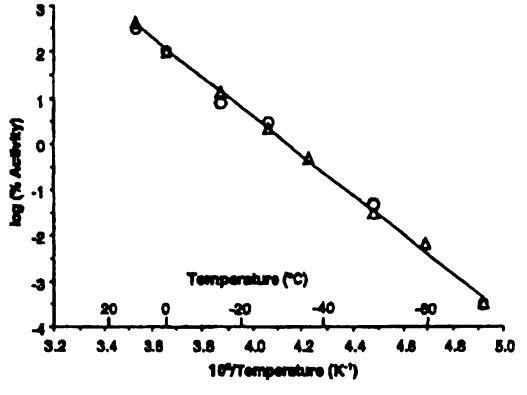

Figure 1 Effect of temperature on the activity of a xylanase enzyme in 70% aqueous methanol

The activity is expressed as the percentage residual activity corresponding to the activity in 70% methanol at 0 °C in hydrogenated (△) and fully deuterated (○) solvents. 100% activity corresponds to 0.57 and 0.62 μmol·min^{-1}·mg^{-1} in the hydrogenated and deuterated solvent, respectively.

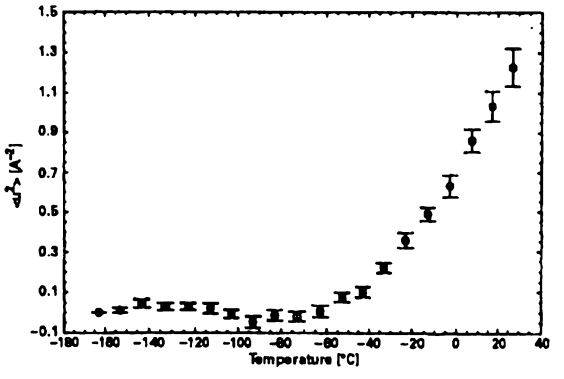

Figure 2 Effect of temperature on the dynamics of a xylanase enzyme in fully deuterated 70% aqueous methanol, as measured by neutron scattering

The dynamic results from the neutron scattering study of xylanase are shown in Figure 2, expressed as $\langle u^2 \rangle$ as a function of temperature. The $\langle u^2 \rangle$ values are scaled to zero at $T = -163$ °C, the lowest temperature used in the experiment. For $T \leqslant -70$ °C, $\langle u^2 \rangle$ remains at zero within experimental error: any small increase in $\langle u^2 \rangle$ over this range due to the increase with temperature of the amplitude of the harmonic vibrations is likely to be below the experimental error. At approx. -50 °C there is a dynamical transition, at which $\langle u^2 \rangle$ begins to rise rapidly, indicating the activation of anharmonic dynamics. In comparison, in the activity data there is no corresponding transition, the Arrhenius plot remaining linear down to at least $T = -70$ °C.

The results in Figures 1 and 2 throw light on the relationship between fast, picosecond motions, and enzyme activity. The slowest step in the catalytic cycle of the xylanase is the rate-limiting step, and can be expressed as the reciprocal of the turnover number. For the xylanase, the timescale of the rate-limiting step is approx. 1 s at 0 °C and this increases by at least 3 orders of magnitude at -50 °C. The mechanism of xylanase action involves multiple steps [31], including rapid equilibration of intermediates, and the crossing of each associated energy barrier may require one or more dynamical modes on the seconds/milliseconds timescale, at -50 °C. This is several orders of magnitude slower than the 100 ps dynamic motions being observed by neutron scattering. The absence of a transition in the activity data corresponding to the observed transition in the dynamic data at -50 °C shows that over the temperature range -50 to -70 °C picosecond anharmonic dynamics are not required for activity (whether this applies at higher temperatures is an open question). Therefore, anharmonic fast motions are not necessarily coupled to the conformational transitions involved in the enzyme reaction, i.e. to the much slower motions required for barrier-crossing transitions along the enzyme reaction coordinate. However, this conclusion should be tempered by consideration of the experimental error in $\langle u^2 \rangle$ in Figure 2, which is of the order of 0.05 Å^2. As $\langle u^2 \rangle$ obtained by the neutron technique is averaged over the sample, it is conceivable that functionally important fast anharmonic motions may be activated locally at the active site, at levels below the noise in Figure 2.

The xylanase used in this work is a very stable enzyme from an extreme thermophile [26,32], chosen to ensure stability in the

cryosolvent. There is no indication that deuterated or non-deuterated cryosolvent has a significant effect on the xylanase activity or stability. While it is not possible to compare the dynamics of the enzyme in cryosolvent with that in aqueous buffer below 0 °C, its dynamic behaviour as evidenced by neutron scattering is similar in a variety of different cryosolvents below 0 °C, including 40% methanol and 40 and 80% DMSO (R. V. Dunn, V. Réat, J. Finney, M. Ferrand, J. C. Smith and R. M. Daniel, unpublished work). The enzyme itself is not atypical [26], and there is already evidence that thermophilic and mesophilic enzymes behave similarly at their respective optimum temperatures in terms of their global dynamics and cryoenzymology [22,30]. Similar results to those obtained for xylanase have been observed for the multi-subunit protein glutamate dehydrogenase. That is, Arrhenius plots showed no break through the temperature of the picosecond dynamic transition [22,30]. The xylanase is a single subunit enzyme that catalyses a simple hydrolytic reaction, whereas the glutamate dehydrogenase is a multi-subunit enzyme that catalyses a complex multi-substrate reaction. The observation that these two dissimilar enzymes both show an independence of anharmonic picosecond dynamics for activity suggests that this finding may be applicable to enzymes generally. This would be consistent with the finding that the activity of two other multi-subunit enzymes, calf intestinal alkaline phosphatase, and beef liver catalase, have been measured down to approx. −100 °C (J. Bragger, R. V. Dunn and R. M. Daniel, unpublished work), without any Arrhenius plot break, although the corresponding dynamical measurements for these enzymes have not yet been performed.

Recent dynamic measurements on glutamate dehydrogenase over slower, nanosecond, timescales have shown dynamical transitions occurring at significantly lower temperatures than observed here, leading to the suggestion that the temperature of the dynamic transition is dependant on the timescale of the experimental technique [33]. As a corollary, it is confirmation of the idea that the anharmonic behaviour of an enzyme is timescale-dependent, and that anharmonic motions on timescales slower than picoseconds (e.g. functionally important dynamics) can occur in the absence of anharmonic picosecond motions. This latest finding has not yet been probed with other enzymes, but suggests that a way forward to understanding the relationship between enzyme dynamics and activity is to measure dynamical transition behaviour on a variety of timescales, and, as in the present work, to compare the results with activity determinations made under similar conditions. A variety of techniques exist for probing longer-timescale protein dynamics [1], including NMR, Mossbauer and fluorescence spectroscopies, neutron spin-echo [34] and molecular dynamics simulation, the latter technique now being feasible up to the microsecond timescale [35]. Although each of these techniques presents particular difficulties, overall prospects for examining enzyme motions on longer timescales are encouraging.

Received 20 September 1999/29 November 1999; accepted 22 December 1999

We thank the Institut Laue-Langevin for the use of neutron beam facilities; Dion Thompson for developing the xylanase purification; the Royal Society of New Zealand for the award of a James Cook Fellowship to R. M. D.; the European Community for a grant to V.R. (contract number ERBFMBICT975595).

REFERENCES

1 Brooks, C. L., Karplus, M. and Pettitt, B. M. (1988) Proteins: A Theoretical Perspective of Dynamics, Structure, and Thermodynamics, John Wiley, New York
2 McCammon, J. A. and Harvey, S. C. (1987) Dynamics of Proteins and Nucleic Acids, Cambridge University Press, New York
3 Frauenfelder, H., Petsko, G. A. and Tsernoglou, D. (1979) Nature **280**, 558–563
4 Artymiuk, P. J., Blake, C. C. F., Grace, D. E. P., Oatley, S. J., Phillips, D. C. and Sternberg, M. J. E. (1979) Nature (London) **280**, 563–568
5 Huber, R. and Bennett, W. S. (1983) Biopolymers **22**, 261–279
6 Bennett, W. S. and Steitz, T. A. (1980) J. Mol. Biol. **140**, 211–230
7 Gerstein, M., Lesk, A. and Chothia, C. (1994) Biochemistry **33**, 6739–6747
8 Creighton, T. E. (1993) Proteins, 2nd edn., Freeman, New York
9 Wrba, A., Schweiger, A., Shultes, V., Jaenicke, R. and Zavodszky, P. (1990) Biochemistry **29**, 7584–7592
10 Daniel, R. M., Bragger, J. and Morgan, H. W. (1990) In Biocatalysis (Abramowicz, D. A., ed.), pp. 243–254, Van Nostrand Reinhold, New York
11 Jaenicke, R. (1991) Eur. J. Biochem. **202**, 715–728
12 Varley, P. G. and Pain, R. H. (1991) J. Mol. Biol. **220**, 531–538
13 Daniel, R. M., Dines, M. and Petach, H. H. (1997) Biochem. J. **317**, 1–11
14 Doster, W., Cusack, S. C. and Petry, W. (1989) Nature (London) **337**, 754–756
15 Parak, F., Knapp, E. W. and Kucheida, D. (1982) J. Mol. Biol. **161**, 177–194
16 Bauminger, E. R., Cohen, S. G., Nowik, I., Ofer, S. and Yariv, J. (1983) Proc. Natl. Acad. Sci. U.S.A. **80**, 736–740
17 Kneller, G. R. and Smith, J. C. (1994) J. Mol. Biol. **242**, 181–185
18 Tilton, R. F., Dewan, J. C. and Petsko, G. A. (1992) Biochemistry **31**, 2469–2481
19 Hartmann, H., Parak, F., Steigmann, W., Petsko, G. A., Ringe Ronzi, D. and Frauenfelder, H. (1982) Proc. Natl. Acad. Sci. U.S.A. **79**, 4967–4971
20 Cusack, S. and Doster, W. (1990) Biophys. J. **58**, 243–251
21 Ferrand, M., Dianoux, A. J., Petry, W. and Zaccai, G. (1993) Proc. Natl. Acad. Sci. U.S.A. **90**, 9668–9672
22 Daniel, R. M., Smith, J. C., Ferrand, M., Hery, S., Dunn, R. and Finney, J. L. (1998) Biophys. J. **75**, 2504–2507
23 Parak, F., Frolov, E. N., Kononenko, A. A., Mossbauer, R. L., Goldanskii, V. I. and Rubin, A. B. (1980) FEBS Lett. **117**, 368–372
24 Rassmussen, B. F., Stock, A. M., Ringe, D. and Petsko, A. G. (1992) Nature (London) **357**, 523–524
25 Saul, D. J., Williams, L. C., Reeves, R. A., Gibbs, M. D. and Bergquist, P. L. (1995) Appl. Environ. Microbiol. **61**, 4110–4113
26 Bergquist, P. L., Gibbs, M. D., Morris, D. D., Uhl, A. M., Thompson, D. and Daniel, R. M. (2000) Methods Enzymol., in press.
27 Douzou, P., Hui Bon Hoa, G., Maurel, P. and Travers, F. (1976) In Handbook of Biochemistry and Molecular Biology, vol. 1 (3rd edn.) (Fasman, G. D., ed.), pp. 520–539, CRC Press, Boca Raton
28 Glasoe, P. K. and Long, F. A. (1960) J. Phys. Chem. **64**, 188–190
29 Smith, J. C. (1991) Q. Rev. Biophys. **25**, 227–293
30 More, R., Daniel, R. M. and Petach, H. H. (1996) Biochem. J. **305**, 17–20
31 Zachel, D. L., Konerman, L., Withers, S. G. O. and Douglas, D. J. (1998) Biochemistry **37**, 7664–7669
32 Simpson, H. D., Haufler, U. R. and Daniel, R. M. (1991) Biochem. J. **277**, 413–417
33 Daniel, R. M., Finney, J. L., Reat, V., Dunn, R., Ferrand, M. and Smith, J. C. (1999) Biophys. J. **77**, 2184–2190
34 Bellissent-Funel, M.-C., Daniel, R., Durand, D., Ferrand, M., Finney, J. L., Pouget, S. and Smith, J. C. (1998) J. Am. Chem. Soc. **120**, 7347–7348
35 Duan, Y. and Kollman, P. A. (1998) Science **282**, 740–744

References

Affleck, R., Haynes, C.A. and Clark, D.S. (1992a) Solvent dielectric effects on protein dynamics. *Proceedings of the National Academy of Sciences of the USA,* **89**, 5167-5170.

Affleck, R., Xu, Z.-F., Suzawa, V., Focht, K., Clark, D.S. and Dordick, J.S. (1992b) Enzymatic catalysis and dynamics in low-water environments. *Proceedings of the National Academy of Sciences of the USA,* **89**, 1100-1104.

Akerlöf, G. (1932) Dielectric constant of some organic solvent-water mixtures at various temperatures. *Journal of the American Chemical Society,* **54**, 4125-4139.

Andrews, F.C. (1971) *Thermodynamics: Principles and Applications,* John-Wiley and Sons, New York.

Angell, C.A. (1995) Formation of glasses from liquids and biopolymers. *Science,* **267**, 1924-1935.

Ansari, A., Berendzen, J., Bowne, S.F., Frauenfelder, H., Iben, I.E.T., Sauke, T.B., Shyamsunder, E. and Young, R.D. (1985) Protein states and proteinquakes. *Proceedings of the National Academy of Sciences of the USA,* **82**, 5000-5004.

Arêas, E.P.G., Arêas, J.A.G., Hamburger, J., Peticolas, W.L. and Santos, P.S. (1996) On the high viscosity of aqueous solution of lysozyme induced by some organic solvents. *Journal of Colloid and Interface Science,* **180**, 578-589.

Arêas, E.P.G., Menenzes, H.H.A., Santos, P.S. and Arêas, J.A.G. (1999) Hydrodynamic, optical and spectroscopic studies of some organic-aqueous binary systems. *Journal of Molecular Liquids,* **79**, 45-58.

Armand, S., Vielle, C., Gey, C., Heyraud, A., Zeikus, G. and Henrissat, B. (1996) Stereochemical course and reaction products of the action of β-xylosidase from *Thermoanaerobacterium saccharolyticum* strain B6A-RI. *European Journal of Biochemistry,* **236**, 706-713.

Artymiuk, P.J., Blake, C.C.F., Grace, D.E.P., Oatley, S.J., Phillips, D.C. and Sternberg, M.J.E. (1979) Crystallographic studies of the dynamic properties of lysozyme. *Nature,* **280**, 563-568.

Austin, R.H., Beeson, K.W., Eisenstein, L., Frauenfelder, H. and Gunsalus, I.C. (1975) Dynamics of ligand binding to myoglobin. *Biochemistry,* **14**, 5355-5373.

Bagnall, D.J. and Wolfe, J. (1982) Arrhenius plots: Information or noise? *Cryo Letters,* **3**, 7-16.

Bahnson, B.J., Colby, T.D., Chin, J.K., Goldstein, B.M. and Klinman, J.P. (1997) A link between protein structure and enzyme catalyzed hydrogen tunneling. *Proceedings of the National Academy of Sciences of the USA,* **94**, 12797-12802.

Barman, T., Travers, F., Balny, C., Hui Bon Hoa, G. and Douzou, P. (1986) New trends in cryoenzymology: probing the functional role of protein dynamics by single-step kinetics. *Biochimie*, **68**, 1041-1051.

Barron, L.D., Hecht, L. and Wilson, G. (1997) The lubricant of life: a proposal that solvent water promotes extremely fast conformational fluctuations in mobile heteropolypeptide structure. *Biochemistry,* **36**, 13143-13147.

Barrow, G.M. (1979) *Physical Chemistry,* 4th edn., McGraw-Hill Book Company, New York.

Bauminger, E.R., Cohen, S.G., Nowik, I., Ofer, S. and Yariv, J. (1983) Dynamics of heme iron in crystals of metmyoglobin and deoxymyoglobin. *Proceedings of the National Academy of Sciences of the USA,* **80**, 736-740.

Bell, G., Halling, P.J., Moore, B.D., Partridge, J. and Rees, D.G. (1995) Biocatalyst behaviour in low-water systems. *Trends in Biotechnology*, **13**, 468-473.

Bell, G., Janssen, A.E.M. and Halling, P.J. (1997) Water activity fails to predict critical hydration level for enzyme activity in polar organic solvents: Interconversion of water concentrations and activities. *Enzyme and Microbial Technology,* **20**, 471-477.

Biely, P., Kratky, Z. and Vršanská, M. (1981a) Substrate-binding site of endo-1,4-β-xylanase of the yeast *Cryptococcus albidus*. *European Journal of Biochemistry,* **119**, 559-564.

Biely, P., Vršanká, M., Tenkanen, M. and Kluepfel, D. (1997) Endo-β-1,4-xylanase families: Differences in catalytic properties. *Journal of Biotechnology,* **57**, 151-166.

Biely, P., Vršanská, M. and Kratky, Z. (1980) Complex reaction pathway of aryl β-xyloside degradation by β-xylanase of *Cryptococcus albidus*. *European Journal of Biochemistry,* **112**, 375-381.

Biely, P., Vršanská, M. and Kratky, Z. (1981b) Mechanisms of substrate digestion by endo-1,4-β-xylanase of *Cryptococcus albidus*. *European Journal of Biochemistry,* **119**, 565-571.

Bilderback, T., Fulmer, T., Mantulin, W.W. and Glaser, M. (1996) Substrate binding causes movement in the ATP binding domain of *Escherichia coli* adenylate kinase. *Biochemistry,* **35**, 6100-6106.

Bone, S. (1987) Time-domain reflectrometry studies of water binding and structural flexibility in chymotrypsin. *Biochimica et Biophysica Acta,* **916**, 128-134.

Bragger, J.M., Dunn, R.V. and Daniel, R.M. (2000) Enzyme activity down to –100°C. *Biochimica et Biophysica Acta,* **1480**, 278-282.

Brooks, III, C.L. and Karplus, M. (1989) Solvent effects on protein motion and protein effects on solvent motion. Dynamics of the active site region of lysozyme. *Journal of Molecular Biology,* **208**, 159-181.

Brooks, III, C.L., Karplus, M. and Pettitt, B.M. (1988) *Proteins: A Theoretical Perspective of Dynamics, Structure and Thermodynamics,* John Wiley and Sons, New York.

Bruice, T.C. and Benkovic, S.J. (2000) Chemical basis for enzyme catalysis. *Biochemistry,* **39**, 6267-6274.

Careri, G., Giansanti, A. and Gratton, E. (1979) Lysozyme film hydration events: an IR and gravimetric study. *Biopolymers,* **18**, 1187-1203.

Careri, G., Giansanti, A. and Rupley, J.A. (1986) Proton percolation on hydrated lysozyme powders. *Proceedings of the National Academy of Sciences of the USA,* **83**, 6810-6814.

Careri, G., Gratton, E., Yang, P.-H. and Rupley, J.A. (1980) Correlation of IR spectroscopic, heat capacity, diamagnetic susceptibility and enzymatic measurements on lysozyme powder. *Nature,* **284**, 572-573.

Chang, Z. and Baust, J.G. (1991) Further inquiry into the cryobehaviour of aqueous solutions of glycerol. *Cryobiology,* **28**, 268-278.

Chin, J.T., Wheeler, S.L. and Klibanov, A.M. (1994) Protein solubility in organic solvents. *Biotechnology and Bioengineering,* **44**, 140-145.

Cioni, P., Gabellieri, E., Gonnelli, M. and Strambini, G.B. (1994) Heterogeneity of protein conformation in solution from the lifetime of tryptophan phosphorescence. *Biophysical Chemistry,* **52**, 25-34.

Cohen, S.G., Bauminger, E.R., Nowik, I., Ofer, S. and Yariv, J. (1981) Dynamics of the iron-containing core in crystals of the iron-storage protein, ferritin, through Mössbauer spectroscopy. *Physical Review Letters,* **46**, 1244-1247.

Copeland, R.A. (2000) *Enzymes:A Practical Introduction to Structure, Mechanism, and Data Analysis,* 2nd edn., John Wiley and Sons, New York.

Cordone, L., Ferrand, M., Vitrano, E. and Zaccai, G. (1999) Harmonic behaviour of trehalose-coated carbon-monoxy-myoglobin at high temperature. *Biophysical Journal,* **76**, 1043-1047.

Cowan, D.A. (1997) Thermophilic proteins: Stability and function in aqueous and organic solvents. *Comparative Biochemistry and Physiology*, **118A**, 429-438.

Creighton, T.E. (1993) *Proteins - Structures and Molecular Properties,* 2nd edn., W.H. Freeman and Company, New York.

Cusack, S. and Doster, W. (1990) Temperature dependence of the low frequency dynamics of myoglobin. *Biophysical Journal,* **58**, 243-251.

Daniel, R.M., Finney, J.L., Réat, V., Dunn, R., Ferrand, M. and Smith, J.C. (1999) Enzyme dynamics and activity: Time-scale dependence of dynamical transitions in glutamate dehydrogenase solution. *Biophysical Journal,* **77**, 2184-2190.

Daniel, R.M., Smith, J.C., Ferrand, M., Hery, S., Dunn, R. and Finney, J.L. (1998) Enzyme activity below the dynamical transition at 220 K. *Biophysical Journal,* **75**, 2504-2507.

Davies, G.J., Wilson, K.S. and Henrissat, B. (1997) Nomenclature for sugar-binding subsites in glycosyl hydrolases. *Biochemical Journal,* **321**, 557-559.

Demmel, F., Doster, W., Petry, W. and Schulte, A. (1997) Vibrational frequency shifts as a probe of hydrogen bonds: thermal expansion and glass transition of myoglobin in mixed solvents. *European Biophysics Journal,* **26**, 327-335.

Diehl, M., Doster, W., Petry, W. and Schober, H. (1997) Water-coupled low-frequency modes of myoglobin and lysozyme observed by inelastic neutron scattering. *Biophysical Journal,* **73**, 2726-2732.

Dixon, M. and Webb, E.C. (1979) *Enzymes,* 3rd edn., Longman Group Ltd., London.

Doster, W., Cusack, S. and Petry, W. (1989) Dynamical transition of myoglobin revealed by inelastic neutron scattering. *Nature,* **337**, 754-756.

Doster, W., Cusack, S. and Petry, W. (1990) Dynamic instability of liquid-like motions in a globular protein observed by inelastic neutron scattering. *Physical Review Letters,* **65**, 1080-1083.

Douzou, P. (1971) Aqueous-organic solutions of enzymes at subzero temperatures. *Biochimie,* **53**, 401-512.

Douzou, P. (1974) The use of subzero temperatures in biochemistry: Slow reactions. *Methods of Biochemical Analysis,* **22**, 401-512.

Douzou, P. (1977) Enzymology at subzero temperatures. *Advances in Enzymology,* **45**, 157-272.

Douzou, P. (1980) Cryoenzymology in aqueous media. *Advances in Enzymology*, **51**, 1-74.

Douzou, P., Hui Bon Hoa, G., Maurel, P. and Travers, F. (1976) Physical and chemical data for mixed solvents used in low temperature biochemistry. In *Handbook of Biochemistry and Molecular Biology: Physical and Chemical Data,* 3rd edn., vol. 1 (Fasman, G.D., ed.), pp. 520-539, CRC Press, Ohio.

Dunn, R.V. (1998) *Effect of Low Temperature on Thermophilic Enzymes.* MSc Thesis, University of Waikato, New Zealand.

Dunn, R.V., Réat, V., Finney, J., Ferrand, M., Smith, J.C. and Daniel, R.M. (2000) Enzyme activity and dynamics: xylanase activity in the absence of fast anharmonic dynamics. *Biochemical Journal,* **346**, 355-358.

Elber, R. and Karplus, M. (1987) Multiple conformational states of proteins: A molecular dynamic analysis of myoglobin. *Science,* **235**, 318-321.

Engelman, D.M., Dianoux, A.J., Cusack, S. and Jacrot, B. (1984) Inelastic neutron scattering studies of hexokinase in solution. In *Neutrons in Biology* (Schoenborn, B.P., ed.), pp. 365-380, Plenum Press, New York.

Fan, Y.-X., McPhie, P. and Miles, E.W. (2000) Regulation of tryptophan synthase by temperature, monovalent cations, and an allosteric ligand. Evidence from Arrhenius plots, absorption spectra, and primary kinetic isotope effects. *Biochemistry,* **39**, 4692-4703.

Faure, P., Micur, A., Perahia, D., Doucet, J., Smith, J.C. and Benoit, M. (1994) Correlated intramolecular motions and diffuse X-ray scattering in lysozyme. *Nature Structural Biology,* **1**, 124-128.

Ferrand, M., Dianoux, A.J., Petry, W. and Zaccai, G. (1993) Thermal motions and function of bacteriorhodopsin in purple membranes: Effects of temperature and hydration studied by neutron scattering. *Proceedings of the National Academy of Sciences of the USA,* **90**, 9668-9672.

Fersht, A. (1985) *Enzyme Structure and Mechanism,* 2nd edn., W.H. Freeman and Company, New York.

Filabozzi, A., Deriu, A. and Andreani, C. (1996) Temperature dependence of the dynamics of superoxide dismutase by quasi-elastic neutron scattering. *Physica B,* **226**, 56-60.

Fink, A. and Geeves, M. (1979) Cryoenzymology: The study of enzyme catalysis at subzero temperatures. *Methods in Enzymology,* **63**, 336-370.

Fink, A.L. (1973) The α-chymotrypsin-catalyzed hydrolysis of N-acetyl-L-tryptophan *p*-nitrophenyl ester in dimethyl sulfoxide at subzero temperatures. *Biochemistry,* **12**, 1736-1742.

Fischer, C.J., Schauerte, J.A., Wisser, K.C., Gafni, A. and Steel, D.G. (2000) Hydrogen exchange at the core of *Escherichia coli* alkaline phosphatase studied by room-temperature tryptophan phosphorescence. *Biochemistry,* **39**, 1455-1461.

Fitter, J. (1999) The temperature dependence of internal molecular motions in hydrated and dry α-amylase: the role of hydration water in the dynamical transition of proteins. *Biophysical Journal,* **76**, 1034-1042.

Fitter, J., Lechner, R.E., Büldt, G. and Dencher, N.A. (1996) Internal molecular motions of bacteriorhodopsin: Hydration-induced flexibility studied by quasielastic incoherent neutron scattering using oriented purple membranes. *Proceedings of the National Academy of Sciences of the USA,* **93**, 7600-7605.

Fitter, J., Lechner, R.E. and Dencher, N.A. (1997) Picosecond molecular motions in bacteriorhodopsin from neutron scattering. *Biophysical Journal,* **73**, 2126-2137.

Franks, F. (1988) Solution properties of proteins. In *Characterization of Proteins* (Franks, F., ed.), pp. 53-94, Humana Press, New Jersey.

Franks, F. (1995) Protein destabilization at low temperatures. *Advances in Protein Chemistry*, **46**, 105-139.

Frauenfelder, H., Hartmann, H., Karplus, M., Kuntz, I.D., Kuriyan, J., Parak, F., Petsko, G.A., Ringe, D., Tilton, J., R.F., Connolly, M.L. and Max, N. (1987) Thermal expansion of a protein. *Biochemistry,* **26**, 254-261.

Frauenfelder, H., Petsko, G.A. and Tsernoglou, D. (1979) Temperature-dependent X-ray diffraction as a probe of protein structural dynamics. *Nature,* **280**, 558-563.

Frauenfelder, H., Sligar, S.G. and Wolynes, P.G. (1991) The energy landscapes and motions of proteins. *Science,* **254**, 1598-1602.

Frolov, E.N., Gvosdev, R., Goldanskii, V.I. and Parak, F.G. (1997) Differences in the dynamics of oxidised and reduced cytochrome c. *Journal of Biological Inorganic Chemistry,* **2**, 710-713.

Gekko, K., Ohmae, E., Kameyama, K. and Takagi, T. (1998) Acetonitrile-protein interactions: amino acid solubility and preferential solvation. *Biochimica et Biophysica Acta,* **1387**, 195-205.

Gerstein, M., Lesk, A.M. and Chothia, C. (1994) Structural mechanisms for domain movements in proteins. *Biochemistry,* **33**, 6739-6749.

Gilkes, N.R., Henrissat, B., Kilburn, D.G., Miller Jr., R.C. and Warren, R.A.J. (1991) Domains in microbial β-1,4-glycanases: Sequence conservation, function, and enzyme families. *Microbiological Reviews,* **55**, 303-315.

Gonser, U. (1975) From a strange effect to Mössbauer spectroscopy. In *Mössbauer Spectroscopy* (Gonser, U., ed.), pp. 1-52, Springer-Verlag, Berlin.

Gottfried, D.S., Peterson, E.S., Sheikh, A.G., Wang, J., Yang, M. and Friedman, J.M. (1996) Evidence for damped hemoglobin dynamics in a room temperature trehalose glass. *Journal of Physical Chemistry,* **100**, 12034-12042.

Guagliardi, A., Manco, G., Rossi, M. and Bartolucci, S. (1989) Stability and activity of a thermostable malic enzyme in denaturants and water-miscible organic solvents. *European Journal of Biochemistry,* **183**, 25-30.

Gutberlet, T., Heinemann, U. and Steiner, M. (2001) Protein crystallography with neutrons - status and perspectives. *Acta Crystallographica Section D,* **D57**, 349-354.

Hagen, S.J., Hofrichter, J. and Eaton, W.A. (1995) Protein reaction kinetics in a room-temperature glass. *Science,* **269**, 959-962.

Hagen, S.J., Hofrichter, J. and Eaton, W.A. (1996) Geminate rebinding and conformational dynamics of myoglobin embedded in a glass at room temperature. *Journal of Physical Chemistry,* **100**, 12008-12021.

Haines, P.J. and Wilburn, F.W. (1995) Differential thermal analysis and differential scanning calorimetry. In *Thermal Methods of Analysis: Principles, Applications and Problems* (Haines, P.J., ed.), pp. 63-122, Blackie Academic and Professional, Oxford.

Halling, P.J. (1990) High-affinity binding of water by proteins is similar in air and in organic solvents. *Biochimica et Biophysica Acta,* **1040**, 225-228.

Haran, G., Haas, E., Szpikowska, B.K. and Mas, M.T. (1992) Domain motions in phosphoglycerate kinase: Determination of interdomain distance distributions by site-specific labeling and time-resolved fluorescence energy transfer. *Proceedings of the National Academy of Sciences of the USA,* **89**, 11764-11768.

Hartmann, H., Parak, F., Steigemann, W., Petsko, G.A., Ringe, P.D. and Frauenfelder, H. (1982) Conformational substates in a protein: Structure and

dynamics of metmyoglobin at 80 K. *Proceedings of the National Academy of Sciences of the USA,* **79**, 4967-4971.

Hay, J.N. (1992) Applications of thermal analysis of polymers. In *Thermal Analysis - Techniques and Applications* (Charsley, E.L. and Warrington, S.B., eds.), pp. 156-179, The Royal Society of Chemistry, Cambridge.

Hays, W.S., VanderJagt, D.J., Bose, B., Serianni, A.S. and Glew, R.H. (1998) Catalytic mechanism and specificity for hydrolysis and transglycosylation reactions of cytosolic β-glucosidase from guinea pig liver. *Journal of Biological Chemistry,* **273**, 34941-34948.

Henrissat, B. (1991) A classification of glycosyl hydrolases based on amino acid sequence similarities. *Biochemical Journal,* **280**, 309-316.

Henrissat, B. and Bairoch, A. (1993) New families in the classification of glycosyl hydrolases based on amino acid sequence similarities. *Biochemical Journal,* **293**, 781-788.

Henrissat, B. and Bairoch, A. (1996) Updating the sequence-based classification of glycosyl hydrolases. *Biochemical Journal,* **316**, 695-696.

Henrissat, B. and Davies, G. (1997) Structural and sequence-based classification of glycoside hydrolases. *Current Opinion in Structural Biology,* **7**, 637-644.

Huber, R. and Bennett, W.S. (1983) Functional significance of flexibility in proteins. *Biopolymers,* **22**, 261-279.

Hui Bon Hoa, G. and Douzou, P. (1973) Ionic strength and protonic activity of supercooled solutions used in experiments with enzyme solutions. *Journal of Biological Chemistry,* **284**, 4649-4654.

Ibel, K. 1994. Guide to Neutron Research Facilities at the ILL. Institut Laue-Langevin, Grenoble.

Iben, I.E.T., Braunstein, D., Doster, W., Frauenfelder, H., Hong, M.K., Johnson, J.B., Luck, S., Ormos, P., Schulte, A., Steinbach, P.J., Xie, A.H. and Young, R.D. (1989) Glassy behaviour of a protein. *Physical Review Letters,* **62**, 1916-1919.

Ishima, R. and Torchia, D.A. (2000) Protein dynamics from NMR. *Nature Structural Biology,* **7**, 740-743.

Jaenicke, R. (1991) Protein stability and molecular adaption to extreme conditions. *European Journal of Biochemistry*, **202**, 715-728.

Jaenicke, R., Schurig, H., Beaucomp, N. and Ostendorp, R. (1996) Structure and stability of hyperstable proteins: Glycolytic enzymes from hyperthermophilic bacterium *Thermotoga maritima*. *Advances in Protein Chemistry*, **48**, 181-269.

Jenkins, J., Leggio, L.L., Harris, G. and Pickersgill, R. (1995) β-Glucosidase, β-galactosidase, family A cellulases, family F xylanases and two barley glycanases form a superfamily of enzymes with 8-fold β/α architecture and with two conserved glutamates near the carboxy-terminal ends of β-strands four and seven. *FEBS Letters,* **362**, 281-285.

John, R.A. (1992) Photometric assays. In *Enzyme Assays: A Practical Approach* (Eisenthal, R. and Danson, M.J., eds.), pp. 80-81, Oxford University Press, Oxford.

Käiväräinen, A.I. (1985) *Solvent-Dependent Flexibility of Proteins and Principles of Their Function,* D. Reidel Publishing Company, Dordrecht.

Karplus, M. and Petsko, G.A. (1990) Molecular dynamics simulations in biology. *Nature,* **347**, 631-639.

Kay, L.E. (1997) NMR methods for the study of protein structure and dynamics. *Biochemistry and Cell Biology,* **75**, 1-15.

Kay, L.E. (1998) Protein dynamics from NMR. *Biochemistry and Cell Biology,* **76**, 145-152.

Keller, H. and Debrunner, P.G. (1980) Evidence for conformational and diffusional mean square displacements in frozen aqueous solutions of oxymyoglobin. *Physical Review Letters,* **45**, 68-71.

Kistiakowsky, G.B. and Lumry, R. (1949) Anomalous temperature effects in the hydrolysis of urea by urease. *Journal of the American Chemical Society,* **71**, 2006-2013.

Kneller, G.R. and Smith, J.C. (1994) Liquid-like side-chain dynamics in myoglobin. *Journal of Molecular Biology,* **242**, 181-185.

Kohen, A., Cannio, R., Bartolucci, S. and Klinman, J.P. (1999) Enzyme dynamics and hydrogen tunnelling in a thermophilic alcohol dehydrogenase. *Nature,* **399**, 496-499.

Kohen, A. and Klinman, J.P. (1998) Enzyme catalysis: Beyond classical paradigms. *Accounts of Chemical Research,* **31**, 397-404.

Kohen, A. and Klinman, J.P. (1999) Hydrogen tunneling in biology. *Chemistry and Biology,* **6**, R191-R198.

Kohen, A. and Klinman, J.P. (2000) Protein flexibility correlates with degree of hydrogen tunneling in thermophilic and mesophilic alcohol dehydrogenases. *Journal of the American Chemical Society,* **122**, 10738-10739.

Koshland, D.E. (1958) Application of a theory of enzyme specificity to protein synthesis. *Proceedings of the National Academy of Sciences of the USA,* **44**, 98-105.

Koshland, D.E.G. (1953) Stereochemistry and the mechanism of enzymatic reactions. *Biology Reviews,* **28**, 416-436.

Kossiakoff, A.A. (1982) Protein dynamics investigated by the neutron diffraction-hydrogen exchange technique. *Nature,* **296**, 713-721.

Kossiakoff, A.A. (1985) The application of neutron crystallography to the study of dynamic and hydration properties of proteins. *Annual Review of Biochemistry,* **54**, 1195-1227.

Kossiakoff, A.A. (1986) Protein dynamics investigated by neutron diffraction. *Methods in Enzymology,* **131**, 433-447.

Krupyanskii, Y.U.F., Parak, F., Goldanskii, V.I., Mössbauer, R.L., Gaubman, E.E., Engelman, H. and Suzdalev, I.P. (1982) Investigation of large intramolecular movements within metmyoglobin by Rayleigh scattering of Moessbauer radiation. *Zeitschrift fur Naturforschung,* **37**, 57-62.

Kvittingen, L. (1994) Some aspects of biocatalysis in organic solvents. *Tetrahedron,* **50**, 8253-8274.

Laidler, K.J. and Peterman, B.F. (1979) Temperature Effects in Enzyme Kinetics. *Methods in Enzymology,* **63**, 234-257.

Lakowicz, J.R. (1980) Fluorescence spectroscopic investigations of the dynamic properties of proteins, membranes and nucleic acids. *Journal of Biochemical and Biophysical Methods,* **2**, 91-119.

Lakowicz, J.R., Kusba, J., Gryczynski, I., Szmacinski, H., Wiczk, W. and Johnson, M.L. (1992) Macromolecular dynamics observed by intramolecular energy transfer using frequency-domain fluorometry. In *Techniques in Protein Chemistry III* (Angeletti, R.H., ed.), pp. 429-436, Academic Press, London.

Lawson, S.L., Wakarchuk, W.W. and Withers, S.G. (1997) Positioning of the acid/base catalyst in a glycosidase: Studies with *Bacillus circulans* xylanase. *Biochemistry,* **36**, 2257-2265.

Lehmann, M.S., Mason, S.A. and McIntyre, G.J. (1985) Study of ethanol-lysozyme interactions using neutron diffraction. *Biochemistry,* **24**, 5862-5869.

Lehmann, M.S. and Stansfield, R.F. (1989) Binding of dimethyl sulfoxide to lysozyme in crystals, studied with neutron diffraction. *Biochemistry,* **28**, 7028-7033.

Lehnert, U., Réat, V., Weik, M., Zaccai, G. and Pfister, C. (1998) Thermal motions in bacteriorhodopsin at different hydration levels studied by neutron scattering: Correlation with kinetics and light-induced changes. *Biophysical Journal,* **75**, 1945-1952.

Lipari, G. and Szabo, A. (1982) Protein dynamics and NMR relaxation: Comparison of simulations with experiment. *Nature,* **300**, 197-198.

Lipscomb, W.N. (1983) Structure and catalysis of enzymes. *Annual Review of Biochemistry,* **52**, 17-34.

Lo Leggio, L., Jenkins, J., Harris, G.W. and Pickersgill, R.W. (2000) X-ray crystallographic study of xylopentaose binding to *Pseudomonas fluorescens* xylanase A. *Proteins: Structure, Function and Genetics,* **41**, 362-373.

Loncharich, R.L. and Brooks, B.R. (1990) Temperature dependence of dynamics of hydrated myoglobin. *Journal of Molecular Biology,* **215**, 439-455.

Londesborough, J. (1980) The causes of sharply bent or discontinuous Arrhenius plots for enzyme-catalysed reactions. *European Journal of Biochemistry,* **105**, 211-215.

Londesborough, J. and Varimo, K. (1979) The temperature-dependence of adenylate cyclase from Baker's yeast. *Biochemical Journal,* **181**, 539-543.

Ly, H.D. and Withers, S.G. (1999) Mutagenesis of glycosidases. *Annual Review of Biochemistry,* **68**, 487-522.

Maier, V.P., Tappel, A.L. and Volman, D.H. (1955) Reversible inactivation of enzymes at low temperatures. Studies of temperature dependence of phosphatase- and peroxidase-catalyzed reactions. *Journal of the American Chemical Society,* **77**, 1278-1280.

Massey, V. (1953) Studies on fumarase 3. The effect of temperature. *Biochemical Journal,* **53**, 72-79.

Matsumura, S., Sakiyama, K. and Toshima, K. (1999) Preparation of octyl-β-d-xylobioside and xyloside by xylanase-catalyzed direct transglycosylation reaction of xylan and octanol. *Biotechnology Letters,* **21**, 17-22.

Maurel, P. (1978) Relevance of the dielectric constant and solvent hydrophobicity to the organic solvent effect in enzymology. *Journal of Biological Chemistry,* **253**, 1677-1683.

Mazurenko, Y.T. (1973) Luminescence polarization of complex molecules during light quenching. *Optika I Spektroskopiya,* **35**, 234-245.

McCammon, J.A. and Harvey, S.C. (1987) *Dynamics of Proteins and Nucleic Acids,* Cambridge University Press, Cambridge.

Middendorf, H.D. (1984) Inelastic scattering from biomolecules: Principles and prospects. In *Neutrons in Biology* (Schoenborn, B.P., ed.), pp. 401-436, Plenum Press, New York.

Middendorf, H.D., Randall, J.T. and Crespi, H.L. (1984) Neutron spectroscopy of hydrogenous and biosynthetically deuterated proteins. In *Neutrons in Biology* (Schoenborn, B.P., ed.), pp. 381-400, Plenum Press, New York.

Miller, G.P. and Benkovic, S.J. (1998) Stetching exercises - flexibility in dihydrofolate reductase catalysis. *Chemistry and Biology,* **5**, R105-R113.

Moore, W.J. (1983) *Basic Physical Chemistry,* Prentice Hall International, Inc., London.

More, N., Daniel, R.M. and Petach, H. (1995) The effect of low temperatures on enzyme activity. *Biochemical Journal,* **305**, 17-20.

Moreau, A., Shareck, F., Kluepfel, D. and Morosoli, R. (1994) Alteration of the cleavage mode and of the transglycosylation reactions of the xylanase A of *Streptomyces lividans* 1326 by site-directed mutagenesis of the Asn173 residue. *European Journal of Biochemistry,* **219**, 261-266.

Morissett, J.D. (1976) The use of spin labels for studying the structure and function of enzymes. In *Spin Labelling, Theory and Applications* (Berliner, L.J., ed.), pp. 274-338, Academic Press, New York.

Murthy, S.S.N. (1998) Some insight into the physical basis of the cryoprotective action of dimethyl sulfoxide and ethylene glycol. *Cryobiology,* **36**, 84-96.

Natesh, R., Bhanumoorthy, P., Vithayathil, P.J., Sekar, K., Ramakumar, S. and Viswamitra, M.A. (1999) Crystal structure at 1.8 Å resolution and proposed amino acid sequence of a thermostable xylanase from *T. aurantiacus. Journal of Molecular Biology,* **288**, 999-1012.

Nocek, J.M., Stemp, E.D.A., Finnegan, M.G., Koshy, T.I., Johnson, M.K., Margoliash, E., Mauk, A.G., Smith, M. and Hoffman, B.M. (1991) Low-temperature, cooperative conformational transition within [Zn-cytochrome *c* peroxidase, cytochrome *c*] complexes: Variation with cytochrome. *Journal of the American Chemical Society,* **113**, 6822-6831.

Ntarima, P., Nerinckx, W., Klarskov, K., Devreese, B., Bhat, M.K., Van Beeumen, J. and Claeyssens, M. (2000) Epoxyalkyl glycosides of d-xylose and xylo-oligosaccharides are active-site markers of xylanases form glycoside hydrolase family 11, not from family 10. *Biochemical Journal,* **347**, 865-873.

Owusu, R.K. and Cowan, D.A. (1989) Correlation between microbial protein thermostability and resistance to denaturation in aqueous:organic solvent two-phase systems. *Enzyme and Microbial Technology,* **11**, 568-574.

Palmer, III, AG. (1997) Probing molecular motion by NMR. *Current Opinion in Structural Biology,* **7**, 733-737.

Palmer, III, A.G., Kroenke, C.D. and Loria, J.P. (2001) Nuclear magnetic resonance methods for quantifying microsecond-to-millisecond motions in biological macromolecules. *Methods in Enzymology,* **339**, 204-238.

Parak, F., Fischer, M., Heidemeiner, J., Engelhard, M., Kohl, K.-D., Hess, B. and Formanek, H. (1990) Investigation of the dynamics of bacteriorhodopsin. *Hyperfine Interactions,* **58**, 2381-2386.

Parak, F., Frolov, E.N., Kononenko, A.A., Mössbauer, R.L., Goldanskii, V.I. and Rubin, A.B. (1980) Evidence for a correlation between the photoinduced electron transfer and dynamic properties of the chromophore membranes from *Rhodospirillum rubrum. FEBS Letters,* **117**, 368-372.

Parak, F., Knapp, E.W. and Kucheida, D. (1982) Protein dynamics: Mössbauer spectroscopy on deoxymyoglobin crystals. *Journal of Molecular Biology,* **161**, 177-194.

Parak, F. and Reinisch, L. (1986) Mössbauer effect if the study of structure dynamics. *Methods in Enzymology,* **131**, 568-607.

Partridge, J., Dennison, P.R., Moore, B.D. and Halling, P.J. (1998) Activity and mobility of subtilisin in low water organic media: hydration is more important than solvent dielectric. *Biochimica et Biophysica Acta,* **1386**, 79-89.

Perez, J., Zanotti, J.M. and Durand, D. (1999) Evolution of the internal dynamics of two globular proteins from dry powder to solution. *Biophysical Journal,* **77**, 454-469.

Poole, P.L. and Finney, J.L. (1983) Hydration-induced conformational and flexibility changes in lysozyme at low water content. *International Journal of Biological Macromolecules,* **5**, 308-310.

Privalov, P.L. (1990) Cold denaturation of proteins. *Critical Reviews in Biochemistry and Molecular Biology*, **25**, 281-305.

Radkiewicz, J.L. and Brooks, III, C.L. (2000) Protein dynamics in enzymatic catalysis: Exploration of dihydrofolate reductase. *Journal of the American Chemical Society,* **122**, 225-231.

Rasmussen, B.F., Stock, A.M., Ringe, D. and Petsko, G.A. (1992) Crystalline ribonuclease A loses function below the dynamical transition at 220 K. *Nature,* **357**, 423-424.

Reading, M. and Haines, P.J. (1995) Thermomechanical, dynamic mechanical and associated methods. In *Thermal Methods of Analysis: Principles, Applications and*

Problems (Haines, P.J., ed.), pp. 123-160, Blackie Academic and Professional, Oxford.

Réat, V., Patzelt, H., Ferrand, M., Pfister, C., Oesterhelt, D. and Zaccai, G. (1998) Dynamics of different functional parts of bacteriorhodopsin: H-^{2}H labeling and neutron scattering. *Proceedings of the National Academy of Sciences of the USA,* **95**, 4970-4975.

Réat, V., Dunn, R., Ferrand, M., Finney, J.L., Daniel, R.M. and Smith, J.C. (2000a) Solvent dependence of dynamic transitions in protein solutions. *Proceedings of the National Academy of Sciences of the USA,* **97**, 9961-9966.

Réat, V., Finney, J.L., Steer, A., Roberts, M.A., Smith, J., Dunn, R., Peterson, M. and Daniel, R. (2000b) Cryosolvents useful for protein and enzyme studies below –100°C. *Journal of Biochemical and Biophysical Methods,* **42**, 97-103.

Ringe, D. (1995) What makes a binding site a binding site. *Current Opinion in Structural Biology,* **5**, 825-829.

Ringe, D. and Petsko, G.A. (1986) Study of protein dynamics by X-ray diffraction. *Methods in Enzymology,* **131**, 389-433.

Rupley, J.A. and Careri, G. (1991) Protein hydration and function. *Advances in Protein Chemistry,* **41**, 37-172.

Rupley, J.A., Gratton, E. and Careri, G. (1983) Water and globular proteins. *Trends in Biochemical Sciences,* **8**, 18-22.

Ryu, K. and Dordick, J.S. (1992) How do organic solvents affect peroxidase structure and function? *Biochemistry,* **31**, 2588-2598.

Saul, D.J., Williams, L.C., Reeves, R.A., Gibbs, M.D. and Bergquist, P.L. (1995) Sequence and expression of a xylanase gene from the hyperthermophile *Thermotoga* sp. strain FjSS3-B.1 and characterization of the recombinant enzyme and its activity on kraft pulp. *Applied and Environmental Microbiology,* **61**, 4110-4113.

Saviotti, M.L. and Galley, W.C. (1974) Room temperature phosphorescence and the dynamic aspects of protein structure. *Proceedings of the National Academy of Sciences of the USA,* **71**, 4154-4158.

Schinkel, J.E., Downer, N.W. and Rupley, J.A. (1985) Hydrogen exchange of lysozyme powders. Hydration dependence of internal motions. *Biochemistry,* **24**, 352-366.

Schmitke, J.L., Wescott, C.R. and Klibanov, A.M. (1996) The mechanistic dissection of the plunge in enzymatic activity upon transition from water to anhydrous solvents. *Journal of the American Chemical Society,* **118**, 3360-3365.

Schulz, G.E. (1992) Induced-fit movements in adenylate kinases. *Faraday Discussions,* **93**, 85-93.

Shah, N.K. and Ludescher, R.D. (1995) Phosphorescence probes of the glassy state in amophous sucrose. *Biotechnology Progress,* **11**, 540-544.

Shapiro, S.M. and Shirane, G. (1991) Neutron diffraction and scattering. In *Encyclopaedia of Physics,* 2nd edn., (Lerner, R.G. and Trigg, G.L., eds.), pp. 800-807, VCH Publishers, New York.

Silvius, J.R., Read, B.D. and McElhaney, R.N. (1978) Membrane enzymes: Artifacts in Arrhenius plots due to temperature dependence of substrate-binding affinity. *Science,* **199**, 902-904.

Simpson, H.D., Haufler, U.R. and Daniel, R.M. (1991) An extremely thermostable xylanase from the thermophilic eubacterium *Thermotoga. Biochemical Journal,* **277**, 413-417.

Singer, S.J. (1962) The properties of proteins in nonaqueous solvents. *Advances in Protein Chemistry,* **17**, 1-65.

Singh, G.P., Parak, F., Hunklinger, S. and Dransfield, K. (1981) Role of adsorbed water in the dynamics of metmyoglobin. *Physical Review Letters,* **47**, 685-688.

Sinnott, M.L. (1990) Catalytic mechanisms of enzymic glycosyl transfer. *Chemical Reviews,* **90**, 1171-1202.

Smith, J., Cusack, S., Tidor, B. and Karplus, M. (1990) Inelastic neutron scattering analysis of low-frequency motions in proteins: harmonic and damped harmonic models of bovine pancreatic trypsin inhibitor. *Journal of Chemical Physics,* **93**, 2974-2991.

Smith, J.C. (1991) Protein dynamics: comparison of simulations with inelastic neutron scattering experiments. *Quarterly Reviews of Biophysics,* **24**, 227-291.

Smith, J.C., Cusack, S., Poole, P.L. and Finney, J.L. (1987) Direct measurement of hydration-related dynamic changes in lysozyme using inelastic neutron scattering spectroscopy. *Journal of Biomolecular Structure and Dynamics,* **4**, 583-588.

Somero, G.N. (1995) Proteins and Temperature. *Annual Review of Physiology,* **57**, 43-68.

Somogyi, B. and Damjanovich, S. (1988) Protein dynamics and fluorescence quenching. *Journal of Molecular Catalysis,* **47**, 165-177.

Somogyi, B., Lakos, Z., Szarka, A. and Nytirai, M. (2000) Protein flexibility as revealed by fluorescence resonance energy transfer: an extension of the method for systems with multiple labels. *Journal of Photochemistry and Photobiology B,* **59**, 26-32.

Strambini, G.B. and Gonnelli, M. (1985) The indole nucleus triplet-state lifetime and its dependence on solvent microviscosity. *Chemical Physics Letters,* **115**, 196-200.

Stryer, L. (1988) *Biochemistry,* 3rd edn., W.H. Freeman and Company, New York.

Stuckey, J.A., Schubert, H.L., Fauman, E.B., Zhang, Z.-Y., Dixon, J.E. and Saper, M.A. (1994) Crystal structure of *Yersinia* protein tyrosine phosphatase at 2.5 Å and the complex with tungstate. *Nature,* **370**, 571-575.

Sumner, J.B. (1921) Dinitrosalicylic acid: a reagent for the estimation of sugar in normal and diabetic urine. *Journal of Biological Chemistry*, **47**, 5-9.

Swartz, H.M., Bolton, J.R. and Borg, D.C. (1972) *Biological Applications of Electron Spin Resonance,* John Wiley and Sons, New York.

Takaizumi, K. and Wakabayashi, T. (1997) The freezing process in methanol-, ethanol-, and propanol-water systems as revealed by differential scanning calorimetry. *Journal of Solution Chemistry,* **26**, 927-939.

Tilton Jr., R.F., Dewan, J.C. and Petsko, G.A. (1992) Effects of temperature on protein structure and dynamics: X-ray crystallographic studies of the protein ribonuclease-A at nine different temperatures from 98 to 320 K. *Biochemistry,* **31**, 2469-2481.

Tipler, P.A. (1991) *Physics,* 3rd edn., Worth Publishers, New York.

Travers, F. and Barman, T. (1995) Cryoenzymology: How to practice kinetic and structural studies. *Biochimie,* **77**, 937-948.

Travers, F. and Douzou, P. (1974) Dielectric constant of mixed solvents used for low temperature biochemistry. *Biochimie,* **56**, 509-514.

Tsitsimpikou, C., Xhirogianni, K., Markopoulou, O. and Kolisis, F.N. (1996) Comparison of the ability of β-glucosidases from almonds and *Fusarium oxysporum* to produce n-alkyl-β-glucosides in organic solvents. *Biotechnology Letters,* **18**, 387-392.

Valivety, R.H., Halling, P.J. and Macrae, A.R. (1992a) *Rhizomucor meihei* lipase remains active at water activity below 0.0001. *FEBS Letters,* **301**, 258-260.

Valivety, R.H., Halling, P.J., Peilow, A.D. and Macrae, A.R. (1992b) Lipases from different sources vary widely in dependence of catalytic activity on water activity. *Biochimica et Biophysica Acta,* **1122**, 143-146.

van Gunsteren, W.F. and Karplus, M. (1982) Protein dynamics in solution and in a crystalline environment: a molecular dynamics study. *Biochemistry,* **21**, 2259-2274.

Vitkup, D., Ringe, D., Petsko, G.A. and Karplus, M. (2000) Solvent mobility and the protein 'glass' transition. *Nature,* **7**, 34-38.

Wagner, G. and Wuthrich, K. (1978) Dynamic model of globular protein conformations based on NMR studies in solution. *Nature,* **275**, 247-248.

Wallenfels, K. and Malhorta, O.P. (1961) Galactosidases. *Advances in Carbohydrate Chemistry,* **16**, 239-298.

Wand, A.J. (2001) Dynamic activation of protein function: A view emerging from NMR spectroscopy. *Nature Structural Biology,* **8**, 926-931.

Weast, R.C. (1974) *Handbook of Chemistry and Physics,* 55th edn., CRC Press, Cleveland.

Wescott, C.R. and Klibanov, A.M. (1994) The solvent dependence of enzyme specificity. *Biochimica et Biophysica Acta,* **1206**, 1-9.

White, A. and Rose, D.R. (1997) Mechanism of catalysis by retaining β-glycosyl hydrolases. *Current Opinion in Structural Biology,* **7**, 645-651.

Williams, R.J.P. (1989) NMR studies of mobility within protein structure. *European Journal of Biochemistry,* **183**, 479-497.

Withers, S.G. (2001) Mechanisms of glycosyl transferases and hydrolases. *Carbohydrate Polymers,* **44**, 325-327.

Yankeelov, J.A. and Koshland, D.E. (1965) Evidence for conformational changes induced by substrates of phosphoglucomutase. *Journal of Biological Chemisty,* **240**, 1593-1602.

Yguerabide, J. (1972) Nanosecond fluorescence spectroscopy of macromolecules. *Methods in Enzymology,* **26**, 498-578.

Zaks, A. and Klibanov, A.M. (1988) The effect of water on enzyme action in organic media. *The Journal of Biological Chemistry,* **263**, 8017-8021.

Zanotti, J.-M., Bellissent-Funel, M.-C. and Parello, J. (1997) Dynamics of a globular protein as studied by neutron scattering and solid-state NMR. *Physica B,* **234-236**, 228-230.

Zanotti, J.-M., Bellissent-Funel, M.-C. and Parello, J. (1999) Hydration-coupled dynamics in proteins studied by neutron scattering and NMR: The case of the typical EF-hand calcium-binding parvalbumin. *Biophysical Journal,* **76**, 2390-2411.

Zechel, D.L. and Withers, S.G. (2000) Glycosidase mechanisms: Anatomy of a finely tuned catalyst. *Accounts of Chemical Research,* **33**, 11-18.